Universidad de Concepción
Dirección de Postgrado
Facultad de Farmacia -Programa de Doctorado en Ciencias y Tecnología Analítica

Desarrollo de una plataforma analítica para el estudio de compuestos (poli)fenólicos en frutos de uva, calafate y para metabolómica en plasma de animales de experimentación sometidos a la ingesta aguda de un extracto de fruto

Tesis para optar al grado de Doctor en Ciencias y Tecnología Analítica

LUIS ALEJANDRO BUSTAMANTE SALAZAR
CONCEPCIÓN-CHILE
2017

Profesor Guía: Dra. Claudia Mardones Peña
Profesor Co-Guía: Dr. Dietrich von Baer von Lochow
Dr. Edgar Pastene Navarrete

Dpto. de Análisis Instrumental, Facultad de Farmacia
Universidad de Concepción

Tabla de contenidos

Índice de Figuras

Índice de Tablas

Resumen

Se desarrolló un conjunto de métodos de análisis con un enfoque metabolómico dirigido y no dirigido, junto a ensayos de capacidad antioxidante como plataforma analítica para estudios de intervención nutricional.

De acuerdo a la estrategia analítica planteada, se caracterizaron frutos de uva de mesa (*Vitis vinífera L.*) Red Globe, Pink Globe y de calafate (*Berberis microphylla*), 3 frutos con elevadas concentraciones de polifenoles. Los resultados obtenidos por HPLC-DAD-ESI-MS/MS indican que el fruto de calafate contiene entre 60 a 400 veces más antocianos que en las uvas estudiadas, seguido por ácidos hidroxicinámicos y flavonoles (45 y 15 veces, respectivamente), por lo que se diseñó un ensayo de ingesta aguda usando calafate. Con el fin de elaborar un extracto liofilizado de Calafate enriquecido en polifenoles, se modificó la extracción usando etanol potable y ácido fórmico, produciendo un extracto seco de calafate que contiene 265.26 µmol de polifenoles por gramo. Una vez producido un lote homogéneo de extracto liofilizado, se administraron 300 mg/kg de éste a 5 grupos de gerbos (n=3). Transcurridas 1, 2, 4, 8 y 12 horas, se extrajo entre 600 y 1000 µL de sangre mediante punción del plexo retroorbital. Un grupo control (n=3) usado como tiempo 0 se incluyó en el diseño. Se logró obtener plasma sin hemólisis y los animales no fueron sacrificados.

A partir de los plasmas obtenidos, se cuantificaron mediante un método GC-MS/MS validado más de 40 productos de metabolización de polifenoles presentes en calafate, análisis metabolómico no dirigido mediante UPLC-QTOF y ensayos de capacidad antioxidante en microplaca.

Los resultados cuantitativos obtenidos por GC-MS/MS muestran aumentos de 9 compuestos asociados al consumo del extracto de calafate. Luego de 1 y 2 horas los compuestos 1,4-dihidroxibenceno, ácidos 3,4-dihidroxifenilacético, 4-hidroxicinámico, 3,5-dimetoxi-4-hidroxibenzoico y 3-metoxi-4-hidroxibenzoico muestran una tendencia al alza, mientras que se observó un aumento significativo de los ácidos 3-hidroxicinámico y 3-metoxi-4-hidroxifenilacético. Además, los ácidos 3-hidroxifenilacético y fenilacético muestran aumentos significativos luego de 4 y 8 horas de administrado el extracto.

El análisis metabolómico no dirigido de las mismas muestras de plasma revela un cambio significativo de 20 compuestos durante los tiempos ensayados. De estos, uno se identificó como adenosina monofosfato y 6 como metabolitos derivados del consumo del extracto de calafate. Los compuestos cumaroil-quinolactona y derivados sulfatados de ácido (iso)vaníllico y un isómero de ácido cafeico aumentan significativamente luego de 1 y 2 horas de administrado el extracto de calafate. Los derivados sulfatados de un segundo isómero de ácido cafeico y ácido (iso)ferúlico aumentan significativamente solo luego de 1 hora y un metoxicatecol-sulfato aumenta luego de 2 horas. Además, el mismo ácido (iso)ferúlico aumenta nuevamente luego de 12 horas de administrado el extracto.

El ensayo ORAC-FL revela un aumento significativo luego de 1 hora, mientras que el ensayo CUPRAC lo alcanza a las 4 horas de administrado el extracto de calafate. Los resultados de Fenoles totales exhiben un aumento significativo a las 1, 4 y 12 horas, relacionándose con los incrementos de los resultados anteriores.

Capítulo 1

Estado del arte.

Caracterización de polifenoles en bayas estudiadas y su metabolización en mamíferos.

Contenidos

Introducción

Los frutos y vegetales funcionales son productos consumidos habitualmente en la dieta, y contienen una serie de componentes beneficiosos para la salud, incluyendo fibra y altas concentraciones de ácidos fenólicos, flavonoides, vitaminas y minerales. También pueden reducir el riesgo de enfermedades crónicas como cáncer, hipertensión, enfermedades cardiovasculares, etc. [1–5].

Sin embargo, la biodisponibilidad de los (poli)fenoles está relacionada con una serie de factores, como la disolución, absorción, distribución, acumulación en tejidos, metabolismo y excreción. Intervenciones en humanos muestran que estas características se ven directamente influenciadas por el contenido de estos compuestos, tipo de matriz en los alimentos consumidos, presencia de microorganismos en el colon y variables genéticas [6,7].

A pesar de que existe mayor evidencia de la baja biodisponibilidad de los (poli)fenoles presentes en los alimentos, el efecto de la digestión a nivel intestinal, el metabolismo hepático de fase I y II y el metabolismo de (poli)fenoles por microorganismos intestinales está actualmente en estudio. Bajo estos términos, se sabe que existe baja excreción fecal y presencia de (poli)fenoles en orina, lo que indica un alto grado de transformación y/o degradación a nivel intestinal [8]. El análisis del fluido ileal luego de la ingesta de alimentos, obtenido de humanos con ileostomía, muestra que incluso cuando los polifenoles son absorbidos por el intestino delgado, gran cantidad de estos alcanzan el intestino grueso [9–12], donde la microbiota intestinal rompe las estructuras conjugadas junto con la aglicona resultante, produciendo moléculas más pequeñas que son altamente variables entre individuos [13] y alteran la bioactividad asociada al consumo de determinados polifenoles [14,15].

Los polifenoles conjugados con grupos glucuronidos, sulfatos y metilos son tratados como xenobióticos, y en vez de acumularse en el sistema circulatorio, son rápidamente removidos mediante excreción por la orina. En algunas circunstancias, la excreción urinaria provee una evaluación más realista en términos de concentración final de los metabolitos. Sin embargo, excluye la posibilidad de estudiar la acumulación en tejidos o los efectos que pueden producir a nivel sistémico [5]. En este sentido, el análisis del plasma entrega mayor información sobre el efecto biológico asociado a la ingesta de polifenoles.

Para abordar esto, se ha propuesto el uso de enfoques metabolómicos, que tienen como característica principal: a) explorar cambios del metaboloma o familias de compuestos en estudio y b) identificar y cuantificar un grupo de compuestos asociados a la ingesta de polifenoles.

Para contextualizar el uso del enfoque metabolómico en la metabolización de polifenoles es necesario conocer su contenido en los alimentos usados para el estudio, junto con los mecanismos de degradación involucrados en este proceso.

Clasificación de compuestos fenólicos

Los compuestos fenólicos se caracterizan por poseer un anillo aromático con uno o más grupos hidroxilos. Sin embargo, existe una amplia diversidad que varían desde aquellos que contienen un solo anillo aromático (C_6; C_6-C_1) hasta complejos polímeros. En la Tabla 1.1 se muestra la clasificación de las estructuras bases de los (poli)fenoles. Éstos pueden ser comúnmente conjugados con azúcares, ácidos orgánicos u otros fenoles [16].

La biosíntesis de flavonoides, estilbenos, ácidos hidroxicinámicos y otros ácidos fenólicos involucran las rutas biosintéticas del ácido shikímico, fenilpropanoide y flavonoide (Figura 1.1).

Tabla 1.1: Estructuras base de (poli)fenoles (modificado de [16])

Esqueleto	Clasificación	Estructura básica
C_6-C_1	Ácidos fenólicos	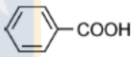
C_6-C_2	Acetofenonas	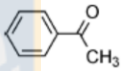
C_6-C_2	Ácidos fenilacéticos	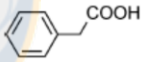
C_6-C_3	Ácidos hidroxicinámicos	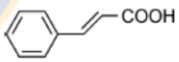
C_6-C_3	Cumarinas	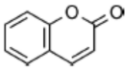
C_6-C_4	Naftoquinonas	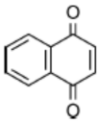
C_6-C_1-C_6	Xantonas	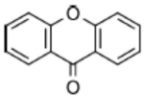
C_6-C_2-C_6	Estilbenos	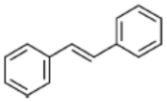
C_6-C_3-C_6	Flavonoides	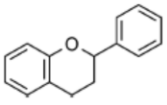

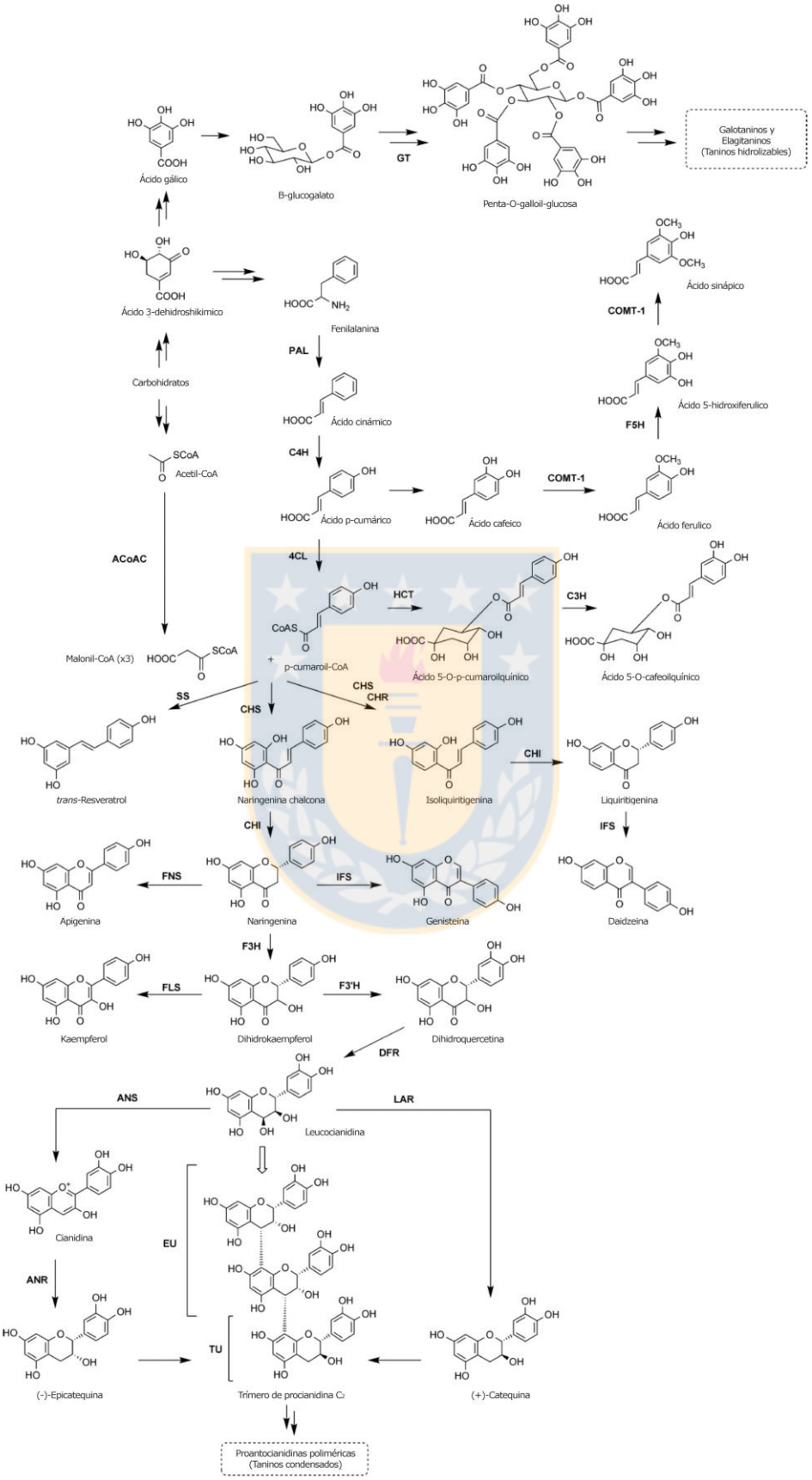
Ácido gálico
B-glucogalato
GT
Penta-O-galloil-glucosa
Galotaninos y
Elagitaninos
(Taninos hidrolizables)
Ácido 3-dehidroshikimico
Fenilalanina
Ácido sinápico
COMT-1
Carbohidratos
PAL
Ácido cinámico
Ácido 5-hidroxiferulico
F5H
Acetil-CoA
C4H
Ácido p-cumárico
Ácido cafeico
COMT-1
Ácido ferulico
ACoAC
4CL
HCT
C3H
Malonil-CoA (x3)
p-cumaroil-CoA
Ácido 5-O-p-cumaroilquínico
Ácido 5-O-cafeoilquínico
SS
CHS
CHS
CHR
CHI
CHI
IFS
trans-Resveratrol
Naringenina chalcona
Isoliquiritigenina
Liquiritigenina
FNS
IFS
Apigenina
Naringenina
Genisteina
Daidzeina
F3H
FLS
F3'H
Kaempferol
Dihidrokaempferol
Dihidroquercetina
DFR
ANS
LAR
Leucocianidina
Cianidina
EU
ANR
TU
(-)-Epicatequina
Trímero de procianidina C2
(+)-Catequina
Proantocianidinas poliméricas
(Taninos condensados)

Figura 1.1: Ruta biosintética y principales enzimas involucrados en la síntesis de taninos hidrolizables y condensados, ácidos hidroxicinámicos, flavonoides y estilbenos. Abreviaciones PAL: fenilalanina amonio liasa; C3H: cinamato 3-hidroxilasa; C4H: cinamato 4-hidroxilasa; COMT-1:ácido cafeico/5-hidroxiferulico O-metiltransferasa; 4CL: p-cumarato:CoA ligasa; F5H: ferulato 5-hidroxilasa; GT: galoiltransferasa; ACoAC: acetilCoA carboxilasa; HCT: hidroxicinamoil transferasa; SS: estilbeno sintasa; CHS: chalcona sintasa; CHR: chalcona reductasa; CHI: chalcona isomerasa; IFS: isoflavona sintasa; FNS: flavona sintasa; FLS: flavonol sintasa; F3´H:flavanona 3´-hidroxi sintasa ; DFR: dihidroflavonol 4-reductasa; ANS: antocianidina sintasa; LAR: leucoantocianidina 4-reductasa; ANR: antocianidina reductasa; EU: unidad de extensión; TU: unidad terminal (modificado de [16]).

La estructura de los flavonoides se forma por la interacción de 2 rutas biosintéticas. El anillo B y la estructura del heteroanillo C se constituye a partir del p-cumaroil-CoA (producto de ruta fenilpropanoide), mientras que el anillo A se origina de la condensación de 3 unidades malonil-CoA.

Los (poli)fenoles están ampliamente distribuidos en el reino vegetal. Dentro de esta familia de compuestos fenólicos, los flavonoides y fenoles relacionados con la ruta biosintética fenilpropanoide representan un grupo importante, los que pueden ser clasificados como flavonoides y no flavonoides.

a) Flavonoides

Su estructura base consiste en 15 carbonos, 2 anillos aromáticos conectados por 3 carbonos (C_6-C_3-C_6, Tabla 1.1). Son los compuestos más numerosos en el reino vegetal, especialmente en hojas, epidermis (piel) y semillas. Las principales subclases se muestran en la Figura 1.2. De estos, los flavonoles, flavonas, flavan-3-oles, antocianidinas, flavanonas e isoflavonas son las más consumidas. Generalmente contienen grupos hidroxilo en las posiciones 4´-, 5- 7- y azúcares en posición 3-O- (aumento de polaridad), además de grupos metilo e isopentilo (disminución de polaridad) [16].

Los antocianos son uno de los grupos más importantes de metabolitos secundarios. En plantas, los antocianos existen en abundancia y confieren los colores azules, rojos, violetas y púrpura a frutas y vegetales. También se pueden encontrar en hojas, ramas, semillas y raíces. Están frecuentemente conjugados con azúcares, ácidos hidroxicinámicos y ácidos orgánicos en la posición 3-O- y 5-O- y sustituidos en los carbono 5-, 7-, 3´-, 4´-, 5´-. Según el grado de sustitución son descritos: 4´-hidroxi, 3´,4´-dihidroxi y 3´,4´,5´-trihidroxi antocianidinas, conocidas como pelargonidina, cianidina y delfinidina, respectivamente. Como producto de la metoxilacion en 3´-O- de cianidina y delfinidina, y la dimetoxilacion en 3´,5´de delfinidina; se producen la peonidina, petunidina y malvidina [17].

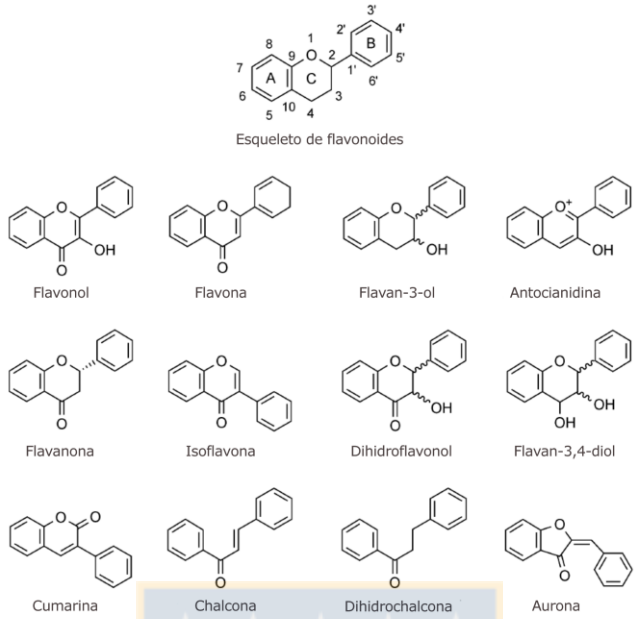

Figura 1.2: Estructuras de subclases de compuestos flavanoides (modificado de [16]).

Los flavonoles son otro grupo de flavonoides ampliamente distribuídos en el reino vegetal. Son frecuentemente conjugados por azúcares en la posición 3-O- y sustituidos en los carbono 5-, 7-, 3´-, 4´-, 5´-. De acuerdo a su grado de sustitución, se describen 6 compuestos principales : 4´-hidroxi, 3´,4´-dihidroxi y 3´,4´,5´-trihidroxi flavonol, conocidos como kaempferol, quercetina y miricetina, respectivamente. Como producto de la metoxilacion en 3´-O- de quercetina y miricetina, y la dimetoxilacion en 3´,5´de miricetina; se producen la isoramnetina, laricitina y siringetina, los que se encuentran en una gran diversidad de bayas [18].

Debido a su C_2 y C_3 insaturado, **los flavan-3-oles** presentan dos centros quirales. Suelen estar sustituidos en los carbono 5-, 7-, 3´-, 4´- y 5´-. Comúnmente se conjugan en la posición 3-O- con ácido gálico, aunque también pueden formar dímeros, oligómeros a polímeros llamados proantocianidinas. Las proantocianidinas tipo B son formadas por (+)-catequina y (-)-epicatequina (estereoisómeros C 5-, 7-, 3´-, 4´- hidroxilados) entre C4 y C6 ó C8, mientras que las de tipo A son formadas por un enlace adicional entre C2 y 7-O- [19]. Las proantocianidinas formadas por unidades de (epi)catequina son llamadas procianidinas, mientras que las formadas por (epi)afzelequina (C 5-, 7-, 4´- hidroxilados) y (epi)galocatequina (C 5-, 7-, 3´-, 4´-,5´- hidroxilados) son llamados propelargonidinas y prodelfinidinas.

Las flavonas pueden ser sustituidas en los carbonos 5-, 7-, 3´-, 4´- y aunque carecen del grupo hidroxilo en posición 3, pueden ser conjugados en la posición 7-O- y normalmente polimetoxilados en el anillo A.

Las isoflavonas tienen el anillo B unido a C3 y se encuentran casi exclusivamente en leguminosas. Son frecuentemente sustituidos en los carbono 5-, 7- y 4´-. Finalmente, **Las flavanonas** presentan un centro quiral en C_2 y están presentes con más frecuencia en frutos cítricos (*Rutaceae*). Son frecuentemente conjugados con azúcares en la posición 7-O- y sustituidos en los carbono 5-, 7-, 3´-y 4´- [16].

b) No flavonoides

Los compuestos no flavonoides más relevantes en la dieta son el ácido gálico junto a galotaninos (p.ej. ésteres de azúcar y ácido gálico), ácido elágico junto a elagitaninos, ácidos hidroxicinámicos (HCA), junto a derivados conjugados (ácido tartárico, ácido quínico) y estilbenoides, principalmente como derivados del resveratrol (3,5,4´-trihidroxiestilbeno) [16]. La identificación y cuantificación de HCAs ha sido ampliamente estudiada en bayas comestibles, café y hierbas medicinales durante los últimos años [20,21]. Los HCAs presentes en plantas se encuentran principalmente como derivados esterificados (ácidos clorogénicos), conformados por un enlace éster entre uno o más ácidos cafeico, cumárico o ferúlico y un ácido quínico, por la vía de los fenilpropanoides (Figura 1.1) [22] . Sin embargo, en algunos casos es posible encontrar enlaces éster entre HCA y ácido aldárico, derivado de las aldosas (principalmente ácido hexárico) [23].

Compuestos fenólicos en calafate y uvas cv. Pink Globe y Red Globe

El calafate (*Berberis microphylla*) es una especie nativa de la familia Berberidaceae presente la Patagonia (Chile y Argentina). Son arbustos de hasta 3 metros de altura con bayas comestibles color azul oscuro de 7 a 11 mm. Es una planta silvestre no cultivada, muchas veces considerada como maleza. En Chile, se distribuye en las regiones de Aysén y Magallanes, aunque se ha descrito desde Curicó hasta la región Antártica. [24].

Por otro lado, la uva (*Vitis vinífera* L.) es una baya de la familia Vitaceae con un alto contenido de compuestos fenólicos que ha sido ampliamente estudiados [25,26]. Aunque el país es más conocido como exportador de vinos, Chile alcanza el primer lugar como exportador de uva de mesa. Dentro de las variedades cultivadas, se encuentra “Red Globe”, que se caracteriza por producir una baya de color rojo oscuro, con un tamaño de 24 – 28 mm, dulce, de semilla astringente, que posee muy buena conservación frigorífica, es resistente al transporte y no presenta problemas fitosanitarios [27,28]. Sin embargo, en los últimos años, se ha encontrado una variante somaclonal de Red Globe, llamada “Pink Globe”, que además de presentar un color rosado, la pulpa es absolutamente blanca, sus semillas son más pequeñas y no son astringentes. En comparación a Red Globe, posee una piel más suave y presenta en promedio 3 a 4 grados Brix más [29].

Dentro de los compuestos fenólicos ampliamente distribuidos, tanto en calafate como en uvas de mesa, se encuentran los flavonoides, principalmente antocianos y flavonoles. También se describen compuestos no flavonoides, como los ácidos hidroxicinámicos. Las uvas se caracterizan adicionalmente por presentar flavan-3-oles, junto con sus derivados poliméricos, ácidos hidroxibenzoicos y estilbenoides [23,25,26].

a) Compuestos flavonoides

Antocianos. El calafate es una baya silvestre rica en antocianos [30]. La concentración media observada en 68 muestras provenientes de las regiones de Aysén y Magallanes obtenidas los años 2011 y 2012 fueron de 21 μmol/g y 17 μmol/g de fruto fresco (FW), respectivamente [31], lo que lo ubica entre las frutas con mayores niveles de este tipo de polifenoles, superando niveles descritos para otras bayas ampliamente consumidas, como el arándano [30,32]. Un estudio reciente comparó los antocianos de calafate con otras bayas nativas que se encuentran en las mismas zonas, detectándose mayores niveles y diversidad en calafate [33]. El principal antociano presente en calafate fue delfinidina-3-glucósido, seguido por petunidina-3-glucósido y malvidina-3-glucósido, siendo detectado un total de 18 antocianos [34]. Adicionalmente, se observó una correlación entre la concentración total de antocianos y la capacidad antioxidante determinada mediante $TEAC_{ABTS}$ [30].

Por otro lado, el contenido de antocianos en uvas Red Globe ha sido ampliamente estudiado. Carreño y col. informaron una concentración de antocianos totales de 167 μg/g de fruto fresco (0.36 μmol/g equivalentes de peonidina-3-glucosido (P3G)), encontrándose mayoritariamente peonidina-3-glucósido, seguido de malvidina-3-glucósido y cianidina-3-glucósido. Adicionalmente se reportaron derivados acetilados, cumarilados y cafeoilados [35]. Sin embargo, Cantos y col. encontraron ligeras diferencias, como una concentración total de 115.3 μg/g de fruto fresco (0.25 μmol/g P3G), concentraciones similares de malvidina-3-glucósido y cianidina-3-glucósido, y la ausencia de derivados acetilados y cafeoilados. Estos autores discuten que las diferencias reportadas están asociadas a factores agronómicos, como composición del suelo, irrigación, intensidad de luz, etc., que son importantes en la composición de compuestos fenólicos en frutos y vegetales a pesar de que sean de la misma especie y variedad [25]. Hasta el desarrollo del presente proyecto (octubre 2013), no hay información científica sobre los niveles de concentración y los perfiles de estos compuestos en uva Pink Globe.

Flavonoles. El calafate muestra perfiles y niveles interesantes de este tipo de compuestos. En una primera aproximación se describieron concentraciones totales de 0.16 μmol/g fruto fresco, lo que equivale 100 veces menos que el contenido de antocianos [30]. Sin embargo, en un estudio más extenso,

que involucro las regiones de Aysén y Magallanes, se encontró que los niveles promedio de flavonoles alcanzan los 1.34 μmol/g [36,37], siendo los más importantes los derivados 3-rutinósidos y 3-galactósidos de quercetina y un derivado rutinósido de isoramnetina.

Cantos y col. determinaron que el contenido de flavonoles totales en uva Red Globe es de 61.3 μg/g, fruto fresco (0.13 μmol/g equivalentes quercetina-3-glucósido), cerca de la mitad de lo reportado para antocianos totales, siendo los de mayor interés los derivados de quercetina (glucósido + rutinósido y glucurónido) [25].

Flavan-3-oles y procianidinas (PC). No hay información sobre la distribución y niveles de PC en calafate, aunque se han reportado bajos niveles de flavan-3-oles en fruto [30].

A pesar que no se encuentra información del contenido de flavan-3-oles específicos en Red Globe, Cantos y col. han reportado una concentración de 40.4 μg/g fruto fresco de flavan-3-oles totales (0.13 μmol/g equivalentes catequina) , mientras que Lutz y col. hallaron 13.07 μg/g fruto fresco de catequina en piel (0.04 μmol/g) [25,26]. No existe información del nivel de flavan-3-oles en uvas Pink Globe. Adicionalmente la comparación con otras variedades de uva de mesa indica que las uvas blancas tienen mayor contenido de flavan-3-oles que las rojas [25].

b) Compuestos no flavonoides

Ácidos hidroxicinámicos (HCAs). Mono-, di- y tri-hidroxicinamoil éster de ácido glucárico, galactárico y 2-hidroxi-glucárico han sido identificados en algunos vegetales [38–40]. En un estudio reciente, 14 ácidos hidroxicinamoil-quínicos (principalmente derivados de ácido cafeico) han sido identificados en calafate, junto con ácidos hidroxicinamoil-glucáricos [41], que fueron posteriormente identificados por NMR como ácidos 3- y 4-cafeoil-glucárico [23]. La concentración promedio de HCAs en calafate fue de 3.79 μmol/g en un total de 68 muestras, siendo el compuesto mayoritario el ácido 5-cafeoilquínico y el ácido 2-cafeoilglucárico.

Cantos y col. determinaron que la concentración de ácidos hidroxicinámicos totales es de 8.4 μg/g fruto fresco (0.03 μmol/g equivalentes ácido cafeoil tartárico) en uvas Red Globe. Los ácidos hidroxicinámicos encontrados fueron el ácido cafeoil-tartárico y *p*-cumaroil-tartárico [25]. Adicionalmente, se encontró presencia de derivados de ácido protocatequínico y ácido gálico, reportado por Lutz y col. [26].

Estilbenoides. Estilbenos como *trans*-resveratrol, *trans*-piceido, dímeros y trímeros de estos compuestos no fueron detectados por LC-MS/MS en bayas de calafate. Por otro lado, existe poca información sobre la presencia de estilbenoides en uva Red Globe. Mientras que Cantos y col. indican

ausencia, Lutz y col. reportan una concentración de 0.77 μg/g fruto fresco (0.003 μmol/g) de resveratrol en piel [25,26]. Hasta la fecha, no existe información de presencia de estilbenoides en uvas Pink Globe.

Metabolismo y biodisponibilidad de compuestos fenólicos.

La metabolización y biodisponibilidad de los compuestos fenólicos es característica para cada grupo. En el caso de los antocianos, los compuestos parentales tienen una muy baja concentración a nivel plasmático y en orina, mientras que para los flavonoles y HCAs estos niveles se ven aumentados. Es importante asociar las características físico-químicas propias de las moléculas en estudio al sistema en que están siendo incorporados. El cambio de las condiciones en que se encuentran normalmente (tejido vegetal) son drásticamente alteradas al consumirlas (por ejemplo, cambio relevante del pH o presencia de enzimas), especialmente a través de todo el tracto digestivo [42].

La absorción de algunos compuestos fenólicos ingeridos en la dieta (como antocianos) puede ocurrir a nivel estomacal luego de ser liberados de su matriz. Sin embargo, una vez que llegan al intestino ocurren una serie de reacciones que modifican los compuestos parentales[43,44].

Para lograr una absorción efectiva por la barrera intestinal, es necesaria la hidrólisis de los glucósidos de flavonoides y ácidos fenólicos esterificados [45], la cual se realiza a nivel de enterocitos. Sin embargo, no es la única forma de ingreso [45]. Aunque la absorción de los compuestos fenólicos puede realizarse mediante difusión pasiva [46,47], ésta se realiza principalmente mediante transportadores de glucosa dependiente de sodio (SGLT), la cual puede posteriormente ser: a) excretado al lumen intestinal mediante proteínas asociadas a resistencia a drogas (MRPs); b) hidrolizada mediante beta-glucosidasa citosólica (CBG); o c) conducida, mediante transportadores de glucosa (GLUT), al sistema portal-hepático. Sin embargo, es posible que los compuestos fenólicos se desconjuguen a nivel apical mediante la lactasa phloridzin hidrolasa (LPH), los que posteriormente pueden ser re-conjugados en menor proporción mediante catecol-O-metiltransferasa (COMT), sulfotransferasa (SULT) o uridina-5-difosfato glucuronosiltransferasa (UGT) a compuestos metilados, sulfatados o glucuronidados, los que pueden ser devueltos al lumen intestinal o llevados al sistema porta-hepático mediante MRPs (Figura 1.3) [5,8]. Luego, a nivel hepático, los polifenoles son altamente glucuronidados y/o sulfatados (metabolismo de fase II), mientras que las reacciones de metabolismo de fase I (oxidación/reducción) ocurren en menor proporción mediante isoformas de citocromo P450 [42,47,48]. Los estudios de farmacocinética en plasma usualmente muestran un segundo pico, atribuído a la circulación entero-hepática [8].

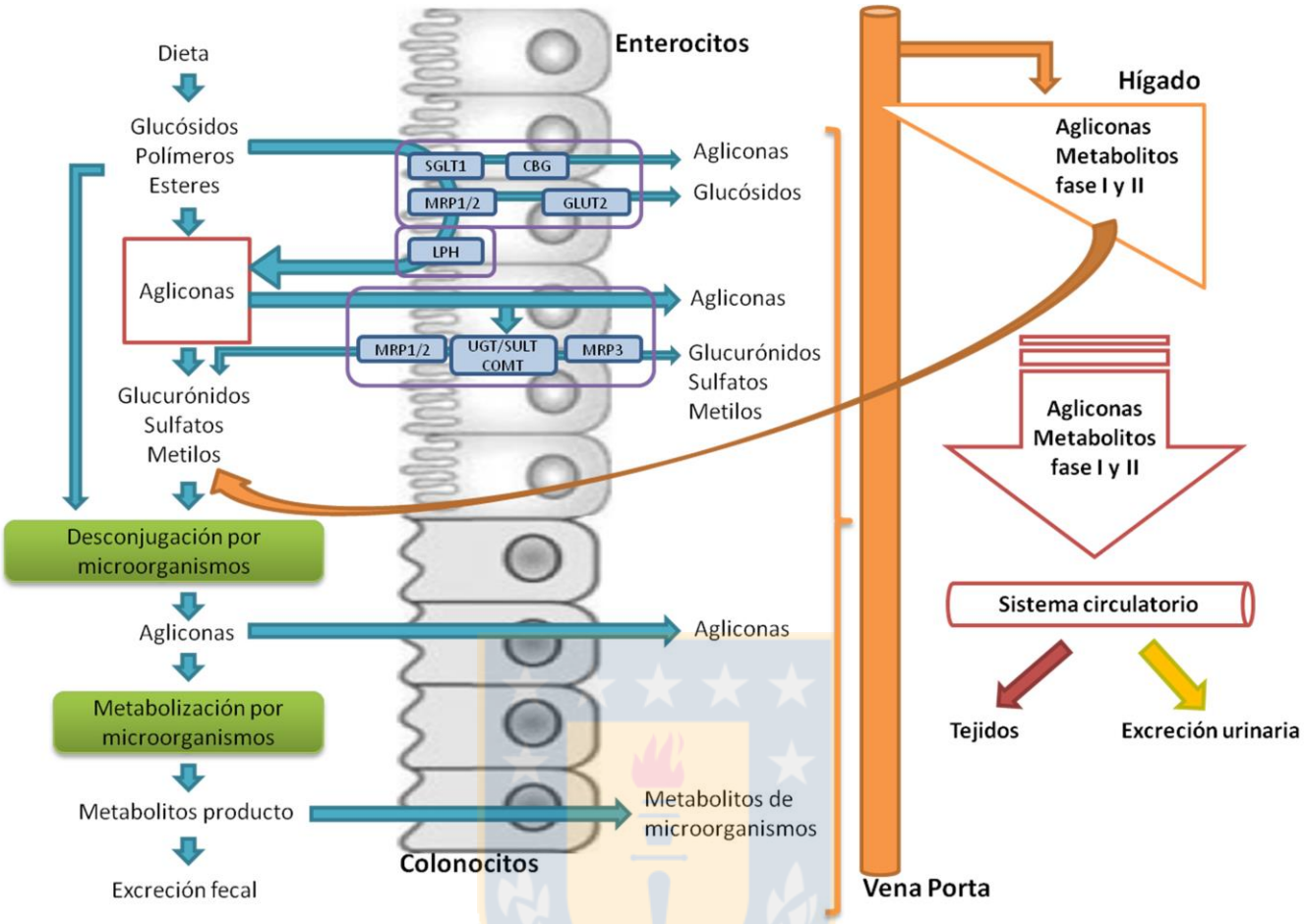

Figura 1.3: Absorción y modificación/hidrólisis por enzimas presentes en enterocitos. CBG; b-glucosidasa citosólica; COMT: catecol-O-metil transferasa; GLUT2: transportador de glucosa; LPH: lactasa phloridzin hidrolasa; MRP1-2–3: proteínas asociadas a resistencia a drogas; SGLT, transportador de glucosa sodio dependiente; SULT, sulfotransferasa; UGT, uridina-5´-difosfato glucuronosil transferasa (modificado de [5,8]).

Los polifenoles conjugados con azúcares que son resistentes a la acción de LPH/CBG no son absorbidos en el intestino delgado, y por lo tanto avanzan directamente al colon [46]. La presencia de microorganismos genera la desconjugación mediante glicosidasas, esterasas, glucuronidasas, sulfatasas y la posterior metabolización de los polifenoles presentes (metabolismo en Fase I), resultando en ácidos benzoicos, fenil-acéticos, fenil-propiónicos e hidroxicinámicos. Los metabolitos originados en Fase I se dirigen al hígado, donde se vuelven a metabolizar, generando nuevamente metabolitos sulfatados, glucuronidados y metilados (metabolismo en Fase II), los que se distribuyen a tejidos y posteriormente

son excretados vía urinaria. La excreción de metabolitos por bilis ocurre a nivel de intestino delgado, donde ocurre reabsorción, remetabolización o excrecion fecal.

a) Antocianos

Los antocianos pueden llegar a ser uno de los principales compuestos fenólicos consumidos en la dieta, con hasta 1 g/día consumido en personas que ingieren rutinariamente bayas y vino tinto. A diferencia de otros flavonoides, que son absorbidos y excretados como derivados glucuronidados o sulfatados, las recuperaciones de antocianos en orina obtenidas en estudios de consumo en humanos alcanzan el 0.1 % del total consumido[49].

El estudio de estos compuestos *in vivo* es muy difícil, ya que existe una gran variedad de agliconas, grupos que se pueden conjugar e incluso interconversiones producto del metabolismo de fase I y II (la metilación convierte la cianidina en peonidina, delfinidina en petunidina y petunudina en malvidina). Al parecer, el 3´-hidroxiantociano, pelargonidina-3-O-glucósido, es metabolizado a un menor número de productos y podría ser más fácilmente absorbido que su análogo 3´,4´-dihidroxiantociano, cianidina-3-O-glucósido.

El catión flavilio predomina a pH 1-3, pero a medida que aumenta el pH por sobre 4, la pseudobase carbinol (hemiacetal) se convierte en el componente principal, junto con cantidades más pequeñas de pseudobase chalcona y base quinoidal [17]. La predominancia en cada compartimento luego de la ingesta (órgano o fluido), en términos de fracción molar porcentual, se visualiza en la Figura 1.4 [43].

Debido a esto, es importante considerar los cambios de pH a través de todo el tracto digestivo. Es así que a nivel bucal, los antocianos pueden ser degradados hasta un 50% debido al pH (~6.8), a la microbiota y proteínas salivales [50,51]. Además pueden ser deglicosiladas por β-glicosidasas microbianas y glucuronidadas (metabolismo de fase II) [52].

Varios estudios reportan concentraciones de antocianos parentales en plasma desde los primeros 30 minutos hasta sobre una hora luego de la ingesta. Esto es debido a que existe una rápida absorción gástrica mediante bilitranslocasas y transportadores de glucosa (SGLT1, GLUT1 y GLUT3) que podrían transferir antocianos glucosilados a la circulación portal antes de los 10 minutos y excretados por la bilis dentro de los 20 minutos , lo que junto a la movilidad gástrica, pH (1-5) y enzimas gástricas libera el contenido de antocianos de la matriz de los alimentos y los acerca a la barrera estomacal [42,50].

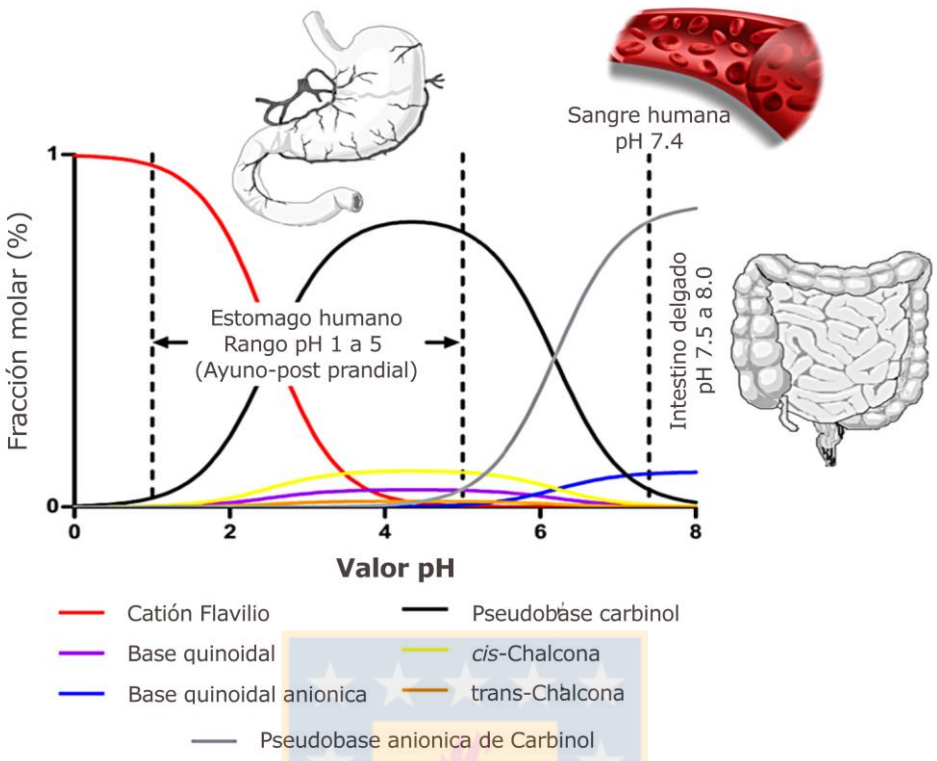

Figura 1.4: Fracción molar (%) en equilibrio, dependiendo del tracto gastrointestinal y pH en el que se encuentra (modificado de [43]).

A nivel intestinal, la absorción de los antocianos no es uniforme. Estudios *in vitro* muestran que la mayor absorción ocurre a nivel del yeyuno, lo cual sumado a la absorción gástrica, resulta en que mayores niveles de delfinidina glucósido administrados vía oral se encuentran en plasma a los 15 y 60 minutos [53].

Estudios sobre el consumo de frambuesas en personas con ileostomía mostraron que el 40% de los antocianos consumidos permanece en el fluido ileal, aunque la recuperación de los compuestos individuales varió enormemente (5.9% para cianidina-3-O-glucósido a 93% de cianidina-3-O-(2"-O-xilosil) rutinósido) [54]. La ingesta de jugo de uva en voluntarios sanos indica que existen niveles trazas de antocianos en plasma, encontrándose solo conjugados de petunidina y delfinidina, probablemente gracias a la absorción en el intestino delgado, ya que el tiempo en donde se encuentran concentraciones máximas de los compuestos glucosilados es entre las 1.3 a 1.4 horas. Por otro lado, las concentraciones máximas de petunidina y delfinidina glucuronidadas, consecuencia de la metabolización de fase II, se obtienen entre las 2.6 a 3.3 horas [55]. De la misma forma, la ingesta de frambuesas en sujetos sanos indica

que la pelargonidina-3-O-glucósido se convierte en pelargonidina-O-glucurónido, la cual alcanza rápidamente el sistema circulatorio (1.1 horas) [56].

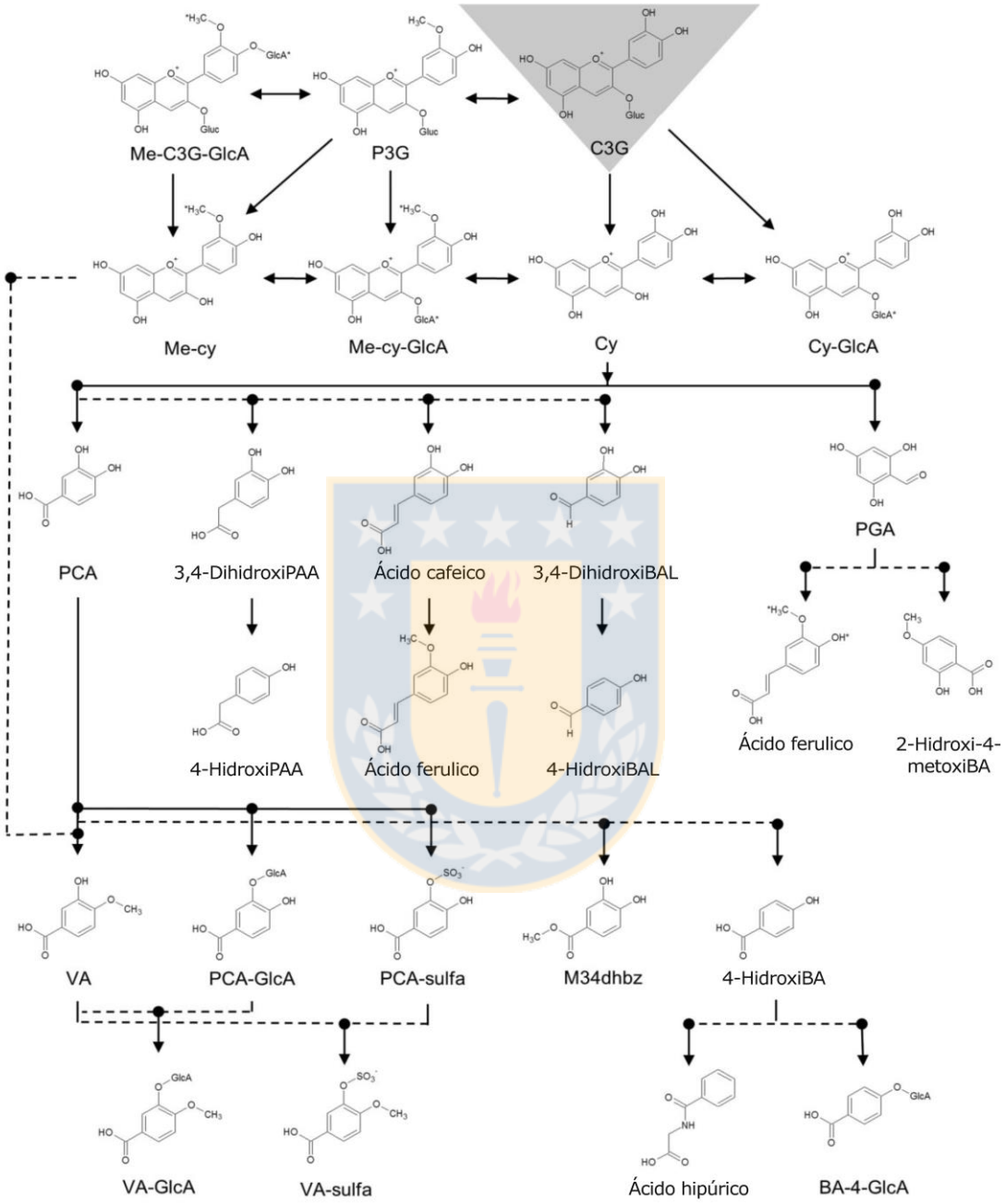

*Figura 1.5**:** Ruta propuesta para la metabolización de cianidina-3-O-glucósido en humanos. *Conjugados sin posición estructural conocida. BA: ácido benzoico; BAL: benzaldehído; C3G: cianidina-3-O-glucosido; Cy: cianidina; GlcA: glucuronido; Me: metoxi; M3,4dhbz: metil-3,4-dihidroxibenzoato; P3G: peonidina-3-glucósido; PAA: ácido fenil acético; PGA: floroglucinaldehído (modificado de [58]).*

Recientemente, un estudio que usó cianidina-3-O-glucósido marcada vía oral muestra que tanto a nivel plasmático, orina y heces, es posible encontrar: a) el antociano parental junto a su análogo mono y di metoxilado; b) los compuestos producidos por la degradación del antociano, resultando del anillo A el floroglucinaldehído y del anillo B el ácido protocatequínico; c) compuestos productos del metabolismo fase II, tanto derivados del antociano parental como de sus productos (de anillo A y B) (Figura 1.5) [57,58].

b) Ácidos hidroxicinámicos (HCAs)

Dupas y col. observaron una absorción limitada, pero significativa, tanto *in vivo* como *in vitro*, por células Caco-2, humanos y ratas, sugiriendo que puede haber absorción de ácidos clorogénicos intactos [59–61]. Mientras tanto, Olthof y col. determinaron que la esterificación del ácido cafeico con ácido quínico reduce la absorción [62]. Hu y col. estudiaron la interacción entre el ácido clorogénico y la albumina mediente un sitio de unión en el subdominio IIA, estableciendo que el mayor componente de las proteínas plasmáticas puede actuar como transportador de HCAs y podría estar explicando la baja detección de este tipo de compuestos si estas proteínas no se desnaturalizan [63]. Stalmach y col. estudiaron el metabolismo de los ácidos clorogénicos en voluntarios sanos y con ileostomía para lograr elucidar los eventos que ocurren a nivel de intestino delgado y colon. Los voluntarios con ileostomía consumieron 385 μmol de ácidos clorogénicos en café, de los cuales se recuperaron 274 μmoles de los compuestos originales, junto a conjugados sulfatados y glucuronidados en fluido ileal recolectado durante 24 horas [64,65]. Por lo tanto, alrededor del 30% es absorbido por el intestino delgado, mientras que el 70% de los ácidos consumidos logran alcanzar el colon, donde son metabolizados por la acción de la microbiota intestinal (Figura 1.6).

Por otro lado, se encontraron bajas concentraciones plasmáticas de derivados de ácidos hidroxicinamicos (cafeoilquinico, cafeoilquinico sulfatados y feruloilquínico), mientras que fueron mayores para el caso de los ácidos cafeoil-3-O-sulfato y ferúlico-4-O-sulfato, luego de transcurrida 1 hora de la ingesta de café. Sin embargo, se observó una mayor concentración de ácido dihidrocafeico y dihidroferulico, junto a sus derivados sulfatados, luego de 5 horas. Estos resultados indican que las modificaciones de los ácidos se deben a alteraciones por el metabolismo hepático de fase II, ya que en el intestino grueso no ocurre la sulfatación de flavonoides ni de ácidos fenólicos. Esta conversión de HCA a dihidro en plasma se explica de mejor manera por el metabolismo de microorganismos en el colon más que por la acción de reacciones de fase I en el hígado [64].

Junto con esto, luego del consumo de jugo de uva en voluntarios sanos, aparecen ácidos hidroxicinámicos (cumárico, cafeico y ferúlico) en plasma después de 0.7 a 1.0 horas, lo que indica una absorción a través del intestino delgado, gracias a la acción de esterasas. Por otro lado, ácidos como el dihidrocumárico, dihidrocumárico-O-sulfato entre otros metabolitos de ácidos dihidrocafeico y dihidroferúlico, alcanzan las concentraciones máximas entre los 3.9 a 6.0 horas [55]. Finalmente, en la orina se encontraron principalmente metabolitos, que en voluntarios sanos alcanzó el 29.2%, mientras que en sujetos con ileostomía alcanzo solo un 8%, demostrando que el colon afecta directamente la biodisponibilidad de los ácidos clorogénicos [55,66].

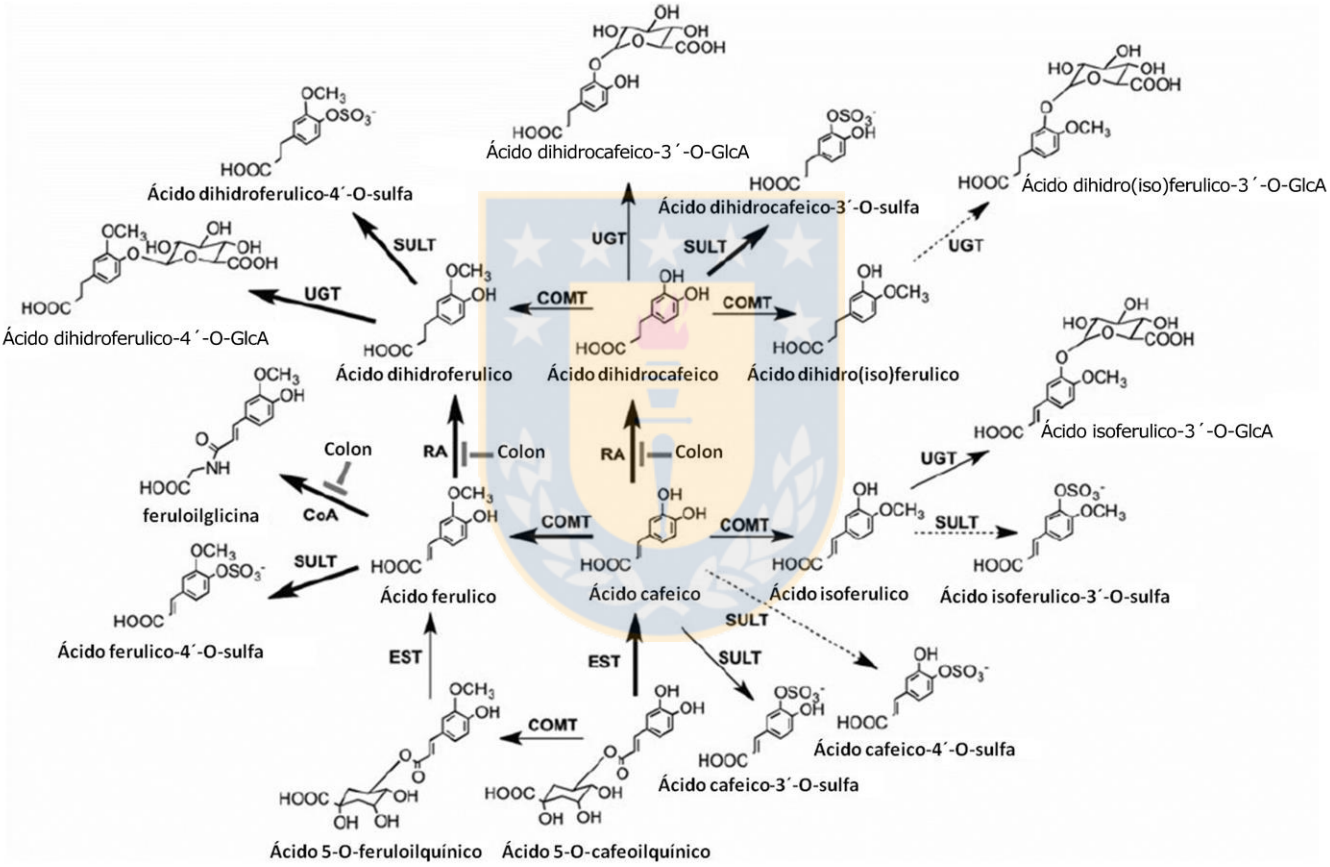

Figura 1.6: Ruta metabólica propuesta para ácidos clorogénicos presentes en fluido ileal, plasma y orina luego de la ingesta de café. Se ejemplifica con el ácido 5-cafeoilquínico y 5-feruloilquínico, aunque sus isómeros podrían ser metabolizados de la misma manera. Co-A: Co-enzima A; EST: esterasa; RA: reductasa. Las flechas marcadas en negrita indican las rutas más favorables, mientras que las flechas punteadas indican las rutas menos favorables. Adicionalmente, se indican las reacciones que ocurren en el colon (modificado de [64,65]).

c) Flavonoles

La ingesta de uno de los principales flavonoles (quercetina) usualmente asociado a un azúcar es de 6 a 18 mg/día, especialmente en personas que consumen lechuga, berries, tomate y manzanas, entre otros [67]. La absorción de flavonoles ocurre a nivel gástrico e intestinal. Sin embargo, no se conoce el mecanismo de la absorción gástrica [68]. Un estudio en humanos que consumieron alimento rico en quercetina-4´-O-glucósido y quercetina-3,4´-diglucósido, resalta la presencia en el sistema circulatorio de quercetina-3-O-sulfato, quercetina-3-O-glucurónido, isoramnetina-3-O-glucurónido, quercetina-O-diglucurónido y quercetina-O-glucurónido-O-sulfato dentro de los primeros 30 minutos luego de la ingesta [69], lo que indica una absorción en el intestino delgado y metabolización de la aglicona por SULTs, UGTs y COMTs de los enterocitos antes de entrar al sistema circulatorio. Sin embargo, al consumir un alimento alto en quercetina-3-O-rutinósido, se obtuvieron concentraciones de quercetina-3-O-glucurónido e isoramnetina-3-O-glucurónido de hasta 25 veces menos, junto con tiempos de concentración máxima en plasma de 5 horas, característico de una absorción en el colon [9,70]. Esto se confirmó con voluntarios con ileostomía, quienes no presentaban metabolitos en plasma u orina, y que al analizar su fluido ileal, se detectó un 86% de la quercetina-3-O-rutinósido ingerida. Finalmente, se respalda con lo reportado por Day y col., quienes concluyen que LPH no es capaz de eliminar el disacárido [46], y que por lo tanto, la eliminación del azúcar se realiza por la microbiota presente en el colon, los que también son capaces de metabolizar la quercetina, resultando principalmente en la producción de ácidos hidroxifenilacéticos, equivalentes al 22% del rutinósido consumido (Figura 1.7).

d) Flavan-3-oles y Procianidinas (PCs)

Ottaviani y col. investigaron la biodisponibilidad de enantiómeros de monómeros de flavan-3-oles. Para ello, hombres adultos consumieron la misma cantidad de (-)-epicatequina, (-)-catequina, (+)-epicatequina, y (+)-catequina en bebida de cacao. Basados en la concentración encontrada en plasma y en orina, la biodisponibildad de los estereoisomeros fue: (-)-epicatequina > (+)-epicatequina = (+)-catequina > (-)-catequina. También se encontraron diferencias en el metabolismo de catequina y epicatequina, reflejados en los niveles de sus metabolitos metilados. Adicionalmente, los niveles de metabolitos de (-) y (+) epicatequina en plasma y orina difieren, demostrando que la esteroquimica de los flavan-3-oles también afecta las rutas metabólicas. Este análisis se realizó con agliconas liberadas por un tratamiento de glucuronidasa/sulfatasa, por lo que no es posible detallar el impacto de los metabolitos sulfatados y glucuronidados [71].

En otro estudio con voluntarios sanos, que consumieron 500 mL de té conteniendo 648 µmol de flavan-3-oles (-)-epicatequina y (+)-catequina, epigalocatequina y derivados galoilados), se analizó el plasma y orina recolectado durante 24 horas [72]. El plasma contenía 12 metabolitos conjugados de (epi)catequina y (epi)galocatequina, junto con (-) epigalocatequina-3-O-galato y (-)-epicatequina-3-O-galato luego de 8 horas, lo que indica una absorción en el intestino grueso. Sin embargo, no se detectó (-)-epigalocatequina-3-O-galato en orina, lo que podría indicar la incapacidad del riñón para eliminar este compuesto del sistema circulatorio, proponiendo la eliminación a través de la bilis [73].

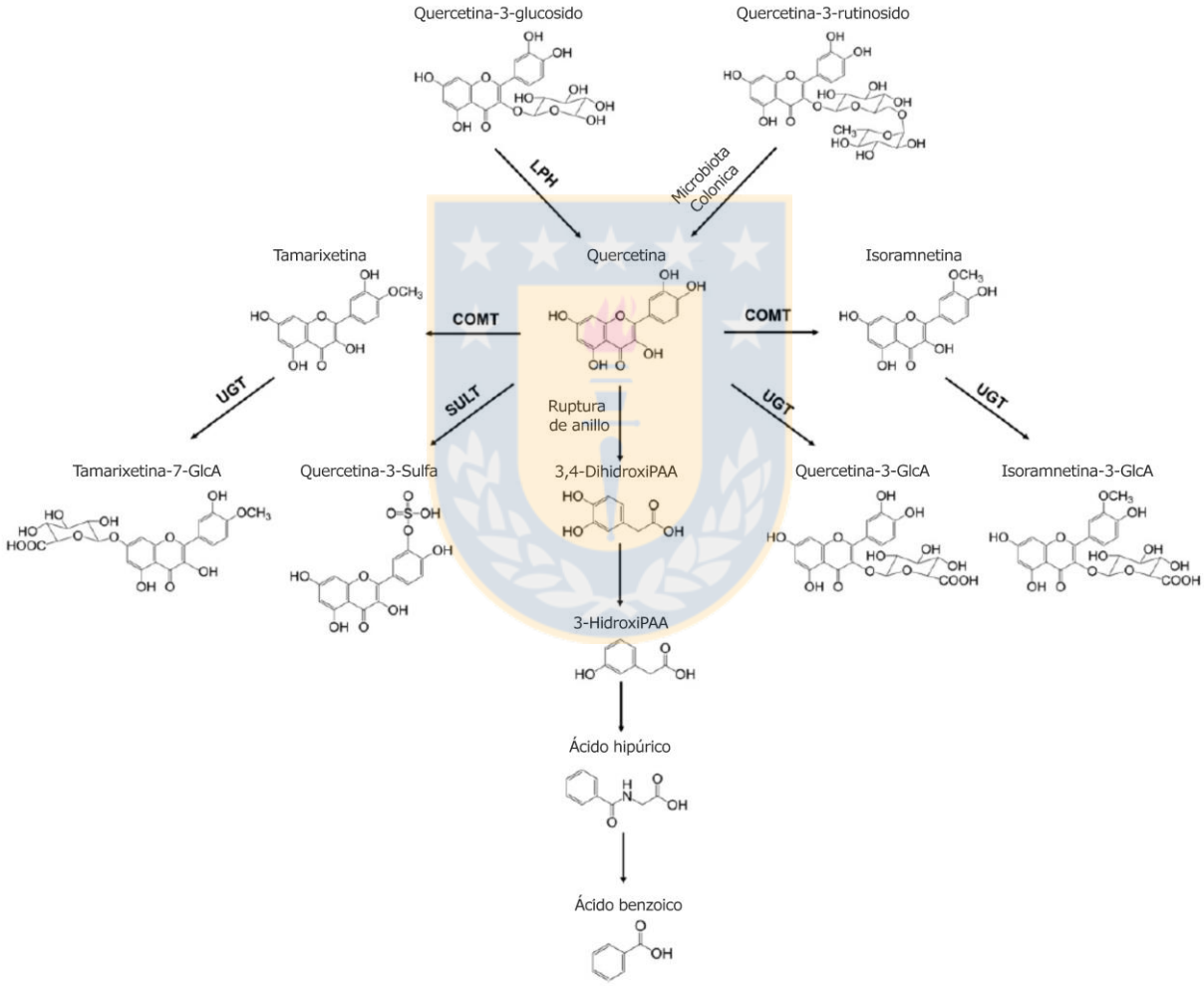

Figura 1.7: Ruta metabólica propuesta para el catabolismo in vitro de quercetina-3-O-rutinósido por bacterias fecales humanas, resultando en la producción de ácido 3,4-dihidroxifenilacético, ácido 3-hidroxifenilacético, junto con ácido benzoico y ácido hipúrico. LPH: lactasa phlorizin hidrolasa; COMT: catecol-O-metil transferasa; UGT: uridina-5´-difosfo-glucuronosil transferasa; SULT: sulfotransferasa (modificado de [67]).

Stalmach y col. estudiaron el mecanismo de metabolización en el intestino, incorporando 634 μmol de flavan-3-oles presentes en té verde a voluntarios con ileostomía [74]. La excreción urinaria fue de un 8% del consumo para metabolitos de (epi)galocatequina y de un 27.4% para los metabolitos de (epi)catequina, similar a lo observado en individuos sanos [72], confirmando que los monómeros pueden ser absorbidos en el intestino delgado. Sin embargo, se observó que un 69% de lo consumido fue recuperado en el fluido ileal, como mezcla de los compuestos encontrados en té y metabolitos. Por lo tanto, en voluntarios sanos, una alto proporción de los flavan-3-oles ingeridos se metabolizarían por la microbiota intestinal. Para lograr entender las reacciones y productos que se forman a este nivel, Roowi y col [75] incubaron en suspensiones fecales 50 μmol de (-)-epicatequina, (-)-epigalocatequina y (-)-epicatequina-3-O-galato, bajo condiciones anaeróbicas, estableciendo que hay compuestos que pueden ser originados por la metabolización de la microbiota intestinal. Adicionalmente, en la Figura 1.8 se muestra la propuesta de degradación de procianidina B1. Cabe considerar que algunos de estos metabolitos, como el ácido 4´-hidroxifenilacético y ácido hipúrico son detectados en orina de sujetos con ileostomía, indicando que son producidos en el cuerpo mediante otros mecanismos.

Información de la degradación de procianidinas obtenida a partir de modelos *in vitro*, indica que se obtienen monómeros de flavan-3-oles fácilmente absorbibles [76], los cuales son metabolizados por la microbiota intestinal, formando valerolactonas y posteriormente una oxidación progresiva, similar que lo propuesto para los monómeros (Figura 1.8). Sin embargo, estudios *in vivo* no concluyen lo mismo, sugiriendo que alrededor de un 10% de los dímeros son convertidos en monómeros [77,78].

e) Estilbenoides.

Estudios de biodisponibilidad en humanos indican una rápida absorción y metabolización de *trans*-resveratrol, aunque hay una baja excreción en orina y fecas. La absorción se realiza a nivel gástrico, lo que explica un pico de resveratrol a los 30 minutos luego de la ingesta [79,80]. Sin embargo, la concentración máxima encontrada es muy baja [81]. El consenso general indica que los metabolitos principales en plasma son el resveratrol-O-glucuronido, sulfato y disulfato. Adicionalmente, se encontraron en plasma y orina dos derivados de *trans*-resveratrol diglucuronidos en voluntarios que ingirieron 128 μmol de *trans*-piceidos [82].

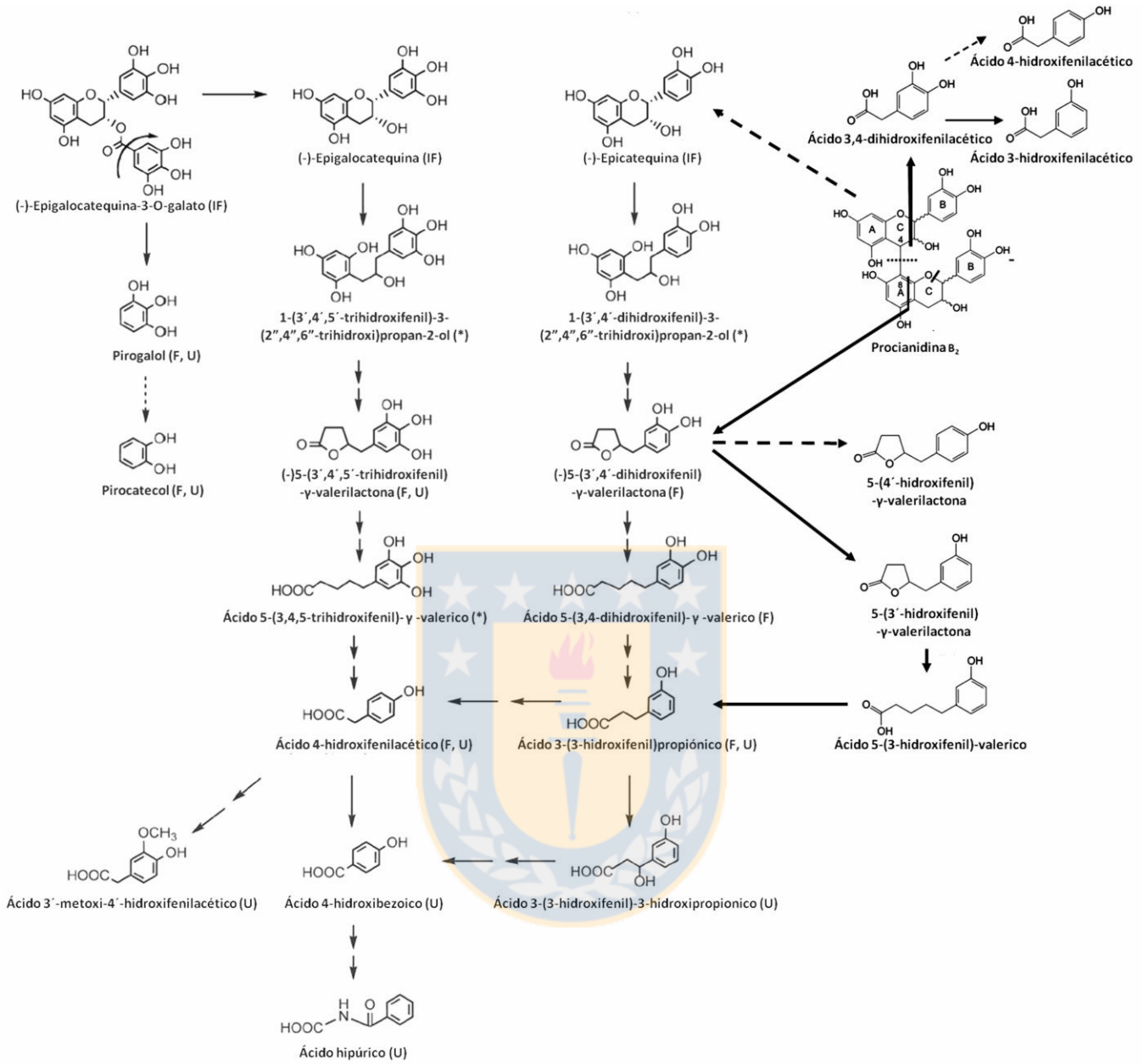

Figura 1.8: Ruta metabólica propuesta que involucra el metabolismo en el colon y excreción urinaria de flavan-3-oles. Las flechas punteadas indican una menor proporción de conversión, las flechas dobles indican conversiones donde los metabolitos no se acumulan y no son conocidos. (IF): compuestos detectados en fluido ileal; (F): compuestos detectados en suspensiones fecales; (U) compuestos detectados en orina; (*) probables compuestos detectados en suspensiones fecales que no se acumulan en cantidades detectables (modificado de [75,77,83]*).*

A partir de todos los estudios sobre metabolismo y biodisponibilidad discutidos en esta sección, se puede concluir que a pesar de que se detectan compuestos fenólicos, originalmente presentes en los alimentos consumidos, o a la forma de conjugados, la mayoría de los compuestos estudiados tienen una posterior metabolización, principalmente producida por los microorganismos presentes en el colon más que por reacciones redox de fase I [47]. Es por esto, que se ha reportado grand variabilid en este tipo de estudios [13], ya que la presencia de bacterias claves podría modificar la conversión de los compuestos fenólicos estudiados [15,84,85] . En general, se discute que los compuestos producto de la metabolización por microorganismos se encuentran en plasma y orina, con algunas modificaciones pequeñas [64,65]. A nivel plasmático, las concentraciones máximas de compuestos fenólicos encontrados se encuentran en el rango nM y es posible encontrarlas principalmente entre 3 tiempos característicos, debido a que ocurre: i) absorción a nivel gástrico ii) absorción a nivel de intestino delgado, y iii) absorción a nivel de intestino grueso (catabolitos).

i) Absorción a nivel gástrico: Los glucósidos de antocianos y flavonoles que se encuentran dentro de los primeros 30 minutos. Al igual que en ii) y iii), son transferidos a través del sistema portal al hígado, en donde pueden sufrir metabolización fase I y/o II, y (re)circular al intestino o al sistema circulatorio.

ii) Absorción a nivel de intestino delgado: Los glucósidos de antocianos se encuentran en plasma entre las 1.3 a 1.4 horas, mientras que los derivados de ácidos hidroxicinámicos glucosilados y sulfatados se detectan en plasma luego de 0.7 a 1 hora. En este caso, los compuestos mayoritarios son los HCA producto de la acción de esterasas, mientras que los sulfatos tienen un origen probable en el intestino delgado por la acción de SULTs. De forma similar, los glucósidos de flavonoles y sus posteriores derivados glucuronidados, sulfatados y metilados se encuentran en plasma luego de 30 minutos, lo que indica un origen probable en el intestino por acción de SULTs, COMTs y UGTs.

iii) Absorción a nivel de intestino grueso: los derivados de antocianos glucuronidados se encuentran en el plasma entre las 2.6 a 3.3 horas, mientras que los productos de flavonoles con azúcares no hidrolizables se detectan en plasma luego de 5 horas. Por otro lado, los derivados dihidrocafeico y dihidroferúlico se observan en plasma luego de 3.9 a 6.0 horas, mientras que en el caso de los flavan-3-oles junto a sus conjugados se encontraron en plasma luego de las 8 horas después de la ingesta. En todos los casos, sus derivados metilados, glucuronidados y sulfatados se originan probablemente gracias al metabolismo de fase II.

Los principales productos de la familia de los flavonoides encontrados en plasma son antocianinas y antocianidinas metiladas y glucoronidadas, flavonoles glucuronidados y sulfatados, derivados de ácido

benzoico y fenilacético, mientras que en orina y suspensiones fecales son derivados de ácido fenilacético, fenilpropiónico, benzoico, hipúrico y mandélico, los cuales también aparecen en plasma. Por otro lado, los productos de la familia HCAs encontrados en plasma son principalmente interconversiones debido a procesos redox, de hidrólisis y metilación/sulfatación/ glucuronidación, como por ejemplo ácido cafeico, ferúlico, isoferúlico, dihidroferulico, dihidrocafeico, dihidrocumárico, feruloilquínico, cafeoilquínico o feruloilglicina, junto a conjugados glucuronidados y sulfatados.

Herramientas utilizadas para el estudio de metabolización de polifenoles

Para asociar correctamente el consumo de polifenoles a un efecto en particular, es necesario identificar y cuantificar los compuestos presentes en el organismo en estudio. Para esto, las herramientas metabolómicas con un enfoque dirigido y no dirigido se consideran como el análisis preferido, ya que es posible su aplicación para un alto número de compuestos de forma simultánea. Adicionalmente, el efecto estudiado pretende conferirle una relevancia a los compuestos biodisponibles, de acuerdo a las concentraciones detectadas.

a) Herramientas metabolómicas

El metaboloma comprende cualquier molécula pequeña que se encuentre en el organismo (metabolitos), quien actúa como intermediario de reacciones bioquímicas para convertirse en compuestos de menor energía libre [86,87]. Estos metabolitos pueden ser estudiados en la célula o en el medio extracelular, dando origen a la definición de endometaboloma o exometaboloma, respectivamente [88]. Para lograr evaluar la complejidad del metaboloma, es posible usar un enfoque global, lo cual es logrado mediante la metabolómica, pudiendo identificar y cuantificar metabolitos [87]. Se han descrito dos tipos de enfoques metabolómicos, dirigido y no dirigido.

i) Metabolómica no dirigida: Este tipo de enfoque ha sido usado para evaluar simultáneamente la mayoría del metaboloma, o todos los compuestos en estudio, alcanzando la capacidad de explorar rutas metabólicas no descritas anteriormente [89] Mediante el uso de este enfoque, se ha logrado explicar, a nivel metabólico, celular o sistémico, respuesta a enfermedades, condiciones ambientales o perturbaciones genéticas [88]. El enfoque no dirigido se usa para generar hipótesis de trabajo, que posteriormente se desarrollaran cuantitativamente con un estudio dirigido [88,90].

Las plataformas analíticas propuestas para este tipo de estudios involucran principalmente técnicas cromatográficas acopladas a detectores de masa de alta resolución [91,92], resonancia magnética nuclear [93], espectroscopia infrarroja con transformada de Fourier [94] y detección con fila de fotodiodos UV-Vis [95],

los cuales están mayoritariamente enfocadas en el análisis de la "huella dactilar" del metaboloma y sus posibles cambios.

En el análisis metabolómico no dirigido, la optimización del procedimiento de pretratamiento de muestra y la eficiencia de ionización en un amplio rango de masas es fundamental, ya que determina el número e intensidad de las señales características analizadas [96], lo que está en estricta relación con la obtención de datos de calidad para un correcto procesamiento de datos[89].

En sistemas cromatográficos, los metabolitos son separados y analizados normalmente por espectrómetros de masa de alta resolución. Luego de la adquisición de datos, se detectan peaks que consideran la dimensión de tiempo de retención y masas (llamados "features"), se agrupan y los tiempos de retención se alinean (Figura 1.9).

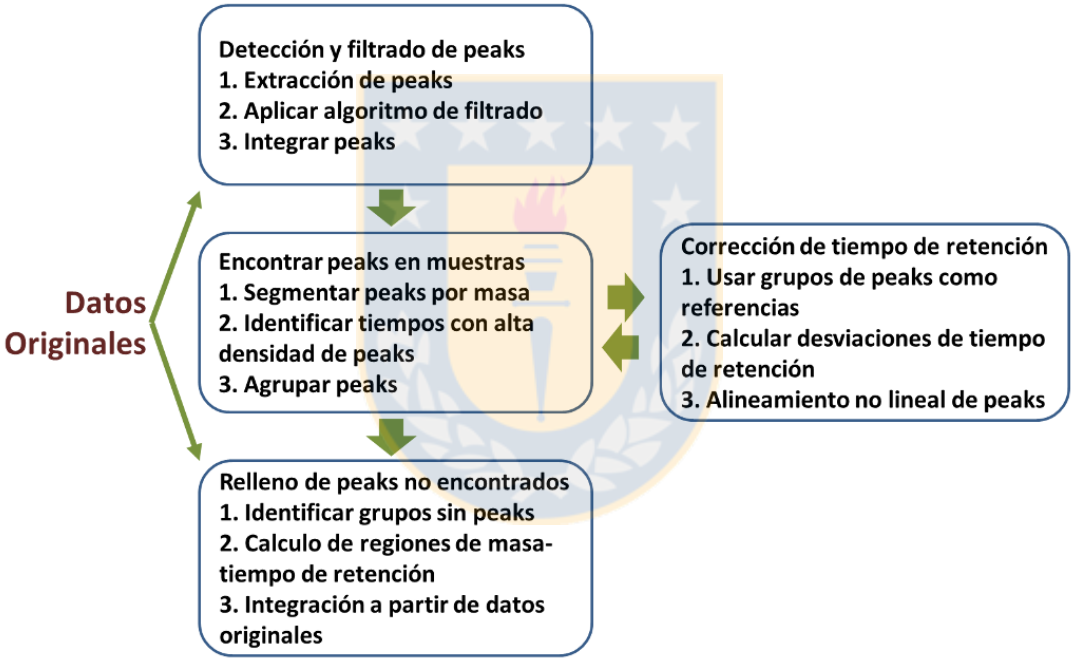

Figura 1.9: Procesamiento de datos en análisis metabolómicos no dirigidos (modificado de [97]).

El algoritmo de detección de peaks divide la dimensión de masas en pequeñas ventanas y logra identificar variaciones en la intensidad de cada sección de masas a lo largo del cromatograma. Normalmente las masas (modo centroide) se pueden ubicar indistintamente en diferentes secciones, por lo que se superponen e integran (Figura 1.10A). Posteriormente, los peaks se filtran con un algoritmo que nuevamente secciona la dimensión de masas (debido a que en espectrómetros de masas de alta resolución la precisión de las masas es mucho mayor a la del tiempo de retención) y se superponen las

secciones vecinas. Para el agrupamiento de peaks, se estiman márgenes dinámicos mediante histograma con suavizado gaussiano (Figura 1.10B) [97]. La gran desventaja de este modo de agrupamiento es que el filtro dependerá de la relación del ancho del suavizado con el ancho del peak cromatográfico, el cual puede variar a lo largo del cromatograma.

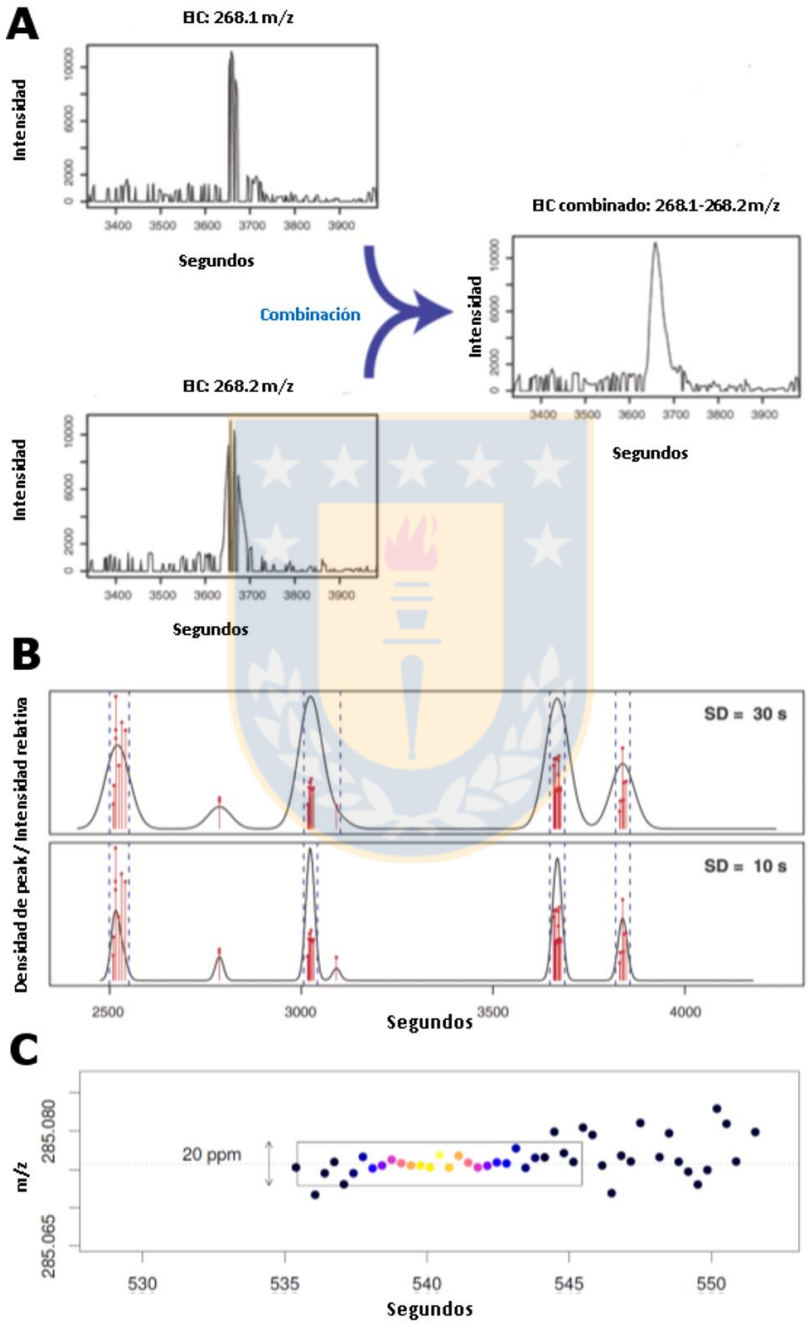

Figura 1.10: Descripción gráfica del procesamiento de datos LC-MS de alta resolución. A. Detección de peaks mediante algoritmo MEND; B. Filtrado y agrupamiento de señales mediante algoritmo MatchFilter; C. Filtrado y agrupamiento de señales mediante algoritmo CentWave (modificado de [97,98]).

Para solucionar este problema, Tautenhahn y col. elaboraron un algoritmo que identifica regiones de interés en datos de LC-MS (m/z vs tiempo de retención), el cual se basa en la mejora de la reproducibilidad de la masa adquirida en función de la intensidad de ésta, como se observa en la Figura 1.10C [98]. De esta forma, el agrupamiento de peaks es independiente de una función gaussiana de ancho definido, disminuyendo la aparición de falsos positivos o perdida de "features".

Finalmente, se comparan las señales de interés con bases de datos, con el fin de obtener identificaciones preliminares, que son confirmadas comparando los espectros de fragmentación y tiempos de retención de estándares[89]. El flujo de trabajo en metabolómica no dirigida se muestra en la Figura 1.11.

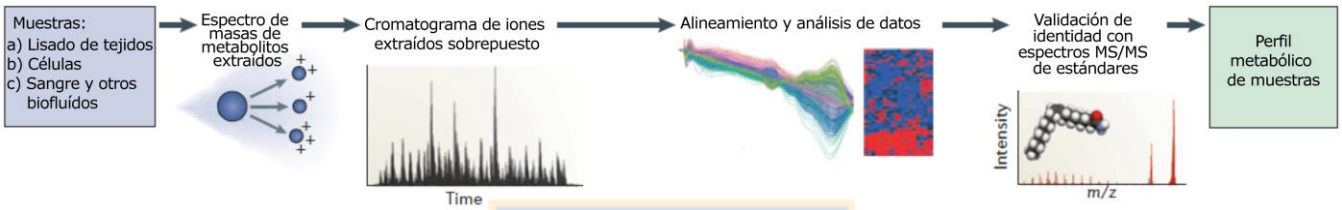

Figura 1.11: Flujo de trabajo en el enfoque metabolómico global. (modificado de [89]).

ii) Metabolomica dirigida: Este tipo de enfoque se ha descrito como una estrategia de "bottom-up" [88], debido a que su principal objetivo es el análisis de uno o un grupo de analitos asociados a una hipótesis. La herramienta más común utilizada para este tipo de enfoque es cromatografía asociada a espectrometría de masas, usando el modo de monitoreo de reacciones múltiples (MRM) [90].

La energía de colisión y la relación masa - carga de iones producto son pre optimizados para cada analito con el fin de obtener la mejor señal. El detector consiste en tres cuadrupolos ubicados en serie. El primer cuadrupolo selecciona el ion precursor o ion padre, el segundo cuadrupolo actúa como celda de colisión, en donde el ion precursor se fragmenta, y el tercer cuadrupolo aísla el ion producto o ion hijo adecuado. Cuando se analizan de esta forma múltiples metabolitos, este proceso es repetido para cada compuesto de manera cíclica. Debido a que cada escaneo de MRM toma un tiempo determinado (dwell time), cada analito es determinado intermitentemente. El número de puntos disponibles para formar el pico cromatográfico depende de la relación de la anchura del pico dividido por el tiempo que tarda un ciclo del conjunto de escaneos MRM programado [99]. Por ello, es necesario tener especial cuidado cuando se trabaja en sistemas de alta eficiencia. Debido a esto, este tipo de métodos provee una medición altamente sensible y robusta a un importante número de metabolitos biológicamente importantes, con un rendimiento alto. Además, los métodos que involucran espectrometría de masas con una configuración de triple cuadrupolo permiten realizar mediciones cuantitativas, por lo que es posible

realizar la cuantificación de metabolitos presentes en bajas concentraciones. El flujo de trabajo en metabolómica dirigida se muestra en la Figura 1.12 [89].

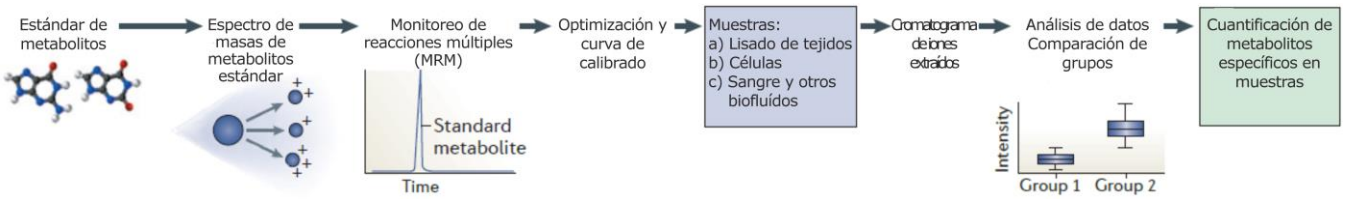

Figura 1.12: Flujo de trabajo en estudio metabolómico dirigido, usando detectores de masas de triple cuadrupolo (QqQ) (modificado de [89]).

iii) Metabolómica de compuestos fenólicos: Se han publicado una serie de estudios que evalúan el metabolismo de compuestos fenólicos mediante el enfoque metabolómico no dirigido, en donde se analizan orina, plasma y otros fluidos [100–104] . Grün y col analizaron ácidos fenólicos previamente desconjugados en plasma, orina y agua residual de heces de 24 voluntarios, a quienes se les administró una mezcla de extracto de vino tinto y jugo de uva roja rica en polifenoles. Mediante el análisis de los perfiles de orina obtenidos por GC-MS, se observó una diferencia en el metabolismo de los voluntarios intervenidos frente al control [105]. Llorach y col. determinaron, mediante cromatografía líquida acoplada a espectrometría de masas (LC-q-TOF), las modificaciones en el metaboloma de orina luego de 24 horas de administrado un extracto rico en compuestos fenólicos de piel de almendra. Se logró determinar la identificación putativa de 34 metabolitos asociados a la intervención, incluyendo conjugados de ácidos hidroxifenilvalérico, hidroxifenilpropiónico e hidroxifenilacético, luego del consumo de flavan-3-oles. Este estudio revela que el enfoque no dirigido puede proveer de nuevos marcadores de ingesta, contribuyendo al desarrollo del metaboloma de alimentos [106]. Por otro lado, Dunn y col. publicaron procedimientos para el análisis del perfil metabólico en suero y plasma usando cromatografía de gases y cromatografía liquida acoplada a espectrometría de masas de alta resolución [107].

El enfoque metabolómico dirigido se ha usado en una serie de publicaciones con el fin de analizar de forma cuantitativa polifenoles y sus metabolitos, que posiblemente se detecten luego de la administración de una dieta rica en compuestos fenólicos. Como es una herramienta que genera datos cuantitativos, puede ser usada para realizar estudios de biodisponibilidad y farmacocinética, usando principalmente cromatografía gaseosa [108] y cromatografía líquida [55,65,66,101,109,110].

Mediante el uso de este tipo de herramientas, se han realizado una serie de estudios en plasma, orina y otros fluidos. Vanzo y col. demostraron que la administración por vía intravenosa de cianidina-3-

glucósido, rápidamente desaparece del plasma, produciendo como metabolito principal peonidina-3-glucósido, el cual, luego de 1 minuto desaparece del plasma y alcanza una concentración máxima en hígado y riñones, siendo rápidamente excretado por la bilis y orina [111]. Gonzáles-Barrio y col. observaron el catabolismo colónico de elagitaninos, ácido elágico y antocianos de frambuesa *in vivo* e *in vitro* mediante un enfoque metabolómico dirigido, usando GC-MS y HPLC-DAD-MS/MS para el análisis cualitativo y cuantitativo. Con esto, se propuso rutas de conversión de conjugados de cianidina a ácidos fenólicos, luego de consumir 300 g de frambuesa roja [112].

El hecho de incorporar sistemas cromatográficos al análisis, puede disminuir su velocidad, pero ofrece dos beneficios. En primer lugar, metabolitos con masas idénticas pero con diferentes tiempos de retención pueden ser diferenciadas entre sí, y en segundo lugar, la separación de los analitos de interés de interferentes permite mejorar su cuantificación [113].

b) Herramientas para la medición de actividad antioxidante

El aumento de reacciones bioquímicas normales, exposición al ambiente y xenobióticos consumidos desde la dieta resulta en el aumento del estrés oxidativo mediante la generación de especies reactivas del oxígeno y nitrógeno (ROS y RNS) [114]. Los antioxidantes son moléculas que detienen la producción de radicales por reacciones en cadena, o puede incluso inhibir la formación de estas especies reactivas y pueden ser clasificados como enzimáticos o no enzimáticos. Dentro de los antioxidantes enzimáticos, se encuentran los antioxidantes endógenos, como la superóxido dismutasa (SOD), catalasa (CAT), glutatión peroxidasa (GSHPX) y glutatión reductasa (GR). Dentro de los antioxidantes no enzimáticos, se encuentra los antioxidantes endógenos como la albúmina, ácido úrico, glutatión (GSH) y externos como vitamina C, E, ácido lipólico y polifenoles derivados del consumo de frutas y hortalizas, como los flavonoides [115]. Estos últimos presentan otro tipo de actividad antioxidante, como actividad quelante de metales, activación de enzimas antioxidantes, inhibición de oxidasas, entre otras [116] Además de proteger del daño oxidativo, se les ha atribuido la participación en la modulación de procesos de proliferación, diferenciación, angiogénesis, apoptosis, inflamación, adhesión celular y hormonas, entre otros [5,114,115,117–119]. Existe evidencia clínica y epidemiológica asociada a los efectos preventivos de enfermedades cardiovasculares, neurodegenerativas y proliferativas con el alto contenido de compuestos fenólicos, vitamina C, E y carotenoides en los alimentos consumidos [120–123].

El estudio del contenido de antioxidantes en alimentos y en el organismo, junto a la capacidad que tienen en la prevención de enfermedades, debido a la disminución de la actividad de radicales libre, se ha convertido en un tema de gran interés. Para el estudio apropiado de estos efectos se han desarrollado

una serie de métodos bajo diferentes condiciones, pero lamentablemente en muchos de ellos hay una falta de correlación entre la concentración de compuestos fenólicos y la actividad antioxidante. Este comportamiento se debe a que existen distintos mecanismos involucrados en el estrés oxidativo, y por lo tanto, no hay un único método para medir capacidad antioxidante precisa, exacta y que sea universal [124]. Sin embargo, existen bases de datos que contienen una serie de valores de capacidad antioxidante en alimentos usando ensayos ORAC [32].

La actividad antioxidante medida por un método refleja sólo la reactividad química bajo las condiciones aplicadas en el ensayo, lo cual es inapropiado si se generaliza como "actividad antioxidante". Por lo tanto, el uso de términos como "capacidad de depuración de radical", "capacidad de depuración de superóxido", "capacidad de reducción de ion férrico" e incluso "capacidad reductora total" detalla de mejor forma la característica que se desea evaluar.

Bajo el punto de vista de las reacciones químicas involucradas, el alto número de ensayos de capacidad antioxidante se pueden dividir en 2 categorías:

1. Ensayos basados en la reacción de transferencia de un átomo de hidrogeno (HAT).
2. Ensayos basados en la reacción de transferencia de un electrón (ET)

Ambos tipos de métodos tienen como finalidad medir la capacidad de depuración del radical y no la capacidad antioxidante preventiva. Los ensayos ET involucran una reacción redox con el oxidante, quien es la sonda utilizada para monitorear la reacción (Ec 1).

Los ensayos HAT, en cambio, monitorean la cinética de reacción por competencia, ya que generalmente se componen por un generador radical sintético, una sonda oxidable y la molécula antioxidante que se quiere evaluar (Ec 2) [114].

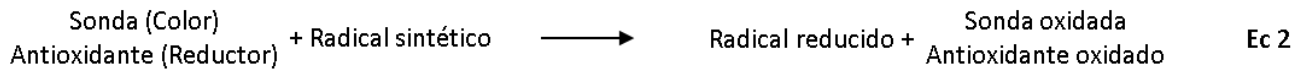

La Tabla 1.2 muestra algunos ensayos que involucran tanto métodos HAT como métodos ET. Estos métodos se consideran, en la mayoría de los casos, como métodos para medir capacidad antioxidante *in vitro*.

La capacidad antioxidante *in vivo* es determinada por una serie de factores. En primer lugar, se encuentra la biodisponibilidad. Los antioxidantes deben ser absorbidos, transportados, distribuidos y retenidos apropiadamente en fluidos biológicos, células y tejidos. Debido a esto, la capacidad observada de algunos antioxidantes es muy diferente *in vivo* que *in vitro*.

A pesar de que es posible evaluar la capacidad antioxidante con métodos *in vitro*, usando ensayos HAT y ET como ORAC y CUPRAC [125–128], es posible usar biomarcadores para evaluar el grado de estrés oxidativo que se presenta bajo las condiciones de trabajo [129].

Para el estudio de capacidad antioxidante es necesario, en primer lugar, elaborar una batería de métodos que determinen distintas propiedades de la capacidad antioxidante total, con la finalidad de englobar todas las características que la propiedad antioxidante estudiada pudiese presentar. Para esto es necesario tener en consideración las condiciones bajo las cuales se trabajará, cuál es la información que entrega el método a utilizar y, por consiguiente, las propiedades de las matrices en las cuales se aplicarán los métodos desarrollados.

Tabla 1.2: *Ensayos de capacidad antioxidante in vitro (Modificado de [114,115]).*

Ensayos que involucran reacciones de transferencia de átomos de hidrogeno (HAT) $ROO^* + AH \rightarrow ROOH + A^*$ $ROO^* + LH \rightarrow ROOH + L^*$	ORAC (Oxygen Radical Absorbance Capacity) TRAP (Total Radical Trapping Antioxidant Parameter) Ensayo de blanqueamiento de crocina IOU (Inhibited Oxygen Uptake) Inhibición de la oxidación de ácido linoleico Inhibición de la oxidación de LDL Peroxidación de fosfolípidos *in vitro*
Ensayos que involucran reacciones de transferencia de electrones (ET) $M^n + e\ (de\ AH) \rightarrow AH^{*+} + M^{n-1}$	ABTS (2,2´-azino-bis(3-ethylbenzthiazoline-6-sulphonic acid) FRAP (Ferric Ion Reducing Antioxidant Parameter) CUPRAC (Cupric ion Reducion Antioxidant Capacity) DPPH (Diphenyl-1-Pycrilhydrazil) Reactivo Folin-Ciocalteu Depuración de anión superóxido TBARS (thiobarbiturate reactive substances)

Donde ROO^*= Radical; AH= Antioxidante; ROOH=Radical estable; A^*=Antioxidante radical; LH= Lípido reducido; L^*=Lípido radical; M^n= Metal oxidado; M^{n-1}=Metal reducido, e=electrones transferidos; AH^{*+}= Antioxidante radical oxidado.

De acuerdo a esto, el objetivo principal es evaluar mediante ensayos químicos, la capacidad reductora y protectora de los compuestos fenólicos en estudio:

i) Medición de la capacidad reductora:

Ensayo $TEAC_{ABTS}$: Dentro de los métodos a utilizar para la medición de la capacidad reductora, ABTS tiene la ventaja de ser simple, rápido, soporta un amplio rango de pH y los antocianos no interfieren la medida fotométrica. El radical ABTS•+ es soluble tanto en solventes acuosos u orgánicos y no se ve afectado por cambios en la fuerza iónica [130].

Ensayo $TEAC_{CUPRAC}$: CUPRAC es lo suficientemente rápido para oxidar antioxidantes que contienen grupos tioles de forma selectiva, debido a que tiene un potencial redox más bajo que otros métodos utilizados (0.6 V). Es más estable, es robusto, tiene un amplio rango lineal (a diferencia de ABTS). La reacción redox se efectúa a pH 7 y el Cu(I) que se produce por la reacción CUPRAC se encuentra quelado, y, por lo tanto, no puede participar como pro-oxidante en la generación de reacciones tipo Fenton [131]. Se ha descrito el uso de este método en la medición de capacidad reductora de polifenoles, vitamina C y E de origen dietético [131,132] y su posterior modificación para la medición de la capacidad reductora en suero total, incluyendo actividad antioxidante de proteínas. La modificación consiste básicamente en el cambio del buffer acetato de amonio (que causa precipitación de proteínas del suero) por buffer urea a pH 7 [127].

ii) Medición de la capacidad depuradora de oxidantes:

Ensayo de competencia ORAC: El ensayo ORAC consiste en la competencia del consumo de radical entre el antioxidante y una sonda fluorescente o coloreada. El consumo de la sonda disminuye la intensidad de emisión (o absorbancia), disminuyendo finalmente el área bajo la curva. Las sondas más utilizadas han sido la fluoresceína (FL) [125], y en algunas aplicaciones el rojo pirogalol (PGR). El uso de PGR tiene ciertas ventajas frente al uso de FL, como el hecho que su reactividad sea mayor para los compuestos evaluados, no posee tiempos de inducción, salvo para vitamina C, por lo que adicionalmente se puede determinar la concentración de este en presencia de antioxidantes totales [126].

Debido a que el efecto ocurre probablemente a nivel plasmático, no es suficiente establecer la capacidad antioxidante del extracto de fruto, sino que es necesario complementarlo con la información obtenida del plasma, ya que es ahí donde se encuentran los metabolitos producto de los microorganismos colónicos, junto con la posterior metabolización realizada por células intestinales y hepáticas.

Hipótesis

"El efecto biológico asociado a la ingesta aguda de bayas en animales de experimentación, puede ser evaluado complementando metabolómica dirigida y no dirigida, con ensayos antioxidantes clásicos".

Objetivo

Desarrollar una plataforma analítica para metabolómica de compuestos fenólicos mediante GC-MS/MS junto con UPLC-ESI-TOF y determinar el efecto biológico de estos metabolitos asociado a capacidad antioxidante en plasma de animales de experimentación.

Objetivo Específico 1: Caracterizar y cuantificar los compuestos fenólicos en uva Pink Globe (*Vitis vinífera L.),* una variante somaclonal de Red Globe, con el objetivo de contrastar el contenido de polifenoles con calafate (*Berberis microphylla*).

Objetivo Específico 2: Implementar, validar y aplicar herramientas metabolómicas dirigidas y no dirigidas para el análisis de compuestos fenólicos y sus metabolitos en plasma de animales de experimentación, mediante el uso de técnicas cromatográficas UPLC-ESI-TOF y GC-MS/MS.

Objetivo Específico 3: Evaluar el efecto a nivel plasmático asociado al consumo agudo de un extracto de bayas rico en polifenoles en animales de experimentación, mediante una plataforma metabolómica contrastada con ensayos de capacidad antioxidante.

Estrategia Analítica

De acuerdo a los objetivos planteados, la estrategia analítica se puede dividir en 4 etapas (Figura 1.13).

Selección de la materia prima: con el fin de realizar los ensayos de ingesta aguda en animales de experimentación, se escogerá el material que aportará los compuestos fenólicos a partir de su concentración por gramo de fruto, tipos de polifenoles, disponibilidad y novedad científica. Específicamente, se trabajará con uva Pink Globe (*Vitis vinífera L.*) y calafate (*Berberis microphylla*).

Implementación de plataforma metabolómica: Se establecerá una plataforma metabolómica para el estudio de compuestos parentales y metabolitos en plasma luego del consumo de compuestos fenólicos por animales de experimentación. Se utilizará UPLC-ESI-TOF como plataforma metabolómica no dirigida y deconjugación-derivatización-GC-MS/MS como plataforma metabolómica dirigida.

Implementación de ensayos antioxidantes miniaturizados: Se implementará una batería de ensayos antioxidantes para evaluar la capacidad antioxidante en bayas y plasma. Para el material vegetal y plasma se establecerán tres métodos de ensayo complementarios; CUPRAC, índice Folin-Ciocalteu (ó fenoles totales) y ORAC-Fluoresceína. Cabe destacar que para el análisis de plasma de animales se utilizará una variante del método CUPRAC en la cual es posible evaluar proteínas plasmáticas.

Ensayo de ingesta aguda en animales de experimentación: se evaluará la cinética de compuestos fenólicos y metabolitos en plasma de gerbos mediante un enfoque semicuantitativo de metabolómica no dirigida mediante UPLC-ESI-ToF y cuantitativo de metabolómica dirigida mediante GC-MS/MS. Los ensayos cinéticos de metabolitos encontrados en plasma se contrastarán con su capacidad antioxidante.

Se cuenta con tres alternativas de bayas como material de estudio. Pink Globe (*Vitis vinífera L.*), una variante somaclonal de Red Globe recientemente descrita, es una baya levemente pigmentada con características organolépticas deseables de la cual no se encuentran reportes de sus niveles de compuestos fenólicos. Por otro lado, el calafate (*Berberis microphylla*) es una baya ampliamente distribuida en la Patagonia chileno-argentina que presenta un muy alto contenido de compuestos fenólicos, entre los que destacan antocianos y en menor proporción flavonoles y ácidos hidroxicinámicos.

Luego de la caracterización de las bayas, se contrastará la concentración de moléculas bioactivas con la capacidad antioxidante, con el fin de generar información sobre la selección del material de estudio. Es por esto que se apuntará al desarrollo de nuevas plataformas analíticas rápidas, selectivas y capaces de cubrir un amplio rango de compuestos fenólicos, para identificar y cuantificar a nivel de nM. Se evaluará la producción de un extracto comestible usando un solvente de extracción no tóxico. Se

realizarán estudios de consumo agudo de extracto de la baya de interés en gerbos, a los cuales se les extraerá sangre a tiempo 0, 1, 2, 4, 8 y 12 horas luego de administrado alrededor de 300 mg/kg de extracto rico en polifenoles vía gavaje (sonda gástrica).

Figura 1.13: Estrategia analítica propuesta.

Bajo este contexto, los cambios en el metaboloma del plasma serán evidenciados mediante el análisis por UPLC-ESI-TOF, empleando un enfoque metabolómico no dirigido para evaluar diferencias globales entre ensayos con y sin tratamiento. Por otro lado, para el estudio cuantitativo de un grupo de compuestos fenólicos y metabolitos de interés, estos pueden ser derivatizados a formas menos polares, con lo que es posible el uso de un enfoque metabolómico dirigido basado en MRM usando GC-EI-MS/MS (Figura 1.14). Con el fin de evaluar el efecto biológico a nivel plasmático de los compuestos fenólicos y sus metabolitos, se contrastará la información cualitativa y cuantitativa con los ensayos de medición de capacidad antioxidante, en términos de capacidad reductora y capacidad protectora, mediante el uso de ensayos CUPRAC y ABTS, o ensayos ORAC, respectivamente (Figura 1.15).

La Figura 1.14 muestra cómo abordar, mediante enfoques metabolómicos, el estudio propuesto, mientras que la Figura 1.15 propone la forma de estudio de la actividad antioxidante en términos de capacidad reductora y protectora.

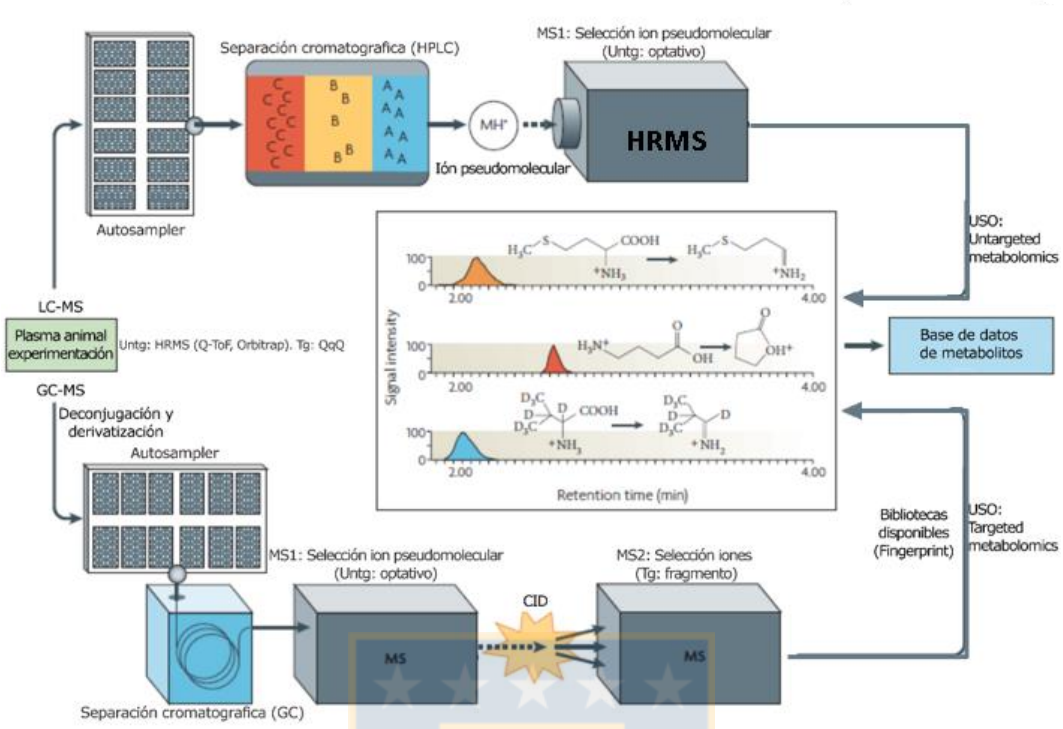

Figura 1.14: Estrategia analítica propuesta para el análisis de compuestos fenólicos y sus metabolitos en bayas y líquidos biológicos, tanto para su caracterización, como para su cuantificación (Modificado de [113]).

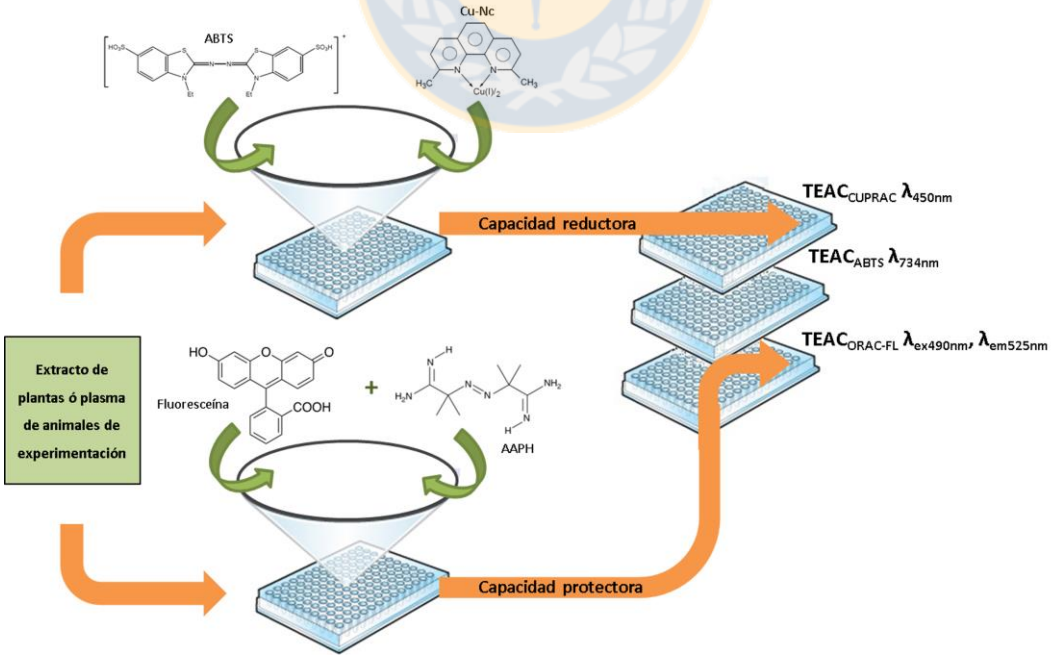

Figura 1.15: Estrategia analítica propuesta para el análisis de capacidad antioxidante de compuestos presentes en frutos y líquidos biológicos.

Referencias

(1) Aluko, R. E. Functional Foods and Nutraceuticals; Heldman, D. R., Ed.; Springer: New York, NY, USA, 2012.

(2) Juurlink, B. H. J.; Azouz, H. J.; Aldalati, A. M. Z.; AlTinawi, B. M. H.; Ganguly, P. Hydroxybenzoic acid isomers and the cardiovascular system. *Nutr. J.* **2014**, *13*, 63.

(3) Folmer, F.; Basavaraju, U.; Jaspars, M.; Hold, G.; El-Omar, E.; Dicato, M.; Diederich, M. Anticancer effects of bioactive berry compounds. *Phytochem. Rev.* **2013**, *13*, 295–322.

(4) Williamson, G. Possible effects of dietary polyphenols on sugar absorption and digestion. *Mol. Nutr. Food Res.* **2013**, *57*, 48–57.

(5) Del Rio, D.; Rodriguez-Mateos, A.; Spencer, J. P. E.; Tognolini, M.; Borges, G.; Crozier, A. Dietary (poly)phenolics in human health: structures, bioavailability, and evidence of protective effects against chronic diseases. *Antioxid. Redox Signal.* **2013**, *18*, 1818–1892.

(6) Bolca, S.; Van De Wiele, T.; Possemiers, S. Gut metabotypes govern health effects of dietary polyphenols. *Curr. Opin. Biotechnol.* **2013**, *24*, 220–225.

(7) van Dorsten, F. A.; Gr un, C. H.; J van Velzen, E. J.; Jacobs, D. M.; Draijer, R.; M van Duynhoven, J. P. The metabolic fate of red wine and grape juice polyphenols in humans assessed by metabolomics. *Mol. Nutr. Food Res.* **2010**, *54*, 897–908.

(8) Kemperman, R. A.; Bolca, S.; Roger, L. C.; Vaughan, E. E. Mini-Review Novel approaches for analysing gut microbes and dietary polyphenols: challenges and opportunities. *Microbiology.* **2010**, *156*, 3224–3231.

(9) Jaganath, I. B.; Mullen, W.; Edwards, C. A.; Crozier, A. The relative contribution of the small and large intestine to the absorption and metabolism of rutin in man. *Free Radic. Res.* **2006**, *40*, 1035–1046.

(10) Kahle, K.; Kraus, M.; Scheppach, W.; Richling, E. Colonic availability of apple polyphenols - A study in ileostomy subjects. *Mol. Nutr. Food Res.* **2005**, *49*, 1143–1150.

(11) Kahle, K.; Kraus, M.; Scheppach, W.; Ackermann, M.; Ridder, F.; Richling, E. Studies on apple and blueberry fruit constituents: Do the polyphenols reach the colon after ingestion? *Mol. Nutr. Food Res.* **2006**, *50*, 418–423.

(12) Marks, D.; Mullen, W.; Borges, G.; Crozier, A. Absorption, metabolism, and excretion of cider dihydrochalcones in healthy humans and subjects with an ileostomy. *J. Agric. Food Chem.* **2009**, *57*, 2009–2015.

(13) Gross, G.; Jacobs, D. M.; Peters, S.; Possemiers, S.; Duynhoven, J. Van; Vaughan, E. E.; De Wiele, T. *In vitro* bioconversion of polyphenols from black tea and red wine/grape juice by human intestinal microbiota displays strong interindividual variability. *J. Agric. Food Chem.* **2010**, *58*, 10236–10246.

(14) Clavel, T.; Borrmann, D.; Braune, A.; Doré, J.; Blaut, M. Occurrence and activity of human intestinal bacteria involved in the conversion of dietary lignans. *Anaerobe.* **2006**, *12*, 140–147.

(15) Boto-Ordonez, M.; Urpi-Sarda, M.; Queipo-Ortuno, M. I.; Tulipani, S.; Tinahones, F. J.; Andres-Lacuevea, C. High levels of *Bifidobacteria* are associated with increased levels of anthocyanin microbial metabolites: a randomized clinical trial. *Food Funct.* **2014**, *5*, 1932–1938.

(16) Crozier, A.; Jaganath, I. B.; Clifford, M. N. Dietary phenolics: chemistry, bioavailability and effects on health. *Nat. Prod. Rep.* **2009**, *26*, 1001–1043.

(17) Clifford, M. N. Anthocyanins — nature, occurrence and dietary burden. *J. Sci. Food Agric.* **2000**, *80*, 1063–1072.

(18) Häkkinen, S. H.; Kärenlampi, S. O.; Heinonen, I. M.; Mykkänen, H. M.; Törrönen, A. R. Content of the flavonols quercetin, myricetin, and kaempferol in 25 edible berries. *J. Agric. Food Chem.* **1999**, *47*, 2274–2279.

(19) Fine, A. Oligomeric proanthocyanidin complexes: history, structure, and phytopharmaceutical applications. *Altern. Med. Rev.* **2000**, *5*, 144–151.

(20) Moze, S.; Polak, T.; Gasperlin, L.; Koron, D.; Vanzo, A.; Ulrich, N.; Abram, V. Phenolics in Slovenian bilberries (*Vaccinium myrtillus L.*) and blueberries (*Vaccinium corymbosum L.*). *J. Agric. food Chem.* **2011**, *59*, 6998–7004.

(21) Paredes-López, O.; Cervantes-Ceja, M. L.; Vigna-Pérez, M.; Hernández-Pérez, T. Berries: Improving human health and healthy aging, and promoting quality life—A Review. *Plant Foods Hum. Nutr.* **2010**, *65*, 299–308.

(22) Pandino, G.; Lombardo, S.; Mauromicale, G.; Williamson, G. Phenolic acids and flavonoids in leaf and floral stem of cultivated and wild *Cynara cardunculus L*. genotypes. *Food Chem.* **2011**, *126*, 417–422.

(23) Ruiz, A.; Mardones, C.; Vergara, C.; Von Baer, D.; Gómez-Alonso, S.; Gómez, M. V.; Hermosín-Gutiérrez, I. Isolation and structural elucidation of anthocyanidin 3,7-β-O- diglucosides and caffeoyl-glucaric acids from calafate berries. *J. Agric. Food Chem.* **2014**, *62*, 6918–6925.

(24) Marticorena, C.; Rodríguez, R. Flora de Chile vol. 2: *Berberidaceae-Betulaceae*; 2003.

(25) Cantos, E.; Espin, J.; Tomas-Barberan, F. Varietal differences among the polyphenol profiles of seven table grape cultivars studied by LC-DAD-MS-MS. *J. Agric. Food Chem.* **2002**, *50*, 5691–5696.

(26) Lutz, M.; Jorquera, K.; Cancino, B.; Ruby, R.; Henriquez, C. Phenolics and antioxidant capacity of table grape (*Vitis vinifera L.*) cultivars grown in chile. *J. Food Sci.* **2011**, *76*, 1088–1093.

(27) Organisation Internationale de la Vigne et du Vin. Description of world vine varieties; Paris, 2009.

(28) Zoffoli, J.; Latorre, B. Chapter 9: Table grape (*Vitis vinifera L.*). In Postharvest biology and technology of tropical and subtropical fruits. Volume: 3.; Yahia, E., Ed.; Woodhead Publishing Limited: Cambridge, 2011; pp 179–207.

(29) Pink Globe, la nueva variedad de uva de mesa chilena que irá a la conquista de China http://www.portalfruticola.com/noticias/2011/12/26/pink-globe-la-nueva-variedad-de-uva-de-mesa-chilena-que-ira-a-la-conquista-de-china/?pais=chile (accessed May 22, 2016).

(30) Ruiz, A.; Hermosín-Gutiérrez, I.; Mardones, C.; Vergara, C.; Herlitz, E.; Vega, M.; Dorau, C.; Winterhalter, P.; Von Baer, D. Polyphenols and antioxidant activity of calafate (*Berberis microphylla*) fruits and other native berries from southern Chile. *J. Agric. Food Chem.* **2010**, *58*, 6081–6089.

(31) Mardones, C. Informe final proyecto Fondecyt 1100944 "Secundary metabolite profiles and genetic study of *Berberis* from Chilean Patagonia with emphasis on phenolic phytochemicals in berries"*;* 2013.

(32) Speisky, H.; López Alarcón, C.; Gómez, M.; Fuentes, J.; Sandoval Acuña, C. First web-based database on total phenolics and Oxygen Radical Absorbance Capacity (ORAC) of fruits produced and consumed within the South Andes Region of South America. *J. Agric. Food Chem.* **2012**, *60*, 8851–8859.

(33) Ruiz, A.; Hermosín-Gutiérrez, I.; Vergara, C.; von Baer, D.; Zapata, M.; Hitschfelda, A.; Obando, L.; Mardones, C. Anthocyanin profiles in south Patagonian wild berries by HPLC-DAD-ESI-MS/MS. *Food Res. Int.* **2013**, *51*, 706–713.

(34) Ruiz, A.; von Baer, D.; Vergara, C.; Hitschfeld, M. A.; Ortega, N.; Hermosín-Gutiérrez, I.; Mardones, C. HPLC-DAD-MS/MS of anthocyanins in native berries from chilean patagonia. In *COLACRO XIV*; 2012; p 315.

(35) Carreno, J.; Almela, L.; Martinez, A.; Fernández-López, J. A. Chemotaxonomical classification of red table grapes based on anthocyanin profile and external colour. *Food Sci. Technol.* **1997**, *30*, 259–265.

(36) Zapata, M. HPLC de flavonoles en frutos nativos chilenos del género *Berberis* utilizando columna convencional, núcleo sólido y UHPLC para su identificación y cuantificación, Universidad de Concepción, 2013.

(37) Ruiz, A.; Zapata, M.; Sabando, C.; Bustamante, L.; Von Baer, D.; Vergara, C.; Mardones, C. Flavonols, alkaloids, and antioxidant capacity of edible wild *Berberis* species from patagonia. *J. Agric. Food Chem.* **2014**, *62*, 12407–12417.

(38) Elliger, C. A.; Lundin, R. E.; Haddon, W. F. Caffeyl esters of glucaric acid in *Lycopersicon esculentum* leaves. *Phytochemistry.* **1981**, *20*, 1133–1134.

(39) Nagels, L.; van Dongen, W.; Parmentier, F. Cestric acid, a caffeic acid ester from *Cestrum euanthes*. *Phytochemistry.* **1982**, *21*, 743–746.

(40) Risch, B.; Herrmann, K.; Wray, V. (E)-O-p-Coumaroyl-, (E)-O-feruloyl-derivatives of glucaric acid in citrus. *Phytochemistry.* **1988**, *27*, 3327–3329.

(41) Ruiz, A.; Mardones, C.; Vergara, C.; Hermosín-Gutiérrez, I.; von Baer, D.; Hinrichsen, P.; Rodriguez, R.; Arribillaga, D.; Dominguez, E. Analysis of hydroxycinnamic acids derivatives in calafate (*Berberis microphylla* G. Forst) berries by liquid chromatography with photodiode array and mass spectrometry detection. *J. Chromatogr. A* **2013**, *1281*, 38–45.

(42) Lila, M. A.; Burton-Freeman, B.; Grace, M.; Kalt, W. Unraveling anthocyanin bioavailability for human health. *Annu. Rev. Food Sci. Technol.* **2016**, *7*, 375–393.

(43) Fernandes, I.; Faria, A.; Calhau, C.; de Freitas, V.; Mateus, N. Bioavailability of anthocyanins and derivatives. *J. Funct. Foods.* **2014**, *7*, 54–66.

(44) Passamonti, S.; Vrhovsek, U.; Vanzo, A.; Mattivi, F. The stomach as a site for anthocyanins absorption from food. *FEBS Lett.* **2003**, *544*, 210–213.

(45) Manach, C.; Scalbert, A.; Morand, C.; Remesy, C.; Jimenez, L. Polyphenols: Food sources and bioavailability. *Am. J. Clin. Nutr.* **2004**, *79*, 727–747.

(46) Day, A. J.; Cañada, F. J.; Díaz, J. C.; Kroon, P. A.; McLauchlan, R.; Faulds, C. B.; Plumb, G. W.; Morgan, M. R. A.; Williamson, G. Dietary flavonoid and isoflavone glycosides are hydrolysed by the lactase site of lactase phlorizin hydrolase. *FEBS Lett.* **2000**, *468*, 166–170.

(47) Lampe, J. W. Interindividual differences in response to plant-based diets : implications for cancer risk. *Am. J. Clin. Nutr.* **2009**, *89*, 1553–1557.

(48) Breinholt, V. M.; Offord, E. A.; Brouwer, C.; Nielsen, S. E.; Brøsen, K.; Friedberg, T. In vitro investigation of cytochrome P450-mediated metabolism of dietary flavonoids. *Food Chem. Toxicol.* **2002**, *40*, 609–616.

(49) Del Rio, D.; Borges, G.; Crozier, A. Berry flavonoids and phenolics: bioavailability and evidence of protective effects. *Br. J. Nutr.* **2010**, *104 Suppl*, S67–S90.

(50) Olivas-Aguirre, F. J.; Rodrigo-García, J.; Martínez-Ruiz, N. D. R.; Cárdenas-Robles, A. I.; Mendoza-Díaz, S. O.; Álvarez-Parrilla, E.; González-Aguilar, G. A.; De La Rosa, L. A.; Ramos-Jiménez, A.; Wall-Medrano, A. Cyanidin-3-O-glucoside: Physical-chemistry, foodomics and health effects. *Molecules* **2016**, *21*, 1–30.

(51) Kamonpatana, K.; Giusti, M.; Chureeporn, C.; MorenoCruz, M.; Riedl, K.; Kumar, P.; Failla, M. Susceptibility of anthocyanins to *ex vivo* degradation in human saliva. *Food Chem* **2012**, *135*, 738–747.

(52) Mallery, S.; Budendorf, D.; Larsen, M.; Pei, P.; Tong, M.; Holpuch, A.; Larsen, P.; Stoner, G.; Fields, H.; Chan, K.; et al. Effects of human oral mucosal tissue, saliva and oral microflora on intraoral metabolism and bioactivation of black raspberry anthocyanins. *Cancer Prev. Res.* **2011**, *4*, 1209–1221.

(53) Fang, J. Bioavailability of anthocyanins. *Drug Metab. Rev.* **2014**, *46*, 508–520.

(54) González-Barrio, R.; Borges, G.; Mullen, W.; Crozier, A. Bioavailability of anthocyanins and ellagitannins following consumption of raspberries by healthy humans and subjects with an ileostomy. *J. Agric. Food Chem.* **2010**, *58*, 3933–3939.

(55) Stalmach, A.; Edwards, C. A.; Wightman, J. D.; Crozier, A. Gastrointestinal stability and bioavailability of (poly)phenolic compounds following ingestion of Concord grape juice by humans. *Mol. Nutr. Food Res.* **2012**, *56*, 497–509.

(56) Mullen, W.; Edwards, C. A.; Serafini, M.; Crozier, A. Bioavailability of pelargonidin-3-O-glucoside and its metabolites in humans following the ingestion of strawberries with and without cream. *J. Agric. Food Chem.* **2008**, *56*, 713–719.

(57) Czank, C.; Cassidy, A.; Zhang, Q.; Morrison, D. J.; Preston, T.; Kroon, P. A.; Botting, N. P.; Kay, C. D. Human metabolism and elimination of the anthocyanin, cyanidin-3-glucoside: A 13C-tracer study. *Am. J. Clin. Nutr.* **2013**, *97*, 995–1003.

(58) De Ferrars, R. M.; Czank, C.; Zhang, Q.; Botting, N. P.; Kroon, P. A.; Cassidy, A.; Kay, C. D. The pharmacokinetics of anthocyanins and their metabolites in humans. *Br. J. Pharmacol.* **2014**, *171*, 3268–3282.

(59) Dupas, C.; Baglieri, A. M.; Ordonaud, C.; Tomé, D.; Maillard, M. N. Chlorogenic acid is poorly absorbed, independently of the food matrix: a Caco-2 cells and rat chronic absorption study. *Mol. Nutr. Food Res.* **2006**, *50*, 1053–1060.

(60) Lafay, S.; Gil-Izquierdo, A.; Manach, C.; Morand, C.; Besson, C.; Scalbert, A. Chlorogenic acid is absorbed in its intact form in the stomach of rats. *J. Nutr.* **2006**, *136*, 1192–1197.

(61) Lafay, S.; Morand, C.; Manach, C.; Besson, C.; Scalbert, A. Absorption and metabolism of caffeic acid and chlorogenic acid in them small intestine of rats. *Br. J. Nutr.* **2006**, *96*, 39–46.

(62) Olthof, M. R.; Hollman, P. C.; Katan, M. B. Chlorogenic acid and caffeic acid are absorbed in humans. *J. Nutr.* **2001**, *131*, 66–71.

(63) Hu, Y.-J.; Chen, C.-H.; Zhou, S.; Bai, A.M.; Ou-Yang, Y. The specific binding of chlorogenic acid to human serum albumin. *Mol. Biol. Rep.* **2012**, *39*, 2781–2787.

(64) Stalmach, A.; Mullen, W.; Barron, D.; Uchida, K.; Yokota, T.; Cavin, C.; Steiling, H.; Williamson, G.; Crozier, A. Metabolite profiling of hydroxycinnamate derivatives in plasma and urine after the ingestion of coffee by humans: Identification of biomarkers of coffee consumption. *Drug Metab. Dispos.* **2009**, *37*, 1749–1758.

(65) Stalmach, A.; Steiling, H.; Williamson, G.; Crozier, A. Bioavailability of chlorogenic acids following acute ingestion of coffee by humans with an ileostomy. *Arch. Biochem. Biophys.* **2010**, *501*, 98–105.

(66) Stalmach, A.; Edwards, C. A.; Wightman, J. D.; Crozier, A. Identification of (poly)phenolic compounds in concord

grape juice and their metabolites in human plasma and urine after juice consumption. *J. Agric. Food Chem.* **2011**, *59*, 9512–9522.

(67) Guo, Y.; Bruno, R. S. Endogenous and exogenous mediators of quercetin bioavailability. *J. Nutr. Biochem.* **2015**, *26*, 201–210.

(68) Crespy, V.; Morand, C.; Besson, C.; Manach, C.; Demigne, C.; Remesy, C. Quercetin, but not its glycosides, is absorbed from the rat stomach. *J. Agric. Food Chem.* **2002**, *50*, 618–621.

(69) Mullen, W.; Edwards, C.; Crozier, A. Absorption, excretion and metabolite profiling of methyl-, glucuronyl-, glucosyl- and sulpho-conjugates of quercetin in human plasma and urine after ingestion of onions. *Br. J. Nutr.* **2006**, *96*, 107–116.

(70) Jaganath, I. B.; Mullen, W.; Lean, M. E. J.; Edwards, C. A.; Crozier, A. *In vitro* catabolism of rutin by human fecal bacteria and the antioxidant capacity of its catabolites. *Free Radic. Biol. Med.* **2009**, *47*, 1180–1189.

(71) Ottaviani, J. I.; Momma, T. Y.; Heiss, C.; Kwik-Uribe, C.; Schroeter, H.; Keen, C. L. The stereochemical configuration of flavanols influences the level and metabolism of flavanols in humans and their biological activity *in vivo*. *Free Radic. Biol. Med.* **2011**, *50*, 237–244.

(72) Stalmach, A.; Troufflard, S.; Serafini, M.; Crozier, A. Absorption, metabolism and excretion of Choladi green tea flavan-3-ols by humans. *Mol. Nutr. Food Res.* **2009**, *53* (SUPPL. 1), 44–53.

(73) Kohri, T.; Nanjo, F.; Suzuki, M.; Seto, R.; Matsumoto, N.; Yamakawa, M.; Hojo, H.; Hara, Y.; Desai, D.; Amin, S.; et al. Synthesis of (-)-[4-3H]epigallocatechin gallate and its metabolic fate in rats after intravenous administration. *J. Agric. Food Chem.* **2001**, *49*, 1042–1048.

(74) Stalmach, A.; Mullen, W.; Steiling, H.; Williamson, G.; Lean, M. E. J.; Crozier, A. Absorption, metabolism, and excretion of green tea flavan-3-ols in humans with an ileostomy. *Mol. Nutr. Food Res.* **2010**, *54*, 323–334.

(75) Roowi, S.; Stalmach, A.; Mullen, W.; Lean, M. E. J.; Edwards, C. A.; Crozier, A. Green tea flavan-3-ols: colonic degradation and urinary excretion of catabolites by humans. *J. Agric. Food Chem.* **2010**, *58*, 1296–1304.

(76) Kahle, K.; Kempf, M.; Schreier, P.; Scheppach, W.; Schrenk, D.; Kautenburger, T.; Hecker, D.; Huemmer, W.; Ackermann, M.; Richling, E. Intestinal transit and systemic metabolism of apple polyphenols. *Eur. J. Nutr.* **2011**, *50*, 507–522.

(77) Appeldoorn, M. M.; Vincken, J. P.; Aura, A. M.; Hollman, P. C.; Gruppen, H. Procyanidin dimers are metabolized by human microbiota with 2-(3,4-dihydroxyphenyl)acetic acid and 5-(3,4-dihydroxyphenyl)-gamma-valerolactone as the major metabolites. *J. Agric. Food Chem.* **2009**, *57*, 1084–1092.

(78) Stoupi, S.; Williamson, G.; Drynan, J. W.; Barron, D.; Clifford, M. N. Procyanidin B2 catabolism by human fecal microflora: Partial characterization of "dimeric" intermediates. *Arch. Biochem. Biophys.* **2010**, *501*, 73–78.

(79) Almeida, L.; Vaz-da-Silva, M.; Falcao, A.; Soares, E.; Costa, R.; Loureiro, A. I.; Fernandes-Lopes, C.; Rocha, J. F.; Nunes, T.; Wright, L.; et al. Pharmacokinetic and safety profile of *trans*-resveratrol in a rising multiple-dose study in healthy volunteers. *Mol. Nutr. Food Res.* **2009**, *53* (SUPPL. 1), 7–15.

(80) Vitaglione, P.; Sforza, S.; Galaverna, G.; Ghidini, C.; Caporaso, N.; Vescovi, P. P.; Fogliano, V.; Marchelli, R. Bioavailability of trans-resveratrol from red wine in humans. *Mol. Nutr. Food Res.* **2005**, *49*, 495–504.

(81) Walle, T.; Hsieh, F.; Delegge, M. H.; Oatis, J. E.; Walle, U. K. High absortion but very low bioavaibility of oral

resveratrol in humans. *Drug Metab. Disposition.* **2004**, *32*, 1377–1382.

(82) Burkon, A.; Somoza, V. Quantification of free and protein-bound trans-resveratrol metabolites and identification of trans-resveratrol-C/O-conjugated diglucuronides - Two novel resveratrol metabolites in human plasma. *Mol. Nutr. Food Res.* **2008**, *52*, 549–557.

(83) Stoupi, S.; Williamson, G.; Drynan, J. W.; Barron, D.; Clifford, M. N. A comparison of the *in vitro* biotransformation of (-)-epicatechin and procyanidin B2 by human faecal microbiota. *Mol. Nutr. Food Res.* **2010**, *54*, 747–759.

(84) Lacombe, A.; Li, R. W.; Klimis-Zacas, D.; Kristo, A. S.; Tadepalli, S.; Krauss, E.; Young, R.; Wu, V. C. H. Lowbush wild blueberries have the potential to modify gut microbiota and xenobiotic metabolism in the rat colon. *PLoS One* **2013**, *8*, 1–8.

(85) Chen, H.; Hayek, S.; Rivera Guzman, J.; Gillitt, N. D.; Ibrahim, S. A.; Jobin, C.; Sang, S. The microbiota is essential for the generation of black tea theaflavins-derived metabolites. *PLoS One* **2012**, *7*, 1–10.

(86) Allwood, J. W.; De Vos, R. C. H.; Moing, A.; Deborde, C.; Erban, A.; Kopka, J.; Goodacre, R.; Hall, R. D. Plant metabolomics and its potential for systems biology research: background concepts, technology, and methodology. *Methods Enzimol.* **2011**, *500*, 299–336.

(87) Villas-Bôas, S.; Roessner, U.; Hansen, M.; Smedsgaard, J.; Nielsen, J. Metabolome analysis an introduction; John Wiley & Sons, Inc: Hoboken, New Jersey, 2007.

(88) Dunn, W. B.; Broadhurst, D. I.; Atherton, H. J.; Goodacre, R.; Griffin, J. L. Systems level studies of mammalian metabolomes: the roles of mass spectrometry and nuclear magnetic resonance spectroscopy. *Chem. Soc. Rev.* **2011**, *40*, 387–426.

(89) Patti, G. J.; Yanes, O.; Siuzdak, G. Metabolomics: the apogee of the omics trilogy. *Nat. Rev. Mol. Cell Biol.* **2012**, *13*, 263–269.

(90) Xiao, J. F.; Zhou, B.; Ressom, H. W. Metabolite identification and quantitation in LC-MS/MS-based metabolomics. *Trends Anal. Chem.* **2012**, *32*, 1–14.

(91) Guo, K.; Peng, J.; Zhou, R.; Li, L. Ion-pairing reversed-phase liquid chromatography fractionation in combination with isotope labeling reversed-phase liquid chromatography–mass spectrometry for comprehensive metabolome profiling. *J. Chromatogr. A* **2011**, *1218*, 3689–3694.

(92) Kamleh, A.; Barrett, M. P.; Wildridge, D.; Burchmore, R. J. S.; Scheltema, R. A.; Watson, D. G. Metabolomic profiling using Orbitrap Fourier transform mass spectrometry with hydrophilic interaction chromatography: a method with wide applicability to analysis of biomolecules. *Rapid Commun. Mass Spectrom.* **2008**, *22*, 1912–1918.

(93) Beckonert, O.; Keun, H. C.; Ebbels, T. M. D. J. B.; Holmes, E.; Lindon, J. C.; Nicholson, J. K. Metabolic profiling, metabolomic and metabonomic procedures for NMR spectroscopy of urine, plasma, serum and tissue extracts. *Nat. Protoc.* **2007**, *2*, 2692–2703.

(94) Suzuki, M.; Kusano, M.; Takahashi, H.; Nakamura, Y.; Hayashi, N.; Kobayashi, M.; Ichikawa, T.; Matsui, M.; Hirochika, H.; Saito, K. Rice-Arabidopsis FOX line screening with FT-NIR-based fingerprinting for GC-TOF/MS-based metabolite profiling. *Metabolomics* **2010**, *6*, 137–145.

(95) Zhou, H.; Liang, J.; Lv, D.; Hu, Y.; Zhu, Y.; Si, J.; Wu, S. Characterization of phenolics of *Sarcandra glabra* by non-targeted high-performance liquid chromatography fingerprinting and following targeted electrospray ionisation

tandem mass spectrometry/time-of-flight mass spectrometry analyses. *Food Chem.* **2013**, *138*, 2390–2398.

(96) Yanes, O.; Tautenhahn, R.; Patti, G.; Siuzdak, G. Expanding coverage of the metabolome for global metabolite profiling. *Anal. Chem.* **2011**, *83*, 2152–2161.

(97) Smith, C. A.; Want, E. J.; O´Maille, G.; Abagyan, R.; Siuzdak, G. XCMS: processing mass spectrometry data for metabolite profiling using nonlinear peak alignment, matching and identification. *Anal. Chem.* **2006**, *78*, 779–787.

(98) Tautenhahn, R.; Bottcher, C.; Neumann, S. Highly sensitive feature detection for high resolution LC/MS. *BMC Bioinformatics* **2008**, *9*, 16.

(99) Lu, W.; Bennett, B. D.; Rabinowitz, J. D. Analytical strategies for LC-MS-based targeted metabolomics. *J. Chromatogr. B.* **2008**, *871*, 236–242.

(100) Jacobs, H.; Koek, G. H.; Peters, R.; Moalin, M.; Tack, J.; Vijgh, W. J. Van Der; Bast, A.; Haenen, G. R. Differences in pharmacological activities of the antioxidant flavonoid MonoHER in humans and mice are caused by variations in its metabolic profile. *Clin. Pharmacol. Ther.* **2011**, *90*, 852–859.

(101) Jacobs, D. M.; Fuhrmann, J. C.; Van Dorsten, F. A.; Rein, D.; Peters, S.; Van Velzen, E. J. J.; Hollebrands, B.; Draijer, R.; Van Duynhoven, J.; Garczarek, U. Impact of short-term intake of red wine and grape polyphenol extract on the human metabolome. *J. Agric. Food Chem.* **2012**, *60*, 3078–3085.

(102) Edmands, W. M. B.; Ferrari, P.; Rothwell, J. A.; Rinaldi, S.; Slimani, N.; Barupal, D. K.; Biessy, C.; Jenab, M.; Clavel-Chapelon, F.; Fagherazzi, G.; et al. Polyphenol metabolome in human urine and its association with intake of polyphenol-rich foods across European countries. *Am. J. Clin. Nutr.* **2015**, *102*, 905–913.

(103) Ma, Y.; Tanaka, N.; Vaniya, A.; Kind, T.; Fiehn, O. Ultrafast polyphenol metabolomics of red wines using microLC-MS/MS. *J. Agric. Food Chem.* **2016**, *64*, 505–512.

(104) Masumoto, S.; Terao, A.; Yamamoto, Y.; Mukai, T.; Miura, T.; Shoji, T. Non-absorbable apple procyanidins prevent obesity associated with gut microbial and metabolomic changes. *Sci. Rep.* **2016**, *6*, 1–10.

(105) Grün, C.; Un, H. G.; Van Dorsten, F. A.; Jacobs, D. M.; Le Belleguic, M.; Van Velzen, E. J. J.; Bingham, M. O.; Janssen, H.-G.; Van Duynhoven, J. P. M. GC–MS methods for metabolic profiling of microbial fermentation products of dietary polyphenols in human and *in vitro* intervention studies. *J. Chromatogr. B* **2008**, *871*, 212–219.

(106) Llorach, R.; Garrido, I.; Monagas, M.; Urpi-sarda, M.; Tulipani, S.; Bartolome, B.; Andres-Lacueva, C. Metabolomics study of human urinary metabolome modifications after intake of almond (*Prunus dulcis* (Mill .) D . A . Webb) skin polyphenols. *J. Proteome Res.* **2010**, *9*, 5859–5867.

(107) Dunn, W. B.; Broadhurst, D.; Begley, P.; Zelena, E.; Francis-McIntyre, S.; Anderson, N.; Brown, M.; Knowles, J. D.; Halsall, A.; Haselden, J. N.; et al. Procedures for large-scale metabolic profiling of serum and plasma using gas chromatography and liquid chromatography coupled to mass spectrometry. *Nat. Protoc.* **2011**, *6*, 1060–1083.

(108) Stalmach, A.; Edwards, C. A.; Wightman, J. D.; Crozier, A. Colonic catabolism of dietary phenolic and polyphenolic compounds from Concord grape juice. *Food Funct.* **2013**, *4*, 52–62.

(109) Prior, R. L.; Rogers, T. R.; Khanal, R. C.; Wilkes, S. E.; Wu, X.; Howard, L. R. Urinary excretion of phenolic acids in rats fed cranberry. *J. Agric. Food Chem.* **2010**, *58*, 3940–3949.

(110) Vitaglione, P.; Donnarumma, G.; Napolitano, A.; Galvano, F.; Gallo, A.; Scalfi, L.; Fogliano, V. Protocatechuic acid is the major human metabolite of cyanidin-glucosides. *J. Nutr.* **2007**, *137*, 2043–2048.

(111) Vanzo, A.; Vrhovsek, U.; Tramer, F.; Mattivi, F.; Passamonti, S. Exceptionally fast uptake and metabolism of cyanidin 3-glucoside by rat Kidneys and liver. *J. Nat. Prod.* **2011**, *74*, 1049–1054.

(112) González-Barrio, R.; Edwards, C. A.; Crozier, A. Colonic catabolism of ellagitannins, ellagic acid, and raspberry anthocyanins : *in vivo* and *in vitro* studies. *Drug Metab. Dispos.* **2011**, *39*, 1680–1688.

(113) Last, R. L.; Jones, a D.; Shachar-Hill, Y. Towards the plant metabolome and beyond. *Nat. Rev. Mol. Cell Biol.* **2007**, *8*, 167–174.

(114) Huang, D.; Boxin, O. U.; Prior, R. L. The chemistry behind antioxidant capacity assays. *J. Agric. Food Chem.* **2005**, *53*, 1841–1856.

(115) Nimse, S. B.; Pal, D. Free radicals, natural antioxidants, and their reaction mechanisms. *RSC Adv.* **2015**, *5*, 27986–28006.

(116) Procházková, D.; Boušová, I.; Wilhelmová, N. Antioxidant and prooxidant properties of flavonoids. *Fitoterapia.* **2011**, *82* (4), 513–523.

(117) Nijveldt, R.; van Nood, E.; van Hoorn, D.; Boelens, P.; van Norren, K.; van Leeuwen, P. Flavonoids: a review of probable mechanisms of action and potential applications. *Am. J. Clin. Nutr.* **2001**, *74*, 418–425.

(118) Liu, R. H. Potential synergy of phytochemicals in cancer prevention: mechanism of action. *J. Nutr.* **2004**, *134* (12 Suppl), 3479S–3485S.

(119) Rodriguez-Mateos, A.; Vauzour, D.; Krueger, C. G.; Shanmuganayagam, D.; Reed, J.; Calani, L.; Mena, P.; Del Rio, D.; Crozier, A. Bioavailability, bioactivity and impact on health of dietary flavonoids and related compounds: an update. *Arch. Toxicol.* **2014**, *88*, 1803–1853.

(120) Kaur, C.; Kapoor, H. C. Antioxidants in fruits and vegetables - The millennium's health. *Int. J. Food Sci. Technol.* **2001**, *36*, 703–725.

(121) Denev, P. N.; Kratchanov, C. G.; Ciz, M.; Lojek, A.; Kratchanova, M. G. Bioavailability and antioxidant activity of black chokeberry (*Aronia melanocarpa*) polyphenols: *in vitro* and *in vivo* evidences and possible mechanisms of action: a review. *Compr. Rev. Food Sci. Food Saf.* **2012**, *11*, 471–489.

(122) Zamora-Ros, R.; Touillaud, M.; Rothwell, J. A.; Romieu, I.; Scalbert, A. Measuring exposure to the polyphenol metabolome in observational epidemiologic studies: current tools and applications and their limits. *Am. J. Clin. Nutr.* **2014**, *100*, 11–26.

(123) Cassidy, A.; Rogers, G.; Peterson, J. J.; Dwyer, J. T.; Lin, H.; Jacques, P. F. Higher dietary anthocyanin and flavonol intakes are associated with anti-inflammatory effects in a population of US adults. *Am. J. Clin. Nutr.* **2015**, *102*, 172–181.

(124) Niki, E. Assessment of antioxidant capacity in vitro and in vivo. *Free Radic. Biol. Med.* **2010**, *49*, 503–515.

(125) Ou, B.; Chang, T.; Huang, D.; Prior, R. L. Determination of total antioxidant capacity by oxygen radical absorbance capacity (ORAC) using fluorescein as the fluorescence probe: First action 2012.23. *J. AOAC Int.* **2013**, *96*, 1372–1376.

(126) Atala, E.; Vásquez, L.; Speisky, H.; Lissi, E.; López-Alarcón, C. Ascorbic acid contribution to ORAC values in berry extracts: An evaluation by the ORAC-pyrogallol red methodology. *Food Chem.* **2009**, *113*, 331–335.

(127) Demirci Çekiç, S.; Kara, N.; Tütem, E.; Sözgen Başkan, K.; Apak, R. Protein–incorporated serum total antioxidant

capacity measurement by a modified CUPRAC (CUPRIC reducing antioxidant capacity) method. *Anal. Lett.* **2012**, *45*, 754–763.

(128) Apak, R.; Güçlü, K.; Demirata, B.; Özyürek, M.; Çelik, S. E.; Bektaşoğlu, B.; Berker, K. I.; Özyurt, D. Comparative evaluation of various total antioxidant capacity assays applied to phenolic compounds with the CUPRAC assay. *Molecules.* **2007**, *12*, 1496–1547.

(129) Wood, L.; Gibson, P.; Garg, M. A review of the methodology for assessing in vivo antioxidant capacity. *J. Sci. Food Agric.* **2006**, *86*, 2057–2066.

(130) Apak, R.; Gorinstein, S.; Böhm, V.; Schaich, K. M.; Özyürek, M.; Güçlü, K. Methods of measurement and evaluation of natural antioxidant capacity/activity (IUPAC Technical Report). *Pure Appl. Chem.* **2013**, *85*, 957–998.

(131) Apak, R.; Güclü, K.; Özyürek, M.; Celik, S. Mechanism of antioxidant capacity assays and the CUPRAC (cupric ion reducing antioxidant capacity) assay. *Microchim. Acta.* **2008**, *160*, 413–419.

(132) Apak, R.; Güclü, K.; Özyürek, M.; Esin, S. Novel total antioxidant capacity index for dietary polyphenols and vitamins C and E, using their cupric ion reducing capability in the presence of neocuproine: CUPRAC Method. *J. Agric. Food Chem.* **2004**, *52*, 7970–7981.

Capítulo 2

Comparación de los perfiles y niveles de concentración de (poli)fenoles en frutos para ensayos de intervención nutricional.

Resumen

Se caracterizó y cuantificó el contenido de (poli)fenoles en frutos de uva Red Globe, Pink Globe y calafate, tres frutos con elevadas concentraciones de compuestos fenólicos.

Pink Globe (*V. vinífera* L.) es una nueva variedad de uva de mesa derivada de Red Globe, más dulce y de maduración más temprana. Los análisis genéticos mediante microsatélite indican que ambos son indiferenciables. Sin embargo, se observaron diferencias cuando se estudió la expresión de reguladores transcripcionales de enzimas clave en la biosíntesis de antocianos. Consecuentemente, mediante análisis por HPLC-DAD-ESI-MS/MS se encontraron menores concentraciones de antocianos en Pink Globe.

Estudios previos del fruto de calafate (*B. microphylla*) han descrito niveles de concentración de antocianos mayores a los reportados en otras bayas ampliamente consumidas. Los estudios realizados por HPLC-DAD indican que el fruto de calafate contiene entre 60 a 400 veces más antocianos que las uvas de mesa estudiadas. Los ensayos de capacidad antioxidante *in vitro* mediante CUPRAC y ABTS indican una capacidad antioxidante 300 veces mayor en fruto de calafate que en las uvas estudiadas.

Mediante análisis HPLC-FLD-ESI-MS/MS se determinaron las concentraciones de flavan-3-oles y de procianidinas en semillas de uvas que superan los 11 µmol/100g, mientras que en semillas de calafate no se encontraron cantidades cuantificables de (+)-catequina, (-)-epicatequina, procianidina B2 y otro dímero de procianidina. A la vista de estos resultados, se decidió utilizar el calafate para los ensayos de ingesta aguda para el cual se elaboró un extracto de calafate apto para el consumo de animales de experimentación. Como solvente de extracción se utilizó etanol potable, obteniendo un extracto inocuo con un rendimiento aceptable.

Contenidos

Section 1

Title: **Differences in *Vvufgt* and *VvmybA1* gene expression levels and phenolic composition in table grape (*Vitis vinifera L.)* 'Red Globe' and its somaclonal variant 'Pink Globe'**

Luis Bustamante[1], Vania Sáez[1], Patricio Hinrichsen[2], María H. Castro[2], Carola Vergara[1], Dietrich von Baer[1] and Claudia Mardones[1]*

[1]Instrumental Analysis Department, Faculty of Pharmacy, University of Concepción, P.O. Box 160-C Concepción, Chile, and [2]Instituto de Investigaciones Agropecuarias, INIA La Platina, Santa Rosa 11610, La Pintana, Santiago, Chile.

*Corresponding Author: Tel: 56-41-2204598, Fax: 56-41-2226382, E-mail address: cmardone@udec.cl

Formato Manuscrito publicado en Journal of Agricultural and Food Chemistry (JAFC). DOI: 10.1021/acs.jafc.6b04817, 8 de marzo del 2017

Abstract

A novel ‘Red Globe’ (RG)-derived grape variety, ‘Pink Globe’ (PG), was described and registered as a new genotype, with earlier ripening and sweeter taste than that of RG. Microsatellite analysis revealed that PG and RG are undifferentiable; however, the PG *VvmybA1c* contains six SNPs within the coding and non-coding region, possible related to the reduced *VvmybA1* expression levels. Conversely, HPLC-DAD-ESI-MS/MS analysis showed significantly lower anthocyanin content in PG skin than in RG skin and PG had no detectable trihydroxylated anthocyanins. Total flavonols did not differ between the variants, although some quercetin derivate concentrations were lower in PG. HPLC-FLD analysis revealed slightly higher concentrations of epicatechin and a procyanidin dimer in PG seeds, although antioxidant capacity of crude extracts from either variety did not differ significantly. These differences, particularly in monomeric anthocyanin content, can be attributed to altered activity of a MYB-type transcription factor reducing *Vvufgt* expression.

.

Keywords: *Vitis vinifera*, Pink Globe, Red Globe, Microsatellite, *Vvufgt*, *VvmybA1*, Phenolic Compounds, HPLC-DAD-MS/MS

Introduction

Over the past decades, numerous studies have reported epidemiologic and mechanistic data that indicates the beneficial effect of phenolic compounds present in fruits and vegetables [1–5]. Many studies have shown the potential benefits of these compounds in cardiovascular and neurodegenerative diseases, as well as cancer treatment and prevention [3,6–11].

Grapes (*Vitis vinifera* L.) have become one of the most important sources of polyphenolic compounds due to the high concentration of these compounds in the fruit and its worldwide availability and consumption [12,13]. Grape berry has been widely studied in order to characterize different families of phenolic compounds synthesized via the phenylpropanoid pathway, including flavonoids and non-flavonoid compounds such as anthocyanins, flavonols, flavan-3-ols, phenolic acids, and stilbenoids, amongst others. These compounds are located mainly in the berry skin epidermal layer and in seeds, where they confer protection against UV, pathogens, and oxidative damage [14,15]. The polyphenolic composition and ripening of grapevine berries determines their quality, and these characteristics depend on the cultivar (genotype), the interaction with the environment (light, temperature, water availability, soil composition), and viticulture practices (pruning, irrigation). The combination of these three variables may result in substantial inter-seasonal variation in fruit quality [12,16,17].

Grape berry development is comprised of three main stages: a cell division growth phase, occurring in early fruit development; a lag phase and a cell expansion growth phase, which occurs when upon ripening. The most relevant compounds during the initial cell division growth phase are organic acids, tannins, hydroxycinnamates, minerals, amino acids, and micronutrients. Once growth ceases, ripening (*véraison*) commences, hallmarked by the appearance of characteristic ripen fruit color, and continues with sugar accumulation, rapid pigmentation, and synthesis of aroma compounds [18]. A relationship exists between the environmental conditions, the presence of endogenous hormones and the berry development stage [18].

In Chile, the area used for the cultivation of wine and table grapes has increased over the past years [19]. Similar to in other countries, ‘Red Globe’ (RG) has become one of the main table grape cultivars because of its excellent postharvest performance [20]. RG has berries with large seeds; red-grey colour, thick skin; and unpigmented, juicy, soft flesh [21]. A limited number of studies have described the phenolic composition of RG, among other table grape cultivars [22,23].

Recently, a novel RG-related grape variety named ‘Pink Globe’ (PG) has been described and registered as a new genotype. PG presumably corresponds to a somaclonal variant of RG [24]. The desirable

characteristics of PG include early ripening and sweeter taste of the fruit compared to RG. Moreover, PG berries differ from RG in that they have a lighter skin color (pink) and thinner skin, qualities which are both particularly valuable in a commercial sense [25]. This berry phenotype suggests that the anthocyanin pathway is altered in the variety.

The production of anthocyanins in the berry is mainly associated with two genes, namely *Vvufgt* and *VvmybA1*, which encode the UDP-glucose:flavonoid-3-O-glucosyltransferase (UFGT) enzyme and a MYB-type transcription factor, respectively [26,27]. The UFGT enzyme catalyzes the glycosylation of anthocyanidins, and it has been suggested that anthocyanidin synthase (ANS) and UFGT form a multienzyme complex to catalyze the leucoanthocyanidin – anthocyanidin – anthocyanin reaction [28]. The MYB-type transcription factor (along with bHLH and WD40 types) regulates expression of the *Vvufgt* gene and other structural genes during the berry ripening [29]. Furthermore, a retrotransposon (GRET-1) inserted upstream of the *VvmybA1* coding sequence suppresses its activity [27,30,31], or in some cases, the *VvmybA1* locus has been deleted [32].

Black grapes have at least one intact copy of *VvmybA1*, while white grapes have both gene copies interrupted by GRET-1 or carry deletions in the functional allele. Pink and red grapes may contain either a 829 bp insertion or a 44 bp deletion in the promoter region, the insertion being associated with excision of GRET-1, or two single nucleotide polymorphisms (SNPs) in the first exon [30–32].

In order to fully understand the grape color phenotype, expression levels of *Vvufgt* and *VvmybA1* in RG and PG grape skin were analyzed in two maturation stages. Gene expression was correlated with results from the study of phenolic composition changes by using optimized HPLC-DAD-ESI-MS/MS and HPLC-FLD methods. Identification and quantification of anthocyanin, flavonols and other phenolic compounds were performed in fruit skin, while flavan-3-ols and procyanidins in seeds. The antioxidant capacity of whole extracts and flavonol/HCAD skin fractions was also explored and correlated with phenolic compound concentrations in order to address the contribution of these compounds to the nutraceutical potential of PG and RG grapes.

Experimental

Reagents, Standards, and Extraction Materials

Commercial standards of peonidin-3-glucoside chloride (95%) were provided by Extrasynthese (Lyon Nord, France). Caffeic acid (98%), (+)-catechin hydrate (98%), (-)-epicatechin (90%), quercetin-3-rutinoside (< 94%), and quercetin-3-rhamnoside (85%) were provided by Sigma (Steinheim, Germany). Quercetin-3-glucoside (99%), (*E*)-piceid (99%), procyanidin B1 (93%), B2 (96%), and C1 (91%) were provided by Phytolab (Vestenbergsreuth, Germany). Formic acid, ammonia, hydrochloric acid, copper (II) chloride, ammonium acetate, sodium acetate, sodium ethylenediaminetetraacetic acid (EDTA), cetyltrimethylammonium bromide (CTAB), □-mercaptoethanol, Tris-HC1, chloroform, octanol, ethanol, sodium borate decahydrate (borax), ethylene glycol bis(β-aminoethyl ether)-N,N′-tetraacetic acid (EGTA), sodium dodecyl sulfate (SDS), dithiothreitol, proteinase K, NaC1, KCl, LiCl, acetonitrile (HPLC grade), methanol (HPLC grade), and water (HPLC grade) were provided by Merck (Darmstadt, Germany). Flavonol cleanup was performed using 150 mg Oasis MCX 6cc mixed phase SPE cartridges from Waters (Milford, Connecticut, USA).

Neocuproine, 6-hydroxy-2,5,7,8-tetramethylchroman-2-carboxylic acid (Trolox), 2,2′-azino-bis(3-ethylbenzothiazoline-6-sulphonic acid) (ABTS), RNase A, and polyvinylpolypyrrolidone (PVP) were provided by Sigma (St. Louis, Missouri, USA).

Plant Material

RG and PG berry samples were collected at 50% *véraison*, e.g., when roughly half of the berries have turned their skin color to redish, and at maturity, defined when a sample of berries from different bunches of similar phenology reached 18°Brix . Intact grape bunches were harvested from the original vineyard where the variety was originally identified (Talagante, RM, Chile; 33°38′26″ S; 70°51′52″ W). Samples were stored in liquid N_2 during transportation, and then maintained at -80°C for those samples used for RNA analyses or at -20°C for those samples used for analysis of anthocyanins, flavonol, phenolic acids and procyanidins profiles and concentrations.

Instruments

An analytical balance from Denver Instrument Company (New York, New York, USA), an ultrasonic bar homogenizer Series 4710 from Cole Palmer (Chicago, Illinois, USA), a Stuart S01 mechanical shaker from Bibby Scientific LTD (Stanford, UK), a Sigma 3-16p centrifuge from Martin Christ (Osterode, Germany), and a rotavapor complemented with a V-700 vacuum pump and V-850 controller

system from Büchi (Flawil, Switzerland) were used for sample preparation. An Epoch™ microplate reader from Biotek Instruments (Winooski, Vermont, USA) was used for antioxidant assays.

HPLC-DAD-ESI-MS/MS analyses for identification of anthocyanins, flavonols, flavan-3-ols, procyanidins, and phenolic acids were carried out using a Nexera UHPLC/HPLC system from Shimadzu Corporation (Kyoto, Japan) equipped with a quaternary LC-30AD pump, a DGU-20A5R degassing unit, a Prominence CTO-20 AC oven, a SIL-30AC autosampler, and an SPD-M20A UV-Vis photodiode array spectrophotometer detector coupled in tandem with a QTrap 3200 LC-MS/MS detector from MDS Sciex (Redwood City, California, USA). Instrument control and data collection were carried out using CLASS-VP DAD Chromatography Data System from Shimadzu Corporation (Kyoto, Japan) and MS/MS analysis was performed using Analyst software version 1.5.2 from AB Sciex (Framingham, Massachusetts, USA).

Quantitative analyses of procyanidins were carried out using a HPLC- fluorescence system composed of a LaChrom Elite L-2130 pump, an L-2200 autosampler, and an L-7485 detector from Hitachi High Technologies Co (Tokyo, Japan), with a CTO-10AVP oven from Shimadzu Corporation (Kyoto, Japan). Data collection was performed using interactive software graphics version 6.2 from Varian Inc. (Palo Alto, California, USA).

Standard PCR and quantitative real-time PCR (qRT-PCR) analyses were performed using a Light Cycler from Roche Diagnostics (Mannheim, Germany) and a NanoDrop ND-1000 from Thermo Fisher Scientific (Wilmington, Delaware, USA) was used to quantify and assess the quality of DNA, RNA and cDNA.

DNA and RNA extraction

DNA was purified from berry skins following the CTAB method described by Lodhi et al. [33]. The quality and quantity of purified DNA were estimated by spectrophotometry as well as by evaluation on a 1.0% agarose gel.

Total RNA was isolated from 3-4 g of frozen tissue using the modified hot borate method [34]. The quantity and quality of purified RNA were assessed by measuring the $A_{260/280}$ ratio and by electrophoresis on a 1.2% formaldehyde-agarose gel. First-strand cDNA was obtained by reverse transcription reactions following standard procedures using 2 µg of total RNA as template, MMLV-RT reverse transcriptase from Promega (Madison, Wisconsin, USA), and oligo dT primers. The concentration of cDNA was determined by measuring the absorbance at 260 nm, and each cDNA sample was diluted to 50 ng/µL prior to its use in qRT-PCR.

Analysis of microsatellites or SSR (Simple sequence repeats)

Microsatellite (SSR) markers were used to determine cultivar identity in key samples. For this purpose, protocols and markers were used that were previously proposed by a number of groups [35–39] (Vitis Microsatellite Consortium) and validated by INIA La Platina in the most commonly used varieties in Chile [40]. Following this, a set of 67 SSR markers were used to find intra-varietal differences (see table S1). PCR products were separated by electrophoresis on 6% polyacrylamide gels and silver-stained using a Silver Sequencing kit from Promega (Madison, Wisconsin, USA) as described by Narváez et al. [40].

Quantitative real-time PCR

The expression levels of selected genes were determined using qRT-PCR. Both *VvmybA1* and *Vvufgt* amplicons were amplified from synthesized first-strand cDNA in presence of SYBR Green used as a fluorescent marker dye. qRT-PCR reaction conditions, procedures and data analysis were as described by Kobayashi et al. [41]. The internal reference gene *elongation factor 1-alfa* (*EF1α*) was used to normalize experimental gene expression. Samples collected from fruit in two developmental stages, namely 50% *véraison* and ripen, were considered.

Characterization of VvmybA1 alleles

In order to amplify the a, b or c allelic variants of *VvmybA1* from each RG and PG sample, specific primers were used as previously described [42]. Amplified fragments were cloned into the pGEM-Easy vector from Promega. Transformation of *E. coli* DH5α and selection of recombinant clones was performed according to Sambrook [43]. Plasmid DNA extraction was performed using a Plasmid Mini Kit II from Promega (Madison, Wisconsin, USA). Sequencing of cloned DNA was carried out using an external service provided by Macrogen (Seoul, Korea).

Sample pre-treatments

Skin Extraction

Whole extract preparation and cleanup were carried out based on the method described by Ruiz et al. [44]. For anthocyanins analyses, crude extract was dried in a rotary evaporator and reconstituted in mobile phase. For flavonol and phenolic acid analyses, a clean-up of the crude skin extracts was performed using Oasis MCX cartridges as described by Castillo-Muñoz et al. [45].

Seed Extraction

Seed samples were ground using a coffee mill, and then subject to a freeze-drying step to remove residual water content. Following Soxhlet degreasing with hexane, 100 mg of seed sample was mixed

with 0.4 mL of an 80/20% v/v ethanol/water mixture and sonicated for 5 minutes with the ultrasonic bar, followed by 15 s of vortex agitation and centrifugation at 1000 rpm for 4 minutes. The separated supernatant was removed and the pellet was washed three more times as described above. The final sample volume was adjusted to 5 mL with ethanol. For procyanidins and flavan-3-ols analyses, this extract was dried in a rotary evaporator and reconstituted in mobile phase.

Anthocyanin analysis

HPLC separation of anthocyanins from grape skin extracts were carried out using a reverse phase C-18 column (YMC-ODS-AM, 5 µm, 250 × 3.0 mm), with a C-18 precolumn (Nova-Pak Waters, 4 µm, 22 × 3.9 mm) at 30°C. The injection volume was 10 µL. The mobile phase gradient used was constituted by a 99.9/0.1% v/v water/trifluoroacetic acid mixture (solvent A) and acetonitrile (solvent B). The flow rate was 0.3 mL/min and the gradient program was initiated with 10 to 20% of solvent B in 15 minutes, then maintained for 6 minutes, then raised to 27% in 5 minutes and maintained for a further 10 minutes followed by 1 minute of washing and 22 minutes of stabilization. Anthocyanin quantification was performed through a DAD extracted chromatogram at 518 nm by external calibration for all detected compounds using a peonidin-3-glucoside calibration curve. Results were expressed as the equivalent of peonidin-3-glucoside in µmol/100 g fresh weight (FW). Relative concentrations were also determined by internal normalization.

Compound identification by MS/MS was carried out using the same chromatographic condition. Positive ionization mode was as follows: +5 V collision energy, +4000 V ionization voltage, capillary temperature at 450°C, and N_2 nebulizer at 15 psi. Analytes identities were assigned by comparison of their retention time (t_R) with those of the available commercial standards and also by comparisons made between characteristic spectral data (MS enhance product ion (MS-EPI) and UV-Visible).

Flavonol analysis

HPLC separation and quantification of flavonols present in the grape skin extracts were carried out using a core-shell reverse phase C-18 column (Kinetex C-18, 2.6 µm, 150 × 4.6 mm), with a C-18 precolumn (SecurityGuard UHPLC for 4,6 mm) at 40°C. The injection volume was 10 µL. The mobile phase gradient used was constituted by a 87/3/10% v/v/v water/acetonitrile/formic acid mix (solvent A) and a 40/50/10% v/v/v water/acetonitrile/formic acid mix (solvent B). The flow rate was 0.38 mL/min and the gradient program was initiated with 6 to 12% of solvent B in 10 minutes, then raised to 25% in 10 minutes, from 25% to 30% in 5 minutes and elevated to 45% for 10 minutes, followed by 5 minutes of washing and 10 minutes of stabilization. Flavonol quantification was performed through a DAD

chromatogram extracted at 360 nm by external calibration using a quercetin-3-glucoside calibration curve. Results were expressed as the equivalent of quercetin-3-glucoside in µmol/100 g FW. Relative concentrations were also determined by internal normalization.

In addition, it was possible to quantify hydroxycinnamic acids and flavan-3-ols through a DAD chromatogram extracted at 320 nm and at 280 nm, using an external calibration of caffeic acid and (+)-catechin, respectively. Results were expressed as the equivalent of caffeic acid or (+)-catechin in µmol/100 g FW.

The identification by MS/MS was carried out using the same chromatographic conditions. Negative ionization mode was as follows: −5 V collision energy, −4000 V ionization voltage, capillary temperature at 450°C, and N_2 nebulizer at 15 psi. Analytes identities were assigned based on comparison of their retention time (t_R) with those of the available commercial standards and also by comparisons made between characteristic spectral data (MS-EPI and UV-Visible).

Procyanidins analysis

Flavan-3-ol and procyanidins quantification in seeds was performed through FL detection with a $\lambda_{excitation}$ of 230 nm and a $\lambda_{emission}$ of 321 nm as described by Nakamura et al. [46] with some modifications. All analyses were carried out using a core-shell reverse phase C-18 column (Kinetex C-18, 2.6 µm, 150 × 4.6 mm), with a C-18 precolumn (SecurityGuard UHPLC for 4,6 mm) at 30°C. The injection volume was 5 µL and the mobile phase gradient used was constituted by a 99.9/0.1% v/v water/formic acid mix (solvent A) and a 69.9/30/0.1% v/v/v water/acetonitrile/formic acid mix (solvent B). Phosphoric acid was substituted with formic acid as mobile phase acid modifier. Flavan-3-ols and procyanidin quantitation was performed using external calibration of (+)-catechin, (-)-epicatechin, procyanidin B1, B2 and C1. All other procyanidins were expressed as equivalents of procyanidin B1 in µmol/100 g FW. Relative concentrations were also determined as internal normalization.

The identification by MS/MS was carried out using the same chromatographic conditions. Negative ionization mode was as follows: −5 V collision energy, −4000 V ionization voltage, capillary temperature at 450°C, and N_2 nebulizer at 15 psi. Analytes identities were assigned by comparison of their retention time (t_R) with those of the available commercial standards and also by comparisons made between characteristic spectral data (MS-EPI).

$TEAC_{CUPRAC}$ and $TEAC_{ABTS}$ assays

Trolox equivalent antioxidant capacity (TEAC) assays were conducted in 96-well microplates. $TEAC_{CUPRAC}$ assay was carried out as described by Ribbero et al. [47]. $TEAC_{ABTS}$ assay was performed as

described by Ruiz et al. [44], but the procedure was modified to microplates. The antioxidant capacities of whole extracts were compared with the SPE fractions containing non-anthocyanin phenolic compounds (as described in section 2.8) and monomeric anthocyanins (fraction obtained as described by Castillo-Muñoz et al. [45]).

Results and Discussion

Genetic Analysis

SSR analysis

To explore the genetic dissimilarity between the two clones analyzed in this study, namely RG and PG, 67 SSR markers were used as the basic marker set able to discriminate most of the known grapevine genotypes, with the exception of some clonal pairs (Table S1). As could be expected for clones that had only recently differentiated, all the 67 SSR markers exhibited the same allelic pattern in RG and PG (data not shown), demonstrating that both genotypes are closely related to each other. In addition, this result suggests that the observed phenotypic differences between RG and PG are due to a single mutation or at most a few mutations. A similar result was obtained by AFLP analysis. In this case, none of the 334 amplicons obtained with eight primer combinations (Table S2) revealed any consistent difference between replicates of each genotype, supporting the genetic similarity between them. Consequently, characterization of key genes of the flavonoid biosynthetic pathway in the two clones were performed.

qRT-PCR amplification of flavonoid biosynthesis related genes

Figure 2.1 A shows that expression of *VvmybA1* was significantly higher at 50% *véraison* stage in RG compared to PG, which displayed only a basal expression level. Moreover, at ripen stage, *VvmybA1* expression in RG also returns to a basal expression level. On the other hand, Figure 2.1 B shows a significantly higher level of *Vvufgt* expression in RG compared to PG, which is observed during both 50% *véraison* and ripen stages. Furthermore, no significant differences were found in *Vvufgt* expression levels during both 50% *véraison* and ripen stages of either genotypes.

A lower *VvmybA1* expression level can be associated with a lower prevalence of the particular MYB transcription factor, which consequently would lead to a lower *Vvufgt* expression level and lower anthocyanin biosynthesis in PG.

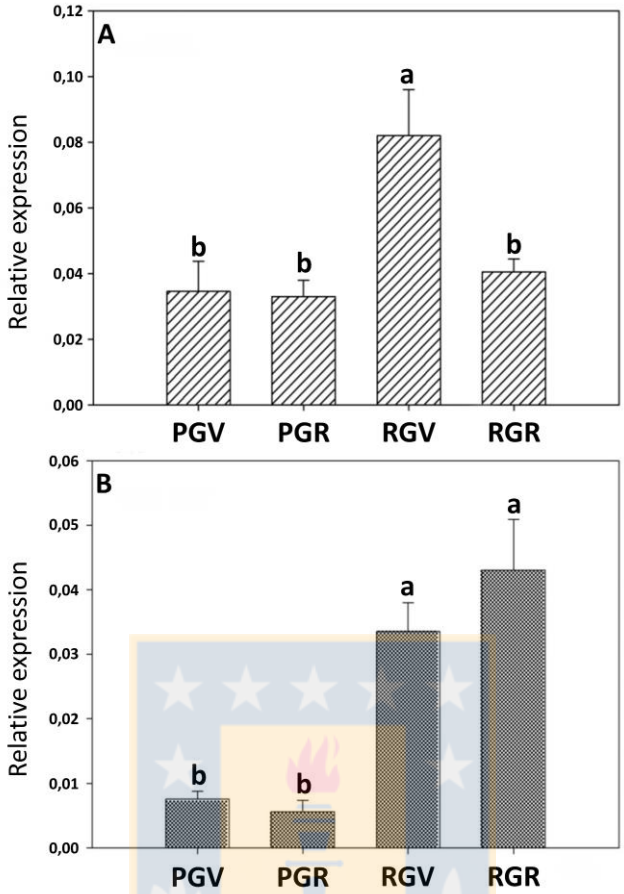

Figure 2.1: Relative expression in Pink Globe (PG) and Red Globe (RG) of (A) VvmybA1, and (B) Vvufgt at véraison (V) and ripening (R) phenological stages. Error bars represent standard error (n = 6) and different letters indicate significant differences ($p < 0.05$).

Identification of VvmybA1 allelic variants

Both RG and PG genotypes carry two *VvmybA1* alleles, namely *VvmybA1a* and *VvmybA1c*, as have been previously described in *V. vinifera* [42] (data not shown).

Fragment of 1,154 bp and 1,166 bp corresponding to *VvmybA1a* and *VvmybA1c*, respectively, were corroborated in both genotypes (Fig. S2.1). Following this, both genes from RG and PG were sequenced and compared with those sequences obtained from the reference grapevine genome PN40024 (Pinot noir-derived line) [48]. No deviation from the reference sequence were found for *VvmybA1a* in both genotypes (Fig. S2.2). However, Figure 2.2 shows a 42 bp insertion following the 218th bp in *VvmybA1c* isolated from PG, which is not present in the reference sequence (Fig. S2.3). This insertion is located in the 5´ region of the gene (noncoding region) and may affect overall expression of the gene, because this

region corresponds to the promoter of the gene, a sequence alteration here could determine the nature of gene expression regulation. However, as this insertion is present in both genotypes (Fig. S2.4), it cannot *per se* be the cause of the difference in RG and PG fruit pigment accumulation.

```
   1  TCCCGTCACTTGGTTGCTTTTTGTCAAGGAAACAGTGGTATCAGAATCCAAATCTTCTACGTAATG   66
  67  TCCCATTCATCCTACCAATGTCCAAATGAATTCCTCTGGACATTAAAATATGGTAGCACGTGGTTG  132
 133  TCTTCGGGATCACACCAGTTTATACATTTGCACCACAAAATAGAGATTGTTCATAAAGGATACTAG  198
 199  TCAGCAATTAATTCCTAAATTTCGCTGTACATTTATAGTAAGTTGATACATAATGGGTAAATATCT  264
 265  CTTATGACACACACCCTTTGTCCATGATGTCCATCGCATTTGGAAGCCAGGTAATGCACCATAAGA  330
 331  AACGTGTCGAATCAACCAATTAGGGGTCTGGTGTCCGAGTCATGAGATAGAACAGGTTCGAGGTTG  396
 397  TTATATATCAATCAATAATTAGAGAAGGAGCCGGTCTCTTGTGTTGAGTTGACTCGATGAAGAGCT  462
 463  TAGGAGTTAGAAAGGGTGCATGGACCCAAGAAGAGGATGTTCTCCTGAGGAAATGCATTGAGAAAT  528
 529  ATGGAGAAGGAAAGTGGCATCTGGTTCCCCTCCGAGCAGGTGACATGAAAGAGAAAGGGATCAGTA  594
 595  TTAATTTGTGTTTTTTTTACTTCTGTTTTGCTTAAAGAGTTTCGTTTTCTTGAGTTTGCAGGGTTG  660
 661  AATAGATGCCTAAAGAGCTGCAGATTGAGATGGCTCAATTATTTGAAGCCAGATATCAAGAGAGGA  726
 727  GAGTTTGCATTAGACGAGGTTGATCTCATGATTAGGCTTCACAATTTGTTGGGGAACAGGCAAGTC  792
 793  TATAATAACTCAAGTACTAGCTTGATAATGATATTATATTAGTTCTGAAGCTGTTCAGAACTTACA  858
 859  AAAGAGCTGTTCAGTTGATACTTTGTCTGATGTTGTGCGTGTATAGATGGTCCTTGATTGCGGGTA  924
 925  GGCTTCCAGGGAGGACTGCTAATGATGTCAAGAACTATTGGCATGGTCACCACCTGAAAAAGAAGG  990
 991  TTCAGTTCCAGGAAGAAGGGAGAAAAAAACCCCAAACACATTCTAAAACCAAAGCTATAAAGCCTC 1056
1057  ACCCTCACAAGTTCTCCAAAGCCTTGCCAAGGTTTGAACTAAAAACTACAGCTGTGGATACTTTTG 1122
1123  ACACACAAGTAAGTACTTCCAGTAAGCCATCATCCACGTCACCACAACCGAATGATGACATCATAT 1188
1189  GGTGGGAAAGCCTGTTAGCTG                                               1209
```

Figure 2.2: PG VvmybA1c sequence obtained using VvmybA1c primers. Point mutations respect of RG nucleotide are marked in red, while those nucleotides in green following the 218th bp were found in both genotypes and represent an insertion in respect to the grapevine reference genome (PN40024).

Of more interest were six SNPs detected when PG and RG *VvmybA1c* sequences were compared. These SNPs occur in the 85th, 305th, 978th, 980th, 1014th and 1016th bp of the amplicon. *In silico* translational analyses carried out in SwissPro revealed differences in two amino acids, located in the 107th and 119th positions, which correspond to phenylalanine and leucine (neutral residues) in RG, and aspartic acid and lysine (acidic and basic residues) in PG, respectively. Further study is required to confirm if these SNPs are responsible for the phenotypic difference(s) observed between RG and PG. For instance, these residues are conserved between RG and the reference genome PN40024. Furthermore, these residues are not part of the HTH (transcription factor) DNA binding motif.

Anthocyanin, flavonol, flavan-3-ol, procyanidins and phenolic acid identification and quantification in Red Globe and Pink Globe grapes

Anthocyanins

Anthocyanin profiles observed in RG and PG skin are shown in Figure 2.3 A. The identification of anthocyanins was carried out according to their UV-Vis profile and $[M-H]^+$ fragments compared with those described in the literature [22,23,44,49]. Table 2.1 presents the retention time and spectral information for the detected anthocyanin signals.

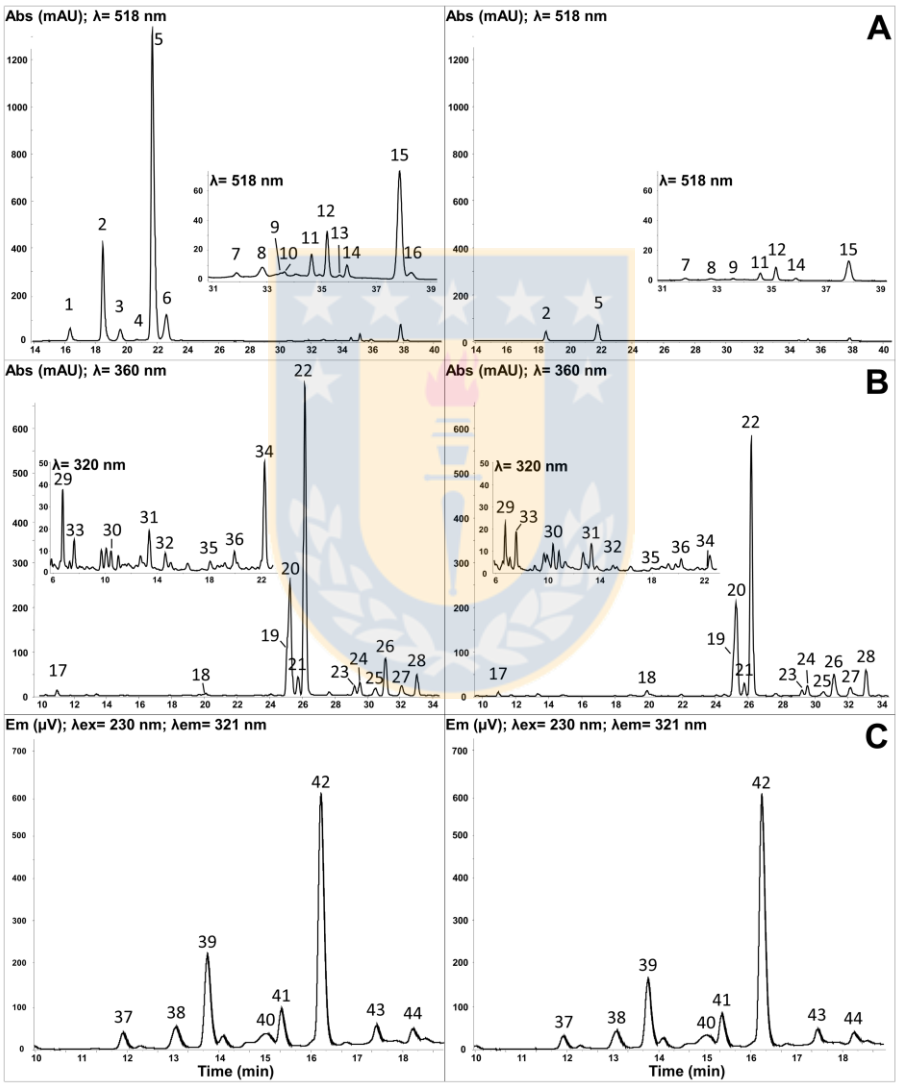

Figure 2.3: Red Globe (left) and Pink Globe (right) polyphenol cromatograms. (A) HPLC-DAD of berry skin anthocyanins at 518 nm. (B) HPLC-DAD of berry skin flavonols at 360 nm and hidroxycinnamic acids at 320 nm. (C) HPLC-FLD of berry seeds using an excitation wavelength of 230 nm and emission wavelength of 321 nm.

Using MS-EPI methods in positive mode, peaks 1 to 6 exhibit a typical neutral loss of 162 amu corresponding to anthocyanin hexoside derivatives. Previous reports shows the same anthocyanin glucosides profile [22,23]. Moreover, peaks 8 and 9 exhibit a neutral loss of 204 amu, produced by the excision of acetyl-glucoside moiety[49,50].

Peak 7 and 11 exhibited a single transition from 611 to 287 and 625 to 301 m/z, with a neutral loss of 324 amu. This could correspond to a dihexoside or caffeoyl-hexoside loss, which have both been previously reported in colored *Vitis vinifera* [50]. To achieve a proper identification, the UV-Vis spectrums were evaluated and matched with a caffeoyl-derivate. Caffeoyl and coumaroyl derivates produce an intense peak around 330 and 310 nm, respectively. Moreover, dihexosides derivates elute before anthocyanins of the 3-glucoside series, and caffeoyl-derivates elute afterwards, as has been previously reported [49,50]. According to these data, the assigned identities corresponded to a cyanidin-3-(6″-caffeoyl)-glucoside and peonidin-3-(6″-caffeoyl)-glucoside.

Moreover, a further two pairs of peaks were elucidated as two different coumaroyl-derivates. Peak 10 and 12 exhibited the same fragmentation from 595 to 287 m/z, with a neutral loss of 308 amu corresponding to a coumaroyl-hexoside derivate. These losses could be explained by a *cis (c)* or *trans (t)* coumaroyl-hexoside derivates as discussed by Castillo-Muñoz et al. [49,51] in other *Vitis vinifera* varieties. Moreover, reported anthocyanin chromatographic profiles indicate that *c*-isomers elute earlier than *t*-isomers, therefore peak 10 was identified as cyanidin-3-(6″-*c*-coumaroyl)-glucoside and peak 12 was identified as cyanidin-3-(6″-*t*-coumaroyl)-glucoside. The other pair of peaks (14 and 16) displayed a 610 to 301 m/z transition, with the same previous neutral loss of 308 amu. Peak 14 was identified as peonidin-3-(6″-*c*- coumaroyl)-glucoside and peak 16 was identified as peonidin-3-(6″-*t*- coumaroyl)-glucoside.

According to the reported anthocyanin elution order, peonidin coumaroyl glucoside isomers elute before malvidin coumaroyl glucoside isomers, and hence the latter peak was identified as malvidin-3-(6″-coumaroyl)-glucoside. Furthermore, petunidin coumaroyl glucoside *c*-isomer elutes following cyanidin coumaroyl glucoside *c*-isomer [49], but was observed here to elute following both cyanidin isomers. Therefore, petunidin isomer identification still remains unclear.

The total monomeric anthocyanin content measured in PG and RG skin was 5.43 ± 0.05 µmol and 35.10 ± 5.25 µmol in 100 g FW of fruit, respectively. Thus, anthocyanin content in PG fruit skin only accounted for 15% of that measured in RG, which is expected due to the observed visual color difference between the fruits. Although some similarities were observed in both of the analyzed grape

skins, functional differences were found when relative concentrations of each anthocyanin were compared.

Table 2.1: *Chromatographic and spectroscopic (UV-vis and MS/MS spectra) characteristics of identified anthocyanins in Pink Globe and Red Globe grape skin extracts by HPLC-DAD-ESI-MS/MS in positive mode.*

Peak	Assignation	t_R (min)	UV-Vis (nm)	$[M-H]^+$ and PI (m/z)	Conc. (µmol/100 g FW)[a]		p value
					PG skin	RG skin	
1	Delphinidin-3-glucoside	16.37	525, 440(sh), 340, 295(sh), 275	465; 303	N.D.	1,23 (±0,21)	<0,05
2	Cyanidin-3-glucoside	18.51	516, 440(sh), 380(sh), 325(sh), 290(sh), 280	449; 287	1,08 (±0,01)	5,69 (±0,89)	<0,05
3	Petunidin-3-glucoside	19.64	525, 445(sh), 350, 295(sh), 275	479; 317	N.D.	1,22 (±0,20)	<0,05
4	Peonidin-3-galactoside	20.72	512, 440(sh), 330(sh), 275	463; 301	N.D.	Traces	-
5	Peonidin-3-glucoside	21.72	516, 440(sh), 380(sh), 330(sh), 290(sh), 280	463; 301	1,70 (±0,02)	19,93 (±2,84)	<0,05
6	Malvidin-3-glucoside	22.63	528, 445(sh), 345, 295(sh), 275	493; 331	N.D.	2,54 (±0,37)	<0,05
7	Cyanidin-3-(6″caffeoyl)-glucoside	31.90	525, 445(sh), 340, 265	611; 287	0,48 (±0,00)	0,46 (±0,09)	>0,05
8	Peonidin-3-(6″acetyl)-glucoside	32.84	518, 450(sh), 355(sh), 305(sh), 278	505; 301	0,48 (±0,00)	0,52 (±0,10)	>0,05
9	Malvidin-3-(6″acetyl)-glucoside	33.51	528, 440(sh), 370(sh), 320(sh), 278	535; 331	Traces	Traces	-
10	Cyanidin-3-(6″-c-coumaroyl)-glucoside	33.64	525, 440(sh), 310(sh), 277	595; 287	N.D.	Traces	-
11	Peonidin-3-(6″caffeoyl)-glucoside	34.64	522, 440(sh), 325(sh), 280	625; 301	Traces	0,55 (±0,10)	<0,05
12	Cyanidin-3-(6″-t-coumaroyl)-glucoside	35.21	522, 440(sh), 310(sh), 280	595; 287	0,55 (±0,01)	0,66 (±0,12)	>0,05
13	Petunidin-3-(6″-coumaroyl)-glucoside	35.67	530, 450(sh), 350(sh), 310(sh), 278	625; 317	N.D.	Traces	-
14	Peonidin-3-(6″-c-coumaroyl)-glucoside	35.94	525, 440(sh), 310(sh), 280	609; 301	0,48 (±0,00)	0,50 (±0,09)	>0,05
15	Peonidin-3-(6″-t-coumaroyl)-glucoside	37.86	521, 440(sh), 312(sh), 282	609; 301	0,66 (±0,01)	1,32 (±0,20)	<0,05
16	Malvidin-3-(6″-coumaroyl)-glucoside	38.29	535, 450 (sh), 306(sh), 280	638; 330	N.D.	0,49 (±0,10)	<0,05
	Total Monomeric Anthocyanin				**5,43 (±0,05)**	**35,10 (±5,25)**	**<0,05**

[a]*Concentrations are expressed as µmol per 100 g of fresh berry weight (FW) in peonidin-3-glucoside equivalents registered at 518 nm. Values are averages (± standard deviation) with n = 3. sh = shoulder.*

Different anthocyanin chromatographic profiles in PG and RG grape skin were observed, as is shown in Figure 2.3 A. Sixteen anthocyanins were detected in RG, with the most abundant being peonidin-3-glucoside (peak 5), followed by cyanidin-3-glucoside (peak 2), which is in agreement with previous reports describing anthocyanin content in RG [22,23]. However, only nine anthocyanins were detected in PG, with the same two major anthocyanins as were observed in RG, as is presented in Table 2.1.

In the 3-glucoside series, the trihydroxylated anthocyanin derivates delphinidin, petunidin, and malvidin comprised approximately 15% of the total anthocyanin content in RG. These compounds were not detected in PG. Moreover, the dihydroxylated anthocyanin derivates cyanidin and peonidin comprised approximately 70% of the total anthocyanin content in RG, and only 51% of total anthocyanin content in PG. In the 3-galactoside series, only peonidin was detected at trace levels in RG.

In the (6″-caffeoyl)-glucoside series, only cyanidin and peonidin (dihydroxylated) derivates were detected. For cyanidin, no differences were observed in total concentration, but relative concentration differed with 1.3% in RG and 8.9% in PG. Peonidin-3-(6″-caffeoyl)-glucoside was present in a quantifiable concentration in RG only, and accounted 1.6% of the total anthocyanin content.

Only two methylated anthocyanin derivates were found in the (6″-acetyl)-glucoside series, namely peonidin and malvidin, although the latter was not present in a quantifiable concentration in either grape skin. Peonidin-3-(6″-acetyl)-glucoside exhibited the same accumulation pattern as was observed for cyanidin-3-(6″-caffeoyl)-glucoside, in that no differences were observed in total concentration, but relative concentration significantly differed with 1.5% in RG and 8.8% in PG.

The (6″-coumaroyl)-glucoside series exhibited the mono- and di-methylated forms of the trihydroxylated anthocyanin derivates petunidin and malvidin. As described above, petunidin and malvidin derivates could not be identified as *c* or *t* isomers. Petunidin derivate was not detected in PG and only traces were found in RG, while malvidin derivate concentration was significantly higher in RG (Table 2.1), although analysis of relative concentration revealed the opposite trend, with 12.1% in PG and 3.75% in RG.

This series also showed the di-hydroxylated anthocyanin derivates cyanidin and peonidin. Interestingly, *c* and *t* coumaroyl glucoside isomers were observed for both compounds. The *c* isomer of cyanidin-3-(6″-coumaroyl)-glucoside was detected at trace levels in RG alone. No significant differences were found in levels of the *t* isomer in both grape skin types, however, relative concentrations strongly differed (1.9% in RG and 10% in PG). Additionally, the *c* isomer of peonidin-3-(6″-coumaroyl)-glucoside was found at a similar concentration in both grape skin types, but analysis of its relative concentration revealed considerable differences, with 1.4% in RG and 8.8% in PG. Finally, the *t* isomer of peonidin-3-(6″-coumaroyl)-glucoside was found only in RG, with a relative concentration of 1.4%.

Flavonols

Flavonol profiles observed in RG and PG skin are shown in Figure 2.3 B. Briefly, 12 flavonols were identified in both genotypes, as is summarized in Table 2.2.

Table 2.2: Chromatographic and spectroscopic (UV-vis and MS/MS spectra) characteristics of identified flavonols and other phenolics (hydroxycinnamic acids (HCADs), flavan-3-ols, and stilbenoids derivates) found in Pink Globe and Red Globe grape skin extracts by HPLC-DAD-ESI-MS/MS in negative mode.

Peak	Assignation	t_R (min)	UV-Vis (nm)	$[M-H]^-$ and PI (m/z)	Conc. (µmol/100 g FW)[a]		p value
					PG skin	RG skin	
17	Quercetin-dihexoside[b]	10.98	352, 285(sh), 266(sh), 245	625; 463, 301	0,14 (±0,00)	0,18 (±0,02)	<0,05
18	Miricetin-3-glucoside[b]	19.91	353, 307(sh), 265(sh), 245	479; 317	0,11 (±0,03)	0,07 (±0,02)	>0,05
19	Quercetin-3-galactoside[b]	25.27	353, 305(sh), 265(sh), 245	463; 301	3,84 (±0,72)	4,59 (±0,82)	>0,05
20	Quercetin-3-glucuronide[b]		353, 302(sh), 265(sh), 245	477; 301			
21	Quercetin-3-rutinoside[c]	25.74	350(sh), 290, 270(sh), 246	609; 301	0,46 (±0,08)	0,49 (±0,09)	>0,05
22	Quercetin-3-glucoside[c]	26.18	353, 305(sh), 265(sh), 254	463; 301	5,08 (±0,90)	7,73 (±0,70)	<0,05
23	Kaempferol-3-galactoside	29.20	344, 325(sh), 300(sh) 265(sh), 246	447; 285	0,30 (±0,00)	0,36 (±0,04)	>0,05
24	Quercetin-formyl-galactoside adduct[d]	29.56	353, 300(sh), 265(sh), 246	491; 463, 301	0,17 (±0,02)	0,24 (±0,01)	<0,05
25	Quercetin-rhamnoside[c]	30.51	348,300(sh), 265(sh), 246	447.5	0,22 (±0,05)	0,29 (±0,06)	>0,05
26	Kaempferol-3-glucoside[b]	31.15	344, 325(sh), 300(sh) 265(sh), 246	447; 285	1,30 (±0,10)	1,49 (±0,12)	>0,05
27	Quercetin-formyl-glucoside adduct[d]	32.17	353, 305(sh), 265(sh), 246	491; 463, 301	0,69 (±0,12)	0,49 (±0,06)	>0,05
28	Isoramnetin-3-glucoside[b]	33.08	353, 302(sh), 265(sh), 246	477; 315	0,62 (±0,08)	0,60 (±0,13)	>0,05
	Total Flavonol				**13,05 (±1,81)**	**15,89 (±0,72)**	>0,05
29	Caffeoyl-hexoside[b]	6,70	328, 300(sh), 248	341; 179, 161	0,76 (±0,31)	0,96 (±0,58)	>0,05
30	Coumaroyl-hexoside[b]	10,45	282, 245	325; 163, 119	N.D.[e]	N.D.[e]	N.D.[e]
31	Cholorogenic acid I[b]	13,36	327, 305(sh), 246	353; 191	0,65 (±0,22)	1,00 (±0,18)	>0,05
32	Cholorogenic acid II[b]	14,60	322, 300(sh). 246	353; 191	N.D.	0,54 (±0,32)	<0,05
	Total HCADs				**1,41 (±0,52)**	**2,50 (±0,69)**	**>0,05**
33	(+)-Catechin[c]	7,60	288, 244	289; 244	0,62 (±0,07)	0,53 (±0,14)	>0,05
	Total flavan-3-ols				**0,62 (±0,07)**	**0,53 (±0,14)**	**>0,05**
34	trans-piceid[c]	22,24	305, 315	389; 227	N.D.	2,24 (±1,36)	<0,05
	Total stilbenoids				**N.D.**	**2,24 (±1,36)**	**<0,05**
	Other compounds						
35	Unknown	18,02	279, 246	366; 204, 186, 142			
36	Unknown	20,15	260(sh), 245	403; 244, 241, 213			

[a]Flavonols concentrations are expressed as µmol per 100 g of fresh berry weight (FW) in quercetin-3-glucoside equivalents registered at 360, HCA derivates concentrations are expressed as 5-caffeoylquinic acid equivalents registered at 320 nm, stilbenoids concentrations are expressed as (E)-piceid equivalents registered at 305 nm, and flavan-3-ol concentrations are expressed as (+)-catechin equivalents registered at 280 nm. Values are averages (± standard deviation) with n = 3. [b]Not quantified due to impurity coelution. sh = shoulder.

The most abundant flavonols in RG were quercetin-3-glucuronide and quercetin-3-glucoside, in agreement with previous reports [22,23]. The identification of flavonols was carried out according to their UV-Vis profiles and $[M-H]^-$ fragments, available in literature [22,23,44,49].

Five flavonols require further analysis in addition UV-Vis max and mass spectra comparisons. Peak 17 was the first detected flavonol, showing a pseudomolecular ion at 625 m/z and a two-step fragmentation at 463 and 301 m/z, which indicted a hexoside excision in two different positions of the quercetin molecule [44]. Peak 21 corresponded to quercetin-3-rutinoside ($[M-H]^-$: 609), which co-eluted with an unidentified compound with UV-Vis max at 290 nm, and peak 25 corresponded to quercetin-3-rhamnoside ($[M-H]^-$: 445). Both of these compounds were further corroborated by comparing their retention times with those of their respective standards. Peak 24 and 27 exhibit a pseudomolecular ion at 491 m/z and a two-step fragmentation at 463 and 301 m/z, which indicates a formyl and hexoside excision and were tentatively assigned as quercetin-formyl-galactoside and glucoside, respectively. This derivative could be formed during extraction procedure due the use of formic acid, however previous reports does not shows formyl derivatives although use the same extraction solvent [22].

Total flavonol content found in PG and RG skin was 13.05 ± 1.81 and 15.89 ± 0.72 µmol in 100 g FW fruit, respectively, which revealed no significant difference in total flavonol content between the two grape skin types ($p > 0.05$) (Table 2.2).

Quercetin-3-galactoside/quercetin-3-glucuronide (coeluting peaks 19/20) and quercetin-3-glucoside (peak 22) were the major flavonols found in both grape skin types. Their combined concentrations were 8.92 and 12.32 µmol in 100 g FW fruit in PG and RG, respectively. Only quercetin-dihexoside, quercetin-3-glucoside and quercetin-formylgalactoside (peak 24) were present at a lower concentration in PG than in RG. Moreover, miricetin-3-glucoside (peak 18), quercetin-3-galactoside/quercetin-3-glucuronide, quercetin-3-rutinoside, kaempferol-3-galactoside (peak 23), kaempferol-3-glucoside (peak 26), quercetin-formylglucoside (peak 27), and isorhamnetin-3-glucoside (peak 28) showed no significant differences in their concentrations in both grapes skin types.

Phenolic acids and other derivates

Hidroxycinnamic acids (HCADs) and stilbenoids were observed in grape skin extracts during the first minutes of the flavonol chromatogram at 320 nm. In RG, three HCADs and one stilbenoid derivate were identified as caffeoyl-hexoside (peak 29), chlorogenic acid I (peak 31), chlorogenic acid II (peak 32), and (*E*)-piceid (peak 34), as is shown in Figure 2.3 B. A further compound identified as coumaroyl-hexoside (peak 30) was also observed coeluting with an impurity. Previous reports indicates presence of

tartaric acid derivatives such as caftaric, fertaric and coutaric acids[22,50]. 311, 325 and 295 m/z pseudomolecular ions along with 179, 193 and 163 m/z fragments were searched to corroborate its presence, however it was not detected. Identities were assigned based on comparisons with UV-vis spectra and $[M-H]^-$ fragments found in the literature [51,52].

Table 2.2 shows that caffeoyl-hexoside and chlorogenic acid I were detected in both genotypes, whereas chlorogenic acid II and (*E*)-piceid were detected in RG only. Total concentrations of HCADs and stilbenoid derivates were not significantly different, although a tendency of both compounds to accumulate in higher amounts was observed in RG.

Flavan-3-ols and Procyanidins

Flavan-3-ols and procyanidins were examined in grape skin and seed extracts. RP-HPLC-FLD was validated (table S2.3) and used to detect them in seeds extract (Figure 2.3 C), and in skin, these compounds were detected in the first minutes of the flavonol chromatograms at 280 nm. In skin extracts, only a single compound, namely (+)-catechin (peak 33), was identified, while in seeds, eight compounds, namely (+)-catechin (peak 39), (-)-epicatechin (peak 42), procyanidin B1 (peak 37), B2 (peak 41), B3 (peak 38), B4 (peak 40), PD (peak 43), and procyanidin C1 (peak 44), were identified. Identification of compounds were based on comparisons with UV-Vis profiles (or selectively observed based on their λex/λem in FLD) and $[M-H]^-$ fragments found in the literature, as well as the elution order of each compound [46,53].

As is shown in Table 2.2, no significant difference in (+)-catechin content was revealed in the two grape skin analized. Furthermore, the levels of flavan-3-ols found in PG seeds were 13% higher than those measured in RG due to a higher abundance of (-)-epicatechin in PG, as is shown in Table 2.3. For procyanidins, only B4 was present at a higher concentration in PG than in RG, with a significant difference of 18%, although no significant difference was observed in total procyanidin content.

In order to comparatively evaluate the metabolic pathways active in PG and RG, a principal components analysis (PCA) was performed using the relative concentrations described above. PCA revealed positive correlation of RG with dihydroxy-anthocyanins (peonidin derivates, with the exception of peonidin-3-(6″acetyl)-glucoside; and cyanidin-3-(6″cis-coumaroyl)-glucoside), trihydroxy-anthocyanins glucosides (delfinidin, malvidin and petunidin 3-glucoside), quercetin-3-glucoside, and quercetin-formyl-galactoside.

Table 2.3: *Chromatographic and spectroscopic (UV-vis and MS/MS spectra) characteristics of identified flavan-3-ols and procyanidins found in Pink Globe and Red Globe seed extracts by HPLC-FL and HPLC-ESI-MS/MS in negative mode.*

Peak (nº)	Assignation	t_R (min)	[M-H]- and PI (m/z)	Concentration (µmol/100 g FW)[a]		p value
				PG seed	RG seed	
39	(+)-Catechin	13,755	289; 245	2,06 (±0,17)	2,33 (±0,04)	>0,05
42	(-)-Epicatechin	16,217	289; 245	7,80 (±0,40)	6,37 (±0,34)	<0,05
	Total Flavan-3-ols			**9,86 (±0,55)**	**8,70 (±0,38)**	<0,05
37	Procyanidin B1	11,928	577; 425, 407, 289	0,59 (±0,03)	0,59 (±0,03)	>0,05
38	Procyanidin B3[b]	13,071	577; 425, 407, 289	0,58 (±0,03)	0,56 (±0,03)	>0,05
40	Procyanidin B4[b]	15,017	577; 425, 407, 289	0,33 (±0,02)	0,27 (±0,02)	<0,05
41	Procyanidin B2	15,362	577; 425, 407, 289	0,63 (±0,02)	0,60 (±0,04)	>0,05
43	PD	17,421	577; 425, 407, 289	0,36 (±0,03)	0,32 (±0,03)	>0,05
44	Procyanidin C1	18,212	865; 577, 289	0,27 (±0,02)	0,26 (±0,02)	>0,05
	Total Procyanidin			**2,77 (±0,14)**	**2,60 (±0,16)**	**>0,05**

[a]*Concentrations are expressed as µmol per 100 g of fresh berry weight (FW) in (+)-Catechin. Procyanidin B1, B2, and C1 equivalents registered at* $\lambda_{exitation}$ *= 230 nm and* $\lambda_{emission}$ *= 321 nm. Procyanidin dimers (PD) are expressed as procyanidin B1 equivalents. Values are averages (± standard deviation) with n = 3.* [b]*Assigned based on elution order according to Tsang et al.*[52].

On the other hand, PG exhibited positive correlation with only dihydroxy anthocyanins, quercetin-formyl-glucoside, its methylated derivate isorhamnetin-3-glucoside, and myricetin-3-glucoside, a trihydroxilated flavonol. These observations could be explained by the metabolic pathway of flavonoids (Figure 2.4).

RG contains tryhydroxylated anthocyanin, probably as a result of higher *Vvufgt* expression, which was discussed previously. PG contains its analogous flavonol (myricetin-3-glucoside) as a result of lower levels of *Vvufgt* expression. That is, in PG, dihydromyricetin only followed the flavonol pathway while in RG, dihydromyricetin also followed the anthocyanin pathway. Moreover, RG showed higher correlation with the methylated dihydroxylated anthocyanin (peonidin-3-glucoside) and its derivates, while in PG this correlation was more important with the non-methylated analogous compound (cyanidin-3-glucoside) and its derivatives. This difference may be attributed to the substrate concentration availability, and not lower expression levels of O-methyltransferase, because PG still shows higher peonidin-3-glucoside concentration than cyanidin-3-glucoside, however a higher ratio value is observed in RG when 3´OMT activity is calculated[54].

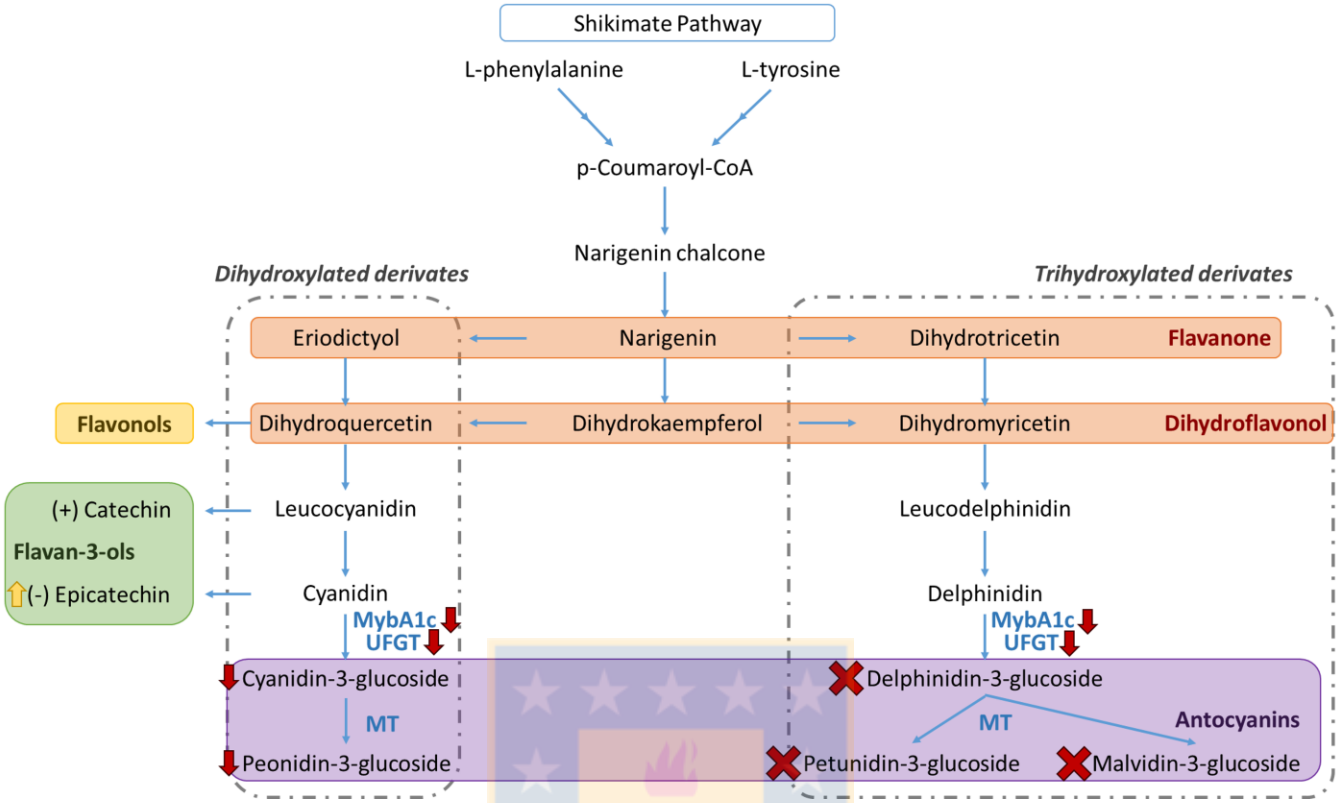

Figure 2.4: Flavonoid pathway of PG (modified from Gutha et al.[55]). Red "x": not detected in skin; red arrow: significant reduction compared to RG in skin; yellow arrow: significant increment compared to RG in seeds. MybA1c: transcription factor MYB-type; UFGT: UDP-glucose:flavonoid-3-O-glucosyltransferase; MT: methyl transferase.

Changes in phenolic compounds during ripening process

Concentrations of phenolics in both grape varieties were studied at two different stages, at 50% *véraison* and ripen, in order to better characterize differences in their phenolics. The obtained concentrations for each family of compounds in skin and seed including total phenolics are summarized in Table 2.4.

PG grape did not show statistical difference for total phenolics in both stages ($p>0.05$). However, this genotype showed an increase of total anthocyanin concentration in the skin and decrease of flavan-3-ol in seed, while the other phenolics not showed statistical differences over the ripening process. On the other hand, RG showed an important increase of total phenolics at expense mainly of anthocyanin increase in the skin; however, this tendency was also observed for all other phenolics with exception of flavan-3-ol and HCADs in skin. The detection of stilbenoids was verified in the ripen RG stage showing only (*E*)-piceid.

Table 2.4: *Total concentrations of phenolics found in Pink Globe and Red Globe skin and seed extracts at véraison and ripen stages.*

	Phenolics	Pink globe		Red Globe	
		Véraison µmol/100 g FW[a]	Ripen µmol/100 g FW[a]	*Véraison* µmol/100 g FW[a]	Ripen µmol/100 g FW[a]
Skin	Total Anthocyanins	3,23 (±0,16)	5,43 (±0,05)[b]	13,32 (±1,63)	35,1 (±5,25)[b]
	Total Flavonols	10,96 (±3,56)	13,05 (±1,81)[c]	12,18 (±0,97)	15,89 (±0,72)[b]
	Total HCADs	1,77 (±0,89)	1,41 (±0,52)[c]	0,88 (±0,34)	2,50 (±0,69)[c]
	Total Flavan-3-ols	0,58 (±0,02)	0,62 (±0,07)[c]	0,35 (±0,10)	0,53 (±0,14)[c]
	Total Stilbenoids	nd	nd	nd	2,23 (±1,36)[b]
Seed	Flavan-3-ol	13,78 (±0,41)	9,87 (±0,55)[b]	7,86 (±0,26)	8,70 (±0,38)[b]
	Procyanidins	2,58 (±0,15)	2,77 (±0,14)[c]	1,65 (±0,12)	2,60 (±0,16)[b]
	Total phenolics[d]	**32,91 (±3,69)**	**33,14 (±1,96)[c]**	**36,25 (±1,94)**	**69,78 (±5,84)[b]**

[a]*Each polyphenols family are expressed as the sum of each family compound (in µmol) per gram of fresh skin weight (FW) as average values (± standard deviation) with n = 3.* [b]*Statistical difference ($p < 0.05$) between both ripening stages.* [c]*No statistical differences ($p > 0.05$) between both ripening stages.* [d]*Obtained as the sum of all quantified phenolics by HPLC-DAD.*

Antioxidant capacity of whole and SPE fractions of PG and RG extracts

In order to comparatively evaluate the antioxidant capacity of both genotypes, ABTS and CUPRAC assays were performed in PG and RG skin methanolic extracts, as well as in non-anthocyanin phenolic compounds and monomeric anthocyanins SPE fractions (Table 2.5).

Table 2.5: *Trolox equivalent antioxidant capacity (TEAC) values obtained from Pink Globe and Red Globe skin extracts using ABTS and CUPRAC methodology.*

	$TEAC_{ABTS}$ (µmol TE / g FW)[a]	$TEAC_{CUPRAC}$ (µmol TE / g FW)[a]
PG skin methanolic extract	16,52 (±1,07)	21,36 (±1,26)
PG Flavonol SPE fraction	3,34 (±0,07)	1,86 (±0,02)
PG Anthocyanin SPE fraction	3,75 (±0,08)	1,14 (±0,08)
RG skin methanolic extract	17,54 (±0,71)	22,15 (±2,04)
RG Flavonol SPE fraction	3,53 (±0,05)	1,92 (±0,16)
RG Anthocyanin SPE fraction	4,85 (±0,04)	3,81 (±0,21)

[a]*Expressed as Trolox equivalents per gram of fresh skin weight (FW) as average values (± standard deviation) with n = 3.*

The sum of the antioxidant capacities of the studied fractions revealed by ABTS assay was approximately 50% of the antioxidant capacity of the crude extract. This was observed for both PG and RG grape skins. For the CUPRAC assay, the sum of the antioxidant capacities of the fractions were 14% and 26% of the PG and RG crude extracts, respectively. These results could be explained by the presence of other reducing compounds in the skin. In addition, these differences could be the result of other compounds with higher relative responses in CUPRAC method conditions. Moreover, the possible synergistic effects of polyphenols when they are present together in a single extract should be considered [56,57].

As is shown in Table 2.5, PG and RG exhibited antioxidant capacity by both assayed methods. Methanolic extract of PG skin revealed no significant difference in $TEAC_{ABTS}$ and $TEAC_{CUPRAC}$ values in respect to RG. These results indicate that, although polyphenol content is lower in PG, nutraceutical potential in terms of antioxidant capacity is not reduced, showing that both analyzed genotypes are equivalent.

Section 2

Title: **Caracterización y cuantificación de compuestos fenólicos en fruto y semilla de calafate (*Berberis microphylla*).**

Abstract

El fruto de calafate (*Berberis microphylla*) es una baya comestible azul oscuro de 7 a 11 mm de diámetro. Es una planta silvestre no cultivada, muchas veces considerada como maleza. Estudios previos de sus frutos han descrito niveles de concentración de antocianos mayores a los encontrados en otras bayas ampliamente consumidas. Los estudios realizados por HPLC-DAD indican que el fruto de calafate contiene entre 60 a 400 veces más antocianos que variedades de uva de mesa estudiadas (Red Globe y Pink Globe). Además, contienen 45 veces más ácidos hidroxicinámicos y 15 veces más flavonoles.

Los estudios de capacidad antioxidante mediante CUPRAC y ABTS indican una actividad antioxidante 300 veces mayor en fruto de calafate que en Red Globe y Pink Globe.

También se estudió el contenido de flavan-3-oles y procianidinas en semillas de calafate, encontrándose niveles no cuantificables de (+)-catequina, (-)-epicatequina, procianidina B2 y otro dímero de procianidina.

Finalmente, se elaboró un extracto apto para el consumo de animales de experimentación, utilizando como solvente de extracción etanol potable. El estudio de recuperación indicó que se alcanza un 84% de polifenoles extraídos en comparación con la extracción clásica con metanol, obteniendo un extracto inocuo con un rendimiento aceptable con una concentración de 265.26 µmol de polifenoles por gramo de extracto.

Experimental

Solventes y estándares

Se utilizaron reactivos detallados en la sección 1, junto con etanol potable (Oxiquim, Concepción, Chile) y ácido 5-cafeoilquínico (Phytolab, Vestenbergsreuth, Germany).

Material vegetal

Se acumuló un lote de 500g de fruto de calafate maduro y congelado proveniente de la región de Magallanes (año 2015), el cual se molió para asegurar homogeneidad y se congelo a -20°C hasta su extracción y/o análisis cromatográfico.

Equipamiento

Los análisis por HPLC-DAD de polifenoles se realizaron con un sistema HPLC shimadzu (Kyoto, Japón) equipado con una bomba cuaternaria LC-10ADVP, una unidad de elución FCV-10ALVP, unidad degasificadora DGU-14A, horno CTO-10AVP y un detector UV-Vis de arreglo de diodos (DAD) SPD-M10AVP. El control del sistema y colección de datos se realizó usando el software de Shimadzu CLASS-VP.

Pretratamiento de muestra

Extracción de fruto y semilla de calafate

Las metodologías de extraccion utilizadas para los análisis de antocianos, flavonoles y ácidos hidroxicinámicos (HCADs) en fruto y de flavan-3-oles y procianidinas en semillas de calafate son las ya descritas para uvas Pink Globe y Red Globe detallado en la sección 1.

Análisis de polifenoles

Análisis de antocianos

Para el análisis de antiocianos en frutos de calafate se utilizó la metodología propuesta por Ruiz y col [44]. Brevemente, se utilizó una columna Kromasil C18 de 250 x 4.6 mm, 5 μm, con una precolumna Nova-Pak (Waters, Milford, Conneticut, USA) C18 de 22 x 3.9 mm, 4 μm a 40°C. Se utilizó agua/acetonitrilo/ácido fórmico (87:3:10% v/v/v) como fase móvil A y agua/acetonitrilo/ácido fórmico (40:50:10% v/v/v) como fase móvil B. El flujo fue de 0.8 mL/min y la cuantificación se realizó a 518 nm mediante interpolación de una curva de calibrado de delfinidina-3-glucósido.

Análisis de flavonoles

Para el análisis de flavonoles en frutos de calafates se utilizó la metodología propuesta por Ruiz y col [58]. Brevemente, se utilizó una columna core-shell C18 Kinetex de 150 x 4.6 mm, 2.6 μm, con una precolumna UHPLC Phenomenex AJ0-9000 de 22 × 3.9 mm, 2.2 μm a 30°C. Se utilizó agua/ácido

fórmico (99.9:0.1% v/v) como fase movil A y acetonitrilo como fase movil B. El flujo usado fue de 0.5 mL/min y la cuantificación se realizó a 360 nm mediante interpolación de una curva de calibrado de quercetina-3-glucósido.

Análisis de ácidos hidroxicinámicos

Para el análisis de HCADs en frutos de calafates se utilizó la metodología propuesta por Ruiz y col [59]. Brevemente, se utilizó una columna Kromasil C18 de 250 x 4.6 mm, 5 μm, con una precolumna Nova-Pak C18 de 22 x 3.9 mm, 4 μm a 40°C. Se utilizó agua/ácido fórmico (99.9:0.1% v/v) como fase movil A y acetonitrilo como fase movil B. El flujo usado fue de 0.5 mL/min y la cuantificación se realizó a 320 nm mediante interpolación de una curva de calibrado de ácido 5-cafeoilquínico.

Análisis de flavan-3-oles, procianidinas y ensayos antioxidantes CUPRAC y ABTS

Las condiciones cromatográficas para el análisis de flavan-3-oles y procianidinas, junto a los ensayos de capacidad antioxidantes son los mismos que aquellos descritos en la sección 1.

Resultados y discusión

Comparación del contenido de compuestos fenólicos en Red Globe, Pink Globe y Calafate

Se contrastaron los niveles de compuestos fenólicos derivados de la vía de los fenilpropanoides obtenidos de uvas Red Globe (RG) y Pink Globe (PG) (n=3) con los obtenidos en Calafate (C) (n=3). Además, se han descrito muy bajas concentraciones de flavan-3-oles en fruto de calafate [44], por lo que estudió el contenido de flavan-3-oles y procianidinas en semillas del fruto.

Contenido de Antocianos y Flavonoles

Los flavonoides son compuestos fenólicos que consisten en dos anillos aromáticos (anillos A y B) conectado por un heteroanillo (anillo C). Dentro de esta familia de metabolitos secundarios, las más altas concentraciones corresponden a los antocianos, seguidos de flavonoles. La Figura 2.5 A muestra las concentraciones totales como suma de cada uno de estas familias obtenidas en fruto de C, RG y PG. En relación a contenido total, C contiene más de 60 veces el contenido de antocianos que RG y más de 400 veces que PG. Por otro lado, C contiene más de 15 veces la concentración de flavonoles que RG y PG. En concordancia con Ruiz y col [44,58], los antocianos mayoritarios en C corresponden a derivados trihidroxilados en el anillo B: delfinidina-3-glucósido, petunidina-3-glucósido y malvidina-3-glucósido, mientras que en RG y PG los antocianos mayoritarios corresponden a derivados dihidroxilados: cianidina-3-glucósido y peonidina-3-glucósido. En relación al contenido de flavonoles mayoritarios en C

corresponden a derivados dihidroxilados: quercetina-3-rutinósido, 3-galactósido e isoramnetina-3-rutinósido.

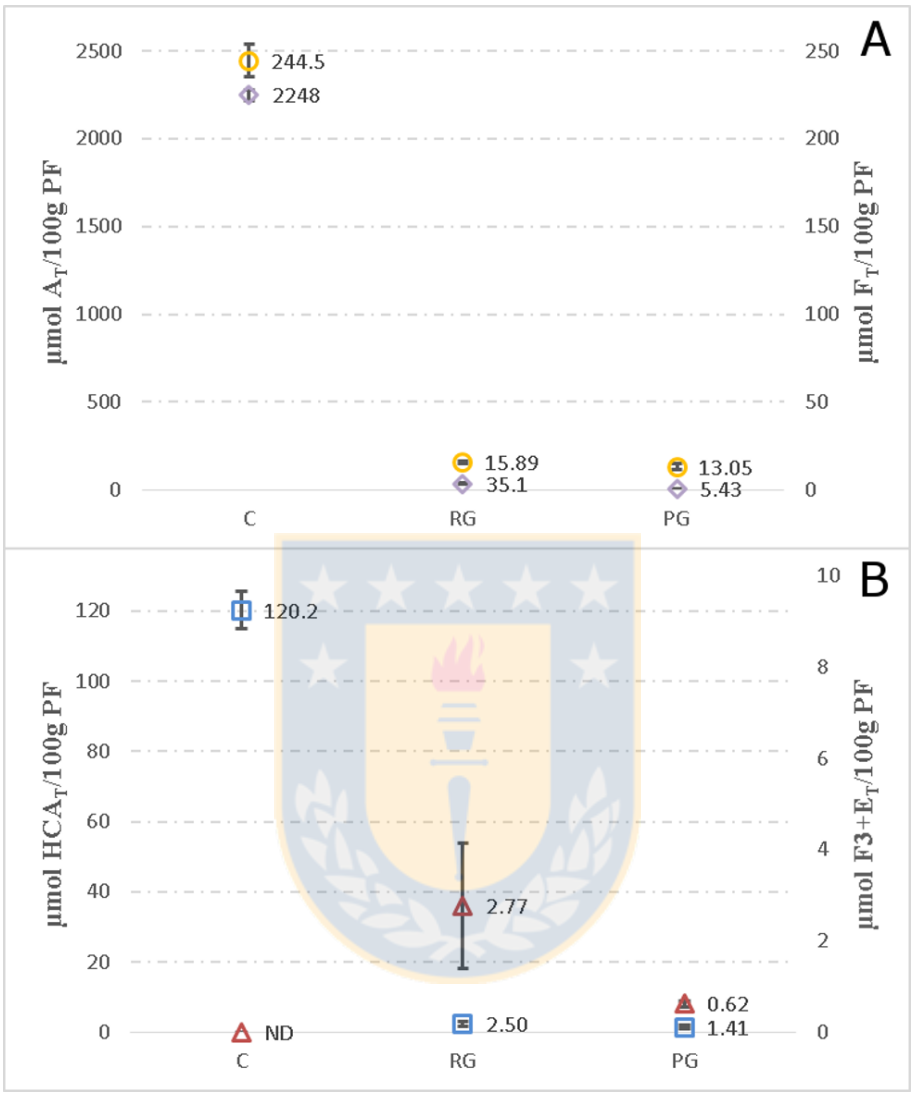

Figura 2.5: Concentraciones de (poli)fenoles en fruto de C, RG y PG. A) Concentraciones de Antocianos totales (A_T) y Flavonoles totales (F_T) en 100 g peso fresco (PF) de fruto. B) Concentraciones de ácidos hidroxicinámicos totales (HCA_T) y Flavan-3-oles + estilbenoides totales ($F3+E_T$) en 100 g PF de fruto (diamante morado indica A_T, circulo amarillo indica F_T, cuadrado azul indica HCA_T y triangulo rojo indica $F3+E_T$).

La concentración, sustitución en el anillo B y la molécula de azúcar son características importantes al evaluar la biodisponibilidad de los flavonoides [60,61]. En ensayos de bioactividad de antocianos se ha observado que los derivados de delfinidina ofrecen mayor protección al evaluar biomarcadores

cardiovasculares y de síndrome metabólico que los derivados de cianidina [60].Por otro lado, el azúcar influye directamente en la absorción. Se ha observado que quercetina-3-glucósido es de-glucosilado mediante lactato phlorizin hidrolasa (LPH) y luego la aglicona es absorbida a nivel de intestino delgado. Sin embargo, esto no ocurre con el rutinósido, el cual alcanza el colon y es subsecuentemente deglucosilado por β-glucosidasas presentes en la microbiota [61].

Contenido de derivados de ácidos hidroxicinámicos

Los derivados de HCADs son compuestos fenólicos con estructura base de fenilacrílico que pueden presentar unidades de ácido quínico, tartárico, glucárico y aminoácidos producto de condensación [59,62]. La Figura 2.5 B muestra el contenido de ácidos totales como suma de HCADs cuantificados por HPLC en C, RG y PG. El fruto C contiene entre 45 a 90 veces la concentración de HCADs totales que la descrita en RG y PG, respectivamente. En los tres casos se encuentran derivados de ácido cafeico. Mientras que en RG y PG se identificaron derivados cafeoil-hexósido y cafeoil-quínico, no se detectaron los derivados tartáricos descritos por Cantos y col [22]. Por otro lado, en C se encontraron como mayoritarios derivados cafeoil-glucáricos y cafeoil-quínicos [59].

Contenido de Flavan-3-oles y estilbenoides

Los flavan-3-oles (F3) son parte de la familia de los flavonoides y se encuentran en menores concentraciones que los compuestos fenólicos anteriormente descritos. Por otro lado, los estilbenoides (E) son moléculas altamente bioactivas y tienen el mismo origen que los flavonoides (vía fenilpropanoide), entre los que se encuentra el *trans*-resveratrol. La Figura 2.5 B muestra el contenido de F3 junto a E totales en frutos de C, RG y PG. En RG y PG se encuentran el F3 (+)-catequina, mientras que sólo en el primero se encuentra *trans*-piceido (derivado glucósido de resveratrol). En C no se detectaron cantidades cuantificables de F3 y E, sin embargo se ha reportado presencia de F3 [44].

Contenido de flavan-3-oles y procianidinas en pepas de calafate

Con el fin de caracterizar el contenido de F3 y procianidinas (PC), se realizó la extracción de estos compuestos fenólicos en semilla de calafate, según lo descrito para semillas de uvas RG y PG.

Debido a la baja absortividad molar a 280 nm de los flavan-3-oles y procianidinas, se acopló un detector de fluorescencia posterior a la cromatografía con el fin de mejorar la sensibilidad. En la tabla 2.6 se enumeran los compuestos encontrados en semilla de calafate. Se encontraron cantidades no cuantificables de (+)-catequina, (-)-epicatequina, procianidina B1 y un posible B2. Adicionalmente, se realizó una búsqueda de compuestos mayoritarios reportados anteriormente en el fruto de calafate mediante espectrometría de masas [58,59].

Tabla 2.6: Características cromatográficas y espectrométricas de flavan-3-oles, procianidinas y otros compuestos fenólicos encontrados en extractos de semilla de Calafate (Berberis microphylla) analizados por HPLC-FL-MS/MS en modo negativo.

N° Peak	Identidad	tR	[M-H]-	MS/MS
1	Ácido gálico-hexósido[a]	5.42	331	169
2	*No identificado*	8.46	315	153
3	*No identificado*	9.88	446	284
4	*No identificado*	10.41	460	298
5	Ácido elágico-hexósido[a]	12.11	463	301
6	Dímero procianidina[a]	12.20	577	-
7	*No identificado*	12.44	479	299
8	Isómero 1 ácido clorogénico[a]	12.88	353	179
9	(+)-Catequina[b]	13.75	289	245
10	Ácido 3-cafeoilquínico[a]	13.89	354	179
11	*No identificado*	14.28	502	340
12	Dímero procianidina B2[b]	15.30	577	289
13	(-)-Epicatequina[b]	16.02	289	245
14	Isómero 3 ácido clorogénico[a]	17.32	354	179
15	Quercetina-rutinósido[a]	20.91	609	301
16	Quercetina-galactósido[a]	22.47	463	301
17	Isoramnetina-rutinósido[a]	25.13	623	315
18	Quercetina-ramnósido[a]	26.82	447	301

[a]Identidad asignada de acuerdo a bibliografía, bibliotecas y MS/MS. [b]Identidad asignada de acuerdo a bibliografía, bibliotecas, MS/MS y tiempo de retención de patrones.

Se encontraron 3 isómeros de ácidos clorogénicos seguidos de derivados de flavonoles. El isómero 2 del ácido clorogénico se encontró en mayor cantidad respecto al isómero 1 y 3. De acuerdo a lo publicado en frutos, el isómero ácido 5-O-cafeoilquínico corresponde al mayoritario, lo cual podría ser cierto en el caso de las semillas [59].

Lo mismo aplica en los derivados de quercetina e isoramnetina. En el caso de quercetina-hexósido se ha reportado anteriormente como mayoritario el derivado galactósido, mientras que el derivado deoxihexósido de quercetina corresponde a ramnósido[44,58]. Finalmente, se encontraron derivados de quercetina e isoramnetina asociado a dos hexosas. El espectro de masas corresponde a una perdida directa de los dos grupos de hexosas característico de disacáridos. Anteriormente, se han reportado estos compuestos como quercetina e isoramnetina-rutinósido [58]. Adicionalmente, se identificó un hexósido de ácido gálico y un probable hexósido de ácido elágico, el cual presenta el mismo ion pseudomolecular y fragmento que quercetina-hexósido, sin embargo eluye mucho antes.

El peak 3 presenta masas características del kampferol-hexósido (flavonol monohidroxilado), sin embargo el tiempo de elución es muy bajo para un compuesto con menor polaridad que quercetina-hexósido. Finalmente, mediante espectrometría de masas se detectó berberina a los 35.37 minutos utilizando ionización positiva [58].

Contenido de polifenoles totales y capacidad antioxidante

Los polifenoles totales han sido calculados como la sumatoria de todos los compuestos fenólicos analizados por HPLC (antocianos + flavonoles + flavan-3-oles + ácidos hidroxicinámicos + estilbenoides). Los ensayos antioxidante utilizados en C son los mismos descritos para RG y PG (Figura 2.6). La concentración de polifenoles totales en C alcanzan los 2612 µmol/100g peso fresco (PF), lo que indica una concentración alrededor de 45 a 125 veces mayor a la obtenida para RG y PG, respectivamente.

El contenido de antocianos totales corresponde a un 86% del total de polifenoles en C, evidenciando la importancia del contenido de antocianos en la capacidad antioxidante. También se ha reportado un alto contenido de vitamina C [44], lo que explica la muy alta capacidad antioxidante presente en C con respecto a RG y PG. Comparativamente, el contenido de antocianos totales en RG y PG es del 62 y 26%, respectivamente, mostrando un mayor aporte de otros compuestos fenólicos en la capacidad antioxidante.

Los valores de capacidad antioxidante CUPRAC indican un muy alto valor para C, siendo sobre 400 veces mayor que RG y PG. Lo mismo se repite para ABTS, observándose en C una capacidad antioxidante sobre 300 veces mayor que RG y PG.

Una explicación para esta diferencia de capacidad antioxidante mediante los dos métodos utilizados tiene que ver con la composición de polifenoles. Como se estableció anteriormente en el calafate, un 86% de los (poli)fenoles totales corresponde a antocianos, mientras que el aporte de esta familia es menor en RG y muy menor en PG. Por otro lado, en C se ha descrito en una concentración promedio de 420 µmol/100 PF de vitamina C y 32.7 µmol/100 PF de berberina, éste último concentrándose particularmente en las semillas [44,59]. Ambos poseen una alta capacidad antioxidante y no fueron contemplados dentro del cálculo de polifenoles totales presentado.

Debido a la amplia diferencia de concentración de polifenoles totales, gran aporte de antocianos trihidroxilados, flavonoles y HCADs por gramo de fruto, junto con la alta capacidad antioxidante presente en C, se seleccionó este fruto como fuente de (poli)fenoles para ser administrado a animales de experimentación.

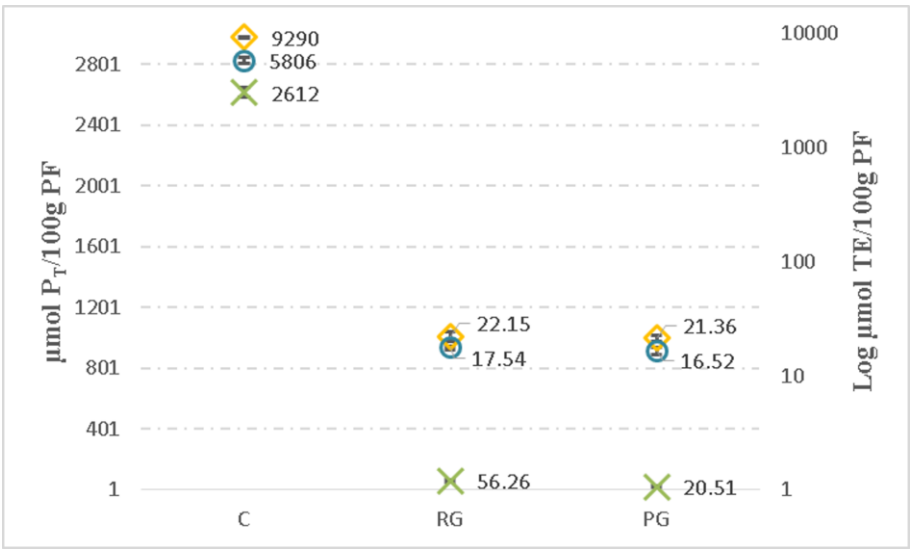

Figura 2.6: Concentraciones de polifenoles totales (PT) en 100 g de PF y escala logarítmica (Log) de capacidad antioxidante, expresada en equivalentes Trolox (TE) por 100 g de PF obtenidos en fruto de C, RG y PG (Diamantes amarillos indican TE para CUPRAC; círculos azules indican TE para ABTS)

Elaboración de extracto liofilizado de calafate

Con el objetivo de contar con un lote homogéneo para los estudios posteriores de consumo agudo, se realizó un cambio en el solvente de extracción para que sea compatible con la administración en animales de experimentación. Esto debido a que cualquier daño asociado al consumo del extracto se evidenciará en los análisis de metabolómica dirigida y no dirigida.

Se evaluó el uso de etanol potable como solvente de extracción como alternativa del metanol, manteniendo la misma concentración de ácido fórmico. La Figura 2.7 muestra el área total de antocianos extraídos por gramo de fruto de calafate, recuperando un 84% de los (poli)fenoles extraídos con metanol a escala analítica.

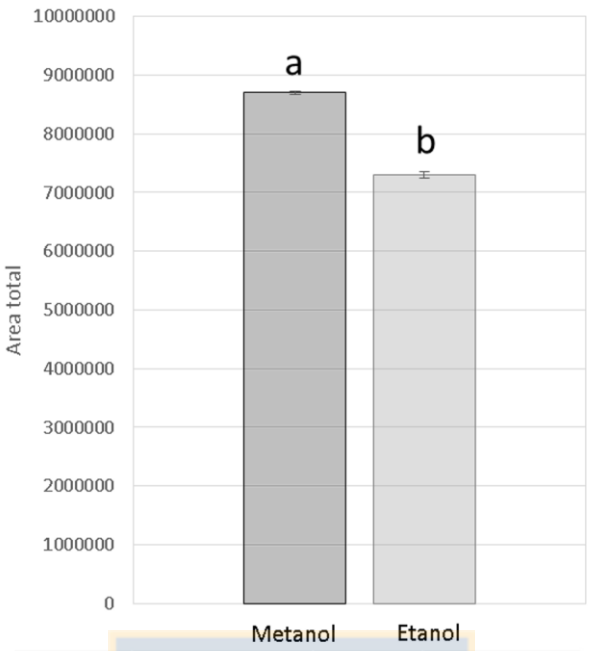

	Promedio (Área/g fruto)	C.V	Porcentaje
Etanol	7301963	0,69	84
Metanol	8699803	0,33	100

Figura 2.7: Evaluación comparativa de extracción de polifenoles en calafate luego de la extracción con metanol/ácido fórmico (97:3% v/v) y etanol potable/ácido fórmico (97:3% v/v). ^{a,b} *estadísticamente distintos.*

Abbreviations Used

RG: Red Globe; PG: Pink Globe; UFGT: UDP-glucose:flavonoid-3-O-glucosyltransferase; ANS: Anthocyanidin synthase; SNP: Single nucleotide polymorphism; EDTA: Ethylenediaminetetraacetic acid; CTAB: Cetyl trimethylammonium bromide; EGTA ethylene glycol-bis(β-aminoethyl ether)-N,N,N',N'-tetraacetic acid; SDS: sodium dodecyl sulfate; ABTS: 2,2′-azino-bis(3-ethylbenzothiazoline-6-sulphonic acid); CUPRAC: Cupric reducing antioxidant capacity; SPE: Solid phase extraction; TEAC: Trolox equivalent antioxidant capacity; PVP: polyvinylpolypyrrolidone; UV-Vis: Ultraviolet-visible; DAD: Diode array detector; MS: Mass spectrometry; FL: Fluorescence; FLD : Fluorescence detector; qRT-PCR: Quantitative real-time PCR; cDNA: complementary DNA; SSR: Simple sequence repeats; EF1α: Elongation factor 1-alfa; MS-EPI; MS enhance product ion; FW: Fresh weight; HCAD: Hydroxycinnamic acid derivative; HTH: Helix-turn-helix motif; *c*: Cis; *t*: Trans; PD: Proxyanidin dimer; λex/λem: Excitation/emission wavelength; PCA: Principal components analysis; sh: shoulder.

Acknowledgement

Authors would like to thank the funding body Conicyt, Chile for award of Fondecyt-1140439, doctoral fellowship and PFB-27.

Supporting Information description

Supporting information is available for list of SSR markers, primers used in AFLP analysis, amplified VvmybA1a and VvmybA1c fragments, sequence analysis.

References

(1) Denev, P. N.; Kratchanov, C. G.; Ciz, M.; Lojek, A.; Kratchanova, M. G. Bioavailability and antioxidant activity of black chokeberry (*Aronia melanocarpa*) polyphenols: *in vitro* and *in vivo* evidences and possible mechanisms of action: a review. *Compr. Rev. Food Sci. Food Saf.* **2012**, *11*, 471–489.

(2) Ziberna, L.; Tramer, F.; Moze, S.; Vrhovsek, U.; Mattivi, F.; Passamonti, S. Transport and bioactivity of cyanidin 3-glucoside into the vascular endothelium. *Free Radic Biol Med.* **2012**, 52, 1750-1759.

(3) Wang, D.; Zou, T.; Yang, Y.; Yan, X.; Ling, W. Cyanidin-3-O-β-glucoside with the aid of its metabolite protocatechuic acid, reduces monocyte infiltration in apolipoprotein E-deficient mice. *Biochem. Pharmacol.* **2011**, *82*, 713–719.

(4) Zamora-Ros, R.; Touillaud, M.; Rothwell, J. A.; Romieu, I.; Scalbert, A. Measuring exposure to the polyphenol metabolome in observational epidemiologic studies: current tools and applications and their limits. *Am. J. Clin. Nutr.* **2014**, *100*, 11–26.

(5) Cassidy, A.; Rogers, G.; Peterson, J. J.; Dwyer, J. T.; Lin, H.; Jacques, P. F. Higher dietary anthocyanin and flavonol intakes are associated with anti-inflammatory effects in a population of US adults. *Am. J. Clin. Nutr.* **2015**, *102*, 172–181.

(6) Juurlink, B. H. J.; Azouz, H. J.; Aldalati, A. M. Z.; Al Tinawi, B. M. H.; Ganguly, P. Hydroxybenzoic acid isomers and the cardiovascular system. *Nutr. J.* **2014**, *13*, 63.

(7) Folmer, F.; Basavaraju, U.; Jaspars, M.; Hold, G.; El-Omar, E.; Dicato, M.; Diederich, M. Anticancer effects of bioactive berry compounds. *Phytochem. Rev.* **2013**, *13*, 295–322.

(8) Williamson, G. Possible effects of dietary polyphenols on sugar absorption and digestion. *Mol. Nutr. Food Res.* **2013**, *57*, 48–57.

(9) Del Rio, D.; Rodriguez-Mateos, A.; Spencer, J. P. E.; Tognolini, M.; Borges, G.; Crozier, A. Dietary (poly)phenolics in human health: structures, bioavailability, and evidence of protective effects against chronic diseases. *Antioxid. Redox Signal.* **2013**, *18*, 1818–1892.

(10) Alvarez-Suarez, J. M.; Dekanski, D.; Ristić, S.; Radonjić, N. V; Petronijević, N. D.; Giampieri, F.; Astolfi, P.; González-Paramás, A. M.; Santos-Buelga, C.; Tulipani, S.; et al. Strawberry polyphenols attenuate ethanol-induced gastric lesions in rats by activation of antioxidant enzymes and attenuation of MDA increase. *PLoS One* **2011**, *6*, e25878.

(11) Jean-Gilles, D.; Li, L.; Ma, H.; Yuan, T.; Chichester, C. O.; Seeram, N. P. Anti-inflammatory effects of polyphenolic-enriched red raspberry extract in an antigen-induced arthritis rat model. *J. Agric. Food Chem.* **2012**, *60*, 5755–5762.

(12) Vivier, M.; Pretorius, I. Genetic improvement of grapevine: tailoring grape varieties for the third millennium - a review. *South African J. Enol. Vitic.* **2000**, *21*, 5–26.

(13) Ali, K.; Maltese, F.; Choi, Y.; Verpoorte, R. Metabolic constituents of grapevine and grape-derived products. *Phytochem. Rev.* **2010**, *9*, 357–378.

(14) Vogt, T. Phenylpropanoid Biosynthesis. *Mol. Plant.* **2010**, *3*, 2–20.

(15) Georgiev, V.; Ananga, A.; Tsolova, V. Review: recent advances and uses of grape flavonoids as nutraceuticals. *Nutrients.* **2014**, *6*, 391–415.

(16) Kuhn, N.; Guan, L.; Dai, Z.; Wu, B.; Lauvergeat, V.; Gomès, E.; Li, S.; Godoy, F.; Arce-Johnson, P.; Delrot, S. Berry ripening: recently heard through the grapevine. *J. Exp. Bot.* **2014**, *65*, 4543–4559.

(17) Dai, Z.; Ollat, N.; Gomès, E.; Decroocq, S.; Tandonnet, J.; Bordenave, L.; Pieri, P.; Hilbert, G.; Kappel, C.; van Leeuwen, C.; et al. Ecophysiological, genetic, and molecular causes of variation in grape berry weight and composition: a review. *Am. J. Enelogy Vitic.* **2011**, *62*, 413–425.

(18) Conde, B.; Silva, P.; Fontes, N.; Dias, A.; Tavares R; Sousa, M.; Agasse, A.; Delrot, S.; Geros H. Biochemical changes throughout grape berry development and fruit and wine quality. *Food.* **2007**, *1*, 1–22.

(19) Bravo, J. Uva de mesa: se ratifica el liderazgo exportador mundial de Chile; Santiago, Chile, 2013.

(20) Zoffoli, J.; Latorre, B. Chapter 9: table grape (*Vitis vinifera L.*). In Postharvest biology and technology of tropical and subtropical fruits. Volume: 3.; Yahia, E., Ed.; Woodhead Publishing Limited: Cambridge, 2011; pp 179–207.

(21) Organisation Internationale de la Vigne et du Vin. Description of world vine varieties; Paris, 2009.

(22) Cantos, E.; Espin, J.; Tomas-Barberan, F. Varietal differences among the polyphenol profiles of seven table grape cultivars studied by LC-DAD-MS-MS. *J. Agric. Food Chem.* **2002**, *50*, 5691–5696.

(23) Baiano, A.; Terracone, C. Varietal differences among the phenolic profiles and antioxidant activities of seven table grape cultivars grown in the south of Italy based on chemometrics. *J. Agric. Food Chem.* **2011**, *59*, 9815–9826.

(24) Julius Kühn-Institut. VIVC 23997 http://www.vivc.de/index.php?r=passport%2Fview&id=23997 (accessed Feb 9, 2017).

(25) Pink Globe, la nueva variedad de uva de mesa chilena que irá a la conquista de China http://www.portalfruticola.com/noticias/2011/12/26/pink-globe-la-nueva-variedad-de-uva-de-mesa-chilena-que-ira-a-la-conquista-de-china/?pais=chile (accessed May 22, 2016).

(26) Boss, P. K.; Davies, C.; Robinson, S. P. Analysis of the expression of anthocyanin pathway genes in developing *Vitis vinifera L.* cv Shiraz grape berries and the implications for pathway regulation. *Plant Physiol.* **1996**, *111*, 1059–1066.

(27) Kobayashi, S.; Goto-Yamamoto, N.; Hirochika, H. Association of VvmybA1 gene expression with anthocyanin production in grape (*Vitis vinifera*) skin-color mutants. *J. Japan Soc. Hortic. Sci.* **2005**, *74*, 196–203.

(28) Nakajima, J. I.; Tanaka, Y.; Yamazaki, M.; Saito, K. Reaction mechanism from leucoanthocyanidin to Anthocyanidin 3-Glucoside, a Key Reaction for Coloring in Anthocyanin Biosynthesis. *J. Biol. Chem.* **2001**, *276*, 25797–25803.

(29) Broun, P. Transcriptional control of flavonoid biosynthesis: A complex network of conserved regulators involved in multiple aspects of differentiation in Arabidopsis. *Curr. Opin. Plant Biol.* **2005**, *8*, 272–279.

(30) Kobayashi, S.; Goto-Yamamoto, N.; Hirochika, H. Retrotransposon-induced mutations in grape skin color. *Science.* **2004**, *80*, *304*, 982.

(31) This, P.; Lacombe, T.; Cadle-davidson, M.; Owens, C. L. Wine grape (*Vitis vinifera L* .) color associates with allelic variation in the domestication gene VvmybA1. *Theor. Appl. Genet.* **2007**, *114*, 723–730.

(32) Walker, A. R.; Lee, E.; Robinson, S. P. Two new grape cultivars, bud sports of Cabernet Sauvignon bearing pale-coloured berries, are the result of deletion of two regulatory genes of the berry colour locus. *Plant Mol. Biol.* **2006**, *62*, 623–635.

(33) Lodhi, M.; Ye, G.N.; Weeden, N. F.; Reisch, B. I. A simple and efficient method for DNA extraction from grapevine cultivars andVitis species. *Plant Mol. Biol. Report.* **1994**, *12*, 6–13.

(34) Wan, C. Y.; Wilkins, T. a. A modified hot borate method significantly enhances the yield of high-quality RNA from cotton (*Gossypium hirsutum L.*). *Anal. Biochem.* **1994**, *223*, 7–12.

(35) This, P.; Jung, A.; Boccacci, P.; Borrego, J.; Botta, R.; Costantini, L.; Crespan, M.; Dangl, G. S.; Eisenheld, C.; Ferreira-Monteiro, F.; et al. Development of a standard set of microsatellite reference alleles for identification of grape

cultivars. *Theor. Appl. Genet.* **2004**, *109*, 1448–1458.

(36) Bowers, J. E.; Dangl, G. S.; Vignani, R.; Meredith, C. P. Isolation and characterization of new polymorphic simple sequence repeat loci in grape (*Vitis vinifera L.*). *Genome.* **1996**, *39*, 628–633.

(37) Bowers, J. E.; Dangl, G. S.; Meredith, C. P. Development and characterization of additional microsatellite DNA markers for grape. *Am. J. Enelogy Vitic.* **1999**, *50*, 243–246.

(38) Sefc, K. M.; Regner, F.; Turetschek, E.; Glössl, J.; Steinkellner, H. Identification of microsatellite sequences in *Vitis riparia* and their applicability for genotyping of different *Vitis* species. *Genome.* **1999**, *42*, 367–373.

(39) Thomas, M. R.; Scott, N. S. Microsatellite repeats in grapevine reveals DNA polymorphisms when analyzed as sequence-tagged sites (STSs). *Theor. Appl. Genet.* **1993**, *86*, 985–990.

(40) Narváez H., C.; Castro P., M. H.; Valenzuela B., J.; Hinrichsen R., P. Patrones genéticos de los cultivares de vides de vinificación más comúnmente usados en Chile basados en marcadores de microsatélites. *Agric. Técnica.* **2001**, *61*, 249–261.

(41) Kobayashi, S.; Ishimaru, M.; Hiraoka, K.; Honda, C. Myb-related genes of the Kyoho grape (*Vitis labruscana*) regulate anthocyanin biosynthesis. *Planta.* **2002**, *215*, 924–933.

(42) Giannetto, S.; Velasco, R.; Troggio, M.; Malacarne, G.; Storchi, P.; Cancellier, S.; De Nardi, B.; Crespan, M. A PCR-based diagnostic tool for distinguishing grape skin color mutants. *Plant Sci.* **2008**, *175*, 402–409.

(43) Sambrook, J.; Russell, D. Molecular cloning a laboratory manual, 3rd Edition.; Cold Spring Harbor Laboratory Press: Cold Spring Harbor, 2000.

(44) Ruiz, A.; Hermosín-Gutiérrez, I.; Mardones, C.; Vergara, C.; Herlitz, E.; Vega, M.; Dorau, C.; Winterhalter, P.; Von Baer, D. Polyphenols and antioxidant activity of calafate (*Berberis microphylla*) fruits and other native berries from Southern Chile. *J. Agric. Food Chem.* **2010**, *58*, 6081–6089.

(45) Castillo-Muñoz, N.; Gómez-Alonso, S.; García-Romero, E.; Hermosín-Gutiérrez, I. Flavonol profiles of *Vitis vinifera* red grapes and their single-cultivar wines. *J. Agric. Food Chem.* **2007**, *55*, 992–1002.

(46) Nakamura, Y.; Tsuji, S.; Tonogai, Y. Analysis of proanthocyanidins in grape seed extracts, health foods and grape seed oils. *J. Heal. Sci.* **2003**, *49*, 45–54.

(47) Ribeiro, J.; Magalhaes, L.; Reis, S.; Lima, J.; Segundo, M. High-throughput total cupric ion reducing antioxidant capacity of biological samples determined using flow injection analysis and microplate-based methods. *Anal. Sci.* **2011**, *27*, 483–488.

(48) Jaillon, O.; Aury, J.-M.; Noel, B.; Policriti, A.; Clepet, C.; Casagrande, A.; Choisne, N.; Aubourg, S.; Vitulo, N.; Jubin, C.; et al. The grapevine genome sequence suggests ancestral hexaploidization in major angiosperm phyla. *Nature* **2007**, *449*, 463–467.

(49) Castillo-Muñoz, N.; Fernández-González, M.; Gómez-Alonso, S.; García-Romero, E.; Hermosín-Gutiérrez, I. Red-color related phenolic composition of garnacha tintorera (*Vitis vinifera L.*) grapes and red wines. *J. Agric. Food Chem.* **2009**, *57*, 7883–7891.

(50) Gomes, L.; Silva, E.; Teixeira, M.; Mota, A.; Stringheta, P.; Da-Silva, R.; Castillo-Muñoz, N.; Gómez-Alonso, S.; Hermosín-Gutiérrez, I. Phenolic composition of the berry parts of hybrid grape cultivar BRS Violeta (BRS Rubea×IAC 1398-21) using HPLC-DAD-ESI-MS/MS. *Food Res. Int.* **2013**, *54*, 354–366.

(51) Silva, E.; Da-Silva, R.; Gomes, E.; García-Romero, E.; Hermosín-Gutiérrez, I. Phenolic composition of the edible parts (flesh and skin) of Bordô grape (*Vitis labrusca*) using HPLC-DAD-ESI-MS/MS. *J. Agric. Food Chem.* **2011**, *59*,

13136–13146.

(52) Buiarelli, F.; Coccioli, F.; Merolle, M.; Jasionowska, R.; Terracciano, A. Identification of hydroxycinnamic acid-tartaric acid esters in wine by HPLC-tandem mass spectrometry. *Food Chem.* **2010**, *123*, 827–833.

(53) Tsang, C.; Auger, C.; Mullen, W.; Bornet, A.; Rouanet, J.-M.; Crozier, A.; Teissedre, P.-L. The absorption, metabolism and excretion of flavan-3-ols and procyanidins following the ingestion of a grape seed extract by rats. *Br. J. Nutr.* **2005**, *94*, 170–181.

(54) Mattivi, F.; Guzzon, R.; Vrhovsek, U.; Stefanini, M.; Velasco, R. Metabolite profiling of grapes: flavonols and anthocyanins. *J Agric Food Chem* **2006**, *54*, 7692–7702.

(55) Gutha, L. R.; Casassa, L. F.; Harbertson, J. F.; Naidu, R. A. Modulation of flavonoid biosynthetic pathway genes and anthocyanins due to virus infection in grapevine (*Vitis vinifera L.*) leaves. *BMC Plant Biol.* **2010**, *10*, 187.

(56) Apak, R.; Güçlü, K.; Demirata, B.; Özyürek, M.; Çelik, S. E.; Bektaşoğlu, B.; Berker, K. I.; Özyurt, D. Comparative evaluation of various total antioxidant capacity assays applied to phenolic compounds with the CUPRAC assay. *Molecules.* **2007**, *12*, 1496–1547.

(57) Skroza, D.; Generalic Mekinic, I.; Svilovic, S.; Simat, V.; Katalinic, V. Investigation of the potential synergistic effect of resveratrol with other phenolic compounds: A case of binary phenolic mixtures. *J. Food Compos. Anal.* **2015**, *38*, 13–18.

(58) Ruiz, A.; Zapata, M.; Sabando, C.; Bustamante, L.; Von Baer, D.; Vergara, C.; Mardones, C. Flavonols, alkaloids, and antioxidant capacity of edible wild *Berberis* species from Patagonia. *J. Agric. Food Chem.* **2014**, *62*, 12407–12417.

(59) Ruiz, A.; Mardones, C.; Vergara, C.; Hermosín-Gutiérrez, I.; von Baer, D.; Hinrichsen, P.; Rodriguez, R.; Arribillaga, D.; Dominguez, E. Analysis of hydroxycinnamic acids derivatives in calafate (*Berberis microphylla* G. Forst) berries by liquid chromatography with photodiode array and mass spectrometry detection. *J. Chromatogr. A* **2013**, *1281*, 38–45.

(60) Lila, M. A.; Burton-Freeman, B.; Grace, M.; Kalt, W. Unraveling anthocyanin bioavailability for human health. *Annu. Rev. Food Sci. Technol.* **2016**, *7*, 375–393.

(61) Guo, Y.; Bruno, R. S. Endogenous and exogenous mediators of quercetin bioavailability. *J. Nutr. Biochem.* **2015**, *26*, 201–210.

(62) El-Seedi, H. R.; El-Said, A. M. a; Khalifa, S..; Göransson, U.; Bohlin, L.; Borg-Karlson, A. K.; Verpoorte, R. Biosynthesis, natural sources, dietary intake, pharmacokinetic properties, and biological activities of hydroxycinnamic acids. *J. Agric. Food Chem.* **2012**, *60*, 10877–10895.

Journal of Agricultural and Food Chemistry

Electronic Supplemental Material

Differences in *Vvufgt* and *VmybA1* expression levels and phenolic composition in table grape (*Vitis vinifera L.)* 'Red Globe' and its somaclonal variant 'Pink Globe'

Luis Bustamante, Vania Saez, Patricio Hinrichsen, María H. Castro, Carola Vergara, Dietrich von Baer and Claudia Mardones*

Instrumental Analysis Department, Faculty of Pharmacy, University of Concepción, P.O. Box 160-C Concepción, Chile, and Instituto de Investigaciones Agropecuarias, INIA La Platina, Santa Rosa 11,610, La Pintana, Santiago, Chile.

*Corresponding Author: Tel: 56-41-2204598, Fax: 56-41-2226382, E-mail address: cmardone@udec.cl

Table S2.1: *List of SSR markers used for comparison of Red Globe and Pink Globe. Markers of the series VVMD (UC-Davis [36, 37]), VVS (CSIRO [39]), VrZAG (Austria [38]) and VMC (Vitis Microsatellite Consortium [35]) are included.*

VMC4H6	VMC1F10	VMC2C7	VMC3A9	VMC4A5	VMC6F1	VrZAG83	VvMD30
VMC2F12	VMC2A10	VMC2D9	VMC3B10	VMC4H5	VMC8G9	VrZAG89	VvMD31
VMC2G2	VMC2A3	VMC2E11	VMC3B9	VMC4H6	VMC9A2-1	VrZAG112	VvMD32
VMC1A12	VMC2A5	VMC2E2	VvZAG93	VMC5C1	VMC9B5	VvS2	VvMD36
VMC1A7	VMC2A7	VMC2E7	VMC3C9	VMC5G7	VrZAG62	VvMD5	
VMC1B11	VMC2B11	VMC2F10	VMC3D12	VMC5G8	VrZAG64	VvMD7	
VMC1C10	VMC2B5	VMC2H4	VMC3E12	VMC5H11	VrZAG67	VvMD25	
VMC1E11	VMC2C10	VMC2H9	VMC3G7	VMC5H2	VrZAG79	VvMD27	
VMC1E8	VMC2C3	VMC3A1	VMC3H5	VMC6C10	VrZAG82	VvMD28	

Table S2.2: *Primers used in the AFLP analysis*.

Primers*	Polymorphisms** (N°)
PM1A (GTA)	51
PM1B (GCG)	51
PM1C (GAC)	50
PM1D (GGT)	57
PM1E (GTT)	48
PM1F (GTC)	44
PM1G (GCA)	36
Total	337

*All combinations used Eco1A Primer (ACC); ** No reproducible polymorphic band were found.

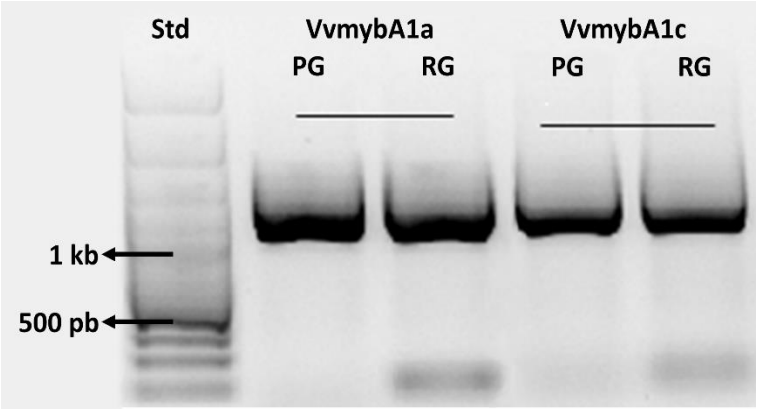

Figure S2.1: *Fragments amplified with VvmybA1a and VvmybA1c specific primers in order to clone fragments of 1154 and 1166 bp amplicons, respectively, corresponding to each allele*.

```
   1  ACCAGCCCTCGGAAAGCCAAACGTCCAAACAGCGCTATCATTGAAACAACATGCTGCCTGGGAATT   66
  67  CCCAGAGTCGCCGGCTCATCATAAATGCCTTTTATGGCTTCCGCACCCCCTCTCGCCACGTGGCTC  132
 133  AGTCAGACGAAGAGACCTCTTCAAAATTCAAAAAGCCAGTTATTTTTTAACCCGCCCATTTTTTGG  198
 199  CAAAATAGGCAAGTTAAAAAGGGGGGCAATGTAGGGACCCCTCCCTCTGGGAAACACGTGGCACGC  264
 265  ACCTCACAGTGACACGCAGCACGTGTTATCAGCCGGACCATCATCATCCGGATTCCCTTAAGGATA  330
 331  CGCATGATGATGGTTCTCCTATCCGGACCGCCTCAAGGAAAAGCACATGACGTTTCAGCTTCTTCT  396
 397  GTCCAAGGAAGAGCAAACGACGCTGACAGAGCATAGACATCCGGACAACCTTCATAATGTATCTGC  462
 463  TCCACTATACAATCCGGATAGTCAGCATGTGACCATCCGGATTTAATCGTCCGGATCATCAATTAA  528
 529  AGTAAAGCAAGTCTTACACGCTATCACGACAACCAGCCATGGCCCACGTCCCATCATCTGCAGAGT  594
 595  GAAAGGACGGGTCGAGGTGACAACAAGTCACTTCCCACGATCATTCTACATGATCATTTCCCACGA  660
 661  TCTCTAGACAGCAGCATCACCTACCACGGTTTCTGACAGCCGCCAGTAGGGTGGCGATGACCATGC  726
 727  TGCCTCCGAATGTCATCATGACAAACATAAAATATCTCCTCGCCATTAATGAGAGGAACAGTACCC  792
 793  CTGAAGCTGTATATATATGCCTTCGCACGAAGAAGAAGGGGATCCTCCTGGTAACTTCTTAATACC  858
 859  TGGTAAAAGGCCAACTAATTTATATTCCTCTCTCTAACCATGGCTAACAAAACCATCGGAGGATGC  924
 925  GTCCAGACACCCTGTCCGGATGCCTTCTTGCAGGAATGACGACTGGATCAAAAACCTTTATGAGTT  990
 991  GAGATCACGCGTCCATCCATCTGGTTACTACGTGGACCGCCAAAGACGCGAGGTAACAACAACACA 1056
1057  CACCCTTTGTCCATGAACTCCAGCGCATTTGGAAGCCAGTAATGCACCATAAGAAACGTGTCGAAT 1122
1123  AAACCAATTAGGGGTCTGGTGTCCGAGTCATG                                    1154
```

Figure S2.2: *Promoter region of VvmybA1 in Pink Globe and Red Globe obtained with primers described by Kobayashi en al. [27]. Red nucleotides indicate the GRET-1 transposon and green nucleotides indicate the LTR3' sequence.*

```
   1   TCCCGTCACTTGGTTGCTTTTTGTCAAGGAAACAGTGGTATCAGAATCCAAATCTTCTACGTAATG   66
  67   TCCCATTCATCCTACCAACGTCCAAATGAATTCCTCTGGACATTAAAATATGGTAGCACGTGGTTG   132
 133   TCTTCGGGATCACACCAGTTTATACATTTGCACCACAAAATAGAGATTGTTCATAAAGGATACTAG   198
 199   TCAGCAATTAATTCCTAAATTTCGCTGTACATTTATAGTAAGTTGATACATAATGGGTAAATATCT   264
 265   CTTATGACACACACCCTTTGTCCATGATGTCCATCGCATTCGGAAGCCAGGTAATGCACCATAAGA   330
 331   AACGTGTCGAATCAACCAATTAGGGGTCTGGTGTCCGAGTCATGAGATAGAACAGGTTCGAGGTTG   396
 397   TTATATATCAATCAATAATTAGAGAAGGAGCCGGTCTCTTGTGTTGAGTTGACTCGATGAAGAGCT   462
 463   TAGGAGTTAGAAAGGGTGCATGGACCCAAGAAGAGGATGTTCTCCTGAGGAAATGCATTGAGAAAT   528
 529   ATGGAGAAGGAAAGTGGCATCTGGTTCCCCTCCGAGCAGGTGACATGAAAGAGAAAGGGATCAGTA   594
 595   TTAATTTGTGTTTTTTTTACTTCTGTTTTGCTTAAAGAGTTTCGTTTTCTTGAGTTTGCAGGGTTG   660
 661   AATAGATGCCTAAAGAGCTGCAGATTGAGATGGCTCAATTATTTGAAGCCAGATATCAAGAGAGGA   726
 727   GAGTTTGCATTAGACGAGGTTGATCTCATGATTAGGCTTCACAATTTGTTGGGGAACAGGCAAGTC   792
 793   TATAATAACTCAAGTACTAGCTTGATAATGATATTATATTAGTTCTGAAGCTGTTCAGAACTTACA   858
 859   AAAGAGCTGTTCAGTTGATACTTTGTCTGATGTTGTGCGTGTATAGATGGTCCTTGATTGCGGGTA   924
 925   GGCTTCCAGGGAGGACTGCTAATGATGTCAAGAACTATTGGCATGGTCACCACTTCAAAAAGAAGG   990
 991   TTCAGTTCCAGGAAGAAGGGAGAGATAAACCCCAAACACATTCTAAAACCAAAGCTATAAAGCCTC   1056
1057   ACCCTCACAAGTTCTCCAAAGCCTTGCCAAGGTTTGAACTAAAAACTACAGCTGTGGATACTTTTG   1122
1123   ACACACAAGTAAGTACTTCCAGTAAGCCATCATCCACGTCACCACAACCGAATGATGACATCATAT   1188
1189   GGTGGGAAAGCCTGTTAGCTG                                               1209
```

Figure S2.3: *Red Globe VvmybA1c gene sequence obtained using VvmybA1c primers. Nucleotide differences in the Pink Globe gene sequence are highlighted in red and green nucleotides indicate an inserted sequence following the 218th bp in respect to the grapevine reference genome PN40024.*

```
   1  TCCCGTCACTTGGTTGCTTTTTGTCTAAGGAAACAGTGGTATCAGAATCCAAATCTTCTACGTAAT   66
  67  GTCCCATTCATCCTACCAATGTCCATATGAATTCCTCTGGACGTTAAAAAATGGTTGCACGTGGTT  132
 133  GTCTTCAGGATCACACCAGTTTATACATTTGGACCACAAAATAGAGATTGTTCATCAAGGATACTA  198
 199  GTCAGCAATTAATTCCTAAATATCTCTTATGACACACACCCTTTGTCCATGAACTCCAGCGCATTT  264
 265  GGAAGCCAGTAATGCACCATAAGAAACGTGTCGAATAAACCAATTAGGGGTCTGGTGTCCGAGTCA  330
 331  TGAGATAGAACAGGTTCGAGGTTGTTATATATCAATCAATAATTAGAGAAGGAGCCGGTCTCTTGT  396
 397  GTTGAGTTGACTCGATGGAGAGCTTAGGAGTTAGAAAGGGTGCATGGATCCAAGAAGAGGATGTTC  462
 463  TCCTGAGGAAATGCATTGAGAAATATGGAGAAGGAAAGTGGCATCTGGTTCCCCTCCGAGCAGGTA  528
 529  ACATGAAAGAGAAAGGGATCAGTATTTATTTGTGTTTTTTTACTTCTGTTTTGCTTAAAGAGTTTC  594
 595  ATTTTCTTGAGTTTGCAGGGTTGAATAGATGCCGAAAAAGCTGCAGGTTGAGATGGCTCAATTATT  660
 661  TGAAGCCGGATATCAAGAGAGGAGAGTTTGCATTAGACGAGGTTGATCTCATGATTAGGCTTCACA  726
 727  ATTTGTTGGGGAACAGGCAAGTCTATAATAACTCAAGTACTAGCTTGATAATGATATTATATTAGT  792
 793  TCTGAAGCTGTTCAGAACTTACAAAAGAGCTGTTCAGTTGATACTTTGTCTGATGTTGTGCGTGTA  858
 859  TAGATGGTCCTTGATTGCGGGTAGGCTTCCAGGGAGGACTGCTAATGATGTCAAGAACTATTGGCA  924
 925  TAGTCACCACTTCAAAAAGGAGGTTCAGTTCCAGGAAGAAGGGAGAGATAAACCCCAAACACATTC  990
 991  TAAAACCAAAGCTATAAAGCCTCACCCTCACAAGTTCTCCAAAGCCTTGCCAAGGTTTGAACTAAA 1056
1057  AACTACAGCTGTGGATACTTTTGACACACAAGTCAGTACTTCCAGTAAGCCATCATCCACGTCACC 1122
1121  ACAACGGAATGATGACATCATATGGTGGGAAAGCCTGTTAGCTG                        1166
```

Figure S2.4: *Pinot Noir (PN40024) VvmybA1c sequence. Green nucleotides indicate differences present in Red Globe, light blue nucleotides indicate differences present in Pink Globe and orange nucleotides indicate differences present in both genotypes, respect to the grapevine reference genome PN40024.*

Capítulo 3

Compuestos fenólicos en plasma de gerbo (*Meriones unguiculatus*) mediante el pretratamiento por micro-extracción de sorbente empacado, microextracción líquido-líquido y derivatización por GC-MS/MS, luego de la ingesta aguda de una extracto de fruto de calafate (*Berberis microphylla*).

Resumen

Se implementó y validó una metodología analítica MRM GC-MS/MS para el análisis cuantitativo de 43 compuestos fenólicos que se proponen como productos de la metabolización del consumo de (poli)fenoles encontrados en el fruto de calafate (*B microphylla*). Para ello fue necesaria la selección de la reacción de derivatización y extracción, optimización y validación del método de cuantificación. Brevemente, la metodología consiste en la deconjugación enzimática con glucuronidasa/sulfatasa de *H. pomatia* comercial previamente purificada, seguido de una extracción líquido-líquido y derivatización con BSTFA/TMCS durante 30 minutos a 90 °C.

El estudio del plasma de gerbo obtenido a 0, 1, 2, 4, 8 y 12 horas luego de la administración de 300 mg/kg de extracto de calafate muestra que existe un aumento de 9 compuestos respecto al nivel basal (0 horas). Luego de 1 y 2 horas los compuestos 1,4-dihidroxibenceno, ácidos 3,4-dihidroxifenilacético, 4-hidroxicinámico, 3,5-dimetoxi-4-hidroxibenzoico y 3-metoxi-4-hidroxibenzoico muestran una tendencia al alza, mientras que se logró determinar un aumento significativo para los ácidos 3-hidroxicinámico y 3-metoxi-4-hidroxifenilacético. Además, los ácidos 3-hidroxifenilacético y fenilacético muestran aumentos significativos luego de 4 y 8 horas de administrado el extracto.

Estos compuestos fenólicos pueden derivar de la reducción, dehidroxilación, metilación y β-oxidación de los polifenoles cuantificados en el extracto de calafate. Se propone que el aumento del ácido 3,5-dimetoxi-3-hidroxibenzoico (ácido siríngico) puede ser exclusivamente atribuido a los antocianos trihidroxilados presentes.

Contenidos

Section 1.

Title: **Evaluation of micro extraction by packed sorbent, liquid-liquid extraction and derivatization pretreatment of diet-derived phenolic acids in plasma by GC-MS/MS.**

Luis Bustamante[1], Diana Cárdenas[1], Dietrich von Baer[1], Edgar Pastene[2], Daniel Duran-Sandoval[3], Carola Vergara[1] and Claudia Mardones[1]*

[1]Department of Instrumental Analysis, Faculty of Pharmacy, Universidad de Concepción, Concepción, Chile

[2]Department of Pharmacy, Faculty of Pharmacy, Universidad de Concepción, Concepción, Chile

[3]Department of Clinical Biochemistry and Immunology, Faculty of Pharmacy, Universidad de Concepción, Concepción, Chile

* To whom correspondence should be addressed. Tel.: 56-41-2204598. Fax: 56-41-2226382 E-mail: cmardone@udec.cl.

Manuscrito enviado al Journal of Separation Science, 29 de marzo del 2017.

Abstract

Miniaturized sample pretreatments for the analysis of phenolic metabolites in plasma involving protein precipitation, enzymatic deconjuation, extraction procedures (microextraction by packed sorbent (MEPS) and liquid - liquid extraction (LLE)) and different derivatization reactions were systematically evaluated. The analysis were conducted by gas chromatography coupled to a triple quadrupole mass detector operating in multiple reaction monitoring mode for the evaluation of 43 possible diet-derived phenolic acids. A previous enzyme purification was necessary for the phenolic deconjugation before extraction. BSTFA/TMCS and two different tetrabutylammonium (TBA) salts for derivatization reactions were compared. The optimum reaction conditions were 50 µL of BSTFA/TMCS at 90 °C for 30 min, while TBA salts were associated with loss of sensitivity due to rapid activation of the inert GC liner. Phenolic acids extractions from plasma, using MEPS and LLE, were optimized in order to achieve reproducible quantification. Optimal MEPS performance was achieved using a C-18 packed bed, and better results for less polar compounds such as methoxylated derivates were observed. Despite the low recovery for some analytes, the repeatability obtained using the automated extraction procedure in the GC inlet was 2.5%. Instead, using LLE, better recoveries (80-110%) for all studied analytes were observed, however, at the expense of repeatability (3.8-18.4%). The analytical investigation of phenolic compounds in biological samples such as gerbil plasma collected before and after the administration of a calafate extract was tested. The miniaturized procedures allows to work with small sample volumes, which is imperative in metabolomics studies using plasma from small laboratory animals.

Keywords: Derivatization, MEPS, MRM, Plasma, Phenolic acids, Metabolomics.

Introduction

In recent decades numerous studies have shown epidemiologic and mechanistic data supporting the beneficial effects of phenolic compounds present in fruits and vegetables [1–5]. Many studies covered the potential benefits of these compounds in diverse pathologies, such as cardiovascular diseases, diabetes and cancer [6,7], however only in the recent years the research has focused in the effects of their metabolites [8–10]. In order to understand their benefits, it is necessary to consider the effects of the parent compound(s) as well as their metabolites generated *in vivo*. The main metabolites produced after the intake of flavonoids and other phenolic compounds are small weight phenolics, such as benzoic, phenylacetic and 3-phenylpropionic acids, which have also been associated with beneficial effects [9,11–14].

It is very important to develop sensitive and reproducible methodologies for metabolomics studies, due to the complexity of the sample matrix, the similar chemical structures of the metabolites and their low concentrations. Recently studies have used LC-MS, but a few of them have been conducted by GC-MS. This is mainly because polar compounds are difficult to analyze using this technique and require derivatization reaction steps [11,15–17]. Regardless, GC-MS is a powerful analytical tool for metabolomics because a GC system with an MS detector has an efficient separation in capillary GC columns and useful tools such as peak deconvolution are available. Moreover, the GC-MS interface is simple and robust, while LC-MS detectors are poorer in this regard as they suffer from ionization suppression and adduct formation, inadequate for studies where low instrumental variability and sample ionization independence are needed [18,19].

Trimethylsilyl (TMS) reagents such as BSTFA/TMCS or oximation/MSTFA are the most widely used for derivatizing phenolics and their metabolites [15–17,20–23]. Recently, alkylation of phenolics using tetrabutylammonium (TBA) salts was reported in an automated procedure in the GC injection port [24]. TMS derivatives have been successfully used especially in the analysis of metabolites in plasma and other biological matrixes [11,15,16]. In contrast, little information is available on the use of the TBA injection-port reaction for these applications [24,25].

Analysis of phenolic metabolites in plasma and other biological fluids requires pre-treatment to eliminate proteins, lipids and other constituents. The more used extraction and clean-up procedures are solid phase extraction (SPE) and liquid-liquid extraction (LLE) [18,26]. However, to the best of our knowledge, there are no studies that compare systematically these pretreatments, nor debate on each approach. Recently, a miniaturized device known as microextraction by packed sorbent (MEPS) has been developed. It consists of a packed sorbent incorporated in a microliter syringe which can be used in a chromatographic

autosampler [27]. It has been proposed as an automated alternative for sample treatment in the analysis of phenolic acids in plasma [24].

Metabolomic approaches require the minimization of variability throughout the entire analytical procedure. This is critical to discriminate analyte changes in pharmacokinetic studies. To achieve this goal, miniaturization and automation in sample pretreatment and derivatization are crucial to reduce sources of error for biological fluids analysis [26,28].

The main aim was focused in the optimization and comparison of miniaturized sample treatments for phenolic metabolites in plasma. Derivatization with TMS reagent and an automated in port reaction with TBA salts were evaluated. The extraction of phenolics from plasma using MEPS was studied to achieve the lowest analytical variation and compare it with LLE. Both procedures (MEPS and LLE) using the better derivatization reaction were compared for quantitation of phenolics in low volumes of gerbil and spiked human plasma samples.

Experimental

Chemicals and materials

Standards of acids 2-butenedioic, butanedioic, 2,3-dihydroxybutanodioic, DL-malic, quinic, shikimic, hippuric, 2-hydroxybenzoic, 3-hydroxybenzoic, 4-hydroxybenzoic, 3,4,5-trihydroxybenzoic, 4-methoxybenzoic, 4-hydroxy-3-methoxybenzoic, 4-hydroxy-3,5-dimethoxybenzoic, 2-acetylbenzoic, 3-hydroxyphenylacetic, 4-hydroxyphenylacetic, 3,4-dihydroxyphenylacetic, 4-hydroxy-3-methoxyphenylacetic, 3-methoxyphenylacetic, 4-methoxyphenylacetic, 3,4-demethoxyphenylacetic, 3-phenylpropionic, 3-(4-hydroxyphenyl)propionic, 3-(3,4-dihydroxyphenyl)propionic, 3-(3-methoxyphenyl)propionic, 3-(4-methoxyphenyl)propionic, 3-(3,4-dimethoxyphenyl)propionic, cinnamic, 3-hydroxycinnamic, 4-hydroxycinnamic, 3,4-dihydroxycinnamic, 4-hydroxy-3-methoxycinnamic, 4-methoxycinnamic and 3,4-dimethoxycinnamic, 4-(2-hydroxyethyl)phenol, 4-hydroxy-3-methoxybezaldehyde, 3,4-dihydroxybenzaldehyde, 1,4 dyhydroxybenzene, 1,2,3-trihydroxybenzene, 1,3,5-trihydroxybenzene, 3,4-dihydroxybenzoic, tetrabutylammonium hydroxide (TBAH) and β-glucuronidase type H-5 from *Helix pomatia* were purchased from Sigma (St. Louis, Missouri, USA). Benzoic acid-d_5, *trans*-cinnamic acid-d_6 and 3,4-dihydroxybenzoic acid 3-O-sulfate sodium salt from Toronto Research Chemicals (Brisbane Rd, Toronto, Canada). BSTFA:TMCS (90:10) was provided by UCT Inc. (Levittown, USA) and MEPS barrel insert and needle (BIN) from SGE Analytical Science (Melbourne, Australia). Tetrabutylammonium chloride (TBACl), sodium acetate p.a., EDTA, Amicron®

ultra centrifugal filters MWCO 100 KDa , methanol, acetonitrile, ethyl acetate, hexane, toluene (LiChrosolv grade), and acetic, trichloroacetic and hydrochloric p.a. acids from Merck (Darmstadt, Germany). Reaction vessels from Supelco (Bellefonte, Pennsylvania, USA), nitrogen evaporator from Pierce (Waltham, Massachusetts, United States) and centrifuge from Thermo Scientific (Waltham, Massachusetts, USA) were used. C-18 and HLB SPE 6 cc catridges were from Waters (Milford, Massachusetts, USA).

Plasma samples

Gerbil (Meriones unguiculatus) blood was collected into EDTA tubes by retro-orbital plexus puncture, centrifuged at 2500 g for 15 min at 5 °C, and stored at -80°C until analysis. A basal sample was obtained before the administration of a calafate (*Berberis microphylla*) berry extract (CBE) via gavage. Two samples were obtained 4 hours after administration of 300 mg kg^{-1} of CBE (M77 and M95). The samples were enzymatically deconjugated, deproteinized and extracted by MEPS and LLE, followed by derivatization and analyzed by GC-MS/MS. Human spiked plasma (1.0 μg mL^{-1} of each phenolic acid) was used for comparison of quantitative performance of extraction methods (MEPS and LLE) under optimized conditions. All procedures involving biological samples were approved by the Bioethical Committee of Universidad de Concepción (submitted in FONDECYT N° 1140439 project).

Enzymatic deconjugation

A solution of 50.000 U mL^{-1} of commercial β-glucuronidase was prepared in acetate buffer 150 mM (pH 4.8). 25 μL of plasma, 50 μL of water or standard mix, 50 μL of EDTA 0.04 % plus sodium acetate buffer 300 mM (pH 4.8) and 10 μL of purified β-glucuronidase (500 U) were incubated at 37°C for deconjugation.

The commercial enzyme contains phenolic compounds, so to avoid interference a previous purification step by ultrafiltration was performed (14.000g during 5 min), followed by buffer addition. The influence of incubation time (30 and 60 min) of purified and non-purified enzyme was evaluated using 25 μL of 3,4-dihydroxybenzoic acid 3-O-sulfate (5 μg mL^{-1}) and the concentration of the deconjugated acid was used as analytical response.

Extraction procedures

In order to evaluate more suitable extraction stationary phases, C-18 and HLB SPE cartridges were assayed. The phases were activated with 5 mL of acetonitrile and 5 mL of trichloroacetic acid at pH 2.0 (TCA). 100 μL of a standard mix (5 mg L^{-1} of each compound) was mixed with 1 mL of TCA and loaded

into the cartridges. TCA (5 mL) were used for clean-up and the elution was carried with acetonitrile (3 x 5 mL). The evaluation was carried out considering recovery and repeatability.

MEPS was evaluated as a miniaturized automatic alternative to SPE managed in the GC autosampler using C-18 and C-8 phases. After deconjugation, protein precipitation was carried out with sample (25 µL), 10% TCA (50 µL) and 2 µg mL^{-1} *trans*-cinnamic acid-d_6 as internal standard (25 µL). The mix was vortexed for 30 s, and centrifuged at 5000 g for 5 min at 5 °C. The liquid fraction was separated and a second extraction was performed using 10% TCA (50 µL) and water (25 µL). Both liquid fractions were pooled and water (350 µL) was added to lower the viscosity. BIN activation was using acetonitrile (250 µL) and HCl 0.1 M, two times at 10 µL s^{-1}. Multivariate optimization was performed with a standard mixture considering the following variables: number of draw-eject cycles (-1:2, 0:6, +1:10), elution volume (-1:30 µL 0:60 µL +1:90 µL) and number of acetonitrile elutions (-1:2, 0:4, +1:8). A wash step with HCl 0.1 M (250 µL) was required.

LLE was performed according to Grün et al [21] with modifications. After enzymatic deconjugation, 2 µg mL^{-1} *trans*-cinnamic acid-d_6 as internal standard (25 µL) and 0.21 M HCl (150 µL) were added to 25 µL of sample, followed by 10 min incubation at 5 °C. Ethyl acetate (700 µL) was added to the sample, vortexed 30 s, centrifuged at 5000 g during 10 min at 5 °C and the superior organic fraction was transferred to a vial. This step was performed three times and the pooled organic fractions were dried under nitrogen before the derivatization process.

Derivatization reactions

Optimization of TMS derivatization was performed based on Zhang and Zuo [29] with modifications. 25 µL of extracted plasma or spiked extracted plasma were transferred to a micro-reaction vessel and evaporated under nitrogen. Toluene (300 µL) was added and evaporated to dryness, followed by 50 µL of BSTFA:TMCS (90:10). Temperature (-1: 70°C, 0: 90°C, +1: 110°C), and time (-1: 0.5 h, 0: 2.25 h, +1: 4.0 h) were evaluated by multivariate optimization using a standard mixture (5 µg mL^{-1} in methanol). The vials were vortexed for 30 s before GC analysis. Normalized areas were used as the analytical response, and benzoic acid-d_5 was used to verify the success of derivatization reactions.

Multivariated optimization of TBA derivatization was based on procedure described by Peters et al with modifications [24]. Standard solutions (20 µg mL^{-1} in methanol) were used in the in-port derivatization (IPD) optimization process. Three parameters were studied; injector temperature (-1: 260°C, 0: 320°C, +1: 380°C), reaction time (-1: 0.67 min, 0: 1.50 min, +1: –2.33 min), and salt concentration (-1: 0.06 M,

0: 0.09 M, +1: 0.12 M). Solutions were mixed with TBAH or TBACl, and evaporated under nitrogen. Acetonitrile (50 µL) was added, vortexed for 30 s and transferred to a GC vial for injection.

GC-MS analysis

An Agilent 7890A GC (Agilent, Palo Alto, CA) with multimode injector, interfaced to an Agilent 7000 GC/MS Triple Quad detector, and fitted with an Agilent CTC PAL autosampler was used. Agilent MassHunter GC/MS acquisition software (Version B.05.00 / Build 5.0.291.0) was used for control system. Chromatographic separations were performed using an HP-5MS fused silica capillary column (30 m x 0.250 mm x 0.25 um, Agilent J&W, Palo Alto, CA) and helium (99.9999% purity, 1 mL min^{-1}) was employed as carrier gas.

The GC conditions for TMS derivatives were one microliter in splitless mode injection at 280 °C. The temperature program was initially 45 °C for 1 min, then raised to 100 °C at 10 °C min^{-1}, and held for 5.5 min, then increased again to 300 °C at 7.5 °C min^{-1} and held for 6.3 min giving a total run time of 45 min. The GC conditions for TBA derivatives were five microliters of the sample injected in programmable temperature vaporizing (PTV) mode. Optimized conditions were: injector temperature 50 °C, held for 1 min with the split vent open and purged at 100 mL min^{-1}, while the column flow was set at 0.63 mL min^{-1}. Once IPD was completed, the split vent valve was opened and the column flow rate increased to 1.5 mL min^{-1}. The initial oven temperature was at 50 °C, held for 3 min, and then ramped to 280 °C at 10 °C min^{-1} being held for 5 min giving a total run time of 45 min.

The MS detector transfer line, quadrupole and ionization source were set to 275, 150 and 230 °C, respectively, using electron impact at 70 eV. The acquisition was performed in scan-mode (from 70 to 450 amu) and in MRM mode. Peak identification was performed by comparing retention times with standards and using mass library (NIST 2.0). Quantitation was performed using *trans*-cinnamic acid-d_6 as internal standard. Calibration curves for each compound were constructed plotting relative area versus concentration.

Multivariate analysis

The optimization of MEPS and derivatizations were carried out with a standard mix of five phenolic compounds, including all reported phenolic metabolite families of flavonoids and hydroxycinnamic acids. This group was selected considering the relevance of phenolic families in the context of their metabolization. The derivatization feasibility with respect to steric hindrance and/or high number of hydroxyl groups was also considered in this selection. The analytes were malic, 4-methoxybenzoic, 3-hydroxyphenylacetic, 3-(4-hydroxyphenyl)propionic and 3-methoxy-4-hydroxycinnamic acids.

Optimization was carried out using a central composite circumscribed design (CCC or full factorial design with star points). The software employed was Modde v 7.0.0.1 (MKS Data Analytics Solutions, San José, CA, USA) and the response were the normalized areas against *trans*-cinnamic acid-d_6. The evaluation was carried out at two levels, with central point in triplicate, assuming heteroscedasticity in the studied interval.

Results and discussion

Derivatization reactions optimization

The TMS and TBA reactions were compared under optimized conditions in order to determine if one of them was analytically advantageous. In the results for TMS derivatization showed in Figure 3.1 A, B, C, D and E, it can be observed that the effect of reaction time cannot be studied without considering the influence of temperature. Indeed, for all studied reaction times, the highest signal was observed at 90 °C. For malic and 4-methoxybenzoic acids (Figure 3.1 A and B), longer reaction times produced higher signal responses, while for the other three compounds the reaction time shows a minor effect and better response in less time. In all cases, temperatures above 90 °C lead to a decrease in signal. The optimum conditions chosen were a compromise between higher signal and short reaction time, i.e., 90 °C and 0.5 h.

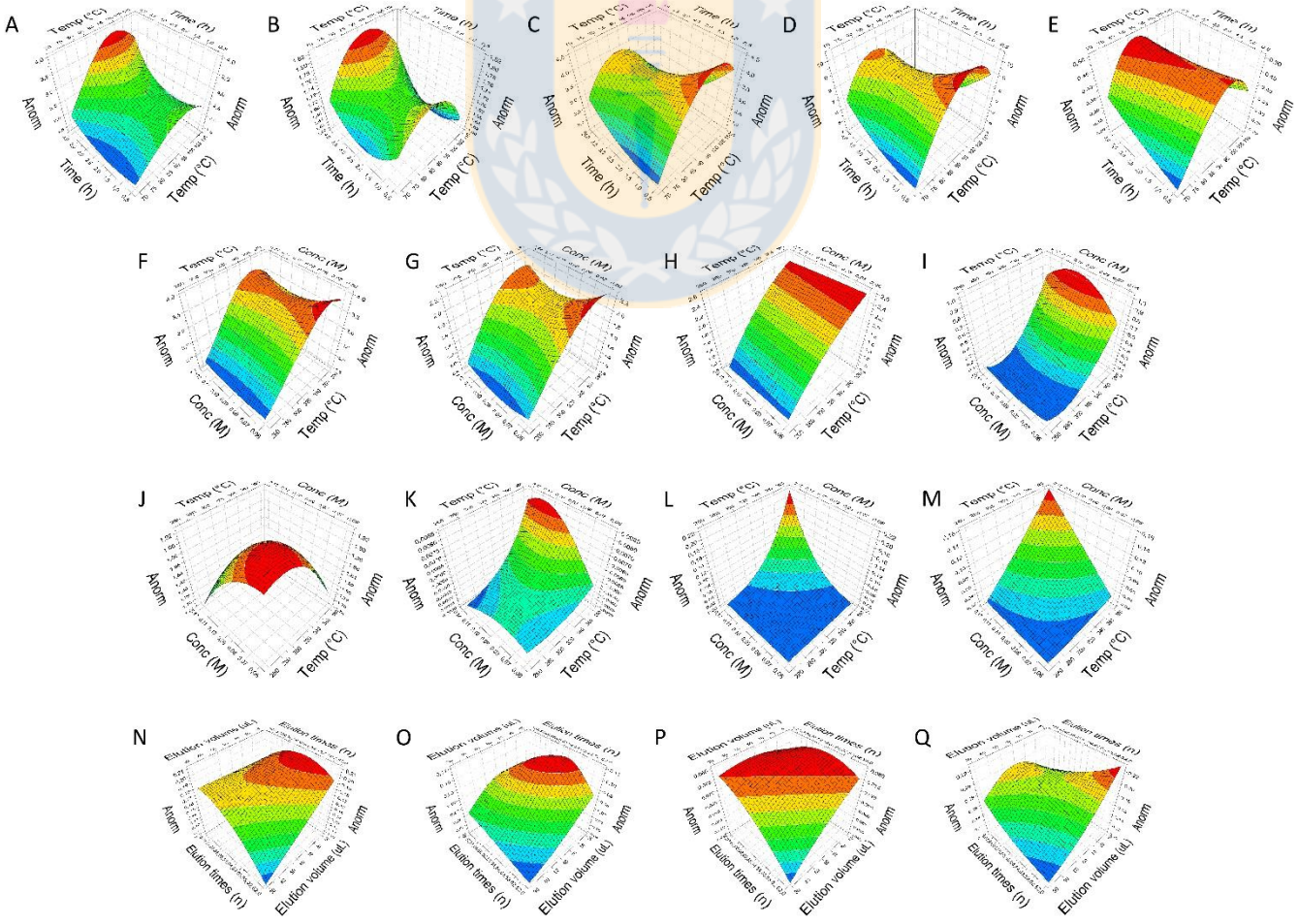

Figure 3.1: *CCC response surface optimization of: i) TMS reaction using time and temperature (Temp) at three levels of five normalized analyte areas; A) malic acid, B) 4-methoxybenzoic acid, C) 3-hydroxyphenylacetic acid, D) 3-(4-hydroxyphenyl)propionic acid, and E) 3-methoxy-4-hydroxycinnamic acid; ii) TBAH reaction using salt concentration (Conc) and Temp at three levels of four normalized analyte areas; F) 4-methoxybenzoic acid, G) 3-hydroxyphenylacetic acid, H) 3-(4-hydroxyphenyl)propionic acid, and I) 3-methoxy-4-hydroxycinnamic acid; iii) TBACl reaction using salt Conc and Temp at three levels of four normalized analyte areas; J) 4-methoxybenzoic acid, K) 3-hydroxyphenylacetic acid, L) 3-(4-hydroxyphenyl)propionic acid, and M) 3-methoxy-4-hydroxycinnamic acid; iv) C18 MEPS BIN using elution time and volume of acetonitrile at three levels of four normalized analyte areas; N) 4-methoxybenzoic acid, O) 3-hydroxyphenylacetic acid, P) 3-(4-hydroxyphenyl)propionic acid, and Q) 3-methoxy-4-hydroxycinnamic acid*.

No systematic study have been made to evaluate TBA derivatization applied to phenolic compounds, therefore an optimization of TBA reaction was carried out with TBAH and TBACl. Both salts does not use any catalyst, so steric hindrance is relevant in the formation of derivatives, like malic acid, a very small molecule bearing three hydroxyl groups. Butylated malic acid was not detected and no response surface plot was generated. Figures 3.1 F, G, H and I show response surfaces for TBAH reaction conditions (salt concentration and temperature) with a fixed reaction time of 1.5 min. The most important factor affecting the IPD was the injector temperature, 380°C was the optimum and the studied TBAH concentration was not relevant. Higher temperatures were not tested to avoid irreversible damage to the GC column and injection port.

The results for TBACl are presented in Figures 3.1 J, K, L and M. The reaction time was established at 1.5 min, allowing evaluation of the effects of salt concentration and temperature. Conflicting results were observed, thus a compromise for the optimum conditions was stablished, which were a TBACl concentration of 0.12M and injector temperature of 380 °C.

TBAH produces higher normalized areas for the four studied analytes than TBACl, which is also true for the net areas, because it gives better reaction yield. The formation of an ion pair between TBA salt and the acid conjugate base is thermally decomposed inside the GC injection port to produce the tributylammonium and a butyl ester derivative [30], which is aided by the use of packed liners to increase the contact surface. When using TBACl, the TBA-conjugate base ion pair is more difficult to establish than TBAH, requiring higher salt concentrations and temperatures, which leads to a secondary pyrolysis reducing dramatically the liner lifespan. Analyte interactions with the active sites of the liner, inhibits the generation of TBA-carboxylate ion pairs, which is a critical step in the butylation process. Liner activation

is due to salt pyrolysis in previous stated reaction conditions. Using liners with higher levels of inertness may not be a solution, because the problem is the high amount of salt deposition on the liner. Consequently, TBACl was no longer pursued. In table S3.1 are presented the validation parameters and polynomial equations for the studied compounds with the three derivatization methods. LDs and LQs from signal-to-noise ratios were estimated for derivatives formed using TMS and TBAH. For the TMS reaction LQ values was below 0.24 µg mL^{-1} in scan mode, while TBAH LQ was over this value. Moreover, a lower acidity of phenol group hinders formation of TBA ion pair, allow incomplete reaction and trap the polar compounds in the liner, increasing uncertainty. Furthermore, our data (not shown) indicates that several peaks are detected when some phenolics are derivatized with TBAH, indicating incomplete reactions under selected conditions. Based on the results, TMS reaction was chosen despite the easy automation and lower moisture sensitivity of the TBAH reaction.

MRM of TMS-GC-MS/MS

MRM method was developed to evaluate 43 phenolic compounds that could be found in an *in vivo* study of dietary phenolics. The evaluated transitions are shown in Table S3.2. MRM mode showed a cleaner chromatogram than scan mode and up to 9 times higher detection limits. However some transitions, such as 147→73, 174→73 and 174→147, were avoided because increase noise [22].

Extraction methods comparison

In the preliminary study carried out with SPE, HLB phase was evaluated due to its wider polarity range compared to C-18. However, the number of retained compounds using C-18 was higher than HLB, 24 analytes were retained with recoveries higher than 80% using C-18, while only 9 of them when HLB was used. Moreover C-18 showed repeatability less than 20 % for 28 compounds while HLB only 11 analytes showed the same behavior. As conclusion, C-18 phase was more appropriated for phenolic acid extraction despite the suitable polarity range of HLB phase. A summary of the recoveries and repeatability of all studied compounds are presented in Table S3.3 and S3.4.

To the best of our knowledge, there are no reports on automated MEPS procedure for phenolic acids before TMS derivatization. Critical steps in MEPS optimization are sample flow rate, if it is set too high (>20 µL s^{-1}) formation of bubbles may produce poor adsorption. Draw-eject cycles must be considered for loading sample and eluting analytes. When MEPS syringe is repeatedly filled with elution solvent, a volume of air is also aspirated, to create a turbulent flow to eliminate solvent fronting and homogenize the eluent. Previous reports of MEPS optimization for other types of analytes included pH, type of elution solvent, % elution solvent in the wash step, number of draw-eject cycles, elution cycles and elution solvent volume

[31–34]. In the present study, the pH was set < 2.0 to ensure protonation of the studied acids, and acetonitrile was used as elution solvent because methanol affected sample derivatization. The study was carried out using 10 draw-eject cycles. The results of the optimization are shown in Figures 3.1 N, O, P and Q. From this, the elution volume was set at 90 µL, and the number of draw-eject cycles of elution solvent to four times (two times for 4-methoxy-3-hydroxycinnamic acid), which is enough to elute all analytes contained in the MEPS BIN. This was further demonstrated as follows. The draw-eject sample step was tested 20 and 30 times. Driving the sample 20 times through the MEPS BIN was enough to ensure maximum adsorption in the stationary phase (data not shown), and it was concluded that 20 cycles, followed by four elution cycles with 90 µL of acetonitrile, were the most suitable settings. In Table S3.1 D are presented the model polynomial equations for the studied compounds.

After set optimized parameters in MEPS procedure, both sample pretreatments (SPE and MEPS) were compared considering recovery and repeatability of procedures. As previously described, C-18 was chosen as appropriate phase for phenolic acid extraction and C-8 phase was also evaluated due to similar retention mechanism, but slightly different selectivity towards more polar compounds. In this study, SPE C-18 retained 24 analytes with recoveries higher than 80%, while other 4 showed more than 30%. In MEPS C-18 only 9 compounds showed recoveries higher than 80% and other 10 higher than 30%, while using MEPS C-8 only 1 compound showed more than 80% of recovery and 12 over 30%. Despite the minor recovery obtained by MEPS, it shows better repeatability (in both MEPS phases it were less than 20% for all evaluated compounds, as is shown in Table S3.4), which is one of the most important parameters to visualize changes produced by the consumption of an extract rich in phenolics. MEPS device allows high repeatability despite the small sample volume available in metabolomics studies, being a good analytical alternative in comparison with another sample pretreatment approach. The MEPS main drawback is the low recoveries when the spiked matrix was evaluated, although it would not be a problem when instrumental detection limits are low, as in MRM mode.

Quantitative performance of MEPS and LLE

Analytical parameters for 43 phenolic compounds, determined using MEPS, TMS derivatization and MRM analysis, all under optimized conditions, were calculated from a calibration curve prepared using a gerbil plasma matrix subjected in triplicate to the overall described procedure. The results are presented in Table 3.1 A. Calibration curves at five concentration levels (between 0.1 and 2 µg mL^{-1}) were analyzed in triplicate. Limits of detection and quantification (LD and LQ) were calculated as 3 and 10 times the standard error of the slope, respectively.

Table 3.1: Analytical parameters of the proposed methodology. A) MEPS methodology; B) LLE methodology.

A)

Compound	Slope (µL µg^{-1})	y-intercept	r^2 ajust.	Linear range (µg mL^{-1})	LD (µg mL^{-1})[1]	LQ (µg mL^{-1})[1]	Recovery (%)[2]	Repeatability (RSD%)[3]
Phenylacetic acid	0.4549	0.0107	0.998	0.1 - 2.0	0.073	0.242	33.6	1.2
Butanedioic acid	N.D	N.D	-	-	-	-	0.0	-
Butenedioic acid	N.D	N.D	-	-	-	-	0.0	-
1,4-dihydroxybenzene	N.D	N.D	-	-	-	-	0.0	-
3-phenylpropionic acid	1.3487	-0.0293	0.999	0.1 - 2.0	0.061	0.205	59.2	0.9
Malic acid	N.D	N.D	-	-	-	-	0.0	-
2-hydroxybenzoic acid	1.3344	-0.0249	0.999	0.1 - 2.0	0.045	0.151	10.8	0.7
4-methoxybenzoic acid	1.3911	-0.0333	0.998	0.1 - 2.0	0.049	0.163	33.0	1.0
3-methoxyphenylacetic acid	0.4801	-0.0126	0.998	0.1 - 2.0	0.052	0.174	34.2	1.1
2-acetylbenzoic acid	N.D	N.D	-	-	-	-	0.0	-
3-methoxy-4-hydroxybenzaldehyde	N.D	N.D	-	-	-	-	0.0	-
4-methoxyphenylacetic acid	1.4236	-0.0096	0.998	0.1 - 2.0	0.051	0.171	39.2	1.2
trans-cinnamic acid	1.5487	-0.0593	0.996	0.1 - 2.0	0.068	0.227	39.8	1.5
1,2,3-trihydroxybenzene	N.D	N.D	-	-	-	-	0.0	-
3-hydroxybenzoic acid	0.0914	0.0016	0.996	0.1 - 2.0	0.093	0.309	3.9	1.7
4-hydroxyphenyl etanol	0.6763	-0.0078	0.998	0.1 - 2.0	0.046	0.152	3.8	1.1
3-hydroxyphenylacetic acid	0.0677	0.0013	0.998	0.1 - 2.0	0.051	0.170	5.3	1.2
3,4-dihydroxybenzaldehyde	N.D	N.D	-	-	-	-	0.0	-
4-hydroxybenzoic acid	0.0764	0.0070	0.997	0.1 - 2.0	0.127	0.424	1.6	2.0
4-hydroxyphenylacetic acid	0.0781	0.0015	0.999	0.1 - 2.0	0.036	0.120	3.0	0.9
3-(3-methoxyphenyl)propionic acid	0.8156	-0.0158	0.999	0.1 - 2.0	0.070	0.233	33.8	1.0
1,3,5-trihydroxybenzene	N.D	N.D	-	-	-	-	0.0	-
3,4-dimethoxyphenylacetic acid	1.8841	-0.0387	0.998	0.1 - 2.0	0.056	0.186	41.7	1.8
2,3-dihydroxybutanodioic acid	N.D	N.D	-	-	-	-	0.0	-
3-(4-methoxyphenyl)propionic acid	0.8103	-0.0071	0.998	0.1 - 2.0	0.050	0.166	50.6	1.0
3-(4-hydroxyphenyl)propionic acid	0.5016	0.0130	0.998	0.1 - 2.0	0.052	0.173	9.2	1.2
3-methoxy-4-hydroxybenzoic acid	0.0946	0.0013	0.997	0.1 - 2.0	0.062	0.207	6.3	1.4
3-methoxy-4-hydroxyphenylacetic acid	0.132	0.0019	0.998	0.1 - 2.0	0.028	0.094	10.4	1.3
Shikimic acid	N.D	N.D	-	-	-	-	0.0	-
3,4-dihydroxybenzoic acid	0.0167	0.0009	0.992	0.1 - 2.0	0.234	0.779	0.6	3.1
4-methoxycinnamic acid	0.3385	-0.0030	0.998	0.1 - 2.0	0.052	0.173	17.3	1.0
3-(3,4-dimethoxyphenyl)propionic acid	0.7675	-0.0133	0.999	0.1 - 2.0	0.058	0.194	52.0	0.9
3,4-dihydroxyphenylacetic acid	N.D	N.D	-	-	-	-	0.0	-
Hippuric acid	N.D	N.D	-	-	-	-	0.0	-
3-hydroxycinnamic acid	0.1087	-0.0002	0.998	0.1 - 2.0	0.054	0.179	18.6	1.0
Quinic acid	N.D	N.D	-	-	-	-	0.0	-
3,5-dimethoxy-4-hydroxybenzoic acid	0.075	0.0007	0.999	0.1 - 2.0	0.030	0.101	27.9	0.5
4-hydroxycinnamic acid	0.0752	0.0013	0.999	0.1 - 2.0	0.045	0.151	7.8	0.6
3-(3,4-dihydroxyphenyl)propionic acid	N.D	N.D	-	-	-	-	0.0	-
3,4,5-trihydroxybenzoic acid	N.D	N.D	-	-	-	-	0.0	-
3,4-dimethoxycinnamic acid	0.0698	-0.0006	0.999	0.1 - 2.0	0.023	0.076	21.3	0.6
3-methoxy-4-hydroxycinnamic acid	0.0207	0.0002	0.999	0.1 - 2.0	0.026	0.088	18.5	0.7
3,4-dihydroxycinnamic acid	0.0148	0.00007	0.995	0.1 - 2.0	0.106	0.354	2.4	2.0

B)

Compound	Slope (µL µg^{-1})	y-intercept	r2 ajust	Linear range (µg mL^{-1})	LD (µg mL^{-1})[1]	LQ (µg mL^{-1})	Recovery (%)[2]	Repeatibility (RSD%)[3]
Phenylacetic acid	0.340	-0.002	0.994	0.10 - 5.0	0.03	0.10	100.1	11.2
Butanedioic acid	0.354	0.162	0.997	0.09 - 5.0	0.03	0.09	98.8	9.1
Butenedioic acid	0.839	0.040	0.999	0.08 - 5.0	0.02	0.08	94.8	6.5
1,4-dihydroxybenzene	1.867	-0.060	0.996	0.10 - 5.0	0.03	0.10	78.2	10.5
3-phenylacetic acid	0.638	-0.011	0.998	0.10 - 5.0	0.03	0.10	101.0	8.2
Malic acid	0.078	0.026	0.995	0.11 - 5.0	0.03	0.11	118.5	12.1
2-hydroxybenzoic acid	2.293	-0.037	0.997	0.10 - 5.0	0.03	0.10	101.7	9.6
4-methoxybenzoic acid	0.975	0.004	0.999	0.07 - 5.0	0.02	0.07	100.3	5.7
3-methoxyphenylacetic acid	0.339	-0.008	0.999	0.08 - 5.0	0.02	0.08	99.0	6.2
2-acetylbenzoic acid	0.363	-0.033	0.993	0.15 - 5.0	0.05	0.15	84.4	14.3
3-methoxy-4-hydroxybenzaldehyde	0.223	0.018	0.999	0.07 - 5.0	0.02	0.07	111.0	5.5
4-methoxyphenylacetic acid	0.836	-0.012	0.999	0.07 - 5.0	0.02	0.07	103.0	5.3
trans-cinnamic acid	0.847	-0.012	0.999	0.06 - 5.0	0.02	0.06	106.4	4.4
1,2,3-trihydroxybenzene	1.315	-0.569	0.999	0.10 - 5.0	0.03	0.10	93.2	6.1
3-hydroxybenzoic acid	0.640	-0.008	0.999	0.05 - 5.0	0.01	0.05	101.0	3.8
4-hydroxyphenyl etanol	3.933	-0.016	0.998	0.09 - 5.0	0.03	0.09	98.4	6.9
3-hydroxyphenylacetic acid	0.426	-0.011	0.999	0.05 - 5.0	0.02	0.05	105.6	4.3
3,4-dihydroxybenzaldehyde	0.414	-0.021	0.996	0.12 - 5.0	0.04	0.12	127.9	10.6
4-hydroxybenzoic acid	1.175	0.006	0.999	0.07 - 5.0	0.02	0.07	100.7	5.3
4-hydroxyphenylacetic acid	0.751	-0.026	0.999	0.05 - 5.0	0.02	0.05	101.7	4.4
3-(3-methoxyphenyl)propionic acid	0.500	-0.016	0.998	0.09 - 5.0	0.03	0.09	100.2	7.4
1,3,5-trihydroxybenzene	0.365	-0.177	0.994	0.24 - 5.0	0.07	0.24	70.8	14.4
3,4-dimethoxyphenylacetic acid	1.040	-0.016	0.999	0.05 - 5.0	0.01	0.05	98.5	3.8
2,3-dihydroxybutanodioic acid	0.035	0.002	0.989	0.29 - 5.0	0.09	0.29	115.3	17.4
3-(4-methoxyphenyl)propionic acid	0.812	-0.028	0.999	0.06 - 5.0	0.02	0.06	102.2	5.0
3-(4-hydroxyphenyl)propionic acid	2.184	-0.087	0.999	0.07 - 5.0	0.02	0.07	98.0	5.3
3-methoxy-4-hydroxybenzoic acid	0.514	-0.018	0.998	0.09 - 5.0	0.03	0.09	97.2	7.5
3-methoxy-4-hydroxyphenylacetic acid	0.625	-0.046	0.997	0.11 - 5.0	0.03	0.11	101.2	8.8
Shikimic acid	0.095	-0.009	0.993	0.22 - 5.0	0.07	0.22	109.0	13.8
3,4-dihydroxybenzoic acid	1.284	-0.098	0.996	0.10 - 5.0	0.03	0.10	101.8	10.3
4-methoxycinnamic acid	0.560	-0.032	0.997	0.11 - 5.0	0.03	0.11	100.8	8.5
3-(3,4-dimethoxyphenyl)propionic acid	0.646	-0.030	0.999	0.08 - 5.0	0.02	0.08	99.7	6.4
3,4-dihydroxyphenylacetic acid	0.577	-0.105	0.997	0.13 - 5.0	0.04	0.13	92.2	10.3
Hippuric acid	0.694	-0.161	0.985	0.13 - 5.0	0.04	0.13	90.2	14.8
3-hydroxycinnamic acid	0.281	-0.030	0.997	0.11 - 5.0	0.03	0.11	102.4	9.6
Quinic acid	0.007	0.003	0.990	0.30 - 5.0	0.09	0.30	93.9	18.4
3,5-dimethoxy-4-hydroxybenzoic acid	0.286	-0.019	0.997	0.11 - 5.0	0.03	0.11	96.3	8.8
4-hydroxycinnamic acid	0.509	-0.046	0.995	0.14 - 5.0	0.04	0.14	101.2	12.4
3-(3,4-dihydroxyphenyl)propionic acid	0.807	-0.112	0.997	0.10 - 5.0	0.03	0.10	93.7	9.0
3,4,5-trihydroxybenzoic acid	0.859	-0.217	0.996	0.17 - 5.0	0.05	0.17	98.4	11.5
3,4-dimethoxycinnamic acid	0.216	-0.013	0.996	0.10 - 5.0	0.03	0.10	89.3	10.3
3-methoxy-4hydroxycinnamic acid	0.112	-0.010	0.997	0.09 - 5.0	0.03	0.09	88.2	9.7
3,4-dihydroxycinnamic acid	0.592	-0.062	0.996	0.12 - 5.0	0.04	0.12	100.5	10.4

[1]Limit of detection (LD) and limit of quantitation (LQ) were estimated using slope error of the first calibration points; [2]Recovery (%) was estimated comparing the whole procedure slope against a standard mix slope without pretreatment; [3]Repeatibility was estimated using slope error of the whole calibration curve.

Recoveries were estimated from the ratio between the calibration curve slopes of the solvent-based and the plasma matrix standard solutions (subjected to the entire analytical method) prepared at the same concentration levels and analyzed in triplicate. The 43 analytes were quantitated using *trans*-cinnamic acid-d_6 as internal standard. Blank samples were found to contain minor phenolics levels, probably from the animal's diet. Because of this, the normalized areas of the blanks were subtracted in all calibration levels.

Small acids such as butanedioic, butenedioic, 2,3-dihydroxybutanedioic acid and malic acid, along with highly polar phenolics, such as 1,2,3-trihydroxybenzene, 1,3,5-trihydroxybenzene, shikimic acid, hippuric acid, quinic acid, 3,4,5-trihydroxybenzoic acid, were not retained on the C18-MEPS cartridge due to weak interactions with the sorbent. Overall, 27 phenolic compounds were evaluated with calculated recoveries varying between 1.6% and 72% with respect to the derivatized standards directly injected into GC.

The quantitative results obtained with the described calibration curve in a spiked human plasma sample (1.0 μg mL^{-1} of each phenolic) subjected to the overall procedure are presented in Table 3.2. In this sample, the 27 phenolic acids were detected.

The difference between added and recovered concentrations were acceptable for at least 23 of the studied analytes. The more significant difference was observed for 3,4-dihydroxycinnamic acids, with errors of 63% which can be explained by the loss of this compound in the extraction procedure. The observed precision for a real sample for the overall procedure was acceptable, with a RSD minor than 5 % for all detected analytes.

The same considerations taken for MEPS were applied in LLE evaluation, in terms of data treatment respect to the blank, calculations of LD and LQ, recoveries and repeatability. Calibration curves were prepared using seven concentrations between 0.05 – 5 μg mL^{-1}, randomly analyzed in triplicate. The results are presented in Table 3.1 B. LLE sample treatment conditions allowed to recover all analyzed compounds with an average of 99.2%. The lower recovery was 70.8% for 1,3,5-trihydroxybenzene, followed by 78.2% for 1,4-dihydroxybenzene. On the other hand, higher recoveries, over 100% were accounted for 3,4-dihydroxybenzaldehyde (127.9%), malic acid (118.5%) and 3-methoxy-4-hydroxybenzaldehyde (111%). All other recoveries were between 80-110%. Nonetheless, repeatability was lower than those obtained for MEPS. Quinic acid was the analyte with highest variability (18.4%), followed by 2,3-dihydroxybutanodioic acid (17.4%). Despite RSD values were under 15%, for only 5 compounds the repeatability was lower than 5%. Figure 3.2 shows chromatographic separation of studied phenolic compounds in gerbil plasma spiked with 1 μg mL^{-1}.

Table 3.2: *Concentration of phenolic compounds in spiked human plasma (1 μg mL^{-1}).*

Compound	Spiked human plasma MEPS		Spiked human plasma LLE	
	Average (μg mL^{-1})	RSD (%)	Average (μg mL^{-1})	RSD (%)
Phenylacetic acid	1.06	2.48	1.58	9.43
Butanedioic acid			1.04	12.09
Butenedioic acid			1.07	3.88
1,4-dihydroxybenzene			0.62	8.37
3-phenylpropionic acid	0.89	2.02	0.92	8.87
Malic acid			1.23	6.88
2-hydroxybenzoic acid	0.89	2.65	1.10	2.80
4-methoxybenzoic acid	0.85	1.95	1.10	1.05
3-methoxyphenylacetic acid	0.72	2.70	0.78	0.13
2-acetylbenzoic acid			0.46	0.36
3-methoxy-4-hydroxybenzaldehyde			0.76	11.71
4-methoxyphenylacetic acid	0.71	2.28	0.90	3.33
trans-cinnamic acid	0.90	2.48	0.86	0.18
1,2,3-trihydroxybenzene			0.87	0.15
3-hydroxybenzoic acid	0.78	1.98	0.92	6.52
4-hydroxyphenyl ethanol	0.82	2.26	0.98	1.46
3-hydroxyphenylacetic acid	0.74	2.14	1.01	2.45
3,4-dihydroxybenzaldehyde			0.96	18.00
4-hydroxybenzoic acid	1.02	2.89	0.93	7.41
4-hydroxyphenylacetic acid	1.08	0.81	1.50	8.41
3-(3-methoxyphenyl)propionic acid	0.77	3.25	0.94	0.30
1,3,5-trihydroxybenzene			1.01	2.96
3,4-dimethoxyphenylacetic acid	0.77	1.94	0.92	2.31
2,3-dihydroxybutanodioic acid			1.20	7.31
3-(4-methoxyphenyl)propionic acid	0.66	2.29	0.86	0.90
3-(4-hydroxyphenyl)propionic acid	0.77	1.39	0.82	1.76
3-methoxy-4-hydroxybenzoic acid	0.73	1.03	1.25	6.05
3-methoxy-4-hydroxyphenylacetic acid	0.67	3.10	0.78	1.01
Shikimic acid			1.11	1.42
3,4-dihydroxybenzoic acid	0.75	4.46	0.82	0.12
4-methoxycinnamic acid	0.88	2.25	0.77	1.68
3-(3,4-dimethoxyphenyl)propionic acid	0.72	1.81	0.99	11.63
3,4-dihydroxyphenylacetic acid			1.05	10.34
Hippuric acid			0.90	12.78
3-hydroxycinnamic acid	0.78	2.53	0.88	4.38
Quinic acid			0.71	3.99
3,5-dimethoxy-4-hydroxybenzoic acid	0.67	1.09	0.74	6.66
4-hydroxycinnamic acid	0.81	2.15	0.72	2.37
3-(3,4-dihydroxyphenyl)propionic acid			0.73	10.7
3,4,5-trihydroxybenzoic acid			1.06	9.60
3,4-dimethoxycinnamic acid	0.73	3.24	0.76	8.28
3-methoxy-4-hydroxycinnamic acid	0.73	0.87	0.98	11.99
3,4-dihydroxycinnamic acid	0.37	3.17	0.89	9.92

As described before, the quantitative results obtained with LLE calibration curve in a spiked human plasma sample (1.0 μg mL^{-1} of each phenolic) subjected to the overall procedure are presented in Table 3.2. In this sample, all 43 analytes were detected, presenting acceptable recovered concentrations for 37

compounds. However, five analytes (phenylacetic acid, malic acid, 4-hydroxyphenylacetic acid, 2,3-dihydroxybutanodioic acid and 3-methoxy-4-hydroxybenzoic acid) showed more than 100% of recovery. The lower recovery was for 2-acetylbenzoic acid with an average error of 54%, probably due to a loss in the extraction procedure. The comparison of quantitative results of both extraction methodologies (MEPS and LLE) showed similar concentrations for most of the phenolics in spiked human plasma, with exception of the five mentioned compounds.

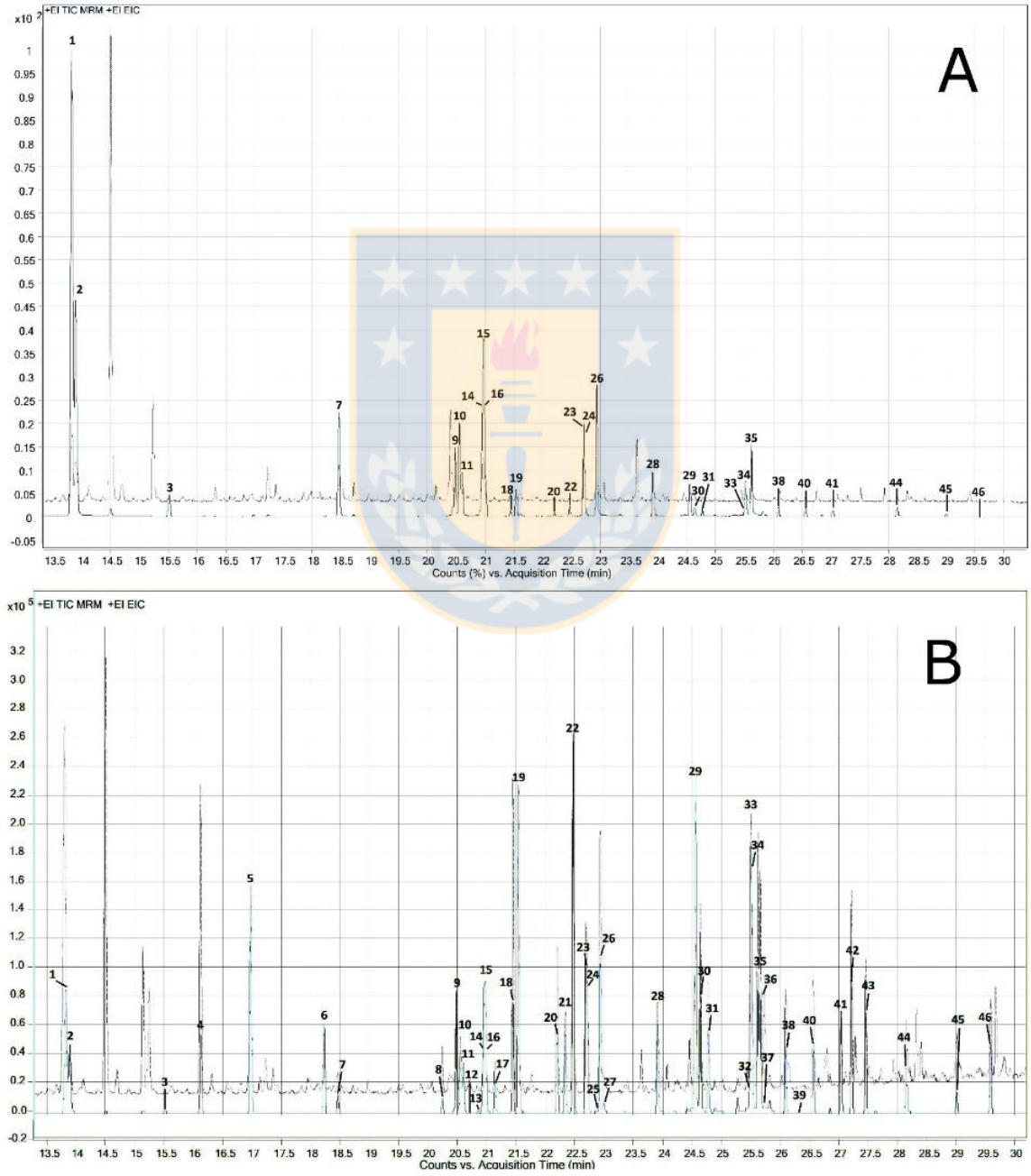

Figure 3.2: GC-chromatogram of gerbil plasma spiked with 1 μg mL^{-1} of 46 phenolic compounds (dotted line correspond to scan mode and solid line correspond to MRM mode). A) MEPS methodology, and B) LLE methodology. Peak annotation: 1. Benzoic acid- d_5, 2. Benzoic acid, 3. Phenylacetic acid, 4. Butanedioic acid, 5. Butenedioic acid, 6. Hydroquinone, 7. 3-(phenyl)propionic acid, 8. DL-malic acid, 9. 2-hydroxybenzoic acid, 10. 4-methoxybenzoic acid, 11. 3-methoxyphenylacetic acid, 12. 2-acetylbenzoic acid, 13. 3-methoxy-4-hydroxybenzaldehyde, 14. Cinnamic acid- d_6, 15. 4-methoxyphenylacetic acid, 16. Cinnamic acid, 17. 1,2,3-trihydroxybenzene, 18. 3-hydroxybenzoic acid, 19. 4-(2-hydroxyethyl)phenol, 20. 3-hydroxyphenylacetic acid, 21. 3,4-dihydroxybenzaldehyde, 22. 4-hydroxybenzoic acid, 23. 4-hydroxyphenylacetic acid, 24. 3-(3-methoxyphenyl)propionic acid, 25. 1,3,5-trihydroxybenzene, 26. 3,4-dimethoxyphenylacetic acid, 27. 2,3-dihydroxybutanedioic acid, 28. 3-(4-methoxyphenyl)propionic acid, 29. 3-(4-hydroxyphenyl)propionic acid, 30. 3-methoxy-4-hydroxybenzoic acid, 31. 3-methoxy-4-hydroxyphenylacetic acid, 32. Shikimic acid, 33. 3,4-dihydroxybenzoic acid, 34. 4-methoxycinnamic acid, 35. 3-(3,4-dimethoxyphenyl)propionic acid, 36. 3,4-dihydroxyphenylacetic acid, 37. Hippuric acid, 38. 3-hydroxycinnamic acid, 39. Quinic acid, 40. 3,5-dimethoxy-4-hydroxybenzoic acid, 41. 4-hydroxycinnamic acid, 42. 3-(3,4-dihydroxyphenyl)propionic acid, 43. 3,4,5-trihydroxybenzoic acid, 44. 3,4-dimethoxycinnamic acid, 45. 3-methoxy-4-hydroxycinnamic acid, 46. 3,4-dihydroxycinnamic acid.

Quantitative analysis of gerbil plasma after calafate berry extract administration

In order to evaluate both procedures with plasma samples obtained from a preliminary ADME (administration, distribution, metabolism and excretion) study, a previous deconjugation step using glucuronidase/sulfatase enzyme was required. After an enzymatic deconjugation of a blank, relevant contamination of other phenolic compounds was found (data not shown). To discard other contamination sources, a purification by ultracentrifugation of the commercial enzyme was evaluated, allowing the elimination of phenolic contamination. Activity comparison of both purified and not purified enzymes was carried out in order to ensure fully functional activity, showing no significant differences between both, when were evaluated for 30 or 60 min. However, the last resulted in a better RSD, employing this incubation time in the enzymatic deconjugation procedure.

Finally, in order to compare the applicability of MEPS and LLE methods, three samples of gerbil plasma were obtained from a preliminary ADME study, whose objective is in the future to evaluate the biological effect of phenolic compounds present in a Patagonian berry (calafate). Table 3.3 shows the results of the application for both procedures to the quantitative determination of phenolics in plasma samples. MEPS procedure allowed to detect five acids in the basal gerbil plasma and further two species were detected only in the post-gavage samples (phenylacetic and 3,4-demethoxycinnamic acids), along with increased concentrations of the others (4-methoxyphenylacetic and 3-hydroxyphenyacetic acids). Such findings

were expected due to dietary intervention. However, observed changes were not conserved in tested samples due to differences in metabolism of each individual animal. LLE procedure showed the presence of eight phenolic acids in the basal gerbil plasma with other four in the post-gavage samples (phenylacetic, 4-methoxyphenylacetic, 3-(4-hydroxyphenyl)propionic and 3,4-dihydroxybenzoic acids). Only two acids found in basal sample had increased concentrations (3-hydroxyphenylacetic and 3-(3,4-dihydroxyphenyl)propionic acids), but not in both tested samples, as previously described. In all analyzed samples, MEPS pretreatment present significantly better overall RSD than LLE.

Despite the variations found in plasma, results show the same trend for both sample pretreatments, finding the same recovered phenolic acids. Nonetheless, in order to accomplish a significant ADME study of this nature, another considerations in the intervention study design must be taken into account, like concentration of polyphenolic extract administrated, if acute or long-term diet will be used, metabolism activity and inter-individual variations.

Table 3.3: *Concentration of phenolic metabolites in gerbil plasma after 4 hours followed the administration via gavage of a polyphenol enriched calafate extract.*

Compound	**Basal MEPS**		**M77 (4h) MEPS**		**M95 (4h) MEPS**		**Basal LLE**		**M77 (4h) LLE**		**M95 (4h) LLE**	
	Average (μg mL^{-1})	**RSD (%)**	**Average (μg mL^{-1})**	**RSD (%)**	**Average (μg mL^{-1})**	**RSD (%)**	**Average (μg mL^{-1})**	**RSD (%)**	**Average (μg mL^{-1})**	**RSD (%)**	**Average (μg mL^{-1})**	**RSD (%)**
Phenylacetic acid	ND	-	0.31	0.30	0.34	2.63	ND	-	0.62	2.80	0.53	4.85
Butanedioic acid							8.23	12.5	2.14	3.26	0.72	3.15
Butenedioic acid							0.33	4.61	ND	-	ND	-
3-phenylpropionic acid	0.35	3.34	ND	-	Trace	-	Trace	-	ND	-	ND	-
2-hydroxybenzoic acid	Trace	-	Trace	-	Trace	-	ND	-	ND	-	ND	-
4-methoxyphenylacetic acid	Trace	-	0.44	7.36	Trace	-	ND	-	Trace	-	Trace	-
4-hydroxybenzoic acid	Trace	-	Trace	-	Trace	-	Trace	-	Trace	-	Trace	-
3-hydroxyphenylacetic acid	Trace	-	0.42	1.00	Trace	-	Trace	-	0.31	15.16	Trace	-
3-(4-hydroxyphenyl)propionic acid	ND	-	ND	-	ND	-	ND	-	Trace	-	ND	-
3,4-dihydroxybenzoic acid	ND	-	ND	-	ND	-	ND	-	Trace	-	ND	-
Quinic acid							2.21	11.2	ND	-	ND	-
3-(3,4-dihydroxyphenyl)propionic acid							0.97	6.25	ND	-	3.23	6.31
3,4-dimethoxycinnamic acid	ND	-	ND	-	Trace	-	ND	-	ND	-	ND	-
3,4-dihydroxycinnamic acid	ND	-	ND	-	ND	-	0.21	6.81	Trace	-	0.12	11.27

Conclusions

ADME studies require reproducible micromethods for quantification of diet-derived phenolic acids in small volumes of biological samples such as gerbil plasma. GC-MS/MS analysis of TMS derivate was shown to be more suitable for the detection and quantification of this kind of compounds. Acids

deconjugation was required using a purified enzyme due to the presence of interfering phenolics. MEPS with C-18 sorbent allows the extraction of diet-derived phenolic acids from plasma, especially less polar acids. Despite the low recovery for some of them, the repeatability using an automated procedure was satisfactory. LLE allowed better recoveries for all studied analytes, at the expense of repeatability. The sensitivity and repeatability of the procedure described using MEPS, TMS derivatization and GC-MS/MS analysis of diet-derived phenolic acids in plasma enables detection of 61% of studied compounds.

Section 2.

Title: Pharmacokinetics of Low Molecular Weight Phenolic Metabolites in Gerbil Plasma by GC-MS/MS after the Consumption of Calafate (*Berberis microphylla*) Berry Extract.

Abstract:

Calafate (*Berberis microphylla*) is shrub with a dark skin berry occurring in Chilean and Argentinean Patagonia. It present high concentrations of vitamin C and phenolic compounds, mainly anthocyanins, followed by flavonols and hydroxycinnamic acids derivatives. No studies about metabolization of calafate fruit phenolic compounds has been carried out to the date.

The quantitative study of over 40 phenolic metabolites was performed by GC-MS/MS analysis using gerbil plasma obtained at 0, 1, 2, 4, 8 and 12 hours after the administration of 300 mg/kg of calafate extract via gavage.

Nine phenolic acids were found to increase in gerbil plasma after calafate intake. After 1 and 2 hours 1,4-dihydroxybenzene, 3,4-dihydroxyacetic, 4-hydroxycinnamic, 3,5-dimethoxy-4-hydroxybenzoic and 3-methoxy-4-hydroxybenzoic acids concentration shows trends to increase. However, 3-hydroxycinnamic and 3-methoxy-4-hydroxyphenylacetic acid concentration show a statistical significant increase. Moreover, 3-hydroxyphenylacetic and phenylacetic acid concentration show statistical significant increase after 4 to 8 hours after calafate intake. The latter, can be product of reduction, dehydroxylation, methylation and β-oxidation of parental compounds found in calafate, and it can be notice the increase in the later time points assayed, indicating entero-hepatic recirculation and/or further metabolization of parent compounds by colonic microbiota, accumulating this molecule through time until achieving high concentrations. Interestingly, 3,5-dimethoxy-3-hydroxybenzoic acid can be attributed to B-ring derivatives of trihydroxylated anthocyanins found in calafate.

Experimental

Animals

Eighteen gerbils were housed in a conventional animal facility maintained at 25±1°C under a 12 h light - 12 h dark photoperiod. Food and water were provided *ad libitum*. Upon arrival, gerbils were acclimatized for three week, 4-6 animals per cage with enriched environment, and fed with D12450H diet (10% fat; Low fat diet: LFD. Open Source Diets; Research Diets, Inc. New Brunswick, NJ, USA) in pellet. A randomization based on gender, blood glucose level and weight of gerbils was carried out. At the end of the study, the animals were fasted for 12h at the beginning of the dark cycle to establish physiological baseline and then blood was collected into EDTA tubes by retro-orbital plexus puncture, centrifuged at 2500 g for 15 min at 5 °C and stored at -80°C until analysis. A basal sample from three animals was obtained before the administration of calafate berry extract (CBE) via gavage. Samples were obtained at 1, 2, 4, 8 and 12 hours after administration of 300 mg kg^{-1} of CBE in triplicate, using a different gerbil to each replicate. All procedures involving animals and biological samples were approved by the Bioethical Committee of Universidad de Concepción (submitted in FONDECYT N° 1140439 project).

Optimized GC-MS/MS targeted analysis

Samples were enzymatically deconjugated as follows. 25 µL of plasma, 50 µL of water or standard mix, 50 µL of EDTA 0.04 % plus sodium acetate buffer 300 mM (pH 4.8) and 10 µL of ultrafiltered β-glucuronidase (500 U) were incubated at 37°C during 1 h. After this, liquid-liquid extraction (LLE) using ethyl acetate was performed to precipitate plasma proteins and extract phenolic acids. Briefly, 25 µL of *trans*-cinnamic acid-d_6 as internal standard (2 µg mL^{-1}) and 0.21 M HCl (150 µL) were added to the mix, followed by 10 min incubation at 5 °C. Ethyl acetate (700 µL) was added to the sample, vortexed 30 s, centrifuged at 5000 g during 10 min at 5 °C and the upper organic fraction was transferred to a vial. This step was performed three times and the pooled organic fractions were dried under nitrogen. For derivatization, 300 µL of toluene was added and evaporated to dryness, followed by addition of 50 µL of BSTFA:TMCS (90:10), vortexed 30 s and incubated at 90 °C during 30 min. The vials were vortexed for 30 s and allowed to achieve room temperature before GC analysis. Normalized areas were used as the analytical response.

Chromatographic separations were performed using an HP-5MS fused silica capillary column (30 m x 0.250 mm x 0.25 um, Agilent J&W, Palo Alto, CA) and helium (99.9999% purity, 1 mL min^{-1}) was employed as carrier gas.

The GC conditions were one microliter in splitless mode injection at 280 °C. The column temperature program was initially 45 °C for 1 min, then raised to 100 °C at 10 °C min^{-1}, and held for 5.5 min, then increased again to 300 °C at 7.5 °C min^{-1} and held for 6.3 min giving a total run time of 45 min.

The MS detector transfer line, quadrupole and ionization source were set to 275, 150 and 230 °C, respectively, using electron impact at 70 eV. The acquisition was performed in scan-mode (from 70 to 450 amu) and in MRM mode. Peak identification was performed by comparing retention times with standards and using mass library (NIST 2.0). Quantitation was performed using *trans*-cinnamic acid-d_6 as internal standard by external calibration.

Results and discussion

Quantitative targeted analysis using GC-MS/MS

A targeted analysis using GC-MS/MS in MRM mode was carried out to monitor over 40 compounds (Section 1). The statistical descriptive analysis reveal that only four compounds show significant differences ($p < 0.10$) between different times after CBE administration and other five exhibit pronounced trends with p values close to 0.10 as it is shown in Figure 3.3. To facilitate comprehension, discussions will be focused in ascending time-points order. Plasma samples obtained 1 h after CBE intake, exhibit higher values than basal condition for three compounds, namely for hydroquinone (1,4-dihydroxybenzene), 3,4-dihydroxyphenylacetic acid and 4-hidroxycinnamic acid, although significant changes could not be properly established (Figure 3.3 A). Following the proposed order, other 4 compounds show a higher concentration 2 h after intake, corresponding to 3-methoxy-4-hydroxybenzoic acid, 3,5-dimethoxy-4-hydroxybenzoic acid, 3-methoxy-4-hydroxyphenylacetic acid and 3-hydroxycinnamic acid, as shown in Figure 3.3 A and B, respectively. Although those four compounds shows the same trend through overall analysis, in the last two a statistical difference was established ($p < 0.05$ and $p < 0.10$, respectively). After 4 h consumption, only 3-hydroxyphenylacetic acid shows a statistical increase ($p < 0.05$). However, this trend is conserved to the next assayed time point (8 h, Figure 3.3 B). At the same time, phenylacetic acid shows a noticeable increase ($p < 0.10$). Finally, previously mentioned compounds show trends at 12 h time point, corresponding to 4-hydroxycinnamic acid, hydroquinone (Figure 3.3 A) and phenylacetic acid (Figure 3.3 B).

Although it is important to establish differences with statistical relevance, trends also gives valuable information to explain the metabolization of phenolics. Accordingly, 3- and 4-hydroxycinnamic acid may be a dehydroxylation product of caffeic acid derivatives present in the extract or B-ring product of trihydroxylated anthocyanins, with concentrations around 0.10 to 0.13 mg/L. Moreover, 3,4-dihydroxy

and 3-methoxy-4-hydroxyphenylacetic acid shows concentration ranges around 0.10 to 0.25 mg/L, although 3-hydroxyphenyl acetic acid shows very low concentration (0.04-0.05 mg/L), contrary those observed for phenylacetic acid (1.0-1.7 mg/L). Phenylacetic acid derivatives can be product of reduction, dehydroxylation, methylation and β-oxidation of parental compounds found in calafate. It is interesting to notice the increase in the later time points assayed, with especial focus on phenylacetic acid, indicating entero-hepatic recirculation and/or further metabolization of parent compounds by colonic microbiota, accumulating this molecule through time until achieve high concentrations.

Finally, benzoic acids and 1,4-dihydroxybenzene are located downstream the metabolism of consumed phenolic compounds. 3-methoxy-4-hydroxybenzoic acid and 1,4-dihydroxybenzene can be a metabolization product of HCADs and anthocyanins contained in the extract. Interestingly, the appearance of 3,5-dimethoxy-4-hydroxybenzoic acid outline the metabolization of trihydroxy anthocyanins. Previous reports of cyanidin feeding shows as major metabolite a dihydroxybenzoic acid [13,35]. However, major calafate anthocyanins corresponds to delphinidin and its methylated derivatives. Assuming the same metabolization, 3,5-dimethoxy-4-hydroxybenzoic can be proposed as a metabolite from delphinidin, petunidin and/or malvidin.

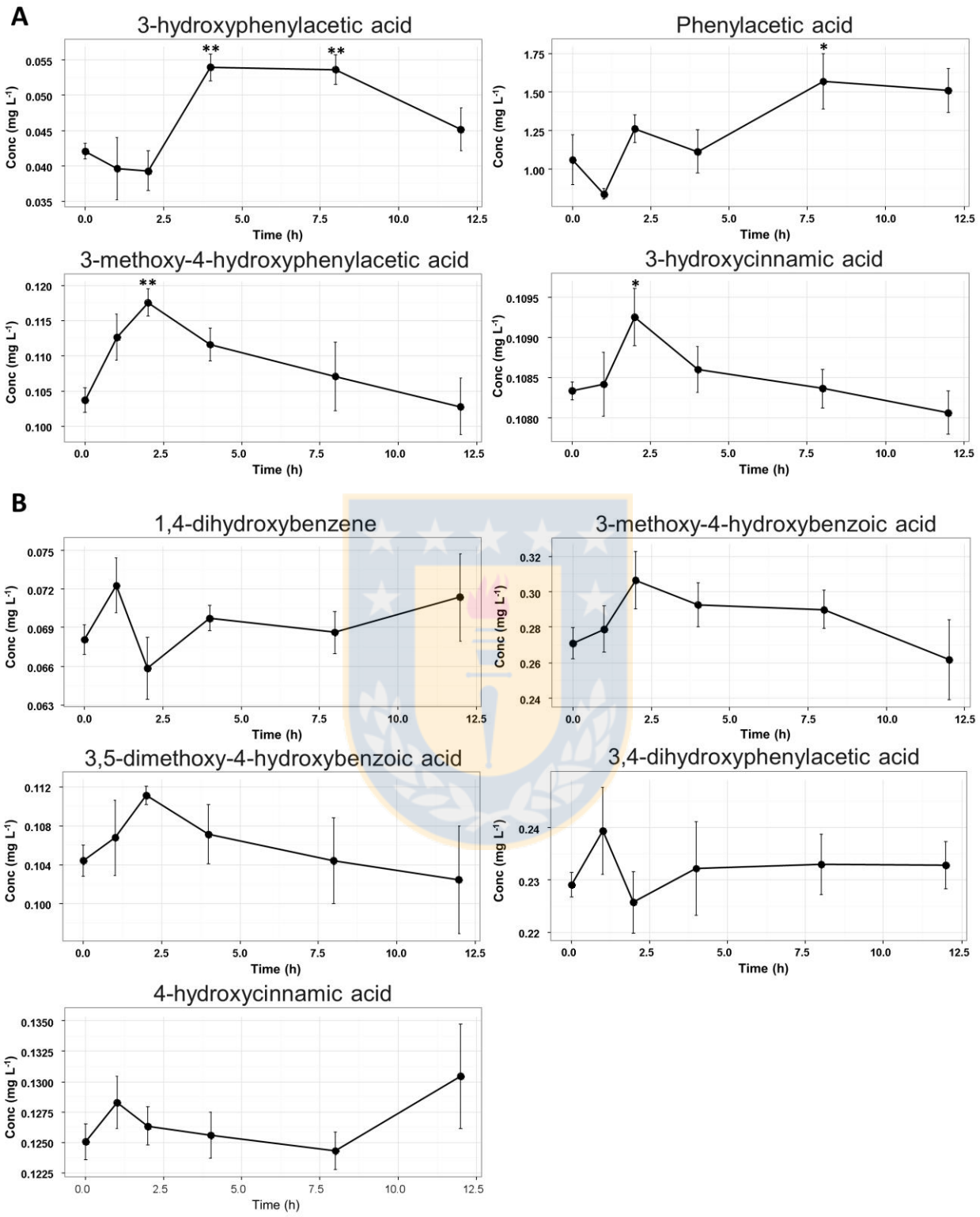

Figure 3.3: Plasmatic concentration of low molecular weight phenolic compounds after administration of 300 mg/kg of CBE. A. Phenolic compounds showing statistical significant increase, * $p<0.10$, ** $p<0.05$; B. Phenolic compound showing trend increase with p value closer to 0.10.

Conclusion

The administration of 300 mg/kg of CBE via gavage increase the concentration of 9 phenolic acids concentration in gerbil plasma. Three core structures increases in the assayed time points, namely hydroxycinnamic acids, benzoic acids and phenylacetic acid derivatives. In terms of their concentrations, the major changes were found in the phenylacetic acids. Interestingly, 3,5-dimethoxy-3-hydroxybenzoic acid was found to increase 2 hours after the administration of CBE and can be attributed to B-ring derivative of trihydroxylated anthocyanins found in calafate. Overall, phenolic concentration changes after one and two hours after intake, and only 3-hydroxyphenylacetic acid and phenylacetic acid show an increase after 4 to 8 hours.

Acknowledgements

Authors would like to thank Fondecyt-1140439, doctoral fellowship, Fondequip-AIC-018 and PFB-27, CONICYT, Chile.

References

[1] P.N. Denev, C.G. Kratchanov, M. Ciz, A. Lojek, M.G. Kratchanova, Bioavailability and antioxidant activity of black chokeberry (*Aronia melanocarpa*) polyphenols: *in vitro* and *in vivo* evidences and possible mechanisms of action: a review, Compr. Rev. Food Sci. Food Saf. 11 (2012) 471–489.

[2] L. Ziberna, F. Tramer, S. Moze, U. Vrhovsek, F. Mattivi, S. Passamonti, Transport and bioactivity of cyanidin 3-glucoside into the vascular endothelium, Free Radic Biol Med. 52 (2012) 1750–1759.

[3] D. Wang, T. Zou, Y. Yang, X. Yan, W. Ling, Cyanidin-3-O-β-glucoside with the aid of its metabolite protocatechuic acid, reduces monocyte infiltration in apolipoprotein E-deficient mice., Biochem. Pharmacol. 82 (2011) 713–9.

[4] R. Zamora-Ros, M. Touillaud, J.A. Rothwell, I. Romieu, A. Scalbert, Measuring exposure to the polyphenol metabolome in observational epidemiologic studies: current tools and applications and their limits., Am. J. Clin. Nutr. 100 (2014) 11–26.

[5] A. Cassidy, G. Rogers, J.J. Peterson, J.T. Dwyer, H. Lin, P.F. Jacques, Higher dietary anthocyanin and flavonol intakes are associated with anti-inflammatory effects in a population of US adults., Am. J. Clin. Nutr. 102 (2015) 172–81.

[6] J.M. Alvarez-Suarez, D. Dekanski, S. Ristić, N. V Radonjić, N.D. Petronijević, F. Giampieri, et al., Strawberry polyphenols attenuate ethanol-induced gastric lesions in rats by activation of antioxidant enzymes and attenuation of MDA increase., PLoS One. 6 (2011) e25878.

[7] D. Jean-Gilles, L. Li, H. Ma, T. Yuan, C.O. Chichester, N.P. Seeram, Anti-inflammatory effects of polyphenolic-enriched red raspberry extract in an antigen-induced arthritis rat model., J. Agric. Food Chem. 60 (2012) 5755–62.

[8] S. Bolca, T. Van de Wiele, S. Possemiers, Gut metabotypes govern health effects of dietary polyphenols, Curr. Opin.

Biotechnol. 24 (2013) 220–225.

[9] G. Williamson, M.N. Clifford, Colonic metabolites of berry polyphenols : the missing link to biological activity ?, Br. J. Nutr. 104 (2010) 48–66.

[10] A.M. Jenner, J. Rafter, B. Halliwell, Human fecal water content of phenolics: The extent of colonic exposure to aromatic compounds, Free Radic. Biol. Med. 38 (2005) 763–772.

[11] A. Stalmach, C.A. Edwards, J.D. Wightman, A. Crozier, Colonic catabolism of dietary phenolic and polyphenolic compounds from Concord grape juice, Food Funct. 4 (2013) 52–62.

[12] H.R. El-Seedi, A.M. El-Said, S. a M. Khalifa, U. Göransson, L. Bohlin, A.K. Borg-Karlson, et al., Biosynthesis, natural sources, dietary intake, pharmacokinetic properties, and biological activities of hydroxycinnamic acids, J. Agric. Food Chem. 60 (2012) 10877–10895.

[13] R.M. De Ferrars, C. Czank, Q. Zhang, N.P. Botting, P.A. Kroon, A. Cassidy, et al., The pharmacokinetics of anthocyanins and their metabolites in humans, Br. J. Pharmacol. 171 (2014) 3268–3282.

[14] M.P. Gonthier, V.R. Cheynier, J.L. Donovan, C. Manach, C. Morand, I. Mila, et al., Nutrient metabolism microbial aromatic acid metabolites formed in the gut account for a major fraction of the polyphenols excreted in urine of rats fed red wine polyphenols 1, J. Nutr. 133 (2003) 461–467.

[15] C. Muñoz-González, M. V Moreno-Arribas, J.J. Rodríguez-Bencomo, C. Cueva, P.J. Martín Álvarez, B. Bartolomé, et al., Feasibility and application of liquid-liquid extraction combined with gas chromatography-mass spectrometry for the analysis of phenolic acids from grape polyphenols degraded by human faecal microbiota., Food Chem. 133 (2012) 526–35.

[16] C.H. Grün, F. van Dorsten, D.M. Jacobs, M. Le Belleguic, E.J.J. van Velzen, M.O. Bingham, et al., GC-MS methods for metabolic profiling of microbial fermentation products of dietary polyphenols in human and in vitro intervention studies, J. Chromatogr. B Anal. Technol. Biomed. Life Sci. 871 (2008) 212–219.

[17] H. Tsugawa, T. Bamba, M. Shinohara, S. Nishiumi, M. Yoshida, E. Fukusaki, Practical non-targeted gas chromatography/mass spectrometry-based metabolomics platform for metabolic phenotype analysis, J. Biosci. Bioeng. 112 (2011) 292–298.

[18] R.F. Venn, Principles and practice of bioanalysis, Second Edition, CRC Press,Taylor & Francis Group, 6000 Broken Sound Parkway N.W., Suite 300. Boca Raton, Florida, United States, 2008.

[19] T. Kind, G. Wohlgemuth, D.Y. Lee, Y. Lu, M. Palazoglu, S. Shahbaz, et al., FiehnLib: mass spectral and retention index libraries for metabolomics based on quadrupole and time-of-flight gas chromatography/mass spectrometry., Anal. Chem. 81 (2009) 10038–48.

[20] E.C.Y. Chan, K.K. Pasikanti, J.K. Nicholson, Global urinary metabolic profiling procedures using gas chromatography-mass spectrometry., Nat. Protoc. 6 (2011) 1483–99.

[21] W.B. Dunn, D. Broadhurst, P. Begley, E. Zelena, S. Francis-McIntyre, N. Anderson, et al., Procedures for large-scale metabolic profiling of serum and plasma using gas chromatography and liquid chromatography coupled to mass spectrometry., Nat. Protoc. 6 (2011) 1060–1083.

[22] H. Tsugawa, Y. Tsujimoto, K. Sugitate, N. Sakui, S. Nishiumi, T. Bamba, et al., Highly sensitive and selective analysis of widely targeted metabolomics using gas chromatography/triple-quadrupole mass spectrometry, J. Biosci.

Bioeng. 117 (2014) 122–128.

[23] L. Xu, M. Jiang, G. Li, Injection port derivatization following sonication-assisted ion-pair liquid-liquid extraction of nonsteroidal anti-inflammatory drugs, Anal. Chim. Acta. 666 (2010) 45–50.

[24] S. Peters, E. Kaal, I. Horsting, H.-G. Janssen, An automated method for the analysis of phenolic acids in plasma based on ion-pairing micro-extraction coupled on-line to gas chromatography/mass spectrometry with in-liner derivatisation, J. Chromatogr. A. 1226 (2012) 71–6.

[25] E. Kaal, A.H.J. Kolk, S. Kuijper, H.G. Janssen, A fast method for the identification of *Mycobacterium tuberculosis* in sputum and cultures based on thermally assisted hydrolysis and methylation followed by gas chromatography-mass spectrometry., J. Chromatogr. A. 1216 (2009) 6319–25.

[26] C. Silva, C. Cavaco, R. Perestrelo, J. Pereira, J. Câmara, Microextraction by packed sorbent (MEPS) and solid-phase microextraction (SPME) as sample preparation procedures for the metabolomic profiling of urine, Metabolites. 4 (2014) 71–97.

[27] M. Abdel-Rehim, Microextraction by packed sorbent (MEPS): A tutorial, Anal. Chim. Acta. 701 (2011) 119–128.

[28] R.-J. Raterink, P.W. Lindenburg, R.J. Vreeken, R. Ramautar, T. Hankemeier, Recent developments in sample-pretreatment techniques for mass spectrometry-based metabolomics, TrAC Trends Anal. Chem. 61 (2014) 157–167.

[29] K. Zhang, Y. Zuo, GC-MS Determination of flavonoids and phenolic and benzoic acids in human plasma after consumption of cranberry Juice, J. Agric. Food Chem. 52 (2004) 222–227.

[30] F. Martin, C. Delrio, F.J. Gonzalezvila, T. Verdejo, Thermally assisted hydrolysis and alkylation of lignins in the presence of tetra-alkylammonium hydroxides, J. Anal. Appl. Pyrolysis. 35 (1995) 1–13.

[31] Z.K. Hoshdel, P.H. Ashemi, M.S. Afdaryan, B.D. Elfan, M.R. Ashidipour, A.B. Adiei, Microextraction in a packed syringe for the analysis of olive biophenols in rat plasma using CMK-3 nanoporous sorbent, Anal. Sci. 29 (2013) 527–532.

[32] S. Magiera, Fast, simultaneous quantification of three novel cardiac drugs in human urine by MEPS–UHPLC–MS/MS for therapeutic drug monitoring, J. Chromatogr. B. 938 (2013) 86–95.

[33] S. Magiera, Ş. Gülmez, A. Michalik, I. Baranowska, Application of statistical experimental design to the optimisation of microextraction by packed sorbent for the analysis of nonsteroidal anti-inflammatory drugs in human urine by ultra-high pressure liquid chromatography, J. Chromatogr. A. 1304 (2013) 1–9.

[34] M. Abdel-Rehim, Recent advances in microextraction by packed sorbent for bioanalysis, J. Chromatogr. A. 1217 (2010) 2569–2580.

[35] P. Vitaglione, G. Donnarumma, A. Napolitano, F. Galvano, A. Gallo, L. Scalfi, et al., Protocatechuic acid is the major human metabolite of cyanidin-glucosides, J. Nutr. 137 (2007) 2043–2048.

Journal of Chromatography B: Biomedical Science and Applications

Electronic Supplemental Material

Evaluation of micro extraction by packed sorbent, liquid-liquid extraction and derivatization pretreatment of diet-derived phenolic acids in plasma by GC-MS/MS.

Luis Bustamante[1], Diana Cárdenas[1], Dietrich von Baer[1], Edgar Pastene[2], Daniel Duran-Sandoval[3], Carola Vergara[1] and Claudia Mardones[1]*

[1]Department of Instrumental Analysis, Faculty of Pharmacy, Universidad de Concepción, Concepción, Chile

[2]Department of Pharmacy, Faculty of Pharmacy, Universidad de Concepción, Concepción, Chile

[3]Department of Clinical Biochemistry and Immunology, Faculty of Pharmacy, Universidad de Concepción, Concepción, Chile

* To whom correspondence should be addressed. Tel.: 56-41-2204598. Fax: 56-41-2226382 E-mail: cmardone@udec.cl.

Table S3.1: Polynomial response and figure of merit of the model for derivatization and MEPS optimization.

A. TBAOH.

4-methoxybenzoic acid	**R2**	**R2 Adj.**	**Q2**	**SDY**	**RSD**	**N**	**Model Validity**	**Reproducibility**
	0,995	0,989	0,966	0,102	0,011	15	0,802	0,992
	Model polynomial ecuation: 0,595 (±0,015) - 0,122 (±0,009)TEMP + 0,0004 (±0,007)TIM + 0,002 (±0,007) CONC +0,100 (±0,016)TEMP*TEMP - 0,025 (±0,012)TIM*TIM - 0,026 (±0,012)CONC*CONC + 0,009 (±0,009) TEMP*CONC							
3-hydroxyphenylacetic acid	**R2**	**R2 Adj.**	**Q2**	**SDY**	**RSD**	**N**	**Model Validity**	**Reproducibility**
	1,000	1,000	0,999	0,217	0,004	13	0,722	1,000
	Model polynomial ecuation: 1,288 (±0,008) + 0,248 (±0,004)TEMP + 0,002 (±0,004)TIM -0,013 (±0,003)CONC -0,163 (±0,009) TEMP*TEMP +0,107 (±0,008)TIM*TIM +0,101 (±0,006)CONC*CONC + 0,007 (0,004) TEMP*TIM -0,016 (±0,004) TEMP*CONC							
3-(4-hydroxyphenyl)propionic acid	**R2**	**R2 Adj.**	**Q2**	**SDY**	**RSD**	**N**	**Model Validity**	**Reproducibility**
	0,926	0,889	0,823	0,685	0,228	16	0,803	0,922
	Model polynomial ecuation: 1,913 (±0,227) + 0,838 (±0,169)TEMP -0,036 (±0,147)TIM – 0,055 (±0,147)CONC -0,210 (±0,223)TEMP*TEMP + 0,281 (±0,198) TIM*TIM							
3-methoxy-4-hydroxycinnamic acid	**R2**	**R2 Adj.**	**Q2**	**SDY**	**RSD**	**N**	**Model Validity**	**Reproducibility**
	0,988	0,978	0,906	0,535	0,080	14	0,725	0,995
	Model polynomial ecuation: 0,486 (±0,124) + 0,584 (±0,064)TEM -0,014 (±0,054)TIM + 0,033 (±0,064)CONC -0,059 (±0,094)TEMP*TEMP +0,323 (±0,083)TIM*TIM -0,141 (±0,094)CONC*CONC							

B. TBACl

	R2	R2 Adj.	Q2	SDY	RSD	N	Model Validity	Reproducibility
4-methoxybenzoic acid	0.971	0.904	0.776	0.04	0.012	14	0.967	0.77
	Model polynomial ecuation: 0,276 (±0,022) + 0,009 (±0,012)TEMP + 0,002 (±0,013)TIM + 0,015 (±0,013) CONC +0,018 (±0,015)TEMP*TEMP + 0,053 (±0,015)TIM*TIM + 0,015 (±0,015)CONC*CONC							
3-hydroxyphenylacetic acid	**R2**	**R2 Adj.**	**Q2**	**SDY**	**RSD**	**N**	**Model Validity**	**Reproducibility**
	0.989	0.964	0.928	0.83	0.158	14	0.991	0.883
	Model polynomial ecuation: 3,773 (±0,289) + 0,279 (±0,127)TEMP + 0,406 (±0,150)TIM -0,048 (±0,150)CONC -0,690 (±0,220) TIM*TIM +0,360 (±0,155)TEMP*TIM - 0,186 (0,155) TEMP*CONC + 0,443 (±0,155) TIM*CONC							
3-(4-hydroxyphenyl)propionic acid	**R2**	**R2 Adj.**	**Q2**	**SDY**	**RSD**	**N**	**Model Validity**	**Reproducibility**
	0.998	0.994	0.991	0.134	0.011	13	0.996	0.977
	Model polynomial ecuation: 0,233 (±0,018) + 0,016 (±0,010)TEMP -0,024 (±0,013)TIM – 0,012 (±0,012)CONC + 0,104 (±0,015)TIM*TIM - 0,102 (±0,013) TEMP*TIM + 0,083 (±0,013)TEMP*CONC – 103 (±0,013)TIM*CONC							
3-methoxy-4-hydroxycinnamic acid	**R2**	**R2 Adj.**	**Q2**	**SDY**	**RSD**	**N**	**Model Validity**	**Reproducibility**
	0.99	0.97	0.812	0.023	0.004	13	0.907	0.961
	Model polynomial ecuation: 0,007 (±0,006) + 0,008 (±0,004)TEM -0,008 (±0,005)TIM + 0,003 (±0,004)CONC -0,037 (±0,007)TIM*TIM - 0,034 (±0,010)TEMP*TIM + 0.030 (±0,010)TEMP*CONC - 0,033 (±0,010)TIM*CONC							

C. BSTFA/TMCS (90:10)

4-methoxybenzoic acid	**R2**	**R2 Adj.**	**Q2**	**SDY**	**RSD**	**N**	**Model Validity**	**Reproducibility**
	0.989	0.976	0.947	0.094	0.015	10	0.973	0.938
	Model polynomial ecuation: 1,710 (±0,027) - 0,006 (±0,015)TEMP + 0,026 (±0,015)TIM - 0,101 (±0,022)TEMP*TEMP + 0,082 (±0,022)TIM*TIM + 0,030 (±0,020)TEMP*TIM							
3-hydroxyphenylacetic acid	**R2**	**R2 Adj.**	**Q2**	**SDY**	**RSD**	**N**	**Model Validity**	**Reproducibility**
	0.989	0.971	0.834	1.286	0.221	9	0.81	0.981
	Model polynomial ecuation: 3,659 (±0,479) + 0,334 (±0,329)TEMP – 0,230 (±0,329)TIM -1,560 (±0,418) TEMP*TEMP +0,508 (±0,418)TIM*TIM - 0,855 (±0,480) TEMP*TIM							
3-(4-hydroxyphenyl)propionic acid	**R2**	**R2 Adj.**	**Q2**	**SDY**	**RSD**	**N**	**Model Validity**	**Reproducibility**
	0.989	0.969	0.886	2.959	0.517	9	0.899	0.959
	Model polynomial ecuation: 8,746 (±1,124) + 0,685 (±0,770)TEMP -0,419 (±0,770)TIM – 3,698 (±0,980)TEMP*TEMP + 0,983 (±0,980) TIM*TIM – 1,923 (±1,126)TEMP*TIM							
3-methoxy-4-hydroxycinnamic acid	**R2**	**R2 Adj.**	**Q2**	**SDY**	**RSD**	**N**	**Model Validity**	**Reproducibility**
	0.981	0.961	0.946	0.082	0.016	9	0.995	0.864
	Model polynomial ecuation: 0,828 (±0,022) + 0,021 (±0,020)TEMP + 0,012 (±0,020)TIM - 0,106 (±0,025)TEMP*TEMP - 0,052 (±0,029)TEMP*TIM							
Malic acid	**R2**	**R2 Adj.**	**Q2**	**SDY**	**RSD**	**N**	**Model Validity**	**Reproducibility**
	0.923	0.862	0.676	0.084	0.031	10	0.79	0.939
	Model polynomial ecuation: 0,810 (±0,054) - 0,052 (±0,030)TEMP - 0,034 (±0,030)TIM + 0,068 (±0,044)TEMP*TEMP - 0,055 (±0,044)TIM*TIM							

D. MEPS.

4-methoxybenzoic acid	**R2**	**R2 Adj.**	**Q2**	**SDY**	**RSD**	**N**	**Model Validity**	**Reproducibility**
	0.964	0.923	0.82	0.044	0.012	14	0.855	0.943
	Model polynomial ecuation: 0,120 (±0,015) + 0,017 (±0,010)DES + 0,023 (±0,009)ACN + 0,003 (±0,010)DEA +0,047 (±0,015)DES*DES - 0,024 (±0,015)DEA*DEA + 0,013 (±0,011)DES*DEA – 0,027 (±0,011)ACN*DEA							
3-hydroxyphenylacetic acid	**R2**	**R2 Adj.**	**Q2**	**SDY**	**RSD**	**N**	**Model Validity**	**Reproducibility**
	0.939	0.868	0.667	192.826	70.141	14	0.86	0.898
	Model polynomial ecuation: 245,478 (±112,884) - 29,479 (±58,798)DES - 128,486 (±49,712)ACN - 75,502 (±58,798)DEA + 90,266 (±75,359) ACN*ACN +109,956 (±60,681)ACN*DEA							
3-(4-hydroxyphenyl)propionic acid	**R2**	**R2 Adj.**	**Q2**	**SDY**	**RSD**	**N**	**Model Validity**	**Reproducibility**
	0.969	0.899	0.643	0.017	0.005	14	0.909	0.865
	Model polynomial ecuation: 0,056 (±0,010) + 0,006 (±0,005)DES - 0,012 (±0,004)ACN + 0,003 (±0,005)DEA + 0,015 (±0,008)DES*DES - 0,009 (±0,005) ACN*DEA							
3-methoxy-4-hydroxycinnamic acid	**R2**	**R2 Adj.**	**Q2**	**SDY**	**RSD**	**N**	**Model Validity**	**Reproducibility**
	0.937	0.864	0.732	27.932	10.291	14	0.954	0.723
	Model polynomial ecuation: 56,468 (±15,038) - 5,167 (±8,339)DES - 18,140 (±7,294)ACN - 6,851 (±8,254)DEA - 16,140 (±12,116)DES*DES + 11,571 (±11,037)ACN*ACN + 19.467 (±8,903)ACN*DEA							

Table S3.2: Extracted ions in scan mode and MRM transitions used in TMS derivatization reaction.

Compound	Extractracted ions (m/z)	Q Transition (m/z)	q1 Transition (m/z)	rel. ab.	q2 Transition (m/z)	rel. ab.
Benzoic acid d5	183.9	184.1 -> 110.1	110.1 -> 82.1	78.2	140.1 -> 112.0	13.7
Benzoic acid	178.8	179.1 -> 105.0	105.0 -> 77.0	80.2	135.0 -> 107.0	19.7
Phenylacetic acid	164.0	164.2 -> 73.0	164.2 -> 137.1	10.6	193.1 -> 75.0	58.7
Butanedioic acid	146.8	247.2 -> 147.1	247.2 -> 73.0	30.0	172.1 -> 73.0	31.3
Butenedioic acid	244.8	245.2 -> 73.0	245.2 -> 147.0	62.6	143.0 -> 75.0	29.4
1,4-dihydroxybenzene	238.8	239.1 -> 73.0	254.1 -> 73.0	63.2	254.1 -> 239.1	98.2
3-phenylpropionic acid	103.9	104.1 -> 78.0	207.1 -> 75.0	63.2	222.1 -> 104.1	39.9
Malic acid	146.9	233.3 -> 73.0	245.1 -> 147.1	26.2	335.2 -> 147.1	10.1
2-hydroxybenzoic acid	266.8	267.1 -> 73.0	267.1 -> 209.0	11.2	149.0 -> 133.0	12.5
4-methoxybenzoic acid	208.8	209.2 -> 135.0	165.1 -> 122.1	39.8	224.1 -> 209.1	36.9
3-methoxyphenylacetic acid	222.8	238.1 -> 73.0	194.1 -> 73.0	64.0	223.1 -> 75.0	76.8
2-acetylbenzoic acid	119.9	120.1 -> 92.0	195.0 -> 75.0	62.4	195.0 -> 177.1	76.0
3-methoxy-4-hydroxybenzaldehyde	223.8	193 -> 137.1	224.1 -> 209.0	54.0	224.1 -> 194.1	60.0
trans-cinnamic acid d6	210.8	137.1 -> 109.1	167.1 -> 150.1	35.8	211.1 -> 167.1	74.9
4-methoxyphenylacetic acid	120.9	179.1 -> 73.0	121.1 -> 78.0	24.1	238.1 -> 179.1	23.8
trans-cinnamic acid	204.8	131.1 -> 103.1	131.1 -> 77.0	70.3	205.1 -> 131.0	65.1
1,2,3-trihydroxybenzene	238.8	239.1 -> 133.1	239.1 -> 211.1	97.3	342.2 -> 239.1	61.6
3-hydroxybenzoic acid	266.8	282.1 -> 267.1	223.1 -> 179.1	20.9	223.1 -> 73.0	63.5
4-hydroxyphenyl etanol	178.9	179.1 -> 73.0	282.2 -> 103.0	1.0	282.2 -> 179.1	16.7
3-hydroxyphenylacetic acid	163.8	164.1 -> 149.0	281.2 -> 147.1	31.4	296.2 -> 73.0	43.2
3,4-dihydroxybenzaldehyde	281.8	282.2 -> 267.2	193.1 -> 137.1	101.5	267.1 -> 73.0	169.4
4-hydroxybenzoic acid	266.8	267.1 -> 223.1	267.1 -> 193.1	98.4	193.1 -> 73.0	70.6
4-hydroxyphenylacetic acid	178.9	179.1 -> 73.0	164.2 -> 149.1	49.6	296.2 -> 73.0	25.4
3-(3-methoxyphenyl)propionic acid	133.9	134.1 -> 104.0	134.1 -> 91.0	98.1	252.1 -> 134.1	79.1
1,3,5-trihydroxybenzene	341.7	342.2 -> 327.2	342.2 -> 268.1	10.2	327.2 -> 73.0	96.8
3,4-dimethoxyphenylacetic acid	133.9	134.1 -> 91.1	121.1 -> 77.0	49.7	252.1 -> 134.1	33.1
2,3-dihydroxybutanodioic acid	146.9	292.2 -> 73.0	189.1 -> 73.0	44.4	219.1 -> 73.0	52.1
3-(4-methoxyphenyl)propionic acid	208.8	209.1 -> 73.0	151.1 -> 107.1	24.2	268.1 -> 73.0	28.1
3-(4-hydroxyphenyl)propionic acid	178.9	179.1 -> 73.0	192.1 -> 73.0	25.1	192.1 -> 177.1	58.1
3-methoxy-4-hydroxybenzoic acid	296.8	297.2 -> 223.1	267.1 -> 193.1	82.2	312.1 -> 297.1	55.9
3-methoxy-4-hydroxyphenylacetic acid	208.9	209.1 -> 73.0	179.0 -> 149.0	33.1	326.2 -> 73.0	29.2
Shikimic acid	203.8	204.2 -> 73.0	204.2 -> 189.1	13.2	255.2 -> 239.1	3.2
3,4-dihydroxybenzoic acid	192.9	193 -> 137.0	193.0 -> 165.0	32.2	370.2 -> 193.1	37.0
4-methoxycinnamic acid	160.9	161.1 -> 133.1	235.1 -> 191.1	61.2	235.1 -> 161.0	73.2
3-(3,4-dimethoxyphenyl)propionic acid	150.9	151.1 -> 107.0	164.1 -> 149.1	65.5	282.2 -> 164.1	66.2
3,4-dihydroxyphenylacetic acid	178.9	179.1 -> 149.0	267.2 -> 179.1	86.1	384.2 -> 267.1	28.6
Hippuric acid	205.9	206.1 -> 73.0	105.1 -> 77.0	31.4	236.1 -> 105.1	9.9
3-hydroxycinnamic acid	202.8	203.1 -> 185.0	293.1 -> 203.1	64.2	308.2 -> 293.2	82.2
Quinic acid	344.8	345.4 -> 73.0	345.4 -> 255.2	74.4	255.2 -> 73.0	30.1
3,5-dimethoxy-4-hydroxybenzoic acid	326.8	327.1 -> 253.1	327.2 -> 297.1	92.5	342.2 -> 327.2	87.4
4-hydroxycinnamic acid	218.8	219.1 -> 73.0	293.2 -> 219.1	75.3	308.2 -> 293.2	45.0
3-(3,4-dihydroxyphenyl)propionic acid	178.9	179.1 -> 149.0	267.2 -> 179.1	51.3	398.2 -> 179.1	34.9
3,4,5-trihydroxybenzoic acid	280.8	281.1 -> 179.0	281.1 -> 253.1	22.7	443.2 -> 281.1	8.2
3,4-dimethoxycinnamic acid	190.8	265.2 -> 191.1	191.1 -> 163.1	80.2	280.2 -> 191.1	71.1
3-methoxy-4-hydroxycinnamic acid	337.7	338.3 -> 323.2	308.1 -> 293.1	91.4	323.2 -> 249.2	91.3
3,4-dihydroxycinnamic acid	218.8	219.1 -> 191.1	219.1 -> 117.1	22.8	396.2 -> 219.1	34.3

Table S3.3: Recoveries of compounds obtained using different phases in SPE and MEPS devices.

Recovery (%)	SPE C-18	SPE HLB	MEPS C-18	MEPS C-8
0 – 10	Benzoic acid Butanedioic acid Butenedioic acid 1,4-dihydroxybenzene Malic acid 1,2,3-trihydroxybenzene 1,3,5-trihydroxybenzene 2,3-dihydroxybutanodioic acid Shikimic acid Quinic acid 3-(3,4-dihydroxyphenyl)propionic acid 3,4,5-trihydroxybenzoic acid	Benzoic acid Butanedioic acid Butenedioic acid Malic acid 2-hydroxybenzoic acid 1,2,3-trihydroxybenzene 3-hydroxyphenylacetic acid 3,4-dihydroxybenzaldehyde 4-hydroxybenzoic acid 1,3,5-trihydroxybenzene 2,3-dihydroxybutanodioic acid 3-(4-hydroxyphenyl)propionic acid Shikimic acid 3,4-dihydroxybenzoic acid 3,4-dihydroxyphenylacetic acid 3-hydroxycinnamic acid Quinic acid 4-hydroxycinnamic acid 3-(3,4-dihydroxyphenyl)propionic acid 3,4,5-trihydroxybenzoic acid 3,4-dihydroxycinnamic acid	Benzoic acid Butanedioic acid Butenedioic acid 1,4-dihydroxybenzene Malic acid 1,2,3-trihydroxybenzene 1,3,5-trihydroxybenzene 2,3-dihydroxybutanodioic acid Shikimic acid 3,4-dihydroxybenzoic acid 3,4-dihydroxyphenylacetic acid Hippuric acid Quinic acid 3,4,5-trihydroxybenzoic acid 2-acetylbenzoic acid	Benzoic acid Butanedioic acid Butenedioic acid 1,4-dihydroxybenzene Malic acid 1,2,3-trihydroxybenzene 4-hydroxyphenyl ethanol 3-hydroxyphenylacetic acid 3,4-dihydroxybenzaldehyde 4-hydroxybenzoic acid 4-hydroxyphenylacetic acid 1,3,5-trihydroxybenzene 2,3-dihydroxybutanodioic acid 3-methoxy-4-hydroxyphenylacetic acid Shikimic acid 3,4-dihydroxybenzoic acid 3,4-dihydroxyphenylacetic acid Hippuric acid Quinic acid 3-(3,4-dihydroxyphenyl)propionic acid 3,4,5-trihydroxybenzoic acid 3,4-dihydroxycinnamic acid
10 – 30	2-hydroxybenzoic acid 3,4-dihydroxybenzaldehyde 3,4-dihydroxyphenylacetic acid	1,4-dihydroxybenzene 3-hydroxybenzoic acid 4-hydroxyphenylacetic acid 3-methoxy-4-hydroxybenzoic acid	3-hydroxybenzoic acid 4-hydroxyphenyl ethanol 3-hydroxyphenylacetic acid 3,4-dihydroxybenzaldehyde 4-hydroxybenzoic acid 4-hydroxyphenylacetic acid 3-methoxy-4-hydroxybenzoic acid 3-(3,4-dihydroxyphenyl)propionic acid 3,4-dihydroxycinnamic acid	2-acetylbenzoic acid 3-hydroxybenzoic acid 3-(4-hydroxyphenyl)propionic acid 3-methoxy-4-hydroxybenzoic acid 3-hydroxycinnamic acid 3,5-dimethoxy-4-hydroxybenzoic acid 4-hydroxycinnamic acid 3-methoxy-4-hydroxycinnamic acid
30 – 80	3-methoxy-4-hydroxybenzaldehyde 4-hydroxyphenyl ethanol 3,4-dihydroxybenzoic acid 3,4-dihydroxycinnamic acid	Phenylacetic acid 3-phenylpropionic acid *trans*-cinnamic acid 4-hydroxyphenyl ethanol 3-methoxy-4-hydroxyphenylacetic acid 4-methoxycinnamic acid 3-methoxy-4-hydroxycinnamic acid 3,5-dimethoxy-4-hydroxybenzoic acid	Phenylacetic acid 3-phenylpropionic acid 3-methoxyphenylacetic acid 3-methoxy-4-hydroxybenzaldehyde 3-(4-hydroxyphenyl)propionic acid 3-methoxy-4-hydroxyphenylacetic acid 3-hydroxycinnamic acid 3,5-dimethoxy-4-hydroxybenzoic acid 4-hydroxycinnamic acid 3-methoxy-4-hydroxycinnamic acid	Phenylacetic acid 3-phenylpropionic acid 4-methoxybenzoic acid 3-methoxyphenylacetic acid *trans*-cinnamic acid 3-(3-methoxyphenyl)propionic acid 3,4-dimethoxyphenylacetic acid 3-(4-methoxyphenyl)propionic acid 4-methoxycinnamic acid 3-(3,4-dimethoxyphenyl)propionic acid 3,4-dimethoxycinnamic acid
80 – 120	Phenylacetic acid 3-phenylpropionic acid 4-methoxybenzoic acid 3-methoxyphenylacetic acid 4-methoxyphenylacetic acid *trans*-cinnamic acid 3-hydroxybenzoic acid 3-hydroxyphenylacetic acid 4-hydroxybenzoic acid 4-hydroxyphenylacetic acid 3-(3-methoxyphenyl)propionic acid	3-methoxyphenylacetic acid 3-methoxy-4-hydroxybenzaldehyde 4-methoxybenzoic acid 4-methoxyphenylacetic acid 3-(3-methoxyphenyl)propionic acid 3,4-dimethoxyphenylacetic acid 3-(4-methoxyphenyl)propionic acid 3-(3,4-dimethoxyphenyl)propionic acid Hippuric acid 3,4-dimethoxycinnamic acid	4-methoxybenzoic acid 4-methoxyphenylacetic acid *trans*-cinnamic acid 3-(3-methoxyphenyl)propionic acid 3,4-dimethoxyphenylacetic acid 3-(4-methoxyphenyl)propionic acid 4-methoxycinnamic acid 3-(3,4-dimethoxyphenyl)propionic acid 3,4-dimethoxycinnamic acid	3-methoxy-4-hydroxybenzaldehyde

	3,4-dimethoxyphenylacetic acid 3-(4-methoxyphenyl)propionic acid 3-(4-hydroxyphenyl)propionic acid 3-methoxy-4-hydroxybenzoic acid 3-methoxy-4-hydroxyphenylacetic acid 4-methoxycinnamic acid 3-(3,4-dimethoxyphenyl)propionic acid Hippuric acid 3-hydroxycinnamic acid 3,5-dimethoxy-4-hydroxybenzoic acid 4-hydroxycinnamic acid 3,4-dimethoxycinnamic acid 3-methoxy-4-hydroxycinnamic acid			
>120	2-acetylbenzoic acid	2-acetylbenzoic acid	2-hydroxybenzoic acid	2-hydroxybenzoic acid 4-methoxyphenylacetic acid

Table S3.4: Precision of extraction of studied compounds using different phases in SPE or MEPS devices.

RSD (%)	SPE C18	SPE HLB	MEPS C18	MEPS C8
0 – 10	2-acetylbenzoic acid 4-hydroxyphenylacetic acid 3,4-dihydroxybenzoic acid 4-methoxycinnamic acid 3-(3,4-dimethoxyphenyl)propionic acid 3-hydroxycinnamic acid 4-hydroxycinnamic acid 3,4-dimethoxycinnamic acid	4-methoxybenzoic acid *trans*-cinnamic acid 3,4-dihydroxybenzaldehyde 4-hydroxyphenylacetic acid 3-(4-hydroxyphenyl)propionic acid 3-methoxy-4-hydroxybenzoic acid Shikimic acid 3,4-dihydroxyphenylacetic acid 3-hydroxycinnamic acid 3-(3,4-dihydroxyphenyl)propionic acid	3-phenylpropionic acid 4-methoxybenzoic acid 3-methoxyphenylacetic acid 4-methoxyphenylacetic acid *trans*-cinnamic acid 3-hydroxybenzoic acid 4-hydroxyphenyl ethanol 3-hydroxyphenylacetic acid 4-hydroxyphenylacetic acid 3-(3-methoxyphenyl)propionic acid 3,4-dimethoxyphenylacetic acid 3-(4-methoxyphenyl)propionic acid 3-(4-hydroxyphenyl)propionic acid 3-methoxy-4-hydroxybenzoic acid 3-methoxy-4-hydroxyphenylacetic acid 3,4-dihydroxybenzoic acid 4-methoxycinnamic acid 3-(3,4-dimethoxyphenyl)propionic acid Hippuric acid 3-hydroxycinnamic acid 3,5-dimethoxy-4-hydroxybenzoic acid 4-hydroxycinnamic acid 3-(3,4-dihydroxyphenyl)propionic acid 3,4,5-trihydroxybenzoic acid 3,4-dimethoxycinnamic acid 3-methoxy-4-hydroxycinnamic acid 3,4-dihydroxycinnamic acid	Phenylacetic acid 3-phenylpropionic acid 2-hydroxybenzoic acid 4-methoxybenzoic acid 3-methoxyphenylacetic acid 3-methoxy-4-hydroxybenzaldehyde 4-methoxyphenylacetic acid *trans*-cinnamic acid 3-hydroxybenzoic acid 4-hydroxyphenyl ethanol 3-hydroxyphenylacetic acid 3,4-dihydroxybenzaldehyde 4-hydroxybenzoic acid 4-hydroxyphenylacetic acid 3-(3-methoxyphenyl)propionic acid 3,4-dimethoxyphenylacetic acid 3-(4-methoxyphenyl)propionic acid 3-(4-hydroxyphenyl)propionic acid 3-methoxy-4-hydroxybenzoic acid 3-methoxy-4-hydroxyphenylacetic acid 4-methoxycinnamic acid 3-(3,4-dimethoxyphenyl)propionic acid Hippuric acid 3-hydroxycinnamic acid 3,5-dimethoxy-4-hydroxybenzoic acid 4-hydroxycinnamic acid 3-(3,4-dihydroxyphenyl)propionic acid 3,4,5-trihydroxybenzoic acid 3,4-dihydroxycinnamic acid
10 – 20	Phenylacetic acid 3-phenylpropionic acid 4-methoxybenzoic acid 3-methoxyphenylacetic acid 4-methoxyphenylacetic acid *trans*-cinnamic acid 3-hydroxybenzoic acid 4-hydroxyphenyl ethanol 3-hydroxyphenylacetic acid 4-hydroxybenzoic acid 3-(3-methoxyphenyl)propionic acid 3,4-dimethoxyphenylacetic acid 3-(4-methoxyphenyl)propionic acid 3-(4-hydroxyphenyl)propionic acid 3-methoxy-4-hydroxybenzoic acid 3-methoxy-4-hydroxyphenylacetic acid Hippuric acid 3,5-dimethoxy-4-hydroxybenzoic acid 3-methoxy-4-hydroxycinnamic acid 3,4-dihydroxycinnamic acid	3-methoxy-4-hydroxycinnamic acid	Phenylacetic acid 2-hydroxybenzoic acid 3-methoxy-4-hydroxybenzaldehyde 3,4-dihydroxybenzaldehyde 4-hydroxybenzoic acid	2-acetylbenzoic acid 3,4-dihydroxybenzoic acid Quinic acid 3,4-dimethoxycinnamic acid 3-methoxy-4-hydroxycinnamic acid
> 20	2-hydroxybenzoic acid 3-methoxy-4-hydroxybenzaldehyde 1,2,3-trihydroxybenzene 3,4-dihydroxybenzaldehyde 3,4-dihydroxyphenylacetic acid Quinic acid 3-(3,4-dihydroxyphenyl)propionic acid 3,4,5-trihydroxybenzoic acid	Phenylacetic acid 3-phenylpropionic acid 3-methoxyphenylacetic acid 2-acetylbenzoic acid 3-methoxy-4-hydroxybenzaldehyde 4-methoxyphenylacetic acid 3-hydroxybenzoic acid 4-hydroxyphenyl ethanol 3-hydroxyphenylacetic acid 3-(3-methoxyphenyl)propionic acid		

3,4-dimethoxyphenylacetic acid
3-(4-methoxyphenyl)propionic acid
3-methoxy-4-hydroxyphenylacetic acid
4-methoxycinnamic acid
3-(3,4-dimethoxyphenyl)propionic acid
Hippuric acid
3,5-dimethoxy-4-hydroxybenzoic acid
4-hydroxycinnamic acid
3,4-dimethoxycinnamic acid

Capítulo 4.

Biodisponibilidad de flavonoides, derivados de ácidos hidroxicinámicos y sus catabolitos en plasma de gerbos (*Meriones unguiculatus)* luego del consumo de un extracto de calafate (*Berberis microphylla*) mediante el metabolómica no-dirigída y ensayos de capacidad antioxidante.

Resumen

Un extracto enriquecido en polifenoles y apto para el consumo de fruto de calafate (*B. microphylla*) fue administrado en una dosis única por sonda gástrica a 6 grupos de gerbos. A cada grupo se le extrajo sangre por una vez a las 0, 1, 2, 4, 8 y 12 horas luego de la administración. El estudio de la metabolización y aparición en el plasma de los compuestos consumidos se realizó usando un enfoque de metabolómica no dirigida mediante UPLC-QTOF. También se estudiaron los niveles de capacidad antioxidante en los plasmas obtenidos mediante los ensayos CUPRAC, ORAC y Folin-Ciocalteau.

Luego del análisis estadístico de los cromatogramas de muestras de plasma, se observa un cambio significativo en 20 compuestos durante los tiempos ensayados. De estos, 6 se identificaron como metabolitos derivados del consumo del extracto de calafate. Los compuestos cumaroil-quinolactona y derivados sulfatados de ácido (iso)vanílico y un isómero de ácido cafeico aumentan significativamente luego de 1 y 2 horas de administrado el extracto de calafate. Los derivados sulfatados de un segundo isómero de ácido cafeico y ácido (iso)ferúlico aumentan significativamente luego de 1 hora y un metoxicatecol-sulfato aumenta luego de 2 horas. Además, el mismo ácido (iso)ferúlico aumenta nuevamente luego de 12 horas administrado el extracto. Adicionalmente, 11 “features” muestran acumulación entre las 4 y 12 horas, mientras que otros 8 presentan disminuciones significativas en los mismos tiempos ($p<0.05$).

El ensayo ORAC-FL revela un aumento significativo de la capacidad antioxidante luego de 1 hora, mientras que para ensayo CUPRAC el máximo se alcanza a las 4 horas de administrado el extracto de calafate. Los resultados de fenoles totales exhiben un aumento significativo a las 1, 4 y 12 horas, relacionándose con los incrementos de los resultados anteriores. El aumento de la capacidad antioxidante puede ser atribuido a los metabolitos identificados, que se desempeñan como reguladores del estrés oxidativo, lo que indirectamente puede contribuir en el aumento evidenciado.

Contenidos

Title: Bioavailavility of Flavonoids, Hydroxycinnamic Acid Derivatives and its Catabolites in Gerbil (*Meriones unguiculatus*) Plasma Following the Consumption of Calafate (Berberis microphylla) Extract, a Study by Untargeted Metabolomics

Luis Bustamante[1], Panagiotis Arapitsas[2], Dietrich von Baer[1], Edgar Pastene[2], Daniel Durán-Sandoval[3], Carola Vergara[1] and Claudia Mardones[1]*

[1]Department of Instrumental Analysis, Faculty of Pharmacy, Universidad de Concepción, Concepción, Chile

[2]Department of Food Quality and Nutrition, Research and Innovation Centre, Fondazione Edmund Mach, via E. Mach 1, San Michele all'Adige, Italy

[3]Department of Pharmacy, Faculty of Pharmacy, Universidad de Concepción, Concepción, Chile

[4]Department of Clinical Biochemistry and Immunology, Faculty of Pharmacy, Universidad de Concepción, Concepción, Chile

* To whom correspondence should be addressed. Tel.: 56-41-2204598. Fax: 56-41-2226382 E-mail: cmardone@udec.cl.

Abstract

An edible calafate berry extract with enriched content of anthocyanins, flavonols and hydroxycinnamic acids was used to fed animals in a single dose to assess the changes in their plasma metabolome. The study was carried out using untargeted metabolomic approach after 0, 1, 2, 4, 8 and 12 hours of calafate extract consumption. The analyses were carried out by UPLC-QTOF and antioxidant capacity of plasma was also studied by CUPRAC, ORAC, ABTS and Folin essays. Twenty metabolites were found to change during the study. Interestingly, six phenolic metabolites were correctly annotated. Coumaroyl-quinolactone, sulfate derivatives of (iso)vanillic and a isomer of caffeic acid were increased at 1 and 2 hours after calafate administration, and a second isomer of caffeic acid sulfate and a (iso)ferulic acid sulfate significantly increased after 1 hour. On the other hand, a methoxycatechol sulfate has an increment at 2 hours and the (iso)ferulic acid sulfate rise at 12 hours after the extract administration. Eleven features mainly shows accumulation at 4 to12 hours, but also a decrease mainly after the same time for 8 features. Antioxidant capacity assays shows increase at 1, 4 and 12 hours after the administration, which can be partially explained by phenolic metabolites, widely attributed as regulators of oxidative stress, however, other molecules can also contribute to the higher antioxidant capacity.

Keywords: UPLC-MS, Plasma, Phenolic acids, Metabolomics, Calafate.

Introduction

Calafate (*Berberis microphylla*) is a shrub with a dark skin berries occurring in Chilean and Argentinean Patagonia. It present high content of vitamin C and phenolic compounds, mainly anthocyanins, followed by flavonols and hydroxycinnamic acids derivatives (HCADs), showing high antioxidant capacity using several antioxidant methods [1–4]. Promising flavonoid and HCADs concentrations are reported in this fruit. The anthocyanin content ranges between 14.21 to 26.13 µmol/g fresh weight (FW) [1], meanwhile flavonol and HCADs content vary between 0.12 to 2.89 and 0.32 to 8.28 µmol/g FW, respectively [1–3]. Comparatively, (poly)phenols concentration found in calafate berry are higher than other widely studied berries [5]. Polyphenolic compounds are classified as secondary metabolites of plants and have several functions in plant defense against pathogens and extreme environment conditions [6]. However, several *in vitro* and clinical studies covered the potential benefits of these compounds in diverse pathologies, such as cardiovascular diseases, diabetes, stress and aging, cancer treatments and prevention [7–13]. Lately, the health promotion studies have been focused in the effects of their metabolites [14–17]. In order to understand their benefits, it is necessary to consider the effects of the parent compound(s) as well as their colonic metabolites generated *in vivo*, in accordance with recommendations discussed by Kay et al [18]. Moreover, it is recognized that gut microbiota has an extensive incidence over polyphenols bioavailability, modifying the presence of aglicones derived from glycosides-glucuronides-sulfated flavonoids as well as major catabolites [17]. The main metabolites produced after the consumption of flavonoids and other phenolic compounds are small weight phenolics, such as benzoic, phenylacetic and 3-phenylpropionic acids [19–22]. According to Ferrars et al, *in vivo* intake study of 1114 µmol of ^{13}C cyanidin-3-glucoside reveal low bioavailability of parent anthocyanin in plasma (<0.2%), with a maximum concentration of 141 nM at 1.8 h, but its metabolites shows 42 times higher concentration at their respective maximum concentrations [22]. Moreover, anthocyanins are rapidly absorbed by stomach and small intestine, achieving peak plasma concentration within the first two hours [23]. Additionally, pH in every gastrointestinal tract (GIT) cavity has relevance because it favors different anthocyanin species. At lower pH the flavylium cation is present (pH < 4.0), but along pH is increasing to physiological ranges, the cation is converted to its hemiketal (pH >= 5.2, hydration) or quinoidal form (pH >=5.5, proton loss), finally reaching an open chalcone (pH >= 6.0) or anionic quinoidal base [24,25]. Added to its pH dependence, microbial catabolism of anthocyanins rise as increase GIT distal passage, explaining the relevant catabolites consequently found in plasma [22,26–29]. Main anthocyanin catabolites are originated from heterocyclic C-ring cleavage. B-ring product correspond to hydroxylated benzoic acid, generally reported as protocatechuic acid (PCA; 3,4-

dihydroxybenzoic acid) because it originates from cyanidin-3-glucoside (a B-ring dihydroxy-anthocyanin), and A-ring conserved product is 2-(2,4,6-trihydroxyphenyl)acetic acid or phloroglucinaldehyde [17,22,30]. From these, several phase I and phase II modifications are followed originating other phenolic compounds. Two ^{13}C tracer cyanidin-3-glucoside studies follows the parent anthocyanin (plus its phase II products) and its metabolites, reporting 32 compounds found in faeces, urine and serum which correspond to anthocyanins, its A and B-ring precursors (phloroglucinaldehyde and PCA), its derived phenolic compounds and phase II derivates [22,30]. Anthocyanin aglycones displays different bioactivities and bioavailability, being more effectives in the attenuation of biomarkers related to metabolic and cardiovascular diseases risk sources containing high concentration of delphinidin and malvidin (blueberry, blackcurrant, bilberry, grape) over sources containing high concentration of cyanidin (elderberry, blood orange, and purple carrot) [23]. Accordingly, intake studies of quercetin derivates shows O-methylation, sulfation and glucuronization of parent compounds and ring fission to originate hydroxyphenylacetic derivates and hippuric acid [31].

Moreover, HCADs bioavailability derived by coffee consumption in ileal fluid, urine and plasma shows phase I and II biotransformation of phenolic compounds through dehydroxylation, demethylation O-methylation, hydrogenation, sulfation, glucuronization and addition of GSH or aminoacids such as glycine [20,32,33]. Proposed metabolites due to HCADs consumption are mainly parent compounds, 3-phenylpropionic, hydroxybenzoic, glycine and hippuric acid derivates [20]

Several human and animal feeding studies focused in berries with high anthocyanin content , such as cranberries, blueberries, raspberries, strawberries, grape among others [34–40]. However, to the best of our knowledge, no reports of intake studies with calafate berry has been performed. The focus of this research has been the study of the gerbil plasma metabolome after the intake of a single dose of calafate berry extract. For this purpose, an untargeted metabolomic approach was developed using UPLC-ESI-QTOF and the measure of antioxidant capacity in gerbil plasma was also included.

Experimental

Chemicals and materials

Potassium persulfate, 6-hydroxy-2,5,7,8-tetramethylchroman-2-carboxylic acid (Trolox), 2,20 -azino-bis(3-ethylbenzothiazoline-6-sulfonic acid) (ABTS), 2,2'-Azobis(2-amidino-propane)dihydrochloride (AAPH), flourescein sodium and neocuproine were purchased from Sigma (St. Louis, Missouri, USA). Delphinidin-3-glucoside, quercetina-3-glucoside and 5-o-caffeoylquinic acid were provided by Phytolab (Vestenbergsreuth, Germany). Methanol and acetonitrile (LiChrosolv grade), sodium carbonate, Folin-Ciocalteu phenol reagent, copper (II) chloride, ammonium acetate, tris(hydroxymethyl)aminomethane (Tris), glycine, tri-sodium citrate, urea and formic acid from Merck (Darmstadt, Germany). Flavonol cleanup was performed using 150 mg Oasis MCX 6cc mixed phase SPE cartridges and plasma cleanup by Ostro 96-weel plates from Waters (Milford, Massachusetts, USA). Distilled ethanol was provided by Oxiquim (Concepción, Chile).

Instrumentation

An analytical balance from Denver Instrument Company (New York, New York, USA), an ultrasonic bar homogenizer Series 4710 from Cole Palmer (Chicago, Illinois, USA), a Stuart S01 mechanical shaker from Bibby Scientific LTD (Stanford, UK), a Sigma 3-16p centrifuge and a Alpha 2-4 LD plus freeze-dryer from Martin Christ (Osterode, Germany), a centrifuge from Thermo Scientific (Waltham, Massachusetts, USA), a rotavapor complemented with a V-700 vacuum pump and V-850 controller system from Büchi (Flawil, Switzerland), a nitrogen evaporator from Pierce (Waltham, Massachusetts, United States) and from Biotage (Uppsala, Sweden), a ultrasonic bath and a positive pressure-96-processor from waters were used for sample preparation. An Epoch™ Synergy HTX microplate reader from Biotek Instruments (Winooski, Vermont, USA) was used for antioxidant assays.

HPTLC analyses of sugars and ascorbic acid were carried out in a CAMAG Automatic TLC sampler 4, equipped with a CAMAG ADC2 automatic developing chamber, a CAMAG Reprostar 3, and a CAMAG TLC Scanner 3 (Muttenz, Switzerland). The control system and data collection were carried out by using CAMAG Wincats software.

HPLC-DAD-ESI-MS/MS analyses for identification of anthocyanins, flavonols and hidroxicinnamic acids were carried out using a Nexera UHPLC/HPLC system from Shimadzu Corporation (Kyoto, Japan) equipped with an SPD-M20A UV-Vis photodiode array spectrophotometer detector coupled in tandem with a QTrap 3200 LC-MS/MS detector from MDS Sciex (Redwood City, California, USA). Instrument

control and data collection were carried out using Shimadzu CLASS-VP DAD Chromatography Data System and MS/MS analysis was performed using AB Sciex Analyst software.

For LC–MS untargeted analysis, a Waters Acquity UPLC was used, coupled to a Synapt ESI HDMS QTOF MS (Waters, Manchester, UK) operating in W-mode and controlled by MassLynx 4.1.

Calafate (*Berberis microphylla*) berry extract (CBE)

CBE was obtained from a pool of grinded frozen berry using a stainless steel mixer as described by Ruiz et al with modifications [1]. Around 20 g of fruit was mixed with 20 mL of potable ethanol:formic acid (97:3), vortexed 30 s and sonicated during 1 min, followed by orbital agitation during 16 h at room temperature. The sample was centrifuged at 3000 g during 10 min and supernatant deposited in an evaporation flask. Other three washing steps were performed as described before, but with 15 min of orbital agitation. A solvent evaporation and water addition was performed, followed by freeze-drying. Dried product was weighed to calculate average solid recovery from berry sample.

Proximate composition and sugar content of CBE

Proximate composition of the CBE was determined according to established methods published by AOAC [41]. Sugar and ascorbic acid content of the CBE was determined according to Morlock and Vega-Herrera [42] and HPTLC CAMAG applications [43], respectively.

CBE (poly)phenol compounds analysis by HPLC-DAD-ESI-MS/MS

Anthocyanins analysis: dried extract was weighed and directly diluted into initial mobile phase. HPLC was carried out using a C18 Kromasil reversed phase column 5 um, 250 x 4.6 mm (AkzoNobel, Bohus, Sweden) with a C18 precolumn (Nova-Pak Waters 4 um, 22 x 3.9 mm) according to Ruiz et al [1]. Oven temperature was set at 40 °C and with a mobile phase flow rate of 0.8 mL min^{-1}. Mobile phase gradient constituted by water/acetonitrile/formic acid (87:3:10% v/v/v) (solvent A) and water/acetonitrile/formic acid (40:50:10% v/v/v) (solvent B). Quantification was performed through a DAD extracted chromatogram at 518 nm by external calibration for all detected compounds using a delphinidin-3-glucoside calibration curve. Results were expressed as the equivalent of delphinidin-3-glucoside in µmol g^{-1}.

Flavonol and HCADs analysis: dried extract was weighed and diluted in water followed by a clean-up step, using Oasis MCX cartridges as described by Castillo-Muñoz et al [44]. Hidroxicinnamic acid analysis was performed with the same column and precolumn described before according to Ruiz et al [2]. Oven temperature was set at 30 °C and the mobile phase flow rate of 0.5 mL min^{-1}. Mobile phase gradient was constituted by water/formic acid (99.9:0.1% v/v) (solvent A) and acetonitrile (solvent B). Quantification

was performed through a DAD chromatogram extracted at 320 nm by external calibration using a 5-O-caffeoylquinic acid calibration curve. All the detected HCADs were quantified using the 5-O-caffeoylquinic acid calibration curve. Results were expressed as the equivalent of 5-O-caffeoylquinic acid in µmol g^{-1}. Finally, flavonol analysis was conducted using a core-shell reverse phase column C18 Kinetex C-18, 2.6 µm, 150 × 4.6 mm (Phenomenex, Torrance, California, USA) with a C-18 precolumn (SecurityGuard Kinetex UHPLC 2.2 µm, 22 x 3.9 mm) as described by Ruiz et al [3]. Oven temperature was set at 30 °C and with a mobile phase flow rate of 0.5 mL min^{-1}. Mobile phase gradient constituted by water/formic acid (99.9:0.1% v/v) (solvent A) and acetonitrile (solvent B). Quantification was performed through a DAD chromatogram extracted at 360 nm by external calibration using a quercetin-3-glucoside calibration curve. All the detected flavonols were quantified using the quercetin-3-glucoside calibration curve. Results were expressed as equivalents of quercetin-3-glucoside in µmol g^{-1}.

Compound identification by MS/MS was carried out using the same chromatographic condition. Positive ionization mode was set as follows: +5 V collision energy, +4000 V ionization voltage, capillary temperature at 450°C, and N_2 nebulizer at 15 psi. On the other hand, negative ionization mode was set as follows: −5 V collision energy, −4000 V ionization voltage, capillary temperature at 450°C, and N_2 nebulizer at 15 psi. Analytes were assigned identities by comparison of their retention time (t_R) with those of the available commercial standards and also by comparisons made between characteristic spectral data (MS enhance product ion (MS-EPI) and UV-Visible) [1–3].

Animals

Eighteen gerbils were housed in a conventional animal facility maintained at 25±1°C under a 12 h light - 12 h dark photoperiod. Food and water were provided *ad libitum*. Upon arrival, gerbils were acclimatized for three week, 4-6 animals per cage with enriched environment, and fed with D12450H diet (10% fat; Low fat diet: LFD. Open Source Diets; Research Diets, Inc. New Brunswick, NJ, USA) in pellet. A randomization based on gender, blood glucose level and weight of gerbils was carried out. Before CBE administration, the animals were fasted for 12h at the beginning of the dark cycle to establish physiological baseline and then blood was collected into EDTA tubes by retro-orbital plexus puncture, centrifuged at 2500 g for 15 min at 5 °C and stored at -80°C until analysis. A basal sample from three animals was obtained before the administration of CBE via gavage. Samples were obtained at 1, 2, 4, 8 and 12 hours after administration of 300 mg kg^{-1} of CBE in triplicate, using a different gerbil for each replicate. All procedures involving animals and biological samples were approved by the Bioethical Committee of Universidad de Concepción.

UHPLC-ESI-TOF untargeted analysis

After plasma collection, samples were freeze-dry and kept at -80 °C until analysis. Then, samples were reconstituted with water and 25 µL were placed into Ostro 96-well plate, followed by addition of 475 µL of chilled acetonitrile/formic acid (99.9:0.1% v/v). After sonication, samples were pushed through sample preparation plate using positive pressure, this step was performed one more time. Solvent was gathered into a 2 mL collection plate, each sample was transferred to a 2 mL amber LC vial and evaporated under nitrogen steam. Samples were reconstituted with 100 µL of mobile phase (water/formic acid (99.9:0.1% v/v), vortexed for 30 s and injected in the UPLC-ESI-QTOF system. Quality control (QC) samples were built using equal portion of each reconstituted plasma sample analyzed in this study.

All samples were analyzed on a reversed phase RP ACQUITY C18 UPLC 1.8 m 2.1 × 150 mm HSS T3 column (Waters) with a C-18 precolumn (Acquity UPLC BEH HSS T3 1.8 m, 2.1 × 5 mm) as described by [45]. Oven column temperature was set at 40 ◦C and with a mobile phase flow rate of 0.28 mL min^{-1}.Water/formic acid (99.9:0.1% v/v) (solvent A) and methanol/formic acid (99.9:0.1% v/v) (solvent B) were used as mobile phase. Mass spectrometric data were collected in ESI mode over a mass range of 50–2000 amu, with scan duration of 0.3 s in centroid mode; for positive and negative ionization a different injection was performed. The transfer collision energy and trap collision energy were set at 6V and 4V. The source parameters were set as follows: capillary 2.5 kV for negative scan, sampling cone 25V, extraction cone 3V, source temperature 150 ◦C, desolvation temperature 500 ◦C, desolvation gas flow 1000 L/h and nebulizer gas 50 L/h. External calibration of mass accuracy and resolution of the MS was performed at the beginning of each batch of analysis by direct infusion of a sodium formate solution (10% formic acid/0.1 M NaOH/acetonitrile with a ratio of 1/1/8), controlling the mass accuracy from 40 to 2000 m/z (less than 3 ppm) and mass resolution (over 14000 FWHM). Lock mass calibration was applied using a solution of leucine enkephaline (0.5 mg/L, m/z 554.2620) at 0.1 mL/min [46]. The injection of samples were carried out following a randomised sequence, where at the beginning of the sequence one blank injection and five QC injections were performed to equilibrate the system, and after every six real sample injections one QC injection was inserted to control instrumental stability.

Metabolomic data processing (peak picking, alignment, grouping and adduct assignation) was performed using Progenesis QI software (Waters, Manchester, UK) and further data analysis was done using GraphPad Prism 5 (GraphPad Software, Inc, La Jolla, CA , USA) and web-based Metaboanalyst 3.0 [47].

Biochemical parameters of gerbil plasma

Colorimetric assays were used to determine plasma triglycerides (TG) and total cholesterol (TC) (Valtek Diagnostics, Chile). Plasma alanine aminotransferase (ALT/GPT) and aspartate aminotransferase (AST/GOT) were measured using kinetic kits (Valtek Diagnostics, Chile). Blood glucose was measured using the Accu-chek Performa Nano glucometer and glucose strips (Accu-chek® Performa, Roche). The quality controls were performed quantifying control serums (Valtrol N, Valtrol P; Valtek Diagnostics, Chile). The measurement was accepted if the values of the respective parameter in control serums were within the tolerance range.

Trolox equivalent antioxidant capacity (TEAC) and total phenolics (TP) assays in CBE and gerbil plasma samples

TEAC and TP assays were conducted in 96-well microplates. $TEAC_{CUPRAC}$ assay for CBE was carried out as described by Ribbero et al [48]**,** while gerbil plasma analysis were essayed as reported from Çekiç et al [49], which was modified in order to incorporate plasma protein into TEAC value. $TEAC_{ORAC\text{-}FL}$ assay for CBE and plasma samples were performed as described by Ou et al [50]. $TEAC_{ABTS}$ and Folin-Ciocalteu method was performed in CBE as described by Ruiz et al [1], but the procedure was modified to microplates lectures.

Results and discussion

CBE polyphenol composition, proximate analysis total phenolics and antioxidant capacity

A batch of 10 g of calafate extract was produced according with experimental section. Table 4.1 shows the concentration of total anthocyanin, flavonol and HCADs obtained in CBE. Major components from each analyzed family are the same as previously reported in fresh fruits [1–3]. Major compounds were delphinidin-3-glucoside (Dp-3-glc), petunidin-3-glucoside (Pt-3-glc) and malvidin-3-glucoside (Mv-3-glc) for anthocyanins; quercetin-3-rutinoside (Q-3-rut) and quercetin-3-rhamnoside (Q-3-rhamn) for flavonols; and 5-O-caffeoylquinic acid (5-CQA) and 3 or 4-*trans*-caffeoyl-glucaric acid (3 or 4-*trans*-CGA) [51] for HCADs. Furthermore, Table S4.1 also shows antioxidant capacity of CBE, namely ORAC-FL, CUPRAC, ABTS and TP. A comparison was made in order to estimate how many times higher is the polyphenol content in CBE regarding calafate berry, using reported data by our group. As expected, total anthocyanins, flavonols and HCADs found in CBE are around ten times higher than calafate berry, evidencing a close relation between weight of the dried extract and phenolic composition, indicating a 10 times of pre-concentration.

Table 4.1: Phenolic content of Calafate berry extract.

Phenolic Content (µmol g-1)	
Dp-3-glc	79.83 ± 1.14
Pt-3-glc	44.78 ± 0.64
Mv-3-glc	29.40 ± 0.41
Total Anthocyanin	224.79 ± 3.02
Q-3-rut	4.35 ± 0.20
Q-3-rhamn	3.31 ± 0.15
Total Flavonol	24.45 ± 0.92
5-CQA	7.16 ± 0.16
3 or 4-*trans*-CGA	4.42 ± 0.08
Total HCAD	12.02 ± 0.54

Moreover, Table S4.2 shows proximate analysis, sugar and ascorbic acid content. Due to its low water content, CBE presents high content of two previously reported sugars, namely glucose and fructose. The sum of both represent 64.3% w w^{-1} of total composition of the extract. Moreover, ascorbic acid, another highly reducing molecule, is present in the dry extract, showing concentrations around those previously reported in calafate [1].

Antioxidant capacity analysis and biochemical parameters of gerbil plasma subjected to CBE administration

To a proper discussion of biochemical parameters and antioxidant capacity analysis of gerbil plasma subjected to CBE administration, it is necessary to estimate the amount of phenolics administrated due to gavage incorporation of around 300 mg of CBE/kg. Table 4.2 presents the concentrations of main studied phenolic compounds, such as total anthocyanins, flavonols and HCADs at the different essayed times after extract administration.

Table 4.2: Polyphenolic content of Calafate berry extract administrated by single dose via gavage.

	1 h (µmol/gerbil)	2 h (µmol/gerbil)	4 h (µmol/gerbil)	8 h (µmol/gerbil)	12 h (µmol/gerbil)
Total Anthocyanin (p>0.05)	4.92 ± 0.71	5.08 ± 1.05	4.65 ± 0.24	4.65 ± 0.24	5.08 ± 1.18
Total HCAD (p>0.05)	0.54 ± 0.08	0.55 ± 0.11	0.51 ± 0.03	0.51 ± 0.03	0.55 ± 0.13
Total Flavonol (p>0.05)	0.26 ± 0.04	0.27 ± 0.06	0.25 ± 0.01	0.25 ± 0.01	0.27 ± 0.06

After the calafate extract administration, plasma samples were treated as was explained in experimental section, 25 µL were used to perform described antioxidant methods. Table S4.3 shows analytical parameters used for validation of antioxidant essays

Figure 4.1 shows antioxidant capacity assays (TP, CUPRAC, ORAC-FL) and Figure S4.1 shows performed biochemical parameters.

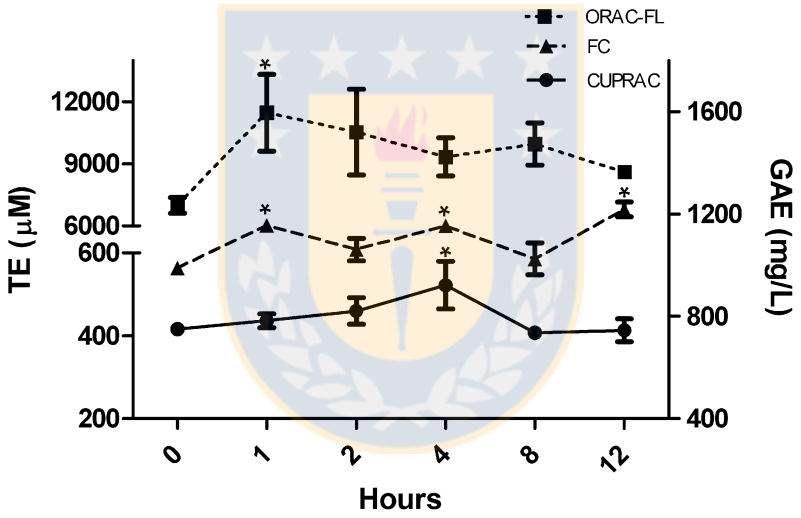

*Figure 4.1: Plasmatic antioxidant capacity values of ORAC-FL, CUPRAC-thiol containing proteins and Folin-Ciocalteu (FC) at different time points after the administration of 300 mg kg^{-1} of CBE; *. p<0.05.*

The antioxidant capacity essays considered plasmatic proteins, reducing sugars, uric acid and phenolic metabolites under physiological pH, obtaining the overall oxidative conditions in analyzed plasma. As is shown in Figure 4.1, ORAC-FL values reveals a 64% increase after 1 h compared to basal. Moreover, CUPRAC shows a 25% increase after 4 h compared to basal samples. Interestingly, TP values shows a similar response than CUPRAC and ORAC-FL values. After 1, 4 and 12 h TP values were statistically higher than basal plasma samples, showing 17% increase at 1 and 4 h and a 23% increase after 12 h CBE was administrated.

Trend differences of antioxidant capacity results may have two main basis. First, all three performed assays have key differences. ORAC-FL is an hydrogen atom transfer (HAT) based assay, which involves the competition of peroxyl radicals produced by an azo compound with other antioxidant molecules presented in plasma to avoid probe decay, measuring a competitive peroxyl radical scavenging capacity [52]. Conversely, CUPRAC and TP using Folin-Ciocalteu reagent (FCR) are electron transfer (ET) based essays. However, observed differences can be explained due to reaction conditions in each assay. CUPRAC is conducted at pH 7 and is based on the mild oxidizing reagent Cu(II)-neocuproine [49], with an standard potential around 0.6 V that may oxidize biologically important antioxidant but no simple sugars or citric acid, however, uric acid and bilirubin may reduce the probe [53]. Contrastingly, although Folin-Ciocalteu method is classified as an ET based assay, the chemical nature is not fully understand. Its conducted in basic media (pH ~10) so phenolate anions reduce FCR, but may also enhance total sample reducing capacity due to the presence of other reducing molecules. Its standard potential is unknown so sugars, uric acid, proteins and other molecules may have a critical contribution [52].

Finally, the key difference between both ET based essays is that in the later, a chaotropic environment is promoted by the addition of urea (8M) into the buffer, allowing the proteins to lose their structure and expose other molecules (in case of carrier proteins such as albumin) or other functional groups capable to reduce the probe, such as thiol-containing proteins or peptides [49].

According to this, CUPRAC assay shows the sum of reducing conditions of plasmatic proteins and its content specially 4 hours after the administration of CBE. Multiple increase at different time points shows that TP may shows a higher response to phenolics, due to at basic pH phenolates increase its reducing power [52,54]. It is interesting to acknowledge that the first increase in TP assay correlates with the increase evidenced in ORAC-FL assay, while the second increase correlates with CUPRAC assay.

Evidenced changes can be attributed to an increase in phenolic metabolites, explaining peaks achieved at different times after CBE consumption. However, antioxidants are also proposed as oxidative stress regulators protecting enzymes and other readily oxidizable molecules, such as the reduced form of glutathione, uric acid, among others [55,56]. These molecules can be also responsible for antioxidant capacity increase, reversing an oxidized environment in plasma samples.

Untargeted analysis using UPLC-ESI-TOF

Phenolics metabolization after CBE consumption can modify several characteristics of parental compounds, due to oxidations, reductions, sulfonation, glucuronidation, methoxylations and hydrolysis, among others in the liver or as byproducts of colonic microbiota metabolization [11]. The analysis conducted

by UPLC-ESI TOF was carried out to evaluate possible consumption markers in gerbil plasma, using 3 biological replicates in each group. After data analysis, possible markers were selected by ANOVA with post-hoc (Fisher´s LSD, $p<0.05$) and max fold change analysis (1.5 fold change) in order to apply the first filter to over a 1600 features detected in both source polarity, the workflow is detailed in Figure 4.2. Moreover, to detect outliers a PCA analysis was carried out to the filtered data, finding two outliers samples at 1 and 4 h in negative mode.

Accordingly, outliers were removed to carry out the data analysis again, avoiding possible missalignments. Once the first filter was applied, a group of 139 features were obtained. To proper analysis, all 139 features were visually inspected and manually integrated in the raw data, including the outlier samples. Again, a second filter was performed to the reintegrated dataset using the same conditions described before, finding only 30 features. Outlier analysis was performed using hierarchical cluster analysis (HCA), standardized residuals and mahalanobis distance of autoescaled dataset (Figure S4.2). The outlier analysis find the same 2 samples (at 1 and 4 h in negative mode), and were properly removed from the following analysis.

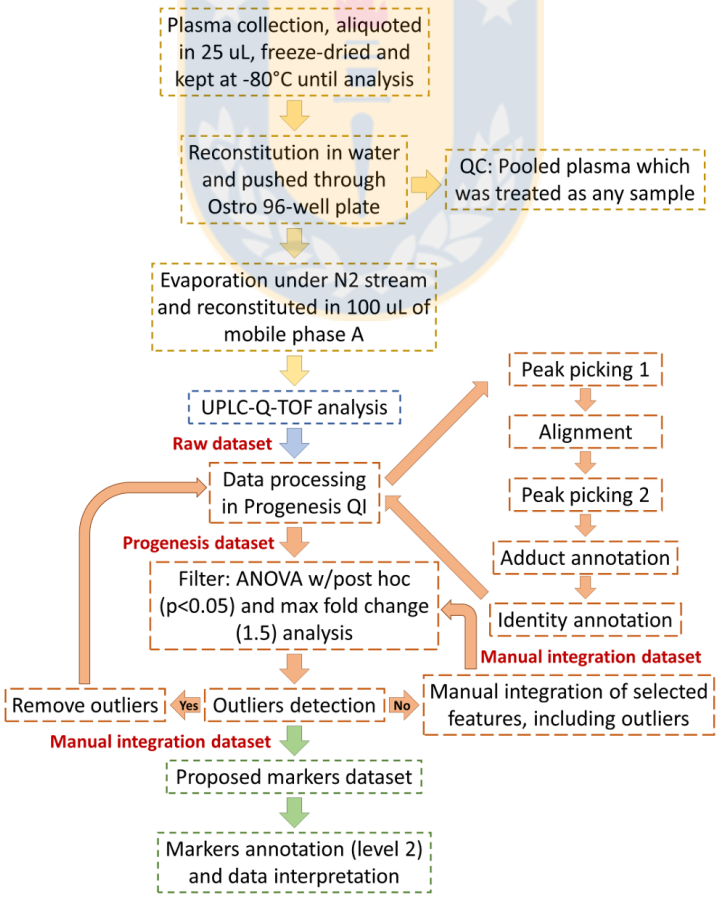

Figure 4.2: Untargeted metabolomic workflow.

To establish the final annotation table for both ionization modes, the QC abundance of each proposed marker was evaluated to discard any variability due to analysis or signal intensity. Table 4.3 shows level 2 annotations of the selected features [57].

Table 4.3: Annotation of proposed markers for CBE consumption in gerbils plasma.

N°	Feature	Proposed formula	Adduct	Mass error (ppm)	Annotation
1	203.0014_9.69	$C_7H_8O_5S$	M-H	0.57	Methoxycatechol sulfate
2a	379.1052_1.49	$C_{16}H_{16}O_7$	M-H+FA	1.75	Coumaroyl-1,5-quinolactone
2b	191.0560_1.49	$C_7H_{12}O_6$	M-H	0.11	Fragment (quinic acid)
3	258.9914_9.13	$C_9H_8O_7S$	M-H	0.40	Caffeic acid sulfate I
4	246.9920_6.56	$C_8H_8O_7S$	M-H	0.20	(Iso)vanillic acid sulfate
5	258.9914_9.84	$C_9H_8O_7S$	M-H	0.40	Caffeic acid sulfate II
6	273.0078_10.57	$C_{10}H_{10}O_7S$	M-H	0.35	(Iso)ferulic acid sulfate
7a	387.1826_20.22	$C_{22}H_{28}O_6$	M-H	1.29	Unknown
7b	455.1721_20.22	$C_{25}H_{28}O_8$	M-H	0.96	Unknown
8	294.1035_11.64	$C_{14}H_{17}N_3O_2$	M+Cl	2.02	Unknown
9	115.0397_5.32	$C_5H_{10}O_4$	M-H_2O-H	0.18	Unknown
10	377.2051_21.84	$C_{19}H_{34}O_5$	M+Cl	4.93	Unknown
11	166.1232_6.31	$C_{10}H_{12}O$	M+NH_4	0.56	Unknown
12a	197.0975_21.86	$C_9H_{18}O_2$	M+K	3.66	Fragment
12b	225.0923_21.86	$C_{15}H_{12}O_2$	M+H	0.00	Fragment
12c	279.1001_21.86	$C_{16}H_{16}O_3$	M+Na	0.94	Unknown
13a	121.0299_21.41				Fragment
13b	245.0781_21.41	$C_{12}H_{14}O_4$	M+Na	0.33	Unknown
14a	215.1064_21.70	$C_{12}H_{16}O_2$	M+Na	2.15	Fragment
14b	352.9906_21.68				Unknown
14c	350.9888_21.68				Unknown
14d	348.9912_21.68	$C_{15}H_{12}O_5$	M+2K+H	3.69	Unknown
15	207.1127_11.60	$C_{11}H_{11}NO_2$	M+NH_4	0.10	Unknown
16a	183.0824_21.73	$C_{13}H_{10}O$	M+Na	1.00	Unknown
16b	105.0353_21.75	$C_4H_8O_S$	M+H	1.56	Fragment
17	277.1062_19.97	$C_{15}H_{16}O_5$	M+H	0.85	Unknown
18a	348.0717_3.14	$C_{10}H_{14}N_5O_7P$	M+H	1.34	Adenosine 2'-phosphate
18b	136.0633_3.15	$C_5H_5N_5$	M+H	1.53	Fragment (Adenine)
19	346.2238_19.54	$C_{18}H_{24}N_4O_2$	M+NH_4	0.05	Unknown
20	335.1634_21.83	$C_{17}H_{28}O_3S$	M+Na	1.73	Unknown

Nine out of thirty features were correctly annotated based on their physicochemical characteristics and mass spectra, 8 were assigned and identified as markers and 2 as fragments.. In supplemental material (Figure S4.3 A and B) are showed the feature correlations to establish them as fragments. As shown in Figure 4.3 A and B and Table 4.3, phenolic metabolites such as coumaroyl-quinolactone, sulfate derivatives of (iso)vanillic and caffeic acid II were found to increase in 1 and 2 h groups ($p<0.05$). However, caffeic acid sulfate I and (iso)ferulic acid sulfate significantly increase after 1h only. On the other hand, methoxycatechol sulfate has an increment after 2h and (iso)ferulic acid sulfate rise after 12 h ($p<0.05$). The time differences can be explained by whether are absorbed and metabolized in the liver during the first two hours or if are further submitted into entero-hepatic recirculation followed by metabolization in the colonic microbiota [11,20,22].

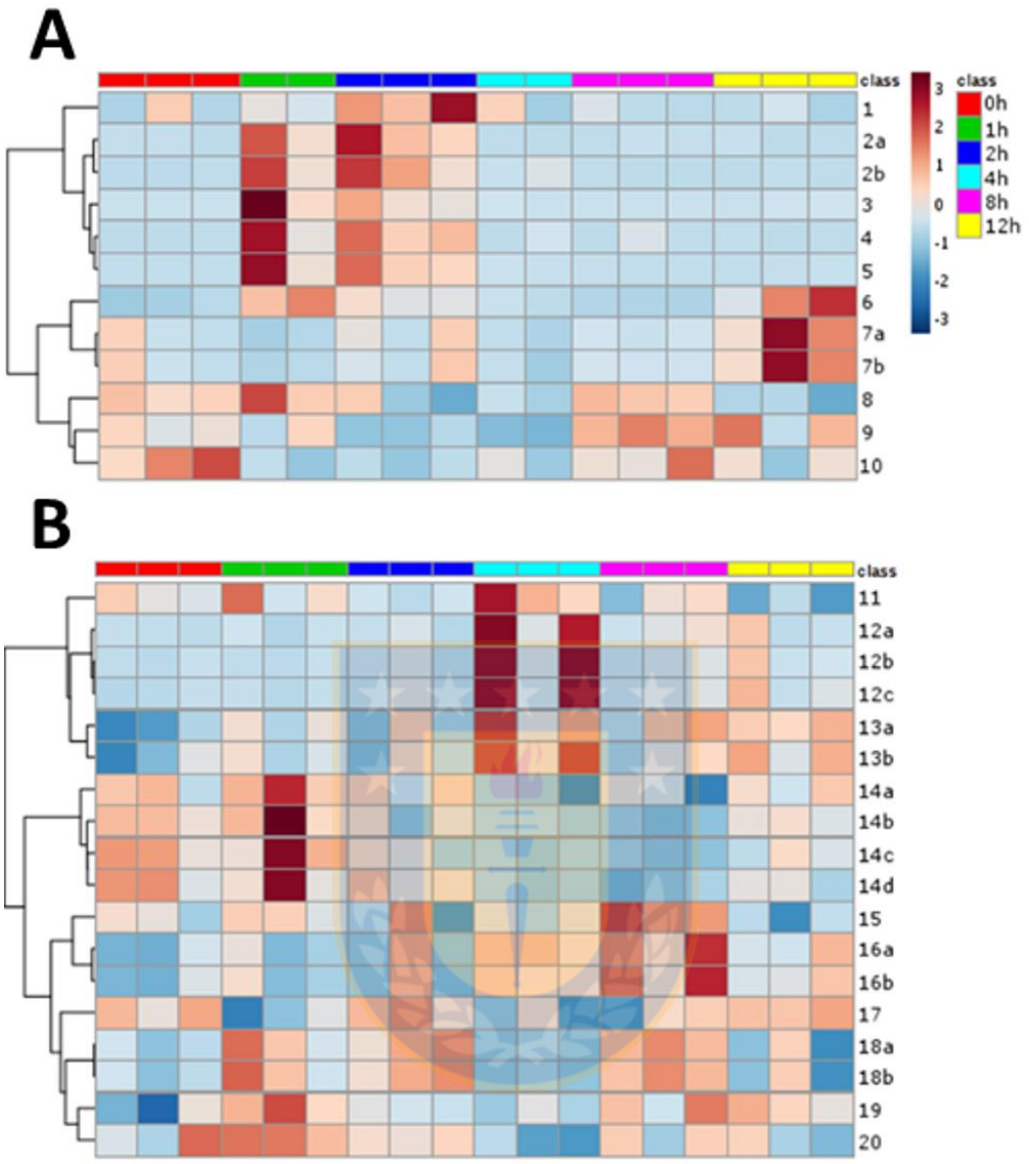

Figure 4.3: Selected features heatmap after applied untargeted metabolomic workflow.

All the described phenolic metabolites can be attributed to methoxylation, β-oxidation, decarboxylation and/or sulfonation of hydroxycinnamic or derivatives from B ring cleavage of anthocyanin contained in CBE. Only (iso)ferulic acid sulfate shows different time trends; the first increase can be explained due to the hydrolysis and methylation of hydroxycinnamic acids in the gastrointestinal tract or liver and the later can be a product of gut microbiota catabolism and/or entero-hepatic recirculation of anthocyanins and hydroxycinnamic acids. Moreover, no described flavonol metabolites was found probably due the high content of quercetin-rutinoside, which cannot be enzymatically deconjugated [58]. However, (iso)vanillic acid can be a product of microbiota catabolism, but the time trends suggest otherwise. Interestingly, level

2 annotation reveals an increase after 1, 2 and 8 h of adenosine monophosphate, an endogenous metabolite product of primary metabolism [59,60]. Other proposed markers mainly shows increments after 4 to12 h for 11 unknown features but also a decrease mainly after the same time for 8 features (Figure 4.3). Figure 4.4 shows possible metabolization pathways of phenolic metabolites found after a single dose of CBE. Accordingly, phenolic metabolites shows an increase at 1, 2 and 12 h suggesting that this compounds may have incidence in the increase of antioxidant capacity measured by ORAC and TP after 1 and 12 h ($p<0.05$). However, only 3 possible phenolic metabolites, namely feature 11, 12 and 13, can explain higher antioxidant capacity after 4 h by CUPRAC and FC.

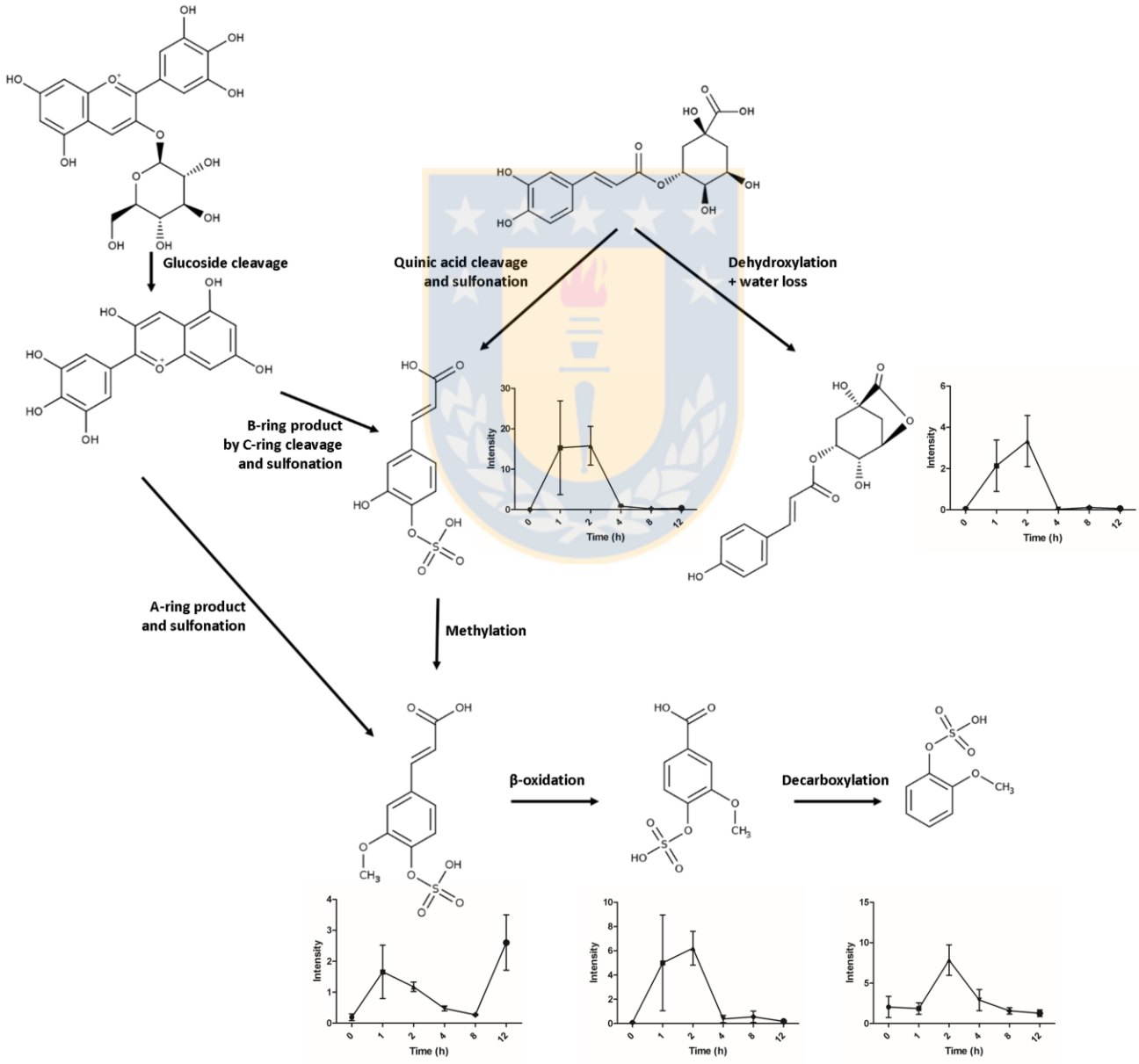

Figure 4.4: Possible sources of phenolic metabolites found after untargeted metabolomic analysis.

Conclusions

For the first time by an untargeted metabolomic approach, 20 markers of phenolic consumption were detected in low volumes of gerbil plasma after a single dose of CBE for the first time using an untargeted metabolomic study approach. From the proposed markers, seven corresponds to phenolic metabolites and two fragments that suggest the relevance of the two related compounds, namely coumaroyl quinolactone and adenosine phosphate. Additionally, previously described phenolic metabolites were detected in gerbils plasma, such as (iso)vanillic, (iso)ferulic, caffeic acid sulfate and methoxycatechol sulfate.

Finally, antioxidant capacity essays were successfully applied using very low volumes of gerbil plasma, showing significant increase at 1, 4 and 12 h after CBE consumption, which can be partially explained by phenolic metabolites markers, widely attributed as regulators of oxidative stress. However, sulfated phenolic compounds may have modified the antioxidant capacity. In addition, other molecules can also contribute to the higher antioxidant capacity, as degradation products of anthocianins, which were the main phenolics in the administrated CBE.

Acknowledgements

Authors would like to thank Fondecyt-1140439, doctoral fellowship, Fondequip-AIC-018 and PFB-27, CONICYT, Chile.

References

(1) Ruiz, A.; Hermosín-Gutiérrez, I.; Mardones, C.; Vergara, C.; Herlitz, E.; Vega, M.; Dorau, C.; Winterhalter, P.; Von Baer, D. Polyphenols and antioxidant activity of calafate (*Berberis microphylla*) fruits and other native berries from Southern Chile. *J. Agric. Food Chem.* **2010**, *58*, 6081–6089.

(2) Ruiz, A.; Mardones, C.; Vergara, C.; Hermosín-Gutiérrez, I.; von Baer, D.; Hinrichsen, P.; Rodriguez, R.; Arribillaga, D.; Dominguez, E. Analysis of hydroxycinnamic acids derivatives in calafate (*Berberis microphylla* G. Forst) berries by liquid chromatography with photodiode array and mass spectrometry detection. *J. Chromatogr. A* **2013**, *1281*, 38–45.

(3) Ruiz, A.; Zapata, M.; Sabando, C.; Bustamante, L.; Von Baer, D.; Vergara, C.; Mardones, C. Flavonols, alkaloids, and antioxidant capacity of edible wild *Berberis* species from patagonia. *J. Agric. Food Chem.* **2014**, *62*, 12407–12417.

(4) Speisky, H.; López Alarcón, C.; Gómez, M.; Fuentes, J.; Sandoval Acuña, C. First web-based database on total phenolics and Oxygen Radical Absorbance Capacity (ORAC) of fruits produced and consumed within the South Andes Region of South America. *J. Agric. Food Chem.* **2012**, *60*, 8851–8859.

(5) Rothwell, J. A.; Urpi-Sarda, M.; Boto-Ordoñez, M.; Llorach, R.; Farran-Codina, A.; Barupal, D. K.; Neveu, V.; Manach, C.; Andres-Lacueva, C.; Scalbert, A. Systematic analysis of the polyphenol metabolome using the Phenol-

Explorer database. *Mol. Nutr. Food Res.* **2016**, *60*, 203–211.

(6) Vogt, T. Phenylpropanoid Biosynthesis. *Mol. Plant* **2010**, *3*, 2–20.

(7) Yang, B.; Kortesniemi, M. Clinical evidence on potential health benefits of berries. *Curr. Opin. Food Sci.* **2015**, *2*, 36–42.

(8) Juurlink, B. H. J.; Azouz, H. J.; Aldalati, A. M. Z.; AlTinawi, B. M. H.; Ganguly, P. Hydroxybenzoic acid isomers and the cardiovascular system. *Nutr. J.* **2014**, *13*, 63.

(9) Williamson, G. Possible effects of dietary polyphenols on sugar absorption and digestion. *Mol. Nutr. Food Res.* **2013**, *57*, 48–57.

(10) Folmer, F.; Basavaraju, U.; Jaspars, M.; Hold, G.; El-Omar, E.; Dicato, M.; Diederich, M. Anticancer effects of bioactive berry compounds. *Phytochem. Rev.* **2013**, *13*, 295–322.

(11) Del Rio, D.; Rodriguez-Mateos, A.; Spencer, J. P. E.; Tognolini, M.; Borges, G.; Crozier, A. Dietary (poly)phenolics in human health: structures, bioavailability, and evidence of protective effects against chronic diseases. *Antioxid. Redox Signal.* **2013**, *18*, 1818–1892.

(12) Alvarez-Suarez, J. M.; Dekanski, D.; Risti, S.; Radonji, N. V; Petronijevi, N. D.; Giampieri, F.; Astolfi, P.; Gonzá Lez-Paramá S, A. M.; Santos-Buelga, C.; Tulipani, S.; et al. Strawberry polyphenols attenuate ethanol-induced gastric lesions in rats by activation of antioxidant enzymes and attenuation of MDA increase. PLoS One. 2011, 6, e25878.

(13) Jean-Gilles, D.; Li, L.; Ma, H.; Yuan, T.; Chichester, C. O.; Seeram, N. P. Anti-inflammatory effects of polyphenolic-enriched red raspberry extract in an antigen-induced arthritis rat model. *J. Agric. Food Chem.* **2012**, *60*, 5755–5762.

(14) Bolca, S.; Van De Wiele, T.; Possemiers, S. Gut metabotypes govern health effects of dietary polyphenols. *Curr. Opin. Biotechnol.* **2013**, *24*, 220–225.

(15) Williamson, G.; Clifford, M. N. Colonic metabolites of berry polyphenols : the missing link to biological activity ? *Br. J. Nutr.* **2010**, *104*, 48–66.

(16) Jenner, A. M.; Rafter, J.; Halliwell, B. Human fecal water content of phenolics: The extent of colonic exposure to aromatic compounds. *Free Radic. Biol. Med.* **2005**, *38*, 763–772.

(17) Stevens, J. F.; Maier, C. S. The chemistry of gut microbial metabolism of polyphenols. *Phytochem. Rev.* **2016**, *15*, 425–444.

(18) Kay, C. D. The future of flavonoid research. *Br. J. Nutr.* **2010**, *104 Suppl* (2010), S91–S95.

(19) Stalmach, A.; Edwards, C. A.; Wightman, J. D.; Crozier, A. Colonic catabolism of dietary phenolic and polyphenolic compounds from Concord grape juice. *Food Funct.* **2013**, *4*, 52–62.

(20) El-Seedi, H. R.; El-Said, A. M. a; Khalifa, S. a M.; Göransson, U.; Bohlin, L.; Borg-Karlson, A. K.; Verpoorte, R. Biosynthesis, natural sources, dietary intake, pharmacokinetic properties, and biological activities of hydroxycinnamic acids. *J. Agric. Food Chem.* **2012**, *60*, 10877–10895.

(21) Gonthier, M.-P.; Cheynier, V. R.; Donovan, J. L.; Manach, C.; Morand, C.; Mila, I.; Lapierre, C.; Ré Mé Sy, C.; Scalbert, A. Nutrient metabolism microbial aromatic acid metabolites formed in the gut account for a major fraction of the polyphenols excreted in urine of rats fed red wine polyphenols. *J. Nutr* **2003**, *133*, 461–467.

(22) De Ferrars, R. M.; Czank, C.; Zhang, Q.; Botting, N. P.; Kroon, P. A.; Cassidy, A.; Kay, C. D. The pharmacokinetics of anthocyanins and their metabolites in humans. *Br. J. Pharmacol.* **2014**, *171*, 3268–3282.

(23) Lila, M. A.; Burton-Freeman, B.; Grace, M.; Kalt, W. Unraveling anthocyanin bioavailability for human health. *Annu. Rev. Food Sci. Technol.* **2016**, *7*, 375–393.

(24) Olivas-Aguirre, F. J.; Rodrigo-García, J.; Martínez-Ruiz, N. D. R.; Cárdenas-Robles, A. I.; Mendoza-Díaz, S. O.; Álvarez-Parrilla, E.; González-Aguilar, G. A.; De La Rosa, L. A.; Ramos-Jiménez, A.; Wall-Medrano, A. Cyanidin-3-O-glucoside: Physical-chemistry, foodomics and health effects. *Molecules.* **2016**, *21*, 1–30.

(25) Fernandes, I.; Faria, A.; de Freitas, V.; Calhau, C.; Mateus, N. Multiple-approach studies to assess anthocyanin bioavailability. *Phytochem. Rev.* **2015**, *14*, 899–919.

(26) Esposito, D.; Damsud, T.; Wilson, M.; Grace, M. H.; Strauch, R.; Li, X.; Lila, M. A.; Komarnytsky, S. Black currant anthocyanins attenuate weight gain and improve glucose metabolism in diet-induced obese mice with intact, but not disrupted, gut microbiome. *J. Agric. Food Chem.* **2015**, *63*, 6172–6180.

(27) Fang, J. Bioavailability of anthocyanins. *Drug Metab. Rev.* **2014**, *46*, 508–520.

(28) Stalmach, A.; Edwards, C. A.; Wightman, J. D.; Crozier, A. Gastrointestinal stability and bioavailability of (poly)phenolic compounds following ingestion of Concord grape juice by humans. *Mol. Nutr. Food Res* **2012**, *56*, 497–509.

(29) González-Barrio, R.; Borges, G.; Mullen, W.; Crozier, A. Bioavailability of anthocyanins and ellagitannins following consumption of raspberries by healthy humans and subjects with an ileostomy. *J. Agric. Food Chem.* **2010**, *58*, 3933–3939.

(30) Czank, C.; Cassidy, A.; Zhang, Q.; Morrison, D. J.; Preston, T.; Kroon, P. A.; Botting, N. P.; Kay, C. D. Human metabolism and elimination of the anthocyanin, cyanidin-3-glucoside: A 13C-tracer study. *Am. J. Clin. Nutr.* **2013**, *97*, 995–1003.

(31) Guo, Y.; Bruno, R. S. Endogenous and exogenous mediators of quercetin bioavailability. *J. Nutr. Biochem.* **2015**, *26*, 201–210.

(32) Stalmach, A.; Mullen, W.; Barron, D.; Uchida, K.; Yokota, T.; Cavin, C.; Steiling, H.; Williamson, G.; Crozier, A. Metabolite profiling of hydroxycinnamate derivatives in plasma and urine after the ingestion of coffee by humans: Identification of biomarkers of coffee consumption. *Drug Metab. Dispos.* **2009**, *37*, 1749–1758.

(33) Stalmach, A.; Steiling, H.; Williamson, G.; Crozier, A. Bioavailability of chlorogenic acids following acute ingestion of coffee by humans with an ileostomy. *Arch. Biochem. Biophys.* **2010**, *501*, 98–105.

(34) Rodriguez-Mateos, A.; Feliciano, R. P.; Cifuentes-Gomez, T.; Spencer, J. P. E. Bioavailability of wild blueberry (poly)phenols at different levels of intake. *J. Berry Res.* **2016**, *6*, 137–148.

(35) Ludwig, I. A.; Mena, P.; Calani, L.; Borges, G.; Pereira-Caro, G.; Bresciani, L.; Del Rio, D.; Lean, M. E. J.; Crozier, A. New insights into the bioavailability of red raspberry anthocyanins and ellagitannins. *Free Radic. Biol. Med.* **2015**, *89*, 758–769.

(36) Sandhu, A. K.; Huang, Y.; Xiao, D.; Park, E.; Edirisinghe, I.; Burton-Freeman, B. Pharmacokinetic characterization and bioavailability of strawberry anthocyanins relative to meal Intake. *J. Agric. Food Chem.* **2016**, *64*, 4891–4899.

(37) Feliciano, R. P.; Boeres, A.; Massacessi, L.; Istas, G.; Ventura, M. R.; Nunes Dos Santos, C.; Heiss, C.; Rodriguez-

Mateos, A. Identification and quantification of novel cranberry-derived plasma and urinary (poly)phenols. *Arch. Biochem. Biophys.* **2016**, *599*, 31–41.

(38) Marques, C.; Fernandes, I.; Norberto, S.; Sá, C.; Teixeira, D.; de Freitas, V.; Mateus, N.; Calhau, C.; Faria, A. Pharmacokinetics of blackberry anthocyanins consumed with or without ethanol: A randomized and crossover trial. *Mol. Nutr. Food Res.* **2016**, *60*, 2319–2330.

(39) Kuntz, S.; Rudloff, S.; Asseburg, H.; Borsch, C.; Fröhling, B.; Unger, F.; Dold, S.; Spengler, B.; Römpp, A.; Kunz, C. Uptake and bioavailability of anthocyanins and phenolic acids from grape/blueberry juice and smoothie *in vitro* and *in vivo*. *Br. J. Nutr.* **2015**, *113*, 1044–1055.

(40) Xie, L.; Lee, S. G.; Vance, T. M.; Wang, Y.; Kim, B.; Lee, J. Y.; Chun, O. K.; Bolling, B. W. Bioavailability of anthocyanins and colonic polyphenol metabolites following consumption of aronia berry extract. *Food Chem.* **2016**, *211*, 860–868.

(41) Horwitz, W.; Association of Official Analytical Chemists, . Official Methods of Analysis of AOAC International, 17th ed.; Horwitz, W., Ed.; Gaithersburg, Md.: Association of Official Analytical Chemists, 2000.

(42) Morlock, G.; Vega-Herrera, M. Two new derivatization reagents for planar chromatographic quantification of sucralose in dietetic products. *J. Planar Chromatogr.* **2007**, *20*, 411–417.

(43) CAMAG. Applications Instrumental Thin-Layer Chromatography.

(44) Castillo-Muñoz, N.; Gómez-Alonso, S.; García-Romero, E.; Hermosín-Gutiérrez, I. Flavonol profiles of *Vitis vinifera* red grapes and their single-cultivar wines. *J. Agric. Food Chem.* **2007**, *55*, 992–1002.

(45) Arapitsas, P.; Ugliano, M.; Perenzoni, D.; Angeli, A.; Pangrazzi, P.; Mattivi, F. Wine metabolomics reveals new sulfonated products in bottled white wines, promoted by small amounts of oxygen. *J. Chromatogr. A.* **2016**, *1429*, 155–165.

(46) Arapitsas, P.; Speri, G.; Angeli, A.; Perenzoni, D.; Mattivi, F. The influence of storage on the chemical age of red wines. *Metabolomics* **2014**, *10*, 816–832.

(47) Xia, J.; Sinelnikov, I. V.; Han, B.; Wishart, D. S. MetaboAnalyst 3.0-making metabolomics more meaningful. *Nucleic Acids Res.* **2015**, *43*, W251–W257.

(48) Ribeiro, J.; Magalhaes, L.; Reis, S.; Lima, J.; Segundo, M. High-throughput total cupric ion reducing antioxidant capacity of biological samples determined using flow injection analysis and microplate-based methods. *Anal. Sci.* **2011**, *27*, 483–488.

(49) Demirci, S.; Ekiç, Ç.; Sözgen, K.; Kan, B.; Tütem, E. Modified cupric reducing antioxidant capacity (CUPRAC) assay for measuring the antioxidant capacities of thiol-containing proteins in admixture with polyphenols. *Talanta* **2009**, *79*, 344–351.

(50) Ou, B.; Chang, T.; Huang, D.; Prior, R. L. Determination of total antioxidant capacity by oxygen radical absorbance capacity (ORAC) using fluorescein as the fluorescence probe: First action 2012.23. *J. AOAC Int.* **2013**, *96*, 1372–1376.

(51) Ruiz, A.; Mardones, C.; Vergara, C.; Von Baer, D.; Gómez-Alonso, S.; Gómez, M. V.; Hermosín-Gutiérrez, I. Isolation and structural elucidation of anthocyanidin 3,7-B-O- diglucosides and caffeoyl-glucaric acids from calafate berries. *J. Agric. Food Chem.* **2014**, *62*, 6918–6925.

(52) Huang, D.; Boxin, O. U.; Prior, R. L. The chemistry behind antioxidant capacity assays. *J. Agric. Food Chem.* **2005**, *53*, 1841–1856.

(53) Apak, R. Total antioxidant capacity assay of human serum using copper(II)- neocuproine as chromogenic oxidant: The CUPRAC method. *Free Radic. Res.* **2005**, *39*, 949–961.

(54) Nimse, S. B.; Pal, D. Free radicals, natural antioxidants, and their reaction mechanisms. *RSC Adv.* **2015**, *5*, 27986–28006.

(55) Micallef, M.; Lexis, L.; Lewandowski, P. Red wine consumption increases antioxidant status and decreases oxidative stress in the circulation of both young and old humans. *Nutr. J.* **2007**, *6*, 27.

(56) Otaolaurruchi, E.; Fernández-Pachón, M. S.; Gonzalez, A. G.; Troncoso, A. M.; García-Parrilla, M. C. Repeated red wine consumption and changes on plasma antioxidant capacity and endogenous antioxidants (uric acid and protein thiol groups). *J. Agric. Food Chem.* **2007**, *55*, 9713–9718.

(57) Sumner, L. W.; Amberg, A.; Barrett, D.; Beale, M. H.; Beger, R.; Daykin, C. A.; Fan, T. W. M.; Fiehn, O.; Goodacre, R.; Griffin, J. L.; et al. Proposed minimum reporting standards for chemical analysis: Chemical Analysis Working Group (CAWG) Metabolomics Standards Initiative (MSI). *Metabolomics* **2007**, *3*, 211–221.

(58) Day, A. J.; Cañada, F. J.; Díaz, J. C.; Kroon, P. A.; McLauchlan, R.; Faulds, C. B.; Plumb, G. W.; Morgan, M. R. A.; Williamson, G. Dietary flavonoid and isoflavone glycosides are hydrolysed by the lactase site of lactase phlorizin hydrolase. *FEBS Lett.* **2000**, *468*, 166–170.

(59) Laboratories, K. KEGG: Kyoto Encyclopedia of Genes and Genomes http://www.genome.jp/kegg/ (accessed Mar 18, 1BC).

(60) Wishart, D. S.; Jewison, T.; Guo, A. C.; Wilson, M.; Knox, C.; Liu, Y.; Djoumbou, Y.; Mandal, R.; Aziat, F.; Dong, E.; et al. HMDB 3.0-The human metabolome database in 2013. *Nucleic Acids Res.* **2013**, *41*, 1–7.

Supplemental Material

Table S4.1: Total antioxidant capacity values of Calafate berry extract.

	Total Antioxidant Capacity (mmol TE[a] g-1)
ORAC-FL	22.29 ± 1.08
CUPRAC	0.95 ± 0.06
ABTS	0.66 ± 0.08
FC[b]	55.27 ± 1.30

[a] TE: Trolox equivalent; [b] FC value is expresed as mg g-1 gallic acid equivalent (GAE)

Table S4.2: Proximate analysis of Calafate berry extract.

Ascorbic acid	98.4 mg%
Total sugars	64.3 g%
Glucose	36.3 g%
Fructose	28.0 g%
Water content	17.70%
Crude Proteins	4.0 % (Nx5.7)
Ether extract	0.90%
Ash	2.80%
Crude Fiber	0.60%
Nitrogen free extractives	74.00%
Calories	319.83 kcal/100g

Table S4.3: Analytical parameters of antioxidant capacity assays in plasma.

	ORAC-FL TE (mM)	CUPRAC Urea TE (mM)	FOLIN GAE (mg L-1)
LD	3.8	0.9	0.6
LQ	12.7	3	2.1
Linear range	12.7-80	2.98-100	2.1-150
Precision (RSD%)	2.4	1.2	1.0

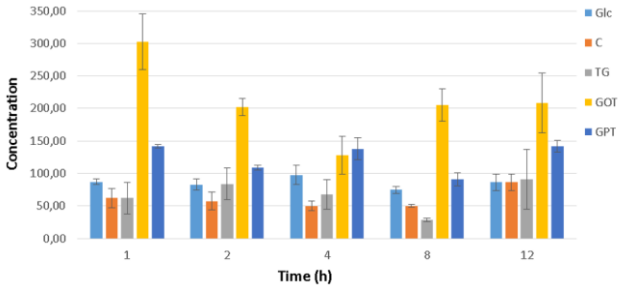

Figure S4.1: Biochemical parameters of gerbil plasma obtained at different time points after the administration of 300 mg kg^{-1} of CBE. Glc: Glucose; C: Cholesterol; TG: Triglycerides; GOT: Glutamic oxoloacetic transaminase; GPT: Glutamate-pyruvate transaminase. Glc, C and TG are expressed in mg dL^{-1}; GOT and GPT are expressed in U L^{-1}.

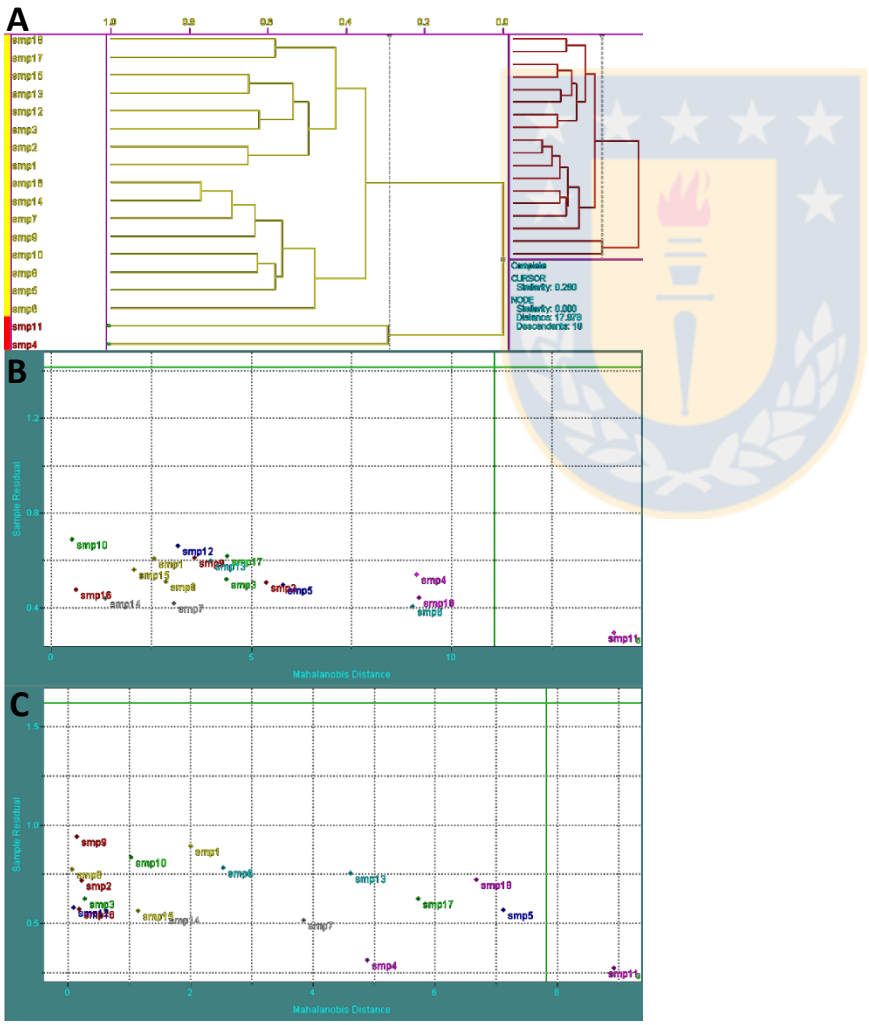

Figure S4.2: Outlier analysis of negative ionization dataset. A: Hierarchical cluster analysis; B and C: Standardized residuals vs Mahalanobis distance analysis.

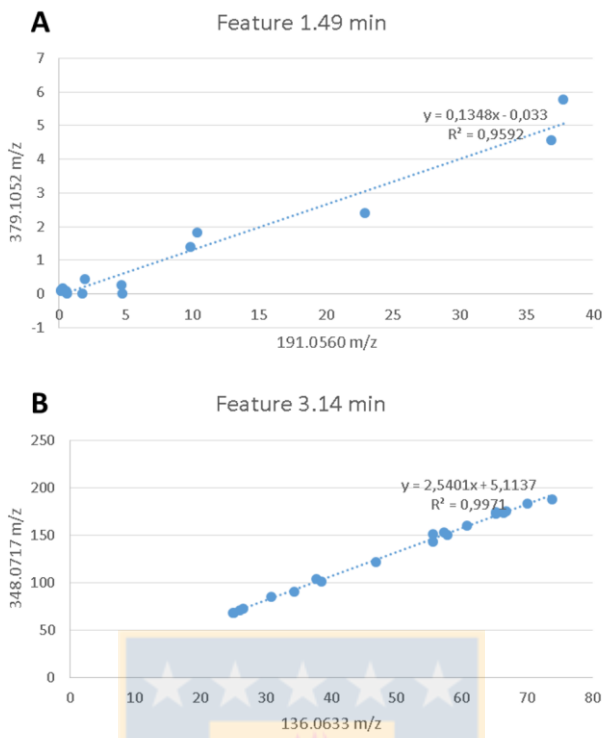

Figure S4.3: Feature correlation found at the same time in the chromatogram. A: Signals correlation at 1.49 minutes (negative mode) B: signals correlation at 3.14 minutes (positive mode).

Capítulo 5

Conclusiones Finales

1. Las menores concentraciones de antocianos encontrados en uvas Pink Globe se deben a la reducción de los niveles de expresión de *VvmybA1*, gen que codifica para un factor de transcripción que regula la expresión de UFGT, enzima clave en la glicosilación de antocianos.

2. El fruto de calafate posee mayor concentración de antocianos, flavonoles y acidos hidroxicinámicos que los contenidos en uvas Red Globe y Pink Globe, siendo hasta 60, 15 y 50 veces más altas, respectivamente. Por otro lado, no presenta cantidades cuantificables de monómeros y dímeros de flavan-3-oles. En base a estos resultados, se utilizó fruto de calafate como fuente de (poli)fenoles para el estudio de su metabolización en animales de experimentación, considerando que hasta la fecha no existe información sobre dicho proceso ni en cambios del metaboloma asociado a su consumo.

3. La modificación del proceso de extracción de (poli)fenoles desde calafate fue necesaria para generar un producto liofilizado sin residuos tóxicos, apto para el consumo en animales de experimentación. La mezcla de etanol potable y ácido fórmico permitió alcanzar una recuperación del 84% en el contenido de (poli)fenoles respecto a la extracción metanólica, alcanzando un compromiso adecuado entre rendimiento e inocuidad.

4. Con el protocolo establecido para la prueba de consumo agudo de calafate se logró obtener un volumen de muestra de plasma de gerbo suficiente para el estudio de metabolización propuesto, sin alterar los parámetros bioquímicos de control experimental.

5. El método MRM GC-MS/MS validado permitió la cuantificación en plasma, con muy alta sensibilidad, de 43 compuestos fenólicos propuestos como productos de metabolización de antocianos, flavonoles y ácidos hidroxicinámicos. La metodología consiste en la deconjugación enzimática, extracción líquido-líquido y derivatización con BSTFA/TMCS (90/10 %v/v), alcanzando límites de cuantificación entre los 0.01 a 0.30 µg/mL.

6. La ingesta aguda de calafate incrementa significativamente la concentración de 4 compuestos fenólicos en plasma y muestra una tendencia al alza de otros 5 compuestos. Entre 1 y 2 horas luego de la administración de calafate, los compuestos 1,4-dihidroxibenzeno, ácido 3,4-dihidroxyacético, 4-hidroxicinámico, 3,5-dimetoxi-4-hidroxibenzoico, 3-metoxi-4-hidroxibenzoico muestran una tendencia al

alza, mientras que para los ácidos 3-hidroxicinámico y 3-metoxi-4-hidroxiacético este aumento es estadísticamente significativo. La concentración de los ácidos 3-hidroxifenilacético y fenilacético también aumentaron significativamente luego de 4 a 12 horas suministrado el extracto. Todos los compuestos fenólicos mencionados son productos de la reducción, dehidroxilación, metilación y/o β-oxidación de derivados del ácido cafeico o productos del anillo B de antocianos trihixroxilados.

7. No fue posible, mediante el método GC-MS/MS desarrollado y aplicado en modalidad scan, desarrollar un análisis metabolómico no dirigido. Esto es debido a que la presencia de artefactos productos de la derivatización genera un alto número de señales que no es posible depurar con las herramientas bioinformáticas disponibles.

8. Se detectaron cambios en el metaboloma de plasma de gerbo sometido al ensayo agudo de ingesta de extracto de calafate, mediante análisis por UPLC-QTOF. Se detectaron 20 marcadores asociados al consumo del extracto de calafate. Estos corresponden a "features" con masas y tiempos de retención característicos, de los cuales 6 se identificaron como metabolitos de compuestos fenólicos, que corresponden a derivados sulfatados de metoxicatecol, ácido cafeico (dos isómeros), ferúlico y vanílico, junto a una quinolactona de ácido cumárico.

9. Los hallazgos por análisis por UPLC-QTOF tienen sentido biológico, considerando el contenido de (poli)fenoles en calafate: Los ácidos cafeicos y ferúlico sulfatados provienen directamente de la hidrolisis y metilación de los ácidos cafeoilquínicos y cafeoilglucáricos, junto con la ruptura del anillo C de los antocianos presentes en el extracto administrado. Consecuentemente, el ácido vanílico y metoxycatecol sulfatados pueden provenir de la β-oxidación del ácido ferúlico y posterior decarboxilación del ácido resultante. Por otro lado, la quinolactona de ácido cumárico puede aparecer como producto de la dehidroxilación del ácido cafeico, aunque es interesante destacar que conserva el ácido quínico (como forma deshidratada). Los 6 marcadores discutidos presentan un aumento característico a las 1 y 2 horas luego de la ingesta de calafate, lo que indica hidrólisis y metabolismo de fase I a nivel de intestino delgado e hígado, ingresando directamente al sistema circulatorio. Sin embargo, el ácido ferúlico sulfatado muestra un segundo peak a las 12 horas probablemente producto de la recirculación entero-hepática de este metabolito o alguno de sus compuestos parentales. Otra posible explicación es la exposición de los

polifenoles consumidos a la microbiota intestinal, generando catabolitos de menor tamaño que son absorbidos y luego modificados (metabolismo de fase II) antes del ingreso al sistema circulatorio.

10. El consumo agudo de calafate produce un aumento de la capacidad antioxidante del plasma. $TEAC_{ORAC\text{-}FL}$ revela un aumento significativo luego de 1 hora, mientras que en $TEAC_{CUPRAC}$ se alcanza a las 4 horas de administrado el extracto de calafate. ORAC-FL muestra una mejor relación con los metabolitos de compuestos fenólicos estudiados.

11. Los cambios de actividad antioxidante del plasma después del consumo de una dosis aguda de calafate pueden estar relacionados con el aumento de metabolitos de compuestos fenólicos, ya sea por una acción directa sobre la sonda de los ensayos o por la capacidad de equilibrar el estrés oxidativo.

12. Los métodos de análisis desarrollados y aplicados para metabolómica no dirigida, análisis cuantitativos de metabolitos de compuestos fenólicos y de capacidad antioxidante permitieron el uso de volúmenes de muestra total menores a los 200 µL, factor crítico en estudios de metabolismo de polifenoles en animales de experimentación pequeños.

Por lo tanto se demuestra que existe un efecto biológico asociado a la ingesta aguda de extracto de calafate en plasma de gerbos (mamífero roedor pequeño), el cual pudo ser evaluado complementando metabolómica dirigida y no dirigida, con ensayos antioxidantes clásicos, demostrándose la hipótesis planteada.